Risques passés et futurs de feux de forêts et leurs incidences sur la résilience de la forêt boréale de l'Est Canadien

Émeline Chaste

THÈSE DE DOCTORAT

de l'Université de recherche Paris Sciences et Lettres
PSL Research University

Préparée dans le cadre d'une cotutelle entre l'École Pratique des Hautes Études et Université du Québec à Montréal

Risques passés et futurs d'incendies, et leurs incidences sur la résilience de la forêt boréale de l'Est Canadien

École doctorale de l'EPHE – ED 472

Spécialité : Systèmes intégrés, environnement et biodiversité

Soutenue par :
Emeline CHASTE
le 20 novembre 2018

Dirigée par :
Christelle Hély
Martin Girardin
Yves Bergeron

COMPOSITION DU JURY :

M Peng Changui
Université du Québec à Montréal
Rapporteur - Président du jury

M David Price
Northern Forestry Center
Rapporteur

Mme Sylvie de Blois
McGill School of Environment
Examinateur

M Roger Prodon
EPHE
Examinateur

Mme Christelle Hély
EPHE
Directrice de thèse

M Martin P. Girardin
Université du Québec à Montréal
Directeur de thèse

M Yves Bergeron
Université du Québec à Montréal
Co-Directeur de thèse

École Pratique des Hautes Études | PSL RESEARCH UNIVERSITY PARIS | UQÀM

AVANT-PROPOS

Outre l'introduction générale et la conclusion générale, cette thèse est composée de trois chapitres, rédigés sous forme d'articles scientifiques. Le chapitre 2 est publié dans une revue à comité de lecture, le chapitre 3 est publié en ligne dans une revue à comité de lecture, alors que le chapitre 4 est actuellement en préparation pour une future soumission. Chaque chapitre répond à un ou plusieurs objectifs de recherche précis et intègre de façon systématique : une introduction qui présente la problématique et les objectifs, une description des données et méthodes utilisées, une présentation des résultats et une discussion qui met en perspective les résultats obtenus. L'ordre des chapitres correspond à l'ordre chronologique dans lequel ils ont été rédigés.

Chapitre 2 - Chaste, E., Girardin, M.P., Kaplan, J.O., Portier, J., Bergeron, Y., Hély, C. The pyrogeography of eastern boreal Canada from 1901 to 2012 simulated with the LPJ-LMfire model. *Biogeosciences*, 15(5), 1273-1292, doi :10.5194/bg-15-1273-2018, 2018.

Chapitre 3 - Chaste, E., Girardin, M.P., Kaplan, J.O., Bergeron, Y., Hély, C. Increases in heat-induced tree mortality could drive reductions of biomass resources in Canada's managed boreal forest. *Landscape Ecology*, (), 1-24, doi.org/10.1007/s10980-019-00780-4, 2019.

Chapitre 4 - Chaste, E., Girardin, M.P., Kaplan, J.O., Bergeron, Y., Hély, C. Holocene dynamics of the boreal forest of Eastern Canada : Untangling the drivers of vegetation change using paleoecological data and models. In prep.

Je suis la première auteure de chacun des chapitres de cette thèse. Martin Girardin, directeur de recherche, Christelle Hély et Yves Bergeron, co-directeurs de recherche, et, Jed Kaplan, membre du comité d'encadrement, ont suivi chaque étape de cette thèse et ont contribué à la réalisation et à la rédaction de tous les chapitres. Le chapitre 1 a fait l'objet d'une collaboration avec Jeanne Portier pour l'acquisition des données, l'étape de validation du modèle et la rédaction de l'article associé.

REMERCIEMENTS

Ce travail de doctorat n'aurait pas pu être réalisé sans le soutien et la participation de nombreuses personnes. Je tiens en premier lieu à exprimer ma profonde reconnaissance envers mon directeur de thèse, Martin Girardin, qui m'a soutenue et encouragée tout au long de cette thèse. Merci Martin, tu as su me transmettre facilement ta grande expertise scientifique et me donner de précieux conseils pour réaliser ce doctorat dans les meilleures conditions. Tes qualités humaines et ta disponibilité font de toi un excellent encadrant. Je remercie également ma co-directrice Christelle Hély qui a su m'apporter un soutien scientifique remarquable malgré la distance. Merci Christelle, tu as su me communiquer tes précieuses connaissances en modélisation et m'a permis d'aller toujours plus loin dans la réflexion. Un énorme merci au professeur Jed Kaplan qui s'est impliqué continuellement dans mon doctorat et m'a encadré comme son étudiante. Merci Jed, nos échanges ont toujours été très enrichissants pour moi tant du point de vue scientifique que personnel. Je remercie enfin mon co-directeur Yves Bergeron, merci Yves d'avoir partagé ton expertise scientifique et m'avoir aidé à amener une vision plus appliquée et concrète de mes travaux de modélisation.

Je tiens à remercier chaleureusement les membres de mon jury d'évaluation de thèse, et particulièrement David Price, pour les nombreux commentaires très constructifs qu'ils ont apportés sur mes travaux de recherche. Je tiens à remercier les professionnels du Centre d'étude de la forêt et Danielle Charron pour leur aide technique et leur soutien tout au long de cette thèse. Un énorme merci à XiaoJing Guo pour sa gentillesse, sa disponibilité et son aide précieuse dans la compilation des bases de données au format NetCDF. Je remercie Daniel Stubbs de Calcul Québec et Compute Canada pour l'aide apportée dans l'utilisation du serveur Briaree et du langage Fortran. Je remercie également Rémi St Amant, Travis Logan, Olivier Marti et Olivier Blarquez pour leur disponibilité et leur aide dans la réalisation de plusieurs étapes importantes de mon doctorat. Je remercie Raphaël Bondu, Olivier Blarquez et Julie Aleman pour les relectures de la thèse. Et enfin, j'aimerais remercier tous les chercheurs avec qui j'ai pu échanger pendant mon parcours car vos conseils ont toujours été enrichissants.

Ce doctorat a été financé par plusieurs organismes que je remercie : le Conseil de Recherches en Sciences Naturelles et en Génie du Canada (CRSNG), le programme Européen NEWFORESTS, l'organisme national canadien Mitacs, le programme FONCER en Modélisation de la complexité de la forêt, le programme Frontenac pour le soutien à la mobilité des doctorants inscrits en cotutelle de thèse franco-québécoise, et le Centre d'étude de la forêt (CEF).

Je remercie également chaleureusement tous les étudiants du Labo de Yves à Montréal, du CEF, du Centre de Foresterie des Laurentides et du réseau des Universités du Québec avec qui j'ai pu me lier d'amitié durant mon parcours. Votre présence à mes côtés m'a apporté énormément de joie et de soutien. Je me souviendrai longtemps de ces nombreux moments « épiques » que nous avons partagés ! Je remercie également mes anciens colocataires, que je suis fière de compter parmi mes amis aujourd'hui, pour tous les bonheurs et les fous rires.

Je conclue ces remerciements pour exprimer toute ma reconnaissance aux membres de ma famille et mes amis hors du Québec. Votre soutien continu durant toutes ces années a été plus qu'essentiel ! Enfin, je remercie énormément Raphaël (pro du LaTeX) pour m'avoir encouragé et épaulé tout au long de cette thèse.

TABLE DES MATIÈRES

LISTE DES FIGURES

LISTE DES TABLEAUX

RÉSUMÉ

Au Canada, la forêt boréale est influencée par le climat et un régime des feux spatialement hétérogène. Des modifications de la composition et de la structure de la forêt boréale sont anticipées en réponse à des conditions climatiques futures plus propices à l'activité des feux et aux stress hydriques. Une diminution importante des stocks de carbone et notamment de biomasse pourrait avoir des effets considérables sur l'industrie forestière et sur le réchauffement global en raison de l'émission vers l'atmosphère d'une quantité importante de carbone, notamment au cours des incendies. Malgré son importance écologique et socioéconomique, l'avenir de la forêt boréale canadienne semble très incertain car les impacts potentiels des changements climatiques futurs sur les processus écosystémiques et les stocks de biomasse sont encore mal compris. Ainsi, il est nécessaire d'approfondir nos connaissances sur les effets des changements climatiques sur la forêt boréale au Canada en lien avec le régime des feux. Ces connaissances devraient contribuer au développement de stratégies d'adaptation fiables au sein du secteur forestier.

L'objectif principal de ce doctorat est d'anticiper les conséquences des changements climatiques sur la dynamique de végétation et des incendies, et de caractériser leurs effets conjoints sur la résilience de la forêt boréale de l'Est canadien de part et d'autre de la limite nordique des forêts sous aménagement. Pour ce faire, des simulations sont réalisées avec le modèle de la dynamique globale de végétation LPJ-LMfire qui modélise la dynamique de la forêt en réponse aux variations climatiques et à l'occurrence des feux. Cette thèse se décline en trois objectifs, chacun présenté sous forme d'un chapitre : (1) reconstruire l'activité de feux en forêt boréale de l'Est canadien durant le dernier siècle (1901-2012) pour analyser l'évolution des tendances spatio-temporelles des feux en relation avec la végétation et le climat, (2) projeter la réponse de la forêt boréale de l'Est canadien aux changements climatiques et à l'augmentation prévue des incendies afin de déterminer si des changements brusques de la biomasse des espèces dominantes sont à envisager dans le futur, (3) simuler les trajectoires temporelles des feux et de la végétation en forêt boréale de l'Est canadien au cours des 6000 dernières années en réponse aux variations climatiques dans le but de comprendre les relations étroites qui ont existé sur une longue échelle de temps entre le climat, le feu et la végétation.

Cette étude propose pour la première fois des simulations effectuées avec le modèle LPJ-LMfire sur une longue échelle temporelle (passé, présent et futur) et à haute résolution spatiale sur la forêt boréale de l'Est canadien. Toutes les simulations réalisées avec LPJ-LMfire ont été effectuées au pas de temps mensuel sur une grille de 100 km^2 de résolution couvrant la forêt boréale qui s'étend de la province du Manitoba à l'Ouest jusqu'à la province maritime de Terre-Neuve à l'Est. LPJ-LMfire a été

paramétré pour quatre types fonctionnels de plantes (PFTs) correspondant aux principaux genres d'arbres présents en forêt boréale de l'Est canadien (*Picea*, *Abies*, *Pinus*, *Populus*). Les capacités prédictives de LPJ-LMfire ont été examinées en comparant nos simulations des taux annuels de combustion et de biomasse aérienne avec des ensembles indépendants de données sur le dernier siècle. En outre, une comparaison des taux annuels de combustion et de biomasse aérienne, simulés sur les 6000 dernières années, a été effectuée avec des reconstructions paléoécologiques obtenues à partir des enregistrements lacustres de charbons et de pollens, respectivement. Enfin, la version de LPJ-LMfire développée ici a été utilisée pour obtenir des trajectoires futures sur le 21$^{\text{ème}}$ siècle à partir d'un ensemble de scénarios climatiques de l'IPCC.

Les résultats principaux de cette étude ont révélé que LPJ-LMfire reproduit correctement les tendances spatio-temporelles de la fréquence de feu observée au cours du dernier siècle, particulièrement au Manitoba et en Ontario. La tendance spatiale simulée de la biomasse aérienne totale des arbres concorde également avec les observations, à l'exception de la biomasse à la limite nord des arbres qui est surestimée, principalement pour le PFT *Picea*. Les trajectoires simulées de la fréquence de feu et des changements de végétation au cours des 6000 dernières années n'étaient pas synchrones avec les reconstructions de la fréquence de feu et de la biomasse arborée pour la région. LPJ-LMfire ne simule pas les changements de la dynamique de la forêt aux bons endroits : trop au sud pour la zone ouest et trop au nord pour la zone est. À première vue, il semblerait que l'écart entre les trajectoires simulées et les reconstructions paléoécologiques soit attribuable aux incertitudes des données climatiques IPSL-CM5A-LR fournies en entrée dans le modèle LPJ-LMfire.

La variabilité climatique et l'occurrence des impacts de foudre sont des facteurs déterminants des tendances spatio-temporelles de la fréquence de feu au cours du dernier siècle. L'influence des effets de rétroaction de la végétation sur les feux s'est révélée être un facteur important contrôlant les tendances spatio-temporelles de la fréquence de feu sur de longues échelles de temps. Nos résultats vont à l'encontre des projections d'augmentation du risque de feu futur car ils suggèrent une diminution de la fréquence de feu d'ici 2100, particulièrement dans les régions sud de notre zone d'étude. Cette diminution sera associée à un changement de composition des forêts, en particulier des taxons résineux vers des taxons feuillus, et à une ouverture des paysages qui du fait de la fragmentation accrue, devrait limiter les allumages et la propagation des feux. Par conséquent, les simulations de la variabilité interannuelle de la fréquence de feu doivent prendre en compte les effets conjoints de l'occurrence des allumages par les impacts de foudre, des conditions climatiques et météorologiques et des conditions du combustible, ainsi que des rétroactions entre les différentes composantes du système.

L'augmentation de la fréquence et de l'intensité des sécheresses induites par les changements climatiques provoqueront une hausse des événements de mortalité des arbres dans les régions au sud de la limite nordique des forêts sous aménagement. La hausse

des températures et des concentrations en CO_2 atmosphérique augmentera la productivité des forêts. Toutefois, cet accroissement de productivité ne sera pas illimité et pourrait être contraint par les effets des sécheresses sur la mortalité des arbres, particulièrement dans les régions sud. Une diminution des stocks de biomasse et de la résilience de la forêt boréale au sud de la limite nordique des forêts sous aménagement pourraient engendrer des retombées économiques négatives importantes sur le secteur forestier. La mise en place de pratiques sylvicoles qui permettent d'augmenter la productivité et maintiennent un niveau de résilience suffisant pour permettre une gestion durable des forêts est proposée.

Mots clés : Modélisation, LPJ-LMfire, Changements climatiques, Aménagement forestier, Forêt boréale, Feux, Dynamique de végétation.

ABSTRACT

In Canada, boreal forest vegetation is modified by climate and heterogeneous wildfire regimes. In the boreal forest, changes in both vegetation composition and structure are anticipated as a result of future climate conditions that will be characterized by increased water stress and more fire prone conditions. The consequences of more severe and frequent fires will include increased release of carbon to the atmosphere, loss of carbon stock, notably in the tree standing biomass compartment, that could in turn have considerable impact on forest industries. Despite its obvious ecological and socioeconomic importance, the future of Canada's boreal forest is highly uncertain considering that future potential climate change impacts on ecosystem processes and biomass stocks are still incompletely understood. Thus, there is an increasing need to better understand the impacts of climate change on boreal forests in relation to fire regime. This should contribute to the development of adaptation strategies to ensure sustainability in the forest sector.

The main objective of this PhD thesis is to evaluate the potential effects of climate change on vegetation and fire dynamics, and to characterize their combined effects on eastern Canada's boreal forest, north and south of the managed forest northern limit. We used simulations from the LPJ-LMfire dynamic global vegetation model which simulates forest dynamics in response to climate variations and fire regime. This main objective has been addressed using three chapters dedicated to : (1) reconstructing fire activity in eastern Canada's boreal forest during the last century (1901-2012) to analyse the dynamics of fire spatio-temporal trends in relation to vegetation and climate, (2) projecting eastern Canada's boreal forest response to climate change and the anticipated increase in fire activity to determine if abrupt changes in dominant species biomass should be expected in the future, (3) simulating fire and vegetation temporal trajectories in eastern Canada's boreal forest over the last 6000 years in response to past climate variations in order to understand the relationships that have persisted over a longer time-scale among climate, fire and vegetation.

For the first time, simulations performed with the LPJ-LMfire model are based on long time-scales covering the past (last 6000 years), the present and the future (present-day to 2100), and at high spatial resolution covering eastern Canada's boreal forest. All LPJ-LMfire simulations were performed with a monthly time step on a 100 km^2 resolution grid covering boreal forest regions from Manitoba to Newfoundland. LPJ-LMfire was parametrized for four Plant Functional Types (PFTs) that correspond to the most abundant tree genera in eastern boreal Canada (*Picea*, *Abies*, *Pinus*, *Populus*). The predictive skills of LPJ-LMfire were examined by comparing our simulations of annual burn rates and biomass with independent data sets from the 20^{th} century. In addition, comparison of annual burn rates and biomass was conducted with palaeoecological reconstructions obtained from lacustrine-charcoal and pollen records, respectively. The current LPJ-LMfire version developed in this study was used to project future trajectories for the 21st century from a multi-model ensemble of IPCC climate scenarios.

We showed that LPJ-LMfire adequately simulates spatio-temporal trends in fire frequency observed over the last century, particularly in Manitoba and Ontario. The general spatial pattern of simulated total tree biomass also matched the observations, with the notable exception of overestimating biomass at the northern treeline, mainly for PFT *Picea*. Simulated trajectories of fire frequency and vegetation changes during the last 6000 years were not synchronous with reconstructions of fire frequency and tree biomass for the region. LPJ-LMfire simulations captured the changes in forest dynamics further south in the west and further north in the east compared to the empirical data. We suggest that the discrepancies between simulated and observed trajectories are associated with uncertainty in the IPSL-CM5A-LR climate dataset that was used as an input to the LPJ-LMfire model.

Climate variability and lightning occurrence are important factors in determining the spatio-temporal trends in fire frequency over the last century. Likewise, vegetation feedback effects related to fuel quantity and quality are important in controlling spatio-temporal trends in fire frequency over multi-millennial time scales. Contrary to the projected increases in future fire risk, our results suggest a decrease in fire frequency by 2100, mainly in southern regions of the study area. This decline will be associated with landscape opening and a shift in forest composition from needleleaf evergreen (softwood) to broadleaf deciduous (hardwood) taxa, which should limit ignition and fire spread. We conclude that simulations of interannual variability of fire frequency should take into account the joint effects of lightning occurrence, climate, weather conditions and fuel conditions, as well as their interactions and feedbacks.

An increase in intensity and frequency of drought induced by climate change will probably trigger a rise in tree mortality events in southern areas of the managed forests northern limit. Rising temperatures and atmospheric CO_2 concentrations appear likely to increase forest productivity. However, this increase in productivity will not be unlimited and could be constrained by heat-induced tree mortality, mainly in southern regions. A decrease in biomass stocks and resilience of boreal forest in the south of the managed forest region could have large negative economic impacts for the forest industry. Implementation of future silvicultural practices that increase productivity and maintain a level of resilience sufficient for sustainable forest management will be needed.

Keywords : Modelling, LPJ-LMfire, Climate change, Forest management, Boreal forest, Wildfires, Vegetation dynamic

Introduction générale

L'augmentation des émissions de gaz à effet de serre, causée par l'intensification des activités anthropiques telles que l'industrialisation et la déforestation depuis l'ère pré-industrielle, est la principale cause du réchauffement global observé depuis le milieu du 20ème siècle (Cook et al., 2016; Oreskes, 2018). Le Groupe d'experts Intergouvernemental sur l'Évolution du Climat (GIEC) indique dans son 5ème rapport (IPCC, 2014) que l'augmentation des émissions de dioxide de carbone (CO_2) imputables à l'usage de combustibles fossiles serait responsable de plus de la moitié de l'augmentation de la température annuelle moyenne à la surface du globe observée depuis 1951, à savoir + 0.12 °C par décennie. Il a également été démontré que les activités humaines auraient eu des répercussions sur les phénomènes météorologiques et climatiques extrêmes, tels que les vagues de chaleur et les fortes précipitations, dans diverses régions du monde depuis les années 1950 (Solow, 2015; Trenberth et al., 2015). Selon l'ensemble des modèles climatiques globaux, ces tendances climatiques observées depuis le début de l'ère industrielle devraient s'accentuer dans le futur avec des changements d'autant plus importants que les émissions anthropiques des gaz à effet de serre seront élevées (IPCC, 2014). L'impact des changements climatiques sur les écosystèmes terrestres a déjà été observé depuis le milieu du 20ème siècle (p. ex. le blanchiment de la Grande Barrière de corail, le dépérissement forestier induit par le climat) et devrait s'accentuer dans le futur à mesure que le réchauffement s'amplifie (IPCC, 2014).

0.1 Interaction végétation-climat-feux en forêt boréale au Canada

La forêt boréale compte parmi les écosystèmes terrestres les plus vulnérables face aux changements climatiques puisque cette forêt, située dans les hautes latitudes de l'hémisphère Nord, est susceptible de subir des changements climatiques de plus fortes amplitudes comparées aux forêts plus méridionales (IPCC, 2014; Mery et al., 2010; Price et al., 2013). La forêt boréale englobe environ 30 % de la superficie forestière mondiale et se situe en majorité en Russie (60 %) et au Canada (28 %) (Figure 1a ; Brandt et al., 2013; Peh et al., 2015). En stockant 32 % du carbone forestier planétaire dans la végétation et les sols (Pan et al., 2011), elle joue un rôle crucial dans le cycle du carbone sur Terre (Deluca and Boisvenue, 2012; Hobbie et al., 2000). La zone dans laquelle s'étend la forêt boréale est caractérisée par un climat continental froid avec des hivers longs et rudes, des saisons de croissance courtes et fraîches, de grandes amplitudes annuelles de température et de faibles précipitations estivales (Brandt et al., 2013; Peh et al., 2015). Le taux de décomposition de la matière organique est lent (Hobbie et al., 2000; Peh et al., 2015) et la disponibilité en nutriment est faible (Deluca and Boisvenue, 2012; Hedwall et al., 2015; Peh et al., 2015). La mosaïque forestière est principalement composée de peuplements de conifères et de feuillus adaptés à des conditions froides (p. ex. *Picea* spp., *Pinus* spp., *Populus* spp.), de parterres forestiers dominés par des mousses et des lichens, ainsi que de lacs, rivières et multiples zones humides telles que des tourbières (Brandt, 2009; Peh et al., 2015). Cette mosaïque paysagère n'est toutefois pas uniforme puisqu'elle est fortement influencée par des gradients climatiques, des régimes de perturbations naturelles hétérogènes et des activités anthropiques dans sa partie la plus méridionale.

Dans l'Est du Canada, la végétation de la forêt boréale est influencée par un gradient de température décroissant du sud vers le nord (Peh et al., 2015) et un gradient de précipitation croissant de l'ouest à l'est (Bergeron et al., 2014). Alors qu'on retrouve essen-

Figure 1. Localisation de (a) la forêt boréale au Canada (en brun) et (b) de la limite nordique des forêts sous aménagement (ligne noire, combinaison de McKenney et al. 2016 et de la limite territoriale des forêts attribuables au Québec adoptée par le Ministère des Forêts, de la Faune et des Parcs en 2016). Le pourcentage de végétation arborée à une résolution de 250 m est extrait de Beaudoin et al. (2014).

tiellement des forêts fermées au sud, les températures froides, entraînant des conditions d'établissement et de croissance des arbres plus difficiles, sont en partie responsables d'une ouverture des paysages forestiers vers le nord pouvant aller jusqu'à un paysage de toundra forestière (Figure 1b ; Brandt et al., 2013). La dynamique de la végétation est également façonnée par le feu, considéré comme la principale perturbation naturelle en forêt boréale au Canada, qui modifie la structure et la composition de la forêt (Gauthier et al., 2000; Boucher et al., 2017; Danneyrolles et al., 2016). Un paysage soumis à une forte activité de feux se caractérise par la présence de peuplements jeunes (Van Wagner, 1987) contenant majoritairement des espèces feuillues de début de succession (p. ex. *Populus* spp., *Betula* spp) et des espèces de conifères adaptées au feu (p. ex. *Pinus* spp., *Picea* spp. ; Boucher et al., 2017). En effet, certaines espèces de conifères telles que le pin gris (*Pinus banksiana*) et l'épinette noire (*Picea mariana*) produisent des cônes sérotineux (ou semi-sérotineux) qui protègent les graines de la chaleur et assurent ainsi une régénération et une colonisation post-incendie rapide (Gauthier et al., 1996). Le feu participe également au rétablissement de la productivité des peuplements en diminuant l'épaisseur de la matière organique à la surface du sol (Fenton et al., 2005) et en redistribuant les nutriments jusqu'alors séquestrés dans la végétation et les sols (Anyomi et al., 2014). La réduction de l'épaisseur de la couche de matière organique, voire sa disparition, est particulièrement favorable à la régénération de forêts fermées composées d'espèces feuillues et du pin gris, des espèces peu tolérantes à une épaisse couche de matière organique (Pacé et al., 2016). À l'inverse, la présence d'une épaisse couche de matière organique favorise l'ouverture des peuplements dominés par les épinettes (Terrier et al., 2014; Pacé et al., 2018). Par ailleurs, des feux successifs très rapprochés dans le temps contribuent à l'ouverture des paysages en diminuant la banque de graines dans les cônes et la production de semences (Le Goff and Sirois, 2004; Sirois, 2000). Dans ce cas, les forêts de conifères fermées se transforment en forêts ouvertes colonisées par des lichens et des éricacées (Girard et al., 2008).

Le régime des feux, généralement décrit par plusieurs attributs tels que la fréquence, l'intensité, la taille, la saisonnalité, le type ou encore la profondeur de brûlage (Keeley, 2009), est hétérogène en forêt boréale (Boulanger et al., 2012). Par exemple, l'activité de feux est plus élevée dans la partie ouest que dans la partie est de la forêt boréale canadienne, et dans les régions septentrionales (Flannigan et al., 2005, 2009; Bergeron et al., 2014; Boulanger et al., 2014). L'activité de feux dépend de la conjoncture de plusieurs facteurs tels que les conditions favorables au départ d'un feu puis à sa propagation, et également de la disponibilité du carburant (Flannigan et al., 2009, 2005;

Moritz et al., 2010). Ces facteurs sont contrôlés par des agents d'allumages tels que les impacts de foudre, les conditions climatiques et météorologiques, l'environnement physique, le type et la quantité de combustible et par les activités anthropiques (Flannigan and Wotton, 2001; Hély et al., 2001; Macias Fauria and Johnson, 2008; Parisien et al., 2011; Peterson et al., 2010; Stocks et al., 2003). La foudre, considérée comme un échange d'énergie électrique entre l'atmosphère et le sol et résultant d'une instabilité atmosphérique, est le principal agent d'allumage en forêt boréale au Canada (Bradshaw and Sykes, 2014; Flannigan et al., 2000; Stocks et al., 2003) et agit sur la fréquence et la densité spatiale des feux en forêt boréale (Flannigan et al., 2005; Peterson et al., 2010). Localement, les conditions météorologiques constituent un déterminant majeur des régimes de feux de forêt puisqu'elles conditionnent l'humidité du combustible et par conséquent l'allumage et la vitesse de propagation du feu (Flannigan et al., 2000; Flannigan and Wotton, 2001). À une échelle plus large, plusieurs facteurs climatiques tels que la température, les précipitations et les vents influencent également l'humidité des combustibles et la propagation des feux (Hély et al., 2001). Par exemple, des phénomènes récurrents de blocage des crêtes de hautes pressions au niveau de la troposphère provoquant un assèchement du combustible favorisent l'occurrence de grands feux dans les régions les plus septentrionales de la forêt boréale (Bonsai and Wheaton, 2005). Certains facteurs environnementaux, tels que la topographie, les lacs et zones humides, et les dépôts de surface, peuvent également influencer le régime des feux en agissant comme barrière dans la propagation des feux (Erni et al., 2017; Portier et al., 2016) ou en conditionnant le drainage des sols (Gauthier et al., 2000; Mansuy et al., 2011). Pour ce qui est du combustible, on note que les risques d'incendies sont plus faibles dans les peuplements jeunes ou composés de feuillus que dans les peuplements vieux ou composés de conifères (Bernier et al., 2016). En effet, les conifères possèdent de nombreux composés chimiques hautement inflammables tels que des terpénoïdes et autres composés organiques volatils, notamment dans leur résine et écorce, associées à une plus faible teneur en eau comparativement aux feuilles des feuillus (Terrier et al., 2013; Van Wagner, 1987). De plus, les feuillus sont souvent associés à une végétation de sous-étage caractérisée par une plus haute teneur en humidité que la végétation de sous-étage associée aux conifères (Hély et al., 2001). Enfin, les activités anthropiques en forêt boréale peuvent affecter l'activité de feux de différentes façons, soit en augmentant l'allumage, soit en diminuant la propagation des feux via la lutte contre les incendies ou en altérant la charge et l'agencement spatial des combustibles à travers l'aménagement forestier (Flannigan et al., 2000, 2005; Stocks et al., 2003; Wotton et al., 2003).

0.2 Aménagement forestier durable et changements climatiques

Depuis le début du 20ème siècle, l'aménagement forestier constitue une part importante de l'économie du Canada (Brandt et al., 2013; Natural Resources Canada, 2017) en raison de la richesse de matière ligneuse que renferme la forêt boréale. Les ventes de bois ont ainsi généré plus de 1,3 milliards de dollars canadiens en 2015 pour une superficie de forêt exploitée égale à 780 000 hectares (Canadian Council of Forest Ministers, 2017). Cependant, la récolte du bois au Canada est contrainte par la limite nordique des forêts sous aménagement (Figure 1B) qui sépare les forêts sous aménagement au sud, des forêts non aménagées et préservées de l'exploitation forestière au nord (Brandt et al., 2013). La limite nordique des forêts sous aménagement s'insère dans le contexte d'aménagement forestier durable adopté par le Canada en 1992 (Natural Resources Canada, 2017). L'aménagement durable de la forêt vise l'obtention d'un certain volume de bois issu d'arbres de dimensions acceptables à l'intérieur d'une période de temps raisonnable. Toutefois, face à l'occurrence de perturbations naturelles et aux conditions climatiques changeantes, la capacité de régénération des écosystèmes doit être suffisante pour maintenir des forêts denses et productives, garantes d'un approvisionnement continuel (Government of Canada, 2003). La limite nordique des forêts sous aménagement a donc pour but de protéger les peuplements forestiers les plus sensibles aux effets cumulatifs du climat, des régimes de perturbations et de l'aménagement forestier. En effet, les peuplements forestiers localisés au nord de la limite nordique des forêts sous aménagement présentent des densités de tiges variables (Figure 1b) et sont généralement peu productifs et donc de faible résilience, cette dernière étant définie comme la capacité de la forêt à se rétablir suite à des perturbations. Ces paysages de plus en plus ouverts vers le nord sont le résultat de conditions édaphiques limitantes, d'un climat rude et d'accidents de régénération post-incendies (Arseneault, 2001; Girard et al., 2008; Payette et al., 2008). Il existe actuellement des pressions économiques importantes en faveur d'une extension de la forêt commerciale vers le nord puisque les prévisions de l'augmentation des températures pourraient supposer une meilleure productivité. Or, certains processus biologiques et écologiques actuellement limités par les conditions climatiques froides pourraient mener à une diminution de la résilience de la forêt boréale au Canada, en lien avec les changements dans les régimes de température et de précipitation.

Les prévisions climatiques pour le Canada indiquent une augmentation des températures entre + 1.8 et + 6.3 °C d'ici la fin du $21^{ème}$ siècle comparativement à la période 1986 - 2005 (CMIP5). Cette augmentation de température devrait se traduire par des hivers plus cléments et plus courts avec notamment des printemps plus précoces (IPCC, 2014; Price et al., 2013). Il est également prévu un déficit hydrique par rapport à l'actuel pour les prochaines décennies en raison d'une hausse des températures que ne compensera pas l'augmentation des précipitations supposée (IPCC, 2013). Par ailleurs, une augmentation de la fréquence et de l'amplitude des événements météorologiques extrêmes tels que les sécheresses est anticipée (IPCC, 2014; Price et al., 2013). Les effets bénéfiques d'une augmentation des températures, de la durée de la saison de croissance et de la concentration en CO_2 atmosphérique sur la productivité de la forêt boréale pourraient être donc contrebalancés par une hausse des stress hydriques entraînant des événements de mortalité des arbres importants (Girardin et al., 2014; Allen et al., 2010). Les observations récentes ont montré que d'importantes baisses de croissance avaient eu lieu en forêt boréale au Canada depuis les années 1950 malgré l'augmentation des températures (Girardin et al., 2016) et ce phénomène pourrait s'amplifier avec les changements climatiques à venir (Girardin et al., 2014). Il existe néanmoins actuellement une controverse majeure sur la balance entre les effets bénéfiques et négatifs des changements climatiques sur la productivité de la forêt boréale (Girardin et al., 2016; D'orangeville et al., 2016; Charney et al., 2016; Boucher et al., 2018; Boulanger et al., 2017) sur laquelle cette thèse de doctorat va apporter de nouveaux éléments de réponse.

Les projections suggèrent une augmentation de la fréquence et de la taille des incendies dans le futur (Flannigan et al., 2009, 2016; Girardin et al., 2013; Girardin and Mudelsee, 2008; Krause et al., 2014; Wotton et al., 2017). Si la relation entre la température printanière et la surface totale brûlée se maintient, les superficies brûlées pourraient être multipliées par trois pour chaque degré de température supplémentaire (Ali et al., 2012). Ces modifications pourraient avoir des effets considérables sur la composition et la structure de la forêt boréale (Boulanger et al., 2017; Taylor et al., 2017). L'augmentation des feux (fréquence et/ou superficie brûlée) au cours des 50 dernières années a déjà entraîné une diminution de 9 % des forêts denses d'épinette noire au profit de peuplements forestiers plus ouverts (Girard et al., 2008). En forêt boréale, l'ouverture prolongée du couvert forestier favorise soit un couvert de lichens sur les sites xériques qui affecte la croissance des arbres en modifiant les conditions nutritives du sol (Pacé et al., 2016), soit un couvert de sphaignes sur les sites hydriques à subhydriques qui entraine une diminution de la productivité des arbres en influençant le contenu en eau de la couche organique (Pacé et al., 2018; Terrier et al., 2014). Par ailleurs, l'augmentation des feux pourrait également avoir des impacts sur le réchauffement global en raison de la libération vers l'atmosphère du carbone séquestré dans la végétation et dans la matière organique des horizons superficiels du sol (Landry and Matthews, 2016). Bien que la majorité des études s'accorde sur une intensification du régime des feux, l'augmentation attendue de peuplements jeunes composés majoritairement de feuillus devrait par rétroaction à moyen terme limiter la capacité de propagation des feux et donc freiner l'intensification des régimes de feux (Hély et al., 2000; Bernier et al., 2016; Marchal et al., 2017). Ces effets de rétroaction négatifs de la modification de la composition du paysage sur le régime des feux ont jusqu'à présent rarement été pris en compte dans les études et tendent à rajouter de l'incertitude dans les prédictions du régime des feux en réponse aux changements climatiques. Le déplacement des aires de répartition des espèces vers des latitudes plus septentrionales est également envisagé alors que de nombreux processus biologiques et écologiques sont limités par les conditions climatiques actuelles (Fei et al., 2017; Fisichelli et al., 2014). Cependant, même si cela reste difficile à quantifier, les zones climatiques pourraient se déplacer plus rapidement vers le nord que ce que la capacité de migration des arbres le permet (Epstein et al., 2007; Gauthier et al., 2015).

Face aux altérations attendues de la composition et de la structure de la forêt boréale au Canada, l'aménagement forestier tel qu'il est pratiqué aujourd'hui est remis en question. Les industries forestières vont en effet devoir adapter leurs pratiques sylvicoles si elles veulent respecter les enjeux écologiques et socio-économiques de l'aménagement forestier durable. Pour réduire les incertitudes, il est par conséquent nécessaire d'approfondir nos connaissances sur les effets des changements climatiques sur la forêt boréale au Canada en relation avec le régime des perturbations naturelles. Ces connaissances devraient contribuer au développement de stratégies d'adaptation fiables au sein du secteur forestier. C'est dans cette démarche que s'inscrit cette thèse de doctorat dont le principal objectif est d'anticiper les conséquences des changements climatiques sur la dynamique de végétation et des incendies, et de caractériser leurs effets conjoints sur la résilience de la forêt boréale de l'Est canadien de part et d'autre de la limite nordique des forêts sous aménagement.

0.3 Une large gamme d'outils de modélisation

Plusieurs outils de modélisation ayant des degrés de complexités variables existent actuellement pour projeter les réponses de la végétation et des feux aux changements climatiques (Fisher et al., 2018; Kerns and Perterson, 2014; Krawchuk et al., 2012; Michetti and Zampieri, 2014). Les modèles les plus simples sont les modèles de distribution d'espèces (« Species Distribution Models », SDMs) qui se basent sur des corrélations entre le climat et les distributions d'espèces (Miller, 2010). Souvent appliqués à des résolutions spatiales fines, ces modèles corrélatifs permettent de simuler rapidement de nombreuses distributions d'espèces (Harris, 2015). Ils ne prennent toutefois pas en compte des processus importants de la réponse de la végétation aux changements climatiques tels que l'efficacité de l'utilisation de l'eau par les plantes en réponse à l'augmentation des concentrations atmosphériques de CO_2 ou encore la dynamique des perturbations. Parmi les modèles les plus complexes, on retrouve les modèles de la dynamique globale de végétation (« Dynamic Global Vegetation Models », DGVMs). Ces modèles mécanistes simulent un certain nombre de processus écophysiologiques, biogéochimiques et hydrologiques impliqués dans les réponses de la végétation et des perturbations aux changements climatiques (Hantson et al., 2016; Peh et al., 2015). De nombreux DGVMs ont été développés par différents groupes de recherche à travers le monde (p. ex. IBIS ; Foley et al., 1996; Kucharik et al., 2000, TRIFFID ; Cox, 2001, LPJ-DGVM ; Sitch et al., 2003, ORCHIDEE ; Krinner et al., 2005). Ces modèles ont à l'origine été paramétrés pour les grands types fonctionnels de plantes (PFTs, "Plant Functional Types") qui composent les grands biomes terrestres (p. ex. la savane, la forêt tempérée, la toundra ; Peh et al., 2015), et appliqués à des résolutions spatiales relativement grossières (p. ex. 0,5 degré) à l'échelle mondiale. Par exemple, le biome forestier boréal est représenté par seulement deux PFTs ligneux qui distinguent les conifères et les feuillus. Cette représentation simplifiée de la végétation entraîne des incertitudes dans les projections de la distribution de la végétation puisqu'elle n'inclut pas toutes les rétroactions internes spécifiques aux différentes espèces présentes dans le biome boréal (Baudena et al., 2015). C'est pourquoi des études récentes se sont concentrées sur la diversification des PFTs et leur reparamétrisation à l'échelle du groupe d'espèces, plutôt qu'à l'échelle du biome (p. ex. Tang et al., 2010; Ruosch et al., 2016; Peaucelle et al., 2017). Des simulations ont également été réalisées à des résolutions spatiales plus fines (p. ex. $\sim$1 km, Shafer et al., 2015) et validées en comparant les sorties de modèles avec des observations provenant de données de terrain et de télédétection (p. ex. Rollinson et al., 2017; Ruosch et al., 2016; Schibalski et al., 2017). Cette étape de validation est importante car, quel que soit le paradigme de modélisation ou le modèle utilisé, les mesures de performance extraites d'un DGVM auront seulement une incidence sur le système réel représenté si le modèle est une bonne représentation de ce système. Ces efforts d'affinement des simulations de DGVMs permettent de combler le fossé qui existe entre notre compréhension écologique et les représentations de la dynamique de la végétation et de perturbations dans les DGVMs, et ce, afin d'améliorer les projections de la réponse de la végétation et des perturbations aux changements climatiques (Baudena et al., 2015).

0.4 Les modèles de dynamique des feux basés sur les processus

Des simulations réalistes de la dynamique de végétation nécessitent l'inclusion dans les DGVMs du régime des perturbations qui, comme nous l'avons expliqué dans la section 1.2, modifie la structure et la composition des peuplements forestiers et influence les bilans globaux de carbone (Pfeiffer et al., 2013). À notre connaissance, il n'existe actuellement aucun DGVM qui inclut toutes les perturbations qui affectent la forêt boréale au Canada (p. ex. feux de forêt, épidémies d'insectes, accidents de régénération, aménagement forestier, ...). Le feu étant la principale perturbation en forêt boréale au Canada, il nous a semblé essentiel d'utiliser un DGVM capable de simuler correctement les feux sur notre zone d'étude. Au cours des dernières années, des efforts considérables ont été déployés pour améliorer les modèles de la dynamique de feux basés sur les processus (p. ex. SPITFIRE ; Thonicke et al., 2010, Reg-FIRM ; Venevsky et al., 2002, MC-FIRE ; Lenihan and Bachelet, 2015, LMfire ; Pfeiffer et al., 2013) et les intégrer dans les DGVMs (p. ex. ORCHIDEE-SPITFIRE, LPJ-LMfire , CTEM-FIRE ; Hantson et al., 2016; Rabin et al., 2017). Cependant, des études récentes ont mis en évidence que chaque DGVM possède ses propres forces, faiblesses et limites (Fisher et al., 2018; Quillet et al., 2010; Xia et al., 2017). Par conséquent, le choix d'un ou de plusieurs DGVM dépend essentiellement de la problématique scientifique et du biome étudié (Quillet et al., 2010). Bien que la plupart des incendies dans le monde soient déclenchés accidentellement ou intentionnellement par les humains (Krause et al., 2014), c'est près de la moitié des incendies qui sont déclenchés par la foudre en forêt boréale au Canada, ces feux étant responsables de 81 % de la superficie totale brûlée (Stocks et al., 2003). La majorité des modèles de la dynamique de feux basés sur les processus génèrent des feux dits « naturels », soit à partir d'une densité d'impacts de foudre constante (p. ex. MC-FIRE, Reg-FIRM, CTEM-FIRE, GlobFIRM), soit à partir de climatologies moyennes mensuelles observées des densités d'impacts de foudre (p. ex. SPITFIRE ; Hantson et al., 2016) réparties sur les jours de pluie dans le mois (p. ex. LPX, LMfire ; Hantson et al., 2016; Pfeiffer et al., 2013; Prentice et al., 2011). Ces techniques ne permettent pas de prendre en compte la variabilité interannuelle de l'occurrence des impacts de foudre qui est une composante essentielle de l'occurrence des feux en forêt boréale (Peterson et al., 2010; Pfeiffer et al., 2013). Par conséquent, ces modèles de feux sous-estiment généralement les aires brûlées annuellement dans les zones où les feux sont principalement causés par la foudre (Pfeiffer et al., 2013). La variabilité interannuelle de l'occurrence des impacts de foudre est prise en compte dans les simulations effectuées avec les modèles LPX et LPJ-LMfire en utilisant l'information d'une série temporelle de l'énergie convective potentielle disponibles (CAPE), un proxy robuste de l'activité de foudre (Peterson et al., 2010; Romps et al., 2014). Les résultats ont montré que la fréquence de feu simulée par LPJ-LMfire en forêt boréale concordait mieux avec les observations que celle simulée par LPX (Pfeiffer et al., 2013; Prentice et al., 2011). En effet, LPJ-LMfire inclut également des processus spécifiques de la dynamique des feux qui reflètent de près le comportement des incendies en forêt boréale (Pfeiffer et al., 2013). Par exemple, LPJ-LMfire permet une propagation et une durée de feu sur plusieurs jours (Pfeiffer et al., 2013) alors que les modèles SPITFIRE et LPX ne permettent pas des durées d'incendie de plus de 4h (Prentice et al., 2011; Thonicke et al., 2010), ce qui n'est pas réaliste pour les feux en forêt boréale (Sedano and Randerson, 2014). De plus, LPJ-LMfire a la particularité de permettre la coalescence de feux (Pfeiffer et al., 2013), contrairement aux autres modèles. Or, les très grands feux, généralement issus de départs multiples, sont importants en forêt boréale puisqu'ils représentent 97 % de l'aire brûlée annuellement, alors qu'ils ne correspondent qu'à seulement 3 % de tous les feux (Stocks et al., 2003). Enfin, la capacité du modèle LPJ-LMfire à simuler la dynamique des feux en forêt boréale a déjà été validée en comparant des simulations effectuées sur l'Alaska avec des jeux de données disponibles pour cette zone (Pfeiffer et al., 2013), alors que celle du modèle LPX n'a quant à elle été évaluée que sur l'Australie, pour des biomes très différents de la forêt boréale au Canada (Kelley et al., 2014).

Dans le cadre de cette thèse, le modèle LPJ-LMfire a ainsi été choisi pour évaluer l'impact des changements climatiques sur la dynamique de végétation et des incendies, et de caractériser leurs effets conjoints sur la résilience de la forêt boréale de l'Est canadien. L'utilisation de ce nouvel outil de modélisation nécessite la paramétrisation pour les espèces de la forêt boréale de l'Est canadien et la validation des simulations à fine résolution.

0.5 Le modèle LPJ-LMfire

Cette section décrit le fonctionnement du modèle LPJ-LMfire qui est une version modifiée du modèle LPJ-SPITFIRE. Ce dernier couple le modèle de dynamique globale de la végétation LPJ-DGVM (Sitch et al., 2003) et le modèle de régime de feu basé sur les processus SPITFIRE (Thonicke et al., 2010). Dans LPJ-LMfire, chaque pixel est simulé indépendamment de ses voisins, et ce, même pour la propagation du feu qui est ainsi contrainte à n'évoluer que dans le pixel où l'allumage se produit. Cela dit, même si la résolution spatiale est fine (10 km x 10 km), celle-ci autorise la propagation de grands feux au sein de chaque pixel. Les sections suivantes présentent les caractéristiques du modèle à l'échelle d'un pixel.

0.5.1 La végétation dans LPJ-LMfire

La végétation est décrite dans LPJ-LMfire en termes de pourcentage de couverture de différents types fonctionnels de plante (PFTs, "Plant Functional Types"). Un PFT peut représenter des espèces ou des groupes d'espèces déterminés conjointement par leurs fonctions et leur utilisation des ressources dans l'écosystème (Nock et al., 2016). Dans la version actuelle de LPJ-LMfire, la végétation est définie par un maximum de neuf PFTs. Chaque PFT est contrôlé par un ensemble de paramètres clés qui définissent la morphologie (p. ex. maximum de la surface du houppier), la phénologie (p. ex. feuilles persistantes ou caduques), la dynamique (p. ex. taux maximal d'établissement de nouveaux individus) et les limites bioclimatiques (p. ex. température minimale du mois le plus froid) des espèces représentées (Smith et al., 2001). Un pixel correspond à une mosaïque de couverture des PFTs, de sol nul et d'une couverture en eau (Figure 2a), la somme des pourcentages de chacune de ces couvertures ne pouvant dépasser 100 %. Les couvertures des PFTs sont distinctes les unes des autres, elles peuvent différer d'un pixel à l'autre, et tous les PFTs ne sont pas forcément représentés sur chaque pixel. Chaque population de PFTs est associée à un nombre d'individus moyen par unité de surface (n ; Figure 2a) et à une surface de sol couverte par le feuillage d'un individu moyen de la population (FPC, "Foliar projective cover" ; Figure 2a). Cette notion d'individu moyen (I_m) signifie que les populations de PFTs sont représentées par des paramètres PFT-spécifiques d'un individu moyen (p. ex. hauteur, aire du houppier ; Figure 2b) appliqués à tous les individus de cette population. Dans ce cas, le postulat est que la valeur d'un paramètre PFT-spécifique correspond à la moyenne de ce paramètre pour tous les individus du PFT, quel que soit l'environnement dans lequel ils se développent et leurs stades de développement (Figure 2c). Les paramètres PFT-spécifiques d'un individu moyen sont mis à l'échelle du pixel en les multipliant par la densité de population *n* et la FPC. Par exemple, le pourcentage du couvert de chaque PFT est obtenu en multipliant la FPC par la surface moyenne du houppier d'un individu moyen et la densité de population *n* (Figure 2a).

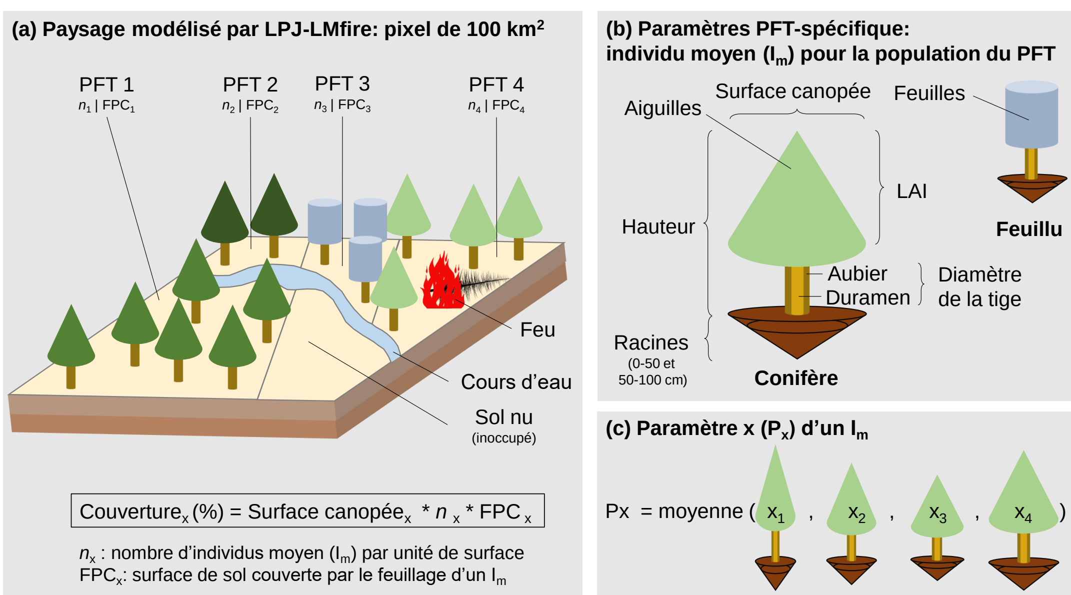

Figure 2. Schéma du processus de simulation des populations de PFTs à l'échelle d'un pixel dans LPJ-LMfire (adapté de Smith et al., 2001). L'indice de surface foliaire (LAI, "Leaf Area Index") est une grandeur sans dimension qui exprime la surface foliaire (m^2) d'un individu moyen (I_m) sur 1 m^2 de surface de sol.

0.5.2 Les données d'entrées

Les données d'entrées de LPJ-LMfire sont de 5 types (Figure 3a) : (i) des climatologies mensuelles, (ii) des contraintes environnementales, (iii) la concentration en CO_2 atmosphérique, (iv) des paramètres PFT-spécifiques, et si possible, (v) des usages anthropiques des terres. Il est important de noter que les perturbations anthropiques n'ont pas été considérées dans ce travail en raison de l'absence de données spatialement explicites couvrant une période de temps suffisante au Canada. Les climatologies mensuelles correspondent à des données spatialisées de températures, d'écarts entre la température minimale et maximale, de précipitations, de nombre de jours de pluie, de densité d'impacts de foudre, de vitesse du vent et de couverture nuageuse (Figure 3a). Ces séries temporelles mensuelles sont données en entrée du modèle LPJ-LMfire sur la période temporelle analysée, mais également en amont sur une période de « spin-up » d'environ 1000 ans afin de remplir les différents compartiments de carbone initialement vides et de simuler la végétation en équilibre avec le climat et le sol (Smith et al., 2001). Les données de contraintes environnementales représentent spatialement la texture et la typologie du sol, la fraction en eau, l'élévation et la pente (Figure 3a). Les données non-spatialisées de la concentration en CO_2 atmosphérique sont données en entrée à LPJ-LMfire au pas de temps annuel. Les paramètres PFT-spécifiques sont au nombre de 53 et leurs valeurs sont définies pour chaque PFT en entrée du modèle avant le démarrage du spin-up.

0.5.3 Le fonctionnement

À partir des données d'entrées, LPJ-LMfire calcule la dynamique de végétation basée sur des processus quotidiens (p. ex. la photosynthèse, l'absorption d'eau, l'évapotranspiration) et annuels (p. ex. l'établissement, la mortalité, l'allocation ; Figure 3b). Le climat mensuel est dérivé en conditions journalières à l'aide d'un générateur météo intégré dans le modèle (Figure 3b). Le carbone est défini dans 4 compartiments tissulaires : les

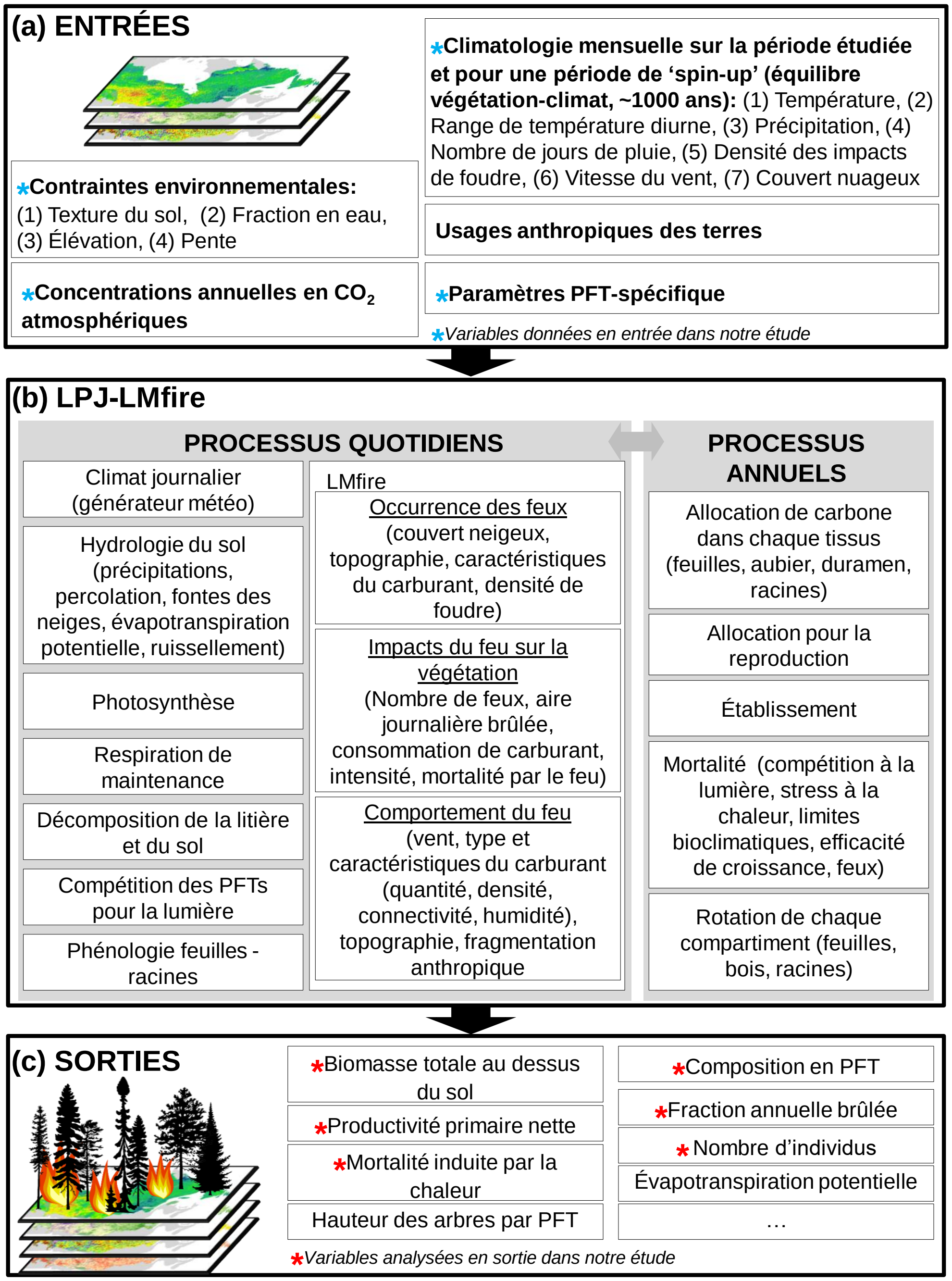

Figure 3. Schéma du fonctionnement de LPJ-LMfire montrant les données d'entrées nécessaires au modèle, les principaux processus calculés quotidiennement ou annuellement, et une liste non-exhaustive des variables de sorties du modèle.

feuilles, l'aubier, le duramen et les racines. L'absorption quotidienne de carbone se fait par la photosynthèse, calculée comme une fonction des radiations photosynthétiques absorbées, des températures, de la longueur du jour et de la conductance de la canopée. L'hydrologie du sol est modélisée sur deux couches de sol d'épaisseurs différentes, mais constantes à l'échelle du pixel, dont la teneur en eau est mise à jour quotidiennement en fonction des précipitations, de la percolation, de l'évapotranspiration, du ruissellement et de la fonte des neiges. La respiration de maintenance est calculée quotidiennement sur la base des ratios carbone/azote, la température, la phénologie et la biomasse des différents tissus. La productivité primaire nette (NPP) est calculée à la fin de chaque année et correspond au résultat net de l'apport de carbone issu de la photosynthèse auquel ont été soustraits les dépenses pour la respiration de maintenance et les coûts associés à la reproduction. Cette NPP est ensuite répartie dans les différents tissus de telle sorte que les contraintes allométriques définies soient satisfaites (p. ex. allocation plus importante dans les racines si stress hydrique). L'établissement des nouveaux individus au sein de la population représentant chaque PFT se produit chaque année en fonction de l'espace disponible et de l'état hydrique. La compétition à la lumière entre PFTs, le stress à la chaleur, les limites bioclimatiques, l'efficacité de croissance et les feux peuvent entraîner de la mortalité dans les populations des PFTs. La biomasse des individus morts est transférée annuellement dans la litière et la matière organique du sol en fonction de paramètres PFT-spécifiques. Au sein des individus vivants, la biomasse de l'aubier est transformée en duramen. Les variables de sorties du modèle LPJ-LMfire sont nombreuses et leur choix dépend des objectifs de l'étude. Le présent travail de recherche s'est concentré sur la biomasse totale au-dessus du sol, la NPP, le pourcentage de couverture des PFTs, la fraction annuelle brûlée et les taux d'établissement de nouveaux individus et de mortalité induite par la sécheresse (Figure 3c).

0.6 Objectifs et structure de la thèse

Ce travail de doctorat vise à évaluer les conséquences des changements climatiques sur la dynamique de végétation et des incendies, et de caractériser leurs effets conjoints sur la résilience de la forêt boréale de l'Est canadien. La thèse a été subdivisée en trois parties qui diffèrent principalement par leurs objectifs et les périodes temporelles étudiées (Figure 4). Tous les chapitres de cette thèse correspondent à des simulations effectuées avec le modèle LPJ-LMfire au pas de temps mensuel sur une grille de 100 km^2 de résolution couvrant la forêt boréale qui s'étend de la province du Manitoba à l'Ouest jusqu'à la province maritime de Terre-Neuve à l'Est.

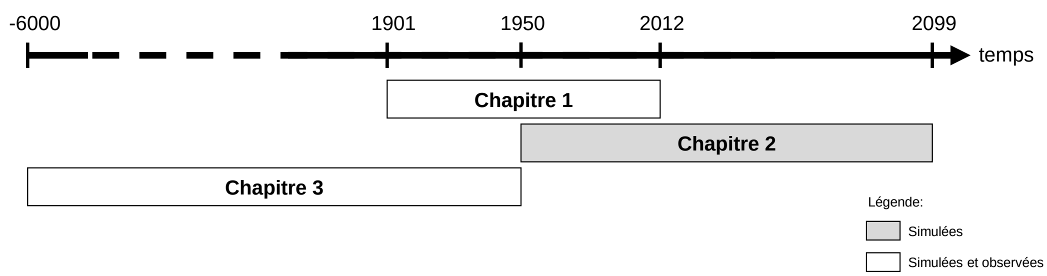

Figure 4. Périodes temporelles d'étude et types de données utilisées dans la thèse de doctorat.

Dans le chapitre 1, intitulé "*The pyrogeography of eastern boreal Canada from 1901 to 2012 simulated with the LPJ-LMfire model*", l'objectif est de reconstruire l'activité de feux en forêt boréale de l'Est canadien durant le dernier siècle (1901-2012) afin d'analyser comment les patrons spatio-temporels des feux ont évolué en relation avec la végétation et le climat. Pour répondre à cet objectif, les principaux genres d'arbres présents en forêt boréale de l'Est canadien (*Picea*, *Abies*, *Pinus*, *Populus*) sont déclinés en PFTs et paramétrés comme entrées de LPJ-LMfire. De plus, certains processus écosystémiques spécifiques à la forêt boréale, non pris en compte dans la version du code source utilisé, sont rajoutés de manière simplifiée mais réaliste dans LPJ-LMfire.

Ainsi, les capacités du modèle LPJ-LMfire à simuler correctement la végétation et les feux sont déterminées en comparant les sorties du modèle avec des ensembles de données empiriques (cartes forestières et archives d'incendies) disponibles pour la forêt boréale de l'Est canadien. En modélisation, cette première étape de calibration-validation est primordiale pour déterminer la robustesse des prédictions fournies. Dans ce souci d'évaluation, l'effet fertilisant de la concentration en CO_2 atmosphérique sur la végétation est également testé en conservant le climat historique (1901-2012) mais en faisant varier la concentration en CO_2.

Dans le chapitre 2, intitulé "*Increases in heat-induced tree mortality could drive reductions of biomass resources in Canada's managed boreal forest*", il s'agit de projeter l'impact des changements climatiques sur la végétation et les feux en forêt boréale de l'Est canadien depuis la deuxième moitié du 20ème siècle jusqu'à la fin du 21ème siècle. L'objectif est de tester l'hypothèse avancée par la communauté scientifique, à savoir que l'augmentation des conditions météorologiques extrêmes, des concentrations en CO_2 atmosphérique et des incendies prévue pour les prochaines décennies devrait provoquer des changements brusques de la biomasse des espèces dominantes dans la forêt boréale de l'Est du Canada. Si cette hypothèse est confirmée, déterminer dans quelle direction devraient se faire les changements de la biomasse est nécessaire pour adapter les pratiques sylvicoles afin de respecter les enjeux écologiques et socio-économiques de l'aménagement forestier durable. Concrètement, un ensemble de scénarios climatiques de l'IPCC sont utilisés en entrée du modèle LPJ-LMfire afin de simuler la plus large gamme de variabilité de la réponse de la végétation et des feux aux changements climatiques. Les simulations sont effectuées entre 1950 et 2099 et permettent l'analyse de la balance entre les gains de productivité induits par un climat plus chaud et des concentrations en CO_2 atmosphériques plus importantes, et les pertes de biomasse éventuellement induites par les feux et le climat. Afin de remettre ces prévisions dans le contexte de l'aménagement forestier durable, des zones particulières (ensemble de pixels), aujourd'hui localisées dans des secteurs où les récoltes de bois sont actuellement élevées, sont analysées plus en détail. Comme pour le chapitre 1, l'effet fertilisant de la concentration en CO_2 atmosphérique future est analysé à la fois à partir des deux scénarios RCP retenus, mais aussi séparément de l'effet du climat et éventuellement de l'effet des feux.

Dans le chapitre 3, intitulé "*Holocene dynamics of the boreal forest of Eastern Canada : Untangling the drivers of vegetation change using paleoecological data and models*", il s'agit de simuler avec le modèle LPJ-LMfire les trajectoires temporelles des feux et de la végétation en forêt boréale de l'Est canadien au cours des 6000 dernières années en réponse aux variations climatiques. Ce chapitre a pour objectif de présenter les avancées réalisées dans l'utilisation d'un DGVM (Lund-Postdam-Jena Lausanne-Mainz, LPJ-LMfire) pour simuler les relations passées climat-feux-végétation au cours de l'Holocène et de discuter de sa performance sur une échelle multi-millénaire. Des simulations climatiques à résolution temporelle continue au cours des 6000 dernières années, extraites du modèle climatique français IPSL, sont utilisées en entrée du modèle LPJ-LMfire. Des comparaisons de la biomasse et des feux simulés par LPJ-LMfire avec des données paléo-écologiques disponibles sur la région servent de deuxième étape de validation du modèle pour confirmer son utilisation pour une large gamme de conditions environnementales. En outre, ce chapitre a pour objectif de déterminer si les relations climat-feux-végétation mis en évidence dans les chapitres 1 et 2 ont déjà été rencontrées dans le passé.

À la suite de ces trois chapitres, la conclusion générale revient sur les principaux résultats et montre en quoi cette recherche contribue significativement à la compréhension de l'impact des changements climatiques sur l'activité de feux et la végétation en forêt boréale de l'Est canadien. Les implications des résultats de ce travail de recherche pour l'aménagement forestier durable à l'Est du Canada y sont également discutées.

CHAPITRE I

THE PYROGEOGRAPHY OF EASTERN BOREAL CANADA FROM 1901 TO 2012 SIMULATED WITH THE LPJ-LMFIRE MODEL

Chaste E., Girardin M. P., Kaplan, J. O., Portier J., Bergeron Y., Hély C. (2018) The pyrogeography of eastern boreal Canada from 1901 to 2012 simulated with the LPJ-LMfire model. *Biogeosciences* 15, 1273-1292.

Résumé

Les feux sont la principale perturbation naturelle qui façonne la structure et la composition de la forêt boréale de l'Est canadien. En moyenne, plus de 700 000 hectares de forêt brûlent chaque année, causant jusqu'à 2,9 millions de dollars de dommages. Bien qu'il est actuellement connu que l'occurrence des feux dépend de la conjoncture de conditions favorables au départ et la propagation du feu ainsi que de la disponibilité du carburant, il reste à évaluer les effets de l'interaction entre ces trois facteurs sur les tendances spatio-temporelles des feux dans l'Est du Canada. L'objectif de cette étude était de reconstituer les tendances spatio-temporelles de l'activité du feu au cours du siècle dernier dans la forêt boréale de l'Est du Canada, en lien avec les changements de densité de foudres, du climat et de la végétation. Pour ce faire, nous avons utilisé le modèle de la dynamique globale de végétation LPJ-LMfire, que nous avons paramétré pour quatre types fonctionnels de plantes (PFTs) correspondant aux principaux genres d'arbres présents en forêt boréale de l'Est canadien (*Picea*, *Abies*, *Pinus*, *Populus*). LPJ-LMfire a été exécuté au pas de temps mensuel entre 1901 et 2012 sur une grille de résolution de 100 km^2 couvrant la forêt boréale du Manitoba à Terre-Neuve. Les sorties de LPJ-LMfire ont été analysées en termes de fréquence d'incendie, de productivité primaire nette (NPP) et de biomasse aérienne. Les capacités prédictives de LPJ-LMfire ont été examinées en comparant nos simulations des taux annuels de combustion et de biomasse aérienne avec des ensembles indépendants de données. Nos résultats montrent que la simulation reproduit correctement le gradient latitudinal de la fréquence des feux au Manitoba et le gradient longitudinal de la fréquence des feux du Manitoba vers le Sud de l'Ontario, ainsi que les tendances temporelles des historiques de feux. En revanche, la simulation entraine une sous-estimation et surestimation de la fréquence des feux aux limites nord et sud de la forêt boréale au Québec. La tendance générale simulée de la biomasse aérienne totale des arbres concorde également avec les observations, à l'exception de la biomasse à la limite nord des arbres qui est surestimée, principalement pour le PFT *Picea*. Dans ces zones septentrionales, la capacité prédictive de LPJ-LMfire est probablement amoindrie par la faible densité des stations météorologiques qui conduit à sous-estimer la force des interactions climat-feu et, par conséquent, la combustion de la végétation durant les années de feux extrêmes. La corrélation entre les tendances spatio-temporelles de la fréquence des feux et les données observées dans une large partie de la zone d'étude tend à confirmer que le feu est fortement limité par l'allumage. Un climat plus sec couplé à une augmentation de la fréquence de la foudre au cours de la seconde moitié du $20^{ème}$ siècle aurait notamment conduit à une augmentation de l'activité de feu. Enfin, nos simulations mettent en évidence l'influence du climat et des feux sur la végétation : malgré une augmentation générale de la NPP induite par le CO_2 dans LPJ-LMfire, la biomasse aérienne forestière est restée relativement stable en raison des effets compensatoires de l'augmentation de l'activité des feux.

Mots-clés

Forêt boréale, LPJ-LMfire, Reconstruction des feux, Climat, Végétation, Foudre.

Abstract

Wildland fires are the main natural disturbance shaping forest structure and composition in eastern boreal Canada. On average, more than 700,000 ha of forest burns annually and causes as much as CAD 2.9 million worth of damage. Although we know that occurrence of fires depends upon the coincidence of favourable conditions for fire ignition, propagation, and fuel availability, the interplay among these three drivers in shaping spatiotemporal patterns of fires in eastern Canada remains to be evaluated. The goal of this study was to reconstruct the spatiotemporal patterns of fire activity during the last century in eastern Canada's boreal forest as a function of changes in lightning ignition, climate, and vegetation. We addressed this objective using the dynamic global vegetation model LPJ-LMfire, which we parametrized for four plant functional types (PFTs) that correspond to the prevalent tree genera in eastern boreal Canada (*Picea*, *Abies*, *Pinus*, *Populus*). LPJ-LMfire was run with a monthly time step from 1901 to 2012 on a 100-km^2 resolution grid covering the boreal forest from Manitoba to Newfoundland. Outputs of LPJ-LMfire were analyzed in terms of fire frequency, net primary productivity (NPP), and aboveground biomass. The predictive skills of LPJ-LMfire were examined by comparing our simulations of annual burn rates and biomass with independent data sets. The simulation adequately reproduced the latitudinal gradient in fire frequency in Manitoba and the longitudinal gradient from Manitoba towards southern Ontario, as well as the temporal patterns present in independent fire histories. However, the simulation led to the underestimation and overestimation of fire frequency at both the northern and southern limits of the boreal forest in Québec. The general pattern of simulated total tree biomass also agreed well with observations, with the notable exception of overestimated biomass at the northern treeline, mainly for PFT *Picea*. In these northern areas, the predictive ability of LPJ-LMfire is likely being affected by the low density of weather stations, which leads to underestimation of the strength of fireweather interactions and, therefore, vegetation consumption during extreme fire years. Agreement between the spatiotemporal patterns of fire frequency and the observed data across a vast portion of the study area confirmed that fire therein is strongly ignition limited. A drier climate coupled with an increase in lightning frequency during the second half of the 20^{th} century notably led to an increase in fire activity. Finally, our simulations highlighted the importance of both climate and fire in vegetation : despite an overarching CO_2-induced enhancement of NPP in LPJ-LMfire, forest biomass was relatively stable because of the compensatory effects of increasing fire activity.

Keywords

Boreal forest, LPJ-LMfire, Fires reconstruction, Climate, Vegetation, Lightning.

1.1 Introduction

Wildland fires are the main natural disturbance shaping forest structure and composition in eastern boreal Canada (Bergeron et al., 1998, 2014). On average, more than 0.7 Mha burns annually across Manitoba, Ontario, Québec, and the Maritime Provinces, which causes as much as CAD 2.9 million worth of damage and property losses (Canadian Council of Forest Ministers, 2017). About 97% of these burned areas are generated by a small proportion (3%) of large fires (fires > 200 ha in area; Stocks et al., 2003). For example, a fire burned 583000 ha within a few days in 2013 near the aboriginal community of Eastmain (province of Québec), which is the equivalent of 31% of the total area burned during that year in Québec (Erni et al., 2017). Studies of the spatial distribution of wildland fires in the past have highlighted that the frequency and size of fires in Canada have continuously increased over the last 50 years or so in response to the ongoing global warming (e.g. Kasischke and Turetsky, 2006; Hessl, 2011; Girardin and Terrier, 2015). Concerns are now being raised about the increasing frequency and severity of extreme climatic events with further warming, which could lead to an increasing concentration of numerous large fires in time and space (Wang et al., 2015). Given these observations and projections, there is growing concern about the capacity of the boreal forest to recover from disturbances (Bond et al., 2004; IPCC, 2013; Kurz et al., 2013; Rogers et al., 2013).

Wildland fire regimes are described by several attributes including the frequency, size, intensity, seasonality, type, and severity of fires (Keeley, 2009). The spatiotemporal variability in a fire regime depends upon the coincidence of favourable conditions for fire ignition, fire propagation, and fuel availability, which are controlled by ignition agents, weather and climate, and vegetation (Flannigan et al., 2009; Moritz et al., 2010). Almost half of the fires that occur in eastern boreal Canada are ignited by lightning and represent 81% of the total area burned (Canadian Forest Service, 2016), while the remaining fires originate from human activities. The capacity of a fire to grow into a large fire is determined by many factors, which include weather and fuel. High temperature, low precipitation, high wind velocity, and low atmospheric humidity can increase the growth of these fires (Flannigan et al., 2000). The intensity, severity, and size of fires are further influenced by species composition within the landscape, with needleleaf species being more fire prone than broad leaf species owing to their high flammability (Hély et al., 2001). Physical variables such as slope, surficial deposits, and soil moisture can also have significant effects on the rate at which fires spread by influencing fuel moisture or creating natural fire breaks (Hély et al., 2001; Mansuy et al., 2011; Hantson et al., 2016). Climate change scenarios for Canada indicate an increase in both temperature and precipitation in the coming decades. However, the increase in precipitation is unlikely to compensate for the increase in temperature (IPCC, 2013), and a greater moisture deficit is expected compared to the current state. Warmer springs and winters that lead to an earlier start of the fire season are anticipated, together with an increase in the frequency of extreme drought years due to more frequent and persistent high-pressure blocking systems (Girardin and Mudelsee, 2008). These phenomena are expected to lead to an increase in the frequency and size of fires in eastern boreal Canada in response to the on-going global warming (Ali et al., 2012). Effects of these changes in seasonal onset and dryness are such that the average size of spring wildfires could be multiplied by a factor of 3 for each additional 1 °C of warming (Ali et al., 2012; Girardin et al., 2013b; Price et al., 2013). An increase in area burned would affect both forest management plans and fire suppression strategies. It could also have subsequent feedback on the global carbon cycle, given that the substantial quantities of carbon currently being stored in these landscapes could be re-emitted back into the atmosphere (Pan et al., 2011).

A number of uncertainties persist concerning future fire projections, and biases still exist regarding our current understanding of the natural variability in fire regimes. Climate has been rapidly changing in recent decades with the expansion of human activities. All of these changes have altered interactions between fire regimes and their various forms of control (Bergeron et al., 2004a). Most fire history studies are based upon observations collected over relatively short time intervals (< 100 years), and reliable observations are often unavailable for many boreal regions prior to the late 1960s (Podur et al., 2002). Moreover, forest management and active fire suppression since the 1970s have contributed to modifying fire patterns and vegetation attributes in Canada (Gauthier et al., 2014). Therefore, it is difficult to determine the contribution of climate alone to fire activity in studies using observations collected since the second half of the 20th century. Furthermore, fire history studies rarely consider the feedback of fire on vegetation, mostly because historical data about vegetation composition are lacking (Danneyrolles et al., 2016). This is particularly true in the case of studies dealing with reconstructions of fire activity using dendrochronological evidence (e.g. Girardin et al., 2006a) or adjusted empirical data sets (Van Wagner, 1987). This problem may be circumvented by investigating past fire regimes over long periods of time through the analysis of charcoal and pollen in soil layers or lacustrine deposits (Payette et al., 2008; Ali et al., 2009). However, these paleoecological methods are costly and time-consuming and do not make it possible to capture the overall spatial variability in fire regimes at annual to decadal scale resolutions. Faced with these gaps, increasing our knowledge of the spatiotemporal patterns of past fires is necessary to perform better predictions in the future.

Simulations using dynamic global vegetation models (DGVMs) make it possible to estimate the spatiotemporal distribution of fires relative to climate and vegetation (Yue et al., 2016; Hantson et al., 2016). Indeed, these models simulate shifts in potential vegetation composition and related fire activity in response to changes in climate or environmental constraints (Smith et al., 2001). Experiments can be conducted on fine to broad spatial scales and validated on relatively short to medium timescales. Validation can be performed in regions where human activities are sufficiently low to allow comparisons with natural potential vegetation, by comparing simulation results with high-resolution satellite products, such as MODIS, on global scales (Tang et al., 2010). DGVM simulations may also be validated on decadal to millennial timescales by comparing them with historical records of vegetation or fire activity that have been reconstructed using indicators derived from pollen and charcoal, amongst others, which are deposited in lacustrine sediments (Molinari et al., 2013). One of these models, the Lund-Potsdam-Jena (LPJ) model, has been the subject of numerous refinements over time, especially concerning simulations of fire patterns (Thonicke et al., 2010; Pfeiffer et al., 2013), and it has been validated in many regions worldwide, excluding eastern boreal Canada (e.g. Prentice et al., 2011; Pfeiffer et al., 2013; Yue et al., 2016; Knorr et al., 2016).

Here, we used the LPJ-LMfire model that was developed by Pfeiffer et al. (2013) to perform a simulation experiment that targeted the boreal forest of eastern Canada and covered the 20th century, with customized parameterization to capture prevalent tree genera in eastern boreal Canada. The DGVM explicitly simulates fire ignition from lightning; hence, it is particularly adapted to the largely ignition-limited fire regimes in our study region. The objectives of this study were (1) to calibrate the LPJ-LMfire model for boreal forests in eastern Canada; (2) to assess the predictive skills of the model with independent data sets from eastern Canada's boreal forests; (3) to reconstruct fire activity, net primary productivity (NPP), and aboveground biomass during the last century; and (4) to determine how the spatiotemporal pattern of these three components has evolved in relation to changes in climate variables.

1.2 Model, experimental set-up, and methods

1.2.1 Study area

The study area encompasses eastern Canada's boreal forest (Brandt, 2009) from Manitoba to Newfoundland, which ranges from 102.86 to 52.64°W and from 46.61 to 64.71°N (Figure 2.1). The most common needleleaf tree species present in this region are black spruce (*Picea mariana* (Mill.) B.S.P.), white spruce (*Picea glauca* (Moench) Voss), balsam fir (*Abies balsamea* (L.) Mill.), jack pine (*Pinus banksiana* Lamb.), white pine (*Pinus strobus* L.), red pine (*Pinus resinosa* Ait.), eastern larch (*Larix laricina* (Du Roi) K. Koch), and eastern white cedar (*Thuja occidentalis* L.). The main broadleaf tree species are trembling aspen (*Populus tremuloides* Michx.) and white or paper birch (*Betula papyrifera* Marsh.) (Ecological Stratification Working Group, 1996; Brandt, 2009; Shorohova et al., 2011). The study area is divided from south to north into four ecozones (Figure 2.1; Ecological Stratification Working Group, 1996). (1) The Boreal Shield (BS) ecozone is characterized by rocky and rugged landscapes influenced by a continental climate (long and cold winters; short and warm summers) and by the cold air masses flowing out from Hudson Bay. Landscapes are dominated by needleleaf tree species in the westernmost areas, and co-dominated by needleleaf and deciduous tree species in temperate eastern areas. (2) The Boreal Plain (BP) ecozone corresponds to drier areas that are characterized by glacial deposits of variable thickness on flat or slightly rolling terrain. Forests are dominated by mixed boreal species, mainly represented by black spruce, trembling aspen, and jack pine. (3) The Hudson Plain (HP) ecozone is characterized by a sparser vegetation, which is dominated by *Sphagnum* and shrubs. Poor drainage conditions constrain southern trees to establish at drier, higher elevations. (4) The Taiga Shield (TS) ecozone, which is split into Eastern (TSE) and Western (TSW) parts, is characterized by colder climate conditions. The landscape becomes more open along a latitudinal gradient from south to north. In all regions, the dominant tree species are black spruce and jack pine. Within the study area, high-intensity crown fires are the most common type of fire events (Flannigan et al., 2016). Fire regimes are heterogeneous, but generally follow a declining trend along a south-westnortheast gradient (Boulanger et al., 2012). During the period of 1961-1990, the highest burn rates occurred in the western part of the BS ecozone (>1% yr^{-1}), while they were the lowest in the TSE ecozone (<0.2% yr^{-1}; Boulanger et al., 2014). Annual burn rates in the BP ecozone and in the eastern part of the BS ecozone varied from 0.2 to 0.5% yr^{-1}, whereas they varied from 0.5 to 1.0% yr^{-1} in the HP ecozone (Boulanger et al., 2014).

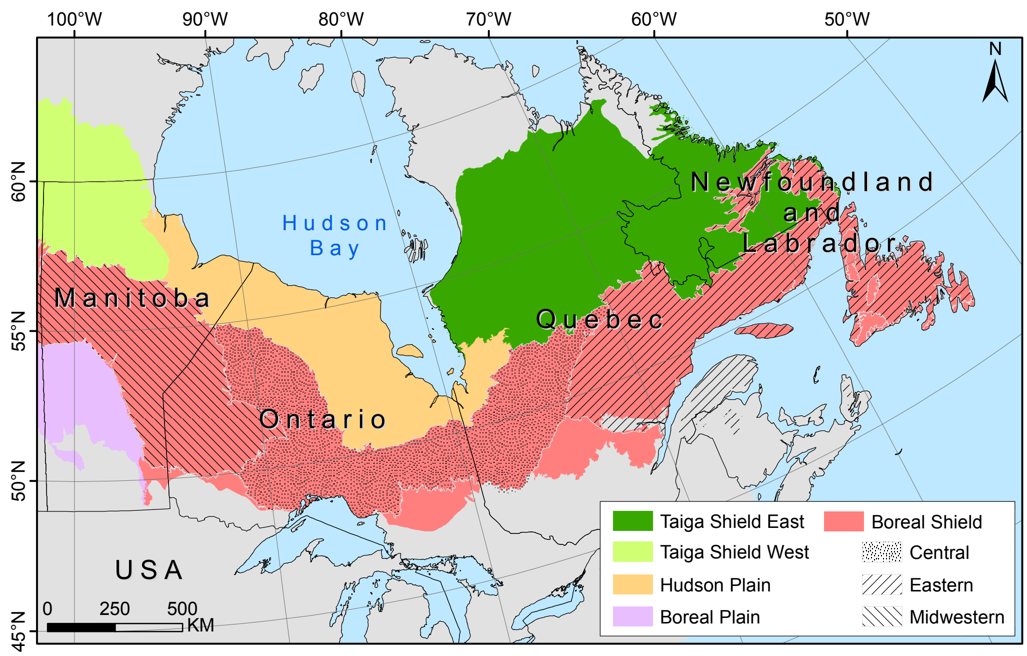

Figure 2.1. Map of eastern Canada's boreal forest from Manitoba to Newfoundland showing ecozones in colour. The Boreal Shield ecozone is divided into three ecoregions: Eastern Canadian forests, Central Canadian Boreal Shield forests, and Midwestern Canadian Shield forests (Ecological Stratification Working Group, 1996).

1.2.2 LPJ-LMfire model

Simulations of the terrestrial ecosystem were carried out using the dynamic global vegetation model LPJ-LMfire, which includes updates of both LPJ and the SPread and InTensity of FIRE (SPITFIRE) wildfire module (Thonicke et al., 2010). The model has been extensively evaluated for boreal forests (Pfeiffer et al., 2013). LPJ-LMfire is designed to simulate regional ecosystem dynamics, structure, and composition, with vegetation and fire events as responses to changes in climate and carbon dioxide (CO_2) concentration (Sitch et al., 2003). LPJ-LMfire describes the state of an ecosystem in terms of annual carbon stocks (living biomass, litter, and soil), NPP, net biome productivity, evapotranspiration, heterotrophic respiration, soil moisture fraction, and forest structure and vertical profile (cover fraction, individual density, crown area, leaf area index). In the present study, changes in the vegetation state are described in terms of NPP and total carbon stocks in living aboveground biomass. In LPJ-LMfire, vegetation is defined by up to nine plant functional types (PFTs). Each PFT represents one or several species sharing the same physiology and dynamics, governed by a short list of vital attributes, and constrained by bioclimatic limits (Sitch et al., 2003). Vegetation dynamics are updated annually based on the simulation of daily and annual processes. Daily processes are defined in terms of photosynthesis, stomatal regulation, soil hydrology, autotrophic respiration, leaf and root phenology, and decomposition. Annual processes are defined in terms of several sources of mortality, seedling establishment, reproduction, allocation, and tissue turnover (Smith et al., 2001; Sitch et al., 2003). The computational core of SPITFIRE is based upon Rothermel-type surface fire behaviour models (Rothermel, 1972; Andrews et al., 2008) and is designed to simulate processes of natural fires and their impacts on vegetation mortality and fire emissions (Thonicke et al., 2010). The LMfire module simulates lightning ignitions based upon a daily time step and uses fuel bulk density and fuel moisture to calculate the fire's rate of spread, intensity, and fire-related mortality. It allows fires to burn over multiple days and simulates fire extinction from changes in weather and fuel (Pfeiffer et al., 2013). As in the original version of SPITFIRE and nearly all other large-scale fire models, LMfire does not simulate the cell-to-cell spread of fire (Hantson et al., 2016; Pfeiffer et al., 2013; Rabin et al., 2017).

1.2.3 Simulation protocol

LPJ-LMfire was run monthly from 1901 to 2012 on 10 x 10 km equal-area grids covering eastern boreal Canada from Manitoba to Newfoundland. Driver data sets were prepared in netCDF format and are described in Table 2.1. Climate data were compiled at a monthly time step, while atmospheric CO_2 concentrations were compiled at an annual time step (see Section 2.2.4). A 1120-year spin-up period was prescribed to equilibrate vegetation and carbon pools with climate at the beginning of the study period (Smith et al., 2001) and to ensure that forest biomass and fire disturbances were in stable condition (Tang et al., 2010). This spin-up run was made using linearly detrended 1901-2012 climate data and repeated 10 times.

1.2.4 Environmental input data sets

1.2.4.1 Climate

Monthly means of temperature, diurnal temperature range, precipitation, number of days with precipitation, and wind speed were extracted for the 1901-2012 period from Environment Canada's historical climate database (Environment Canada, 2013) using BioSIM software (v.10.3.2; Régnière et al., 2014). Gridded climate data were prepared in BioSIM by interpolating weather data from the four weather stations that were closest to each 10 x 10 km grid, adjusted for elevation and location differentials with regional gradients, and averaged using inverse distance weighting ($1/d^2$, where d is distance). Missing wind speed values between 1901 and 1968 and those for 2010-2012 were set to the monthly 1969-2010 averages.

Table 2.1. Climate and other data sets used to drive LPJ-LMfire.

	Variables (units)	Period	Datasets	Reference
Climate data	Monthly mean temperature (°C) and monthly mean diurnal temperature range (°C)	1901-2012	Model "climatic monthly", software BioSIM	Environment Canada (2013)
	Monthly mean precipitation (mm) and number of days per month with precipitation			
	Monthly mean of wind speed (m s^{-1})	1969-2010		
	Monthly mean of total cloud cover percentage	1901-2012	20^{th} century reanalysis	Compo et al. (2011)
	Monthly mean convectible available potential energy (J kg^{-1})			
	Lightning flashes (number day^{-1} km^{-2})	1999-2010	Canadian lightning detection network	Orville et al. (2011)
Environmental constraints	Soil particle size distribution and volume fraction of coarse fragments (%)	-	ISRIC - World Soil Information	Hengl et al. (2014)
	Elevation (m) and slope (°)	-	Canada 3-D	Natural Resources Canada (2007)
	Water fraction area	-	National Hydro Network (NHN)	Natural Resources Canada (2010)
	Atmospheric CO_2 concentrations (ppm)	-	Composite CO_2 time series	Keeling et al. (2009); Pfeiffer et al. (2013)

Monthly means of total cloud cover percentage for the entire atmosphere and convective available potential energy (CAPE) were interpolated on our grid from the NOAA-CIRES 20th Century Reanalysis v2 data set at a $\sim$2.0° latitude and 1.75° longitude resolution (Compo et al., 2011). For a given grid cell, the annual monthly CAPE anomaly was calculated as the difference between the annual value and the monthly normal for CAPE, which was computed between 1961 and 1990.

1.2.4.2 Lightning

The Canadian Lightning Detection Network (CLDN) data set, covering the 1999-2010 period (Orville et al., 2011), was used to reconstruct the monthly cloud-to-ground lightning strike density (number day^{-1} km^{-2}) between 1901 and 2012. Given the strong correlation between lightning strikes and the product of CAPE and precipitation (e.g. Peterson et al., 2010; Romps et al., 2014), we computed daily lightning strike density using CAPE data and distributed the lightning strikes over the daily fraction of monthly rainy days (Pfeiffer et al., 2013). Across Canada and within our study area, July was the month with the maximum number of lightning strikes between 1999 and 2010 (Figure S2.1A in Supplement S2.1) and, in turn, interannual lightning strike variability (hereafter, referred to as min-to-mean and max-to-mean ratios) ranged from 0.1 to 7.5 times the July mean (Figure S2.1B in Supplement S2.1). This interannual variability in lightning strikes was preserved in our reconstruction by applying these two ratios to the normalized CAPE anomalies (values ranging between -1 and +1), which were then added to the 1999-2010 flash climatology (Pfeiffer et al., 2013, see Supplement S2.1 for further details).

1.2.4.3 Soils

The volume fraction of coarse fragments together with the 0-100 cm deep soil texture fractions of sand and clay were interpolated on the 10 x 10 km grids from the 1 km resolution ISRIC - World Soil Information data set (Hengl et al., 2014). For topography, we interpolated the 30 arcsec gridded digital elevation model (DEM) of Canada (Natural Resources Canada, 2007). We calculated slopes in degrees at 30 arcsec with the DEM map using ArcGIS 10.4.1 and interpolated the data to our 10 x 10 km grids. To calculate the percentage of land (i.e. removing lakes and water course areas) in each grid cell, we rasterized the water fraction of the National Hydro Network (NHN) data set at 100 m resolution (Natural Resources Canada, 2010). We calculated the water fraction at a 10 km resolution from 100 m resolution grid cells that had a percentage of water fraction > 50%. The land fraction was defined as the inverse of the water fraction. Roads, power lines, dams, mines, and other human-made structures, and areas of bare rock, were not considered in this study.

1.2.4.4 Atmospheric CO_2 concentration

Monthly mean atmospheric CO_2 concentrations covering the periods from 1901 to 1980 and from 1981 to 2012 were obtained from Pfeiffer et al. (2013) and the Mauna Loa data set (Keeling et al., 2009), respectively. Annual mean atmospheric CO_2 concentration varied from 296.23 ppm in 1901 to 392.48 ppm in 2012, which corresponds to an increase of 32.5%.

1.2.5 PFT definitions and LPJ-LMfire model modifications

LPJ-LMfire was calibrated for four PFTs that corresponded to the predominant tree genera currently present in the boreal forest of Canada: *Picea*, *Abies*, *Pinus*, and *Populus*. PFT-related parameters, e.g. fraction of roots in the upper soil layer or minimum and maximum temperatures of the coldest month for establishment, were assigned values from the published literature or global databases (see Table S2.1 in Supplement S2.2 for further details).

1.2.5.1 Edaphic limits to establishment

Establishment and growth of boreal tree species are influenced by a wide range of soil properties that are related to soil nutrient availability, which include pH, parent material, soil particle size, and water content, among others (Girardin et al., 2001; Beauregard and de Blois, 2014; Gewehr et al., 2014). Not all ecosystem processes linking these properties to tree establishment are simulated in the current version of LPJ-LMfire. Notably, the model does not simulate the development of peatlands or the process of paludification, and it does not include a complete module of biogeochemical cycling in soils that would emulate processes leading to acidification, for instance. As proposed by Beauregard and de Blois (2014), however, some edaphic variables may be indicative of certain soil processes at the stand level. In this study, correlations between the abundance of specific tree genera and soil clay content led to the implementation of a simple scheme to limit tree establishment in LPJ-LMfire (Figure S2.2A in Supplement S2.3). Edaphic limits to establishment were defined here in the same way that bioclimatic limits are used in LPJ. The correlations between the genus-specific tree cover fraction from Beaudoin et al. (2014) and clay volume fraction from Hengl et al. (2014) were analyzed at a 10 km resolution. For each PFT, the percentage of clay corresponding to the upper limit of the 90% confidence interval (CI) of its distribution, for grid cells with at least 10% of PFT cover, was used in the model as a threshold above which the given PFT could not establish. The upper limit of the 90% CI of the clay percentage distribution was 20, 13, 18, and 23% for *Picea*, *Abies*, *Pinus*, and *Populus*, respectively (Figure S2.2A and B in Supplement S2.3). The 20% threshold essentially results in the exclusion of the *Picea* and *Populus* PFTs in the HP ecozone, while the threshold of 13% leads to the additional exclusion of other PFTs, especially *Pinus*, in the Midwestern Canadian Shield forest ecoregion and in the BP ecozone (Figure S2.2C in Supplement S2.3).

1.2.5.2 Post-fire recruitment

Recruitment of *Pinus banksiana* requires the heat of fires to release seeds from serotinous cones (Gauthier et al., 1996). This condition was implemented in the current LPJ-LMfire version specifically for the *Pinus* PFT by inhibiting seedling establishment during years without fire in a given 100 km^2 gridcell. Such fire effects on seed dispersal are also observed for *Picea mariana*, which has semi-serotinous cones. Given that black spruce cones can open gradually over time in the absence of fire (Messaoud et al., 2007), *Picea* PFT establishment was not constrained by fire occurrence, neither was that of the *Abies* and *Populus* PFTs. No other modifications were made to the Pfeiffer et al. (2013) version of LPJ-LMfire.

1.2.6 Model evaluation

We assessed the performance of our customized LPJ-LMfire by comparing simulation results with previously published data sets on fire and maps of genus-specific aboveground biomass for Canadas forests.

1.2.6.1 Fire activity

The simulated burned area fraction was evaluated against three fire data products. First, annual burn rates for 1980-2012 were compiled from the Natural Resources Canada fire database (M. A. Parisien, personal communication, 2016) using Canada's national fire polygons with the hexagonal cells approach from Héon et al. (2014), but extended to our study area. We used 365 hexagonal cells to cover our study area and to compute the 1980-2012 simulated mean annual burn rates with 95% CI for each hexagonal cell. The second fire data product originated from stand-replacing fire history studies. Here, historical annual proportions of burned areas were obtained for 26 locations (Figure S2.3 in Supplement S2.4) using post-fire stand initiation reconstructions based upon field and archival data that were digitized and included in GIS databases (Girardin et al., 2013a; Héon et al., 2014; Portier et al., 2016). Using a 100 km radius around each location centroid, we calculated the simulated mean annual burn rates between 1911 and 2012, together with the 95% CI. Differences between our simulated 95% CI estimates and these two fire data products were considered qualitatively as "not different" if the observed annual burn rate fell within the 95% CI of the simulated mean burn rate. Note that as the period covered by the historical fire data often extended further back in time into the 19^{th} or 18^{th} centuries for southern locations (Table S2.2 in Supplement S2.4), some important differences could be expected in the comparison process. Finally, a third validation of fire simulations was made by comparing time series of total simulated annual burned areas in boreal forests of Manitoba, Ontario, and Québec with provincial fire statistics (point data) from the Canadian National Fire Database (CNFDB; Canadian Forest Service, 2016) covering the 1959-2012 period. Human-caused fires were excluded from these analyses. Spearman's rank correlation (r_s) was used to quantify the agreement between observed and simulated data. The agreement between simulation and observation was further evaluated in terms of fire seasonality by comparing their respective distributions of mean monthly areas that burned from 1959 to 2012.

1.2.6.2 Aboveground biomass

Published maps of total aboveground biomass at the genus level (Beaudoin et al., 2014) were used to evaluate model simulations. Maps that were created by Beaudoin et al. (2014) were constructed at a 250 m spatial resolution using remote sensing MODIS data sets, combined with photo-plot observations of Canada's National Forest Inventory (NFI), mainly in the southern areas (see non-hatched area in Figure 2.4). We aggregated the 250 m data to a 10 km resolution and applied a correction for the vegetated treed fraction of the landscape, as defined by Beaudoin et al. (2014). The vegetated treed fraction corresponds to the fraction of the grid cells that are covered by tree species of any size on at least 10% of the grid cell.

Total aboveground biomass, estimated using two other methods reported by Margolis et al. (2015), was used for a second evaluation of model simulations for the five ecozones under study. The BS ecozone was divided into three ecoregions for comparison purposes (Figure 2.1); ecoregions correspond to the classification of ecological regions on a finerscale than ecozones. The first method of biomass estimation is based upon the Geoscience Lidar Altimetry System (GLAS) method, which estimates total aboveground biomass from the waveforms recorded over vegetated land using lidar instruments. The second method is based upon NFI photo-plot estimates of total aboveground biomass using allometric equations.

1.2.7 History of the eastern boreal forest of Canada described by LPJ-LMfire

The outputs of LPJ-LMfire for the eastern boreal forest of Canada were analyzed in terms of annual burn rates, NPP, and total aboveground biomass. Significant changes in each temporal series were highlighted by a regime shift calculation developed by Rodionov (2004, 2006). A sequential application of Student's *t* test on 1000 randomly chosen grid cells was used (Rodionov, 2004, 2006). To be statistically significant at $P = 0.10$, the difference (diff) between mean values of two subsequent periods that was determined according to Student's *t* test should satisfy the condition

$$\text{diff} = t\sqrt{2\sigma_i^2/l}$$

where t is the value from the t distribution with $2l - 2$ degrees of freedom at the given probability level P, l is the cut-off length of the growth phase to be determined (hereafter set to periods of 20 years), and σ_i^2 is the average variance for running l-year intervals. The sample proportion, representing the fraction of k cells (integer ≥ 0) of a given population N (integer > 0), which was identified positively as recording a growth decline (or release), a biomass reduction (or biomass increase), and an increase in fire activity (or decrease), was computed for each sampled year from 1920 to 2007.

1.2.8 Sensitivity analysis to CO_2 fertilization

In terrestrial ecosystem models, changes in atmospheric CO_2 concentration in the recent past and future often have a more important influence on vegetation than does climate change (Girardin et al., 2011). Therefore, their inclusion has a very important effect on simulated changes in productivity. Here, the effect of CO_2 fertilization was explored using two experiments. In the first experiment, "Climate + CO_2", we ran the model with increases in CO_2 concentration as presented in Section 2.4.4. This experiment was used throughout our evaluation of LPJ-LMfire simulations. In the second experiment, "Climate-only", we ran the model with a constant CO_2 concentration from 1901 to 2012, which was fixed at 296.23 ppm (year 1901 value). In this case, there was no response of vegetation gross primary production (GPP) or fire to changes in CO_2 concentration. The effect of CO_2 fertilization on vegetation was determined by the difference between simulations "Climate + CO_2" and "Climate-only". Due to the post-fire recruitment rules established in LPJ-LMfire (see Section 2.2.5.2), the effect of CO_2 fertilization on fire was only determined by comparing the spatial pattern of annual burn rates simulated with the "Climate + CO_2" and "Climate-only" experiments.

1.3 Results

We report on the evaluation of process-based model performance in adequately simulated spatial patterns of fire frequency and fuel conditions (as indicated by the aboveground biomass of the four PFTs and total NPP) in eastern boreal Canada. We also report on changes in fire activity during the last century as simulated by LPJ-LMfire, with associated changes in vegetation features.

1.3.1 Predictive skills of the LPJ-LMfire model

1.3.1.1 Fire activity

For the recent 1980-2012 period, mean and maximum simulated annual burn rates were 0.36 and 1.49% yr^{-1}, respectively (Figure 2.2b), while mean and maximum observed annual burn rates were 0.28 and 2.03% yr^{-1} (Figure 2.2a). Observed and simulated burn rates were not significantly different in more than 80% of the studied hexagonal cells (295 out of 365; Figure 2.2c). Therefore, LPJ-LMfire was able to capture the amplitude of interregional variation. Decreases in fire activity observed along both the latitudinal gradient in Manitoba and the longitudinal gradient from Manitoba to southern Ontario were well reproduced by the simulation (Figure 2.2a and b). Furthermore, more than half of the observed historical annual burn rates fell within the 95% CI of their corresponding simulated annual burn rates (for further details, see Table S2.2 in Supplement S2.3). LPJ-LMfire overestimated annual burn rates from south of the Hudson Bay in Ontario to southwestern Québec (Figure 2.2c), while it underestimated annual burn rates in the western area of the central boreal forest in Québec (Figure 2.2c). Spearman's correlation coefficients (r_s) of time series of observed versus simulated area burned are 0.41 for Québec and 0.50 for Ontario and Manitoba (Figure 2.3a). As revealed by these coefficients, LPJ-LMfire was also able to emulate year-to-year variability in annual areas that were burned in Manitoba and Ontario, but less so in Québec. High fire activity years over the temporal series were also captured in the simulations, including 1961, 1968, 2003, and 2005, mostly in Manitoba and Ontario (Figure 2.3a). However, three extreme fire years were not reproduced: 1983, 1989, and 2002 (Figure 2.3a). Based upon the comparison of monthly percentage of total areas that were burned between 1959 and 2012 in eastern boreal Canada, the simulated fire season generally started and ended 1 month earlier than what was observed (Figure 2.3b).

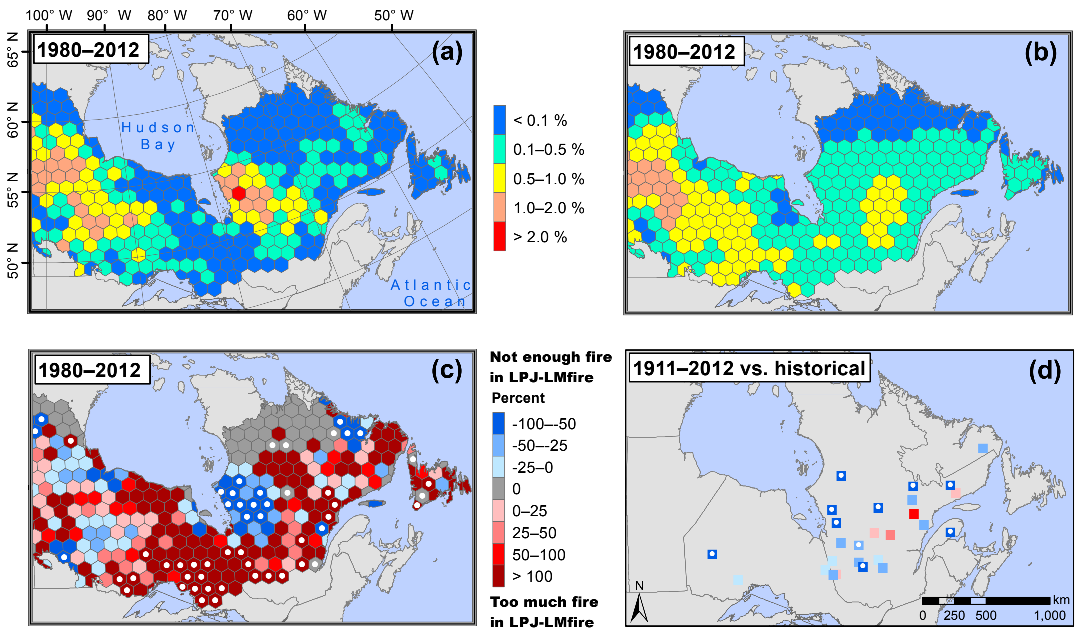

Figure 2.2. Observed versus LPJ-LMfire-simulated annual burn rates across eastern boreal Canada. (a) Observed annual burn rates computed for 365 hexagonal cells between 1980 and 2012 (data from Natural Resources Canada, 2017). (b) LPJ-LMfire simulated annual burn rates computed over the same period and hexagonal cells. (c) Percentage of difference between observed and simulated annual burn rates. (d) Percentage of difference between historical annual burn rates reconstructed from stand-replacing fire history studies (data from Girardin et al., 2013a; Héon et al., 2014; Portier et al., 2016) and LPJ-LMfire-simulated annual burn rates between 1911 and 2012 (see Supplement S2.4 for further details). White points indicate where the observed (and historical) annual burn rate lies outside the 95% confidence interval (95% CI) of the averaged annual burn rates in hexagonal cells simulated by LPJ-LMfire.

1.3.1.2 Fuels

Overall, the general latitudinal pattern of simulated total tree biomass agreed with the pattern of observed total tree biomass (Figure 2.4a). Median simulated total tree biomass (with 90% CI) in the southern areas (non-hatched) was 77 T ha^{-1} (33-108 T ha^{-1}), while median observed total tree biomass in the same areas was 73 T ha^{-1} (36-100 T ha^{-1}). In the BS ecozone, percentage differences between mean total tree biomass that was simulated and that which was estimated using NFI-based and GLAS-based methods were 31 and -7.8%, respectively, and decreased along a westward gra-

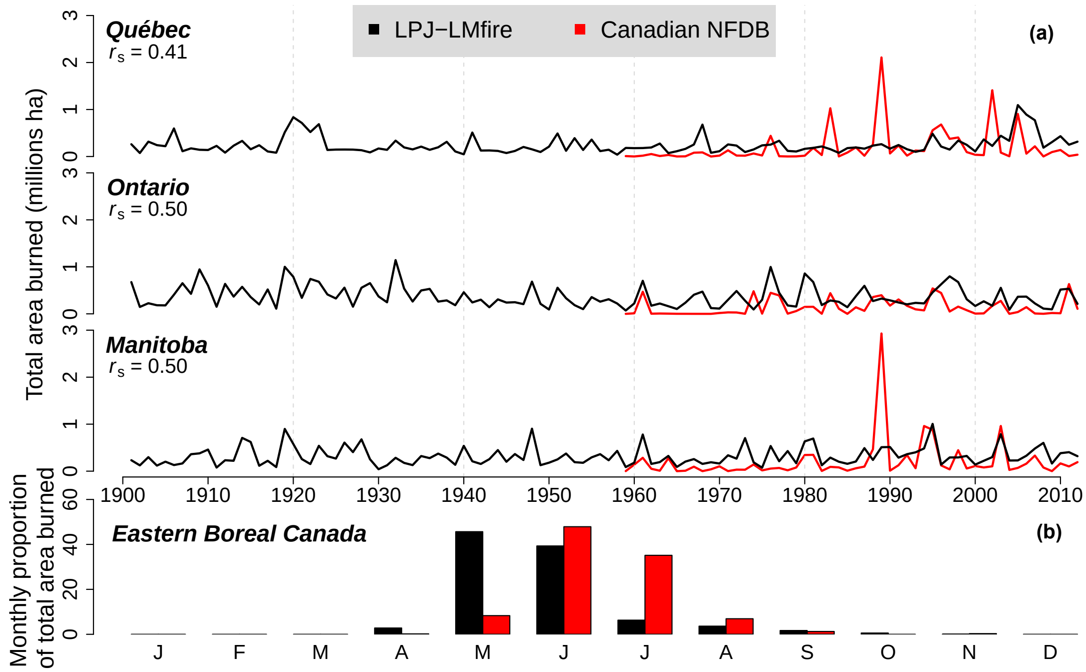

Figure 2.3. (a) Observed versus simulated total annual areas burned in three provinces of eastern Canada. Observed data (1959 to 2012) are from the Canadian National Fire Database (CNFDB). Spearman's rank correlation between data is shown (correlations are significant at $P < 0.05$ for Québec and $P < 0.001$ for the other provinces). (b) Monthly percentage of total areas burned between 1959 and 2012 in eastern boreal Canada.

dient from Québec to Manitoba (Table 2.2). We greatly overestimated mean total tree biomass in the BP ecozone because these differences were -60 and -50%. For the TS ecozone in Québec and Manitoba, which corresponds to less intensively sampled northern regions (hatched areas), total tree biomass was largely overestimated, mostly in Québec, due to the high genus-specific biomass of the *Picea* PFT (Figure 2.4b). In this ecozone, relative differences with GLAS-based estimates ranged from 1.3% in the west to 63.6% in the east, whereas it was only 1.6% in comparison with NFI-based estimates (Table 2.2). Greater relative differences were observed in the HP ecozone (Table 2.2), where we overestimated total tree biomass for grid cells in which edaphic limits were not too restrictive and where vegetation could establish (Figure 2.4a). This overestimation was mainly due to the high biomass of the *Picea* and *Populus* PFTs

(Figure 2.4b). Despite local-scale overestimates, the range of genus-specific biomass variability in the *Abies* and *Populus* PFTs was well captured.

1.3.2 Fire history simulated by LPJ-LMfire

1.3.2.1 Fire activity

In the "Climate+only" experiment, simulated burn rates displayed multi-decadal variation over the 20th century, mostly in Manitoba and Ontario (Figure 2.5a). The high fire activity that was reported for the 1910-1930 period was followed by a decrease in fire activity until the 1970s, and then increased to levels similar to those of the early 20th century (Figure 2.5a). Since the 1970s, annual burn rates have increased in central Manitoba and western Ontario and in the south-central area of Québec (Figure 2.5a). Episodes of successive years of intense fire activity have occurred in 1908-1910, 1919-1923, 1995-1998, and 2002-2007 (Figure S2.5A in Supplement S2.6). A similar temporal pattern of annual burn rates between 1901 and 2012 was reported in the "Climate-only" experiment, but with lower annual burn rates (Figure S2.7 in Supplement S2.6).

The simulated fire season was not stationary: a fire seasonality index (FSI) was computed as the percentage of difference between spring and summer total burned areas (Figure S2.5B in Supplement S2.6) and varied between 0.17 and 83%. The period extending from the end of the 1960s to end of the 1990s corresponds to a period during which several years of high FSI were observed compared with the entire time series. A FSI greater than 50% was calculated for 1968, 1977, 1980, and 1993 (Figure S2.5B in Supplement S2.6). May and June were consistently the spring months with the largest burned areas, while summer months recorded fewer and fewer burned areas over the course of the 20th century.

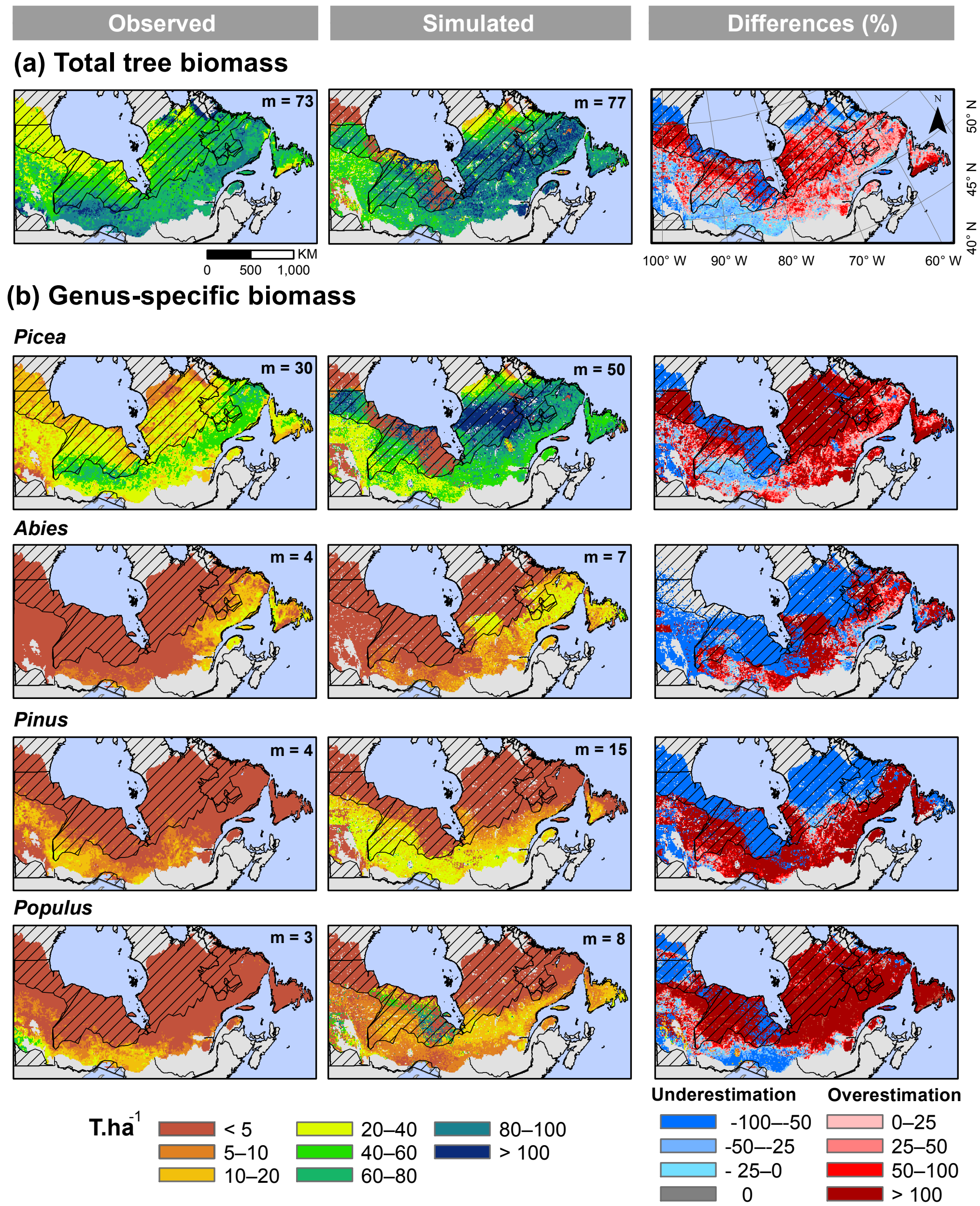

Figure 2.4. Observed, LPJ-LMfire simulated in the "Climate+only" experiment, and differences (%) in (a) mean total aboveground biomass and (b) genus-specific aboveground biomass (T ha^{-1}) between 2000 and 2006 across eastern boreal Canada. The observed aboveground biomass maps across Canada were predicted and validated with photo-plot information in the southern areas (non-hatched areas) and data published by Beaudoin et al. (2014). Median (m) aboveground biomass values are also indicated for each map; these were calculated for the non-hatched areas at a 10 km resolution.

Table 2.2. LPJ-LMfire vs. Margolis et al. (2015) mean total aboveground biomass estimates (with standard deviations) between 2000 and 2006 across five ecozones in eastern boreal Canada. The Boreal Shield ecozone was divided into three ecoregions (ecozone subdivisions) for comparison.

Zones	Ecozones	Ecoregions	Mean total aboveground biomass (T ha^{-1})			
			LPJ-LMfire	GLAS	NFI	kNN
North	Taiga Shield East	-	72.8 (30.0)	44.5	54.8	39.8
	Taiga Shield West	-	38.6 (33.2)	38.1		25
	Hudson Plain	-	59.0 (43.1)	26.1	24.4	37.2
South	Boreal Shield	Eastern Canadian forests	88.7 (17.7)	67.9	81.4	64.7
		Central Canadian Boreal Shield forests	78.8 (17.3)	68.4		67.8
		Midwestern Canadian Shield forests	57.6 (15.1)	56.4		52.8
	Boreal Plain	-	31.9 (23.5)	64.0	79.9	55.5

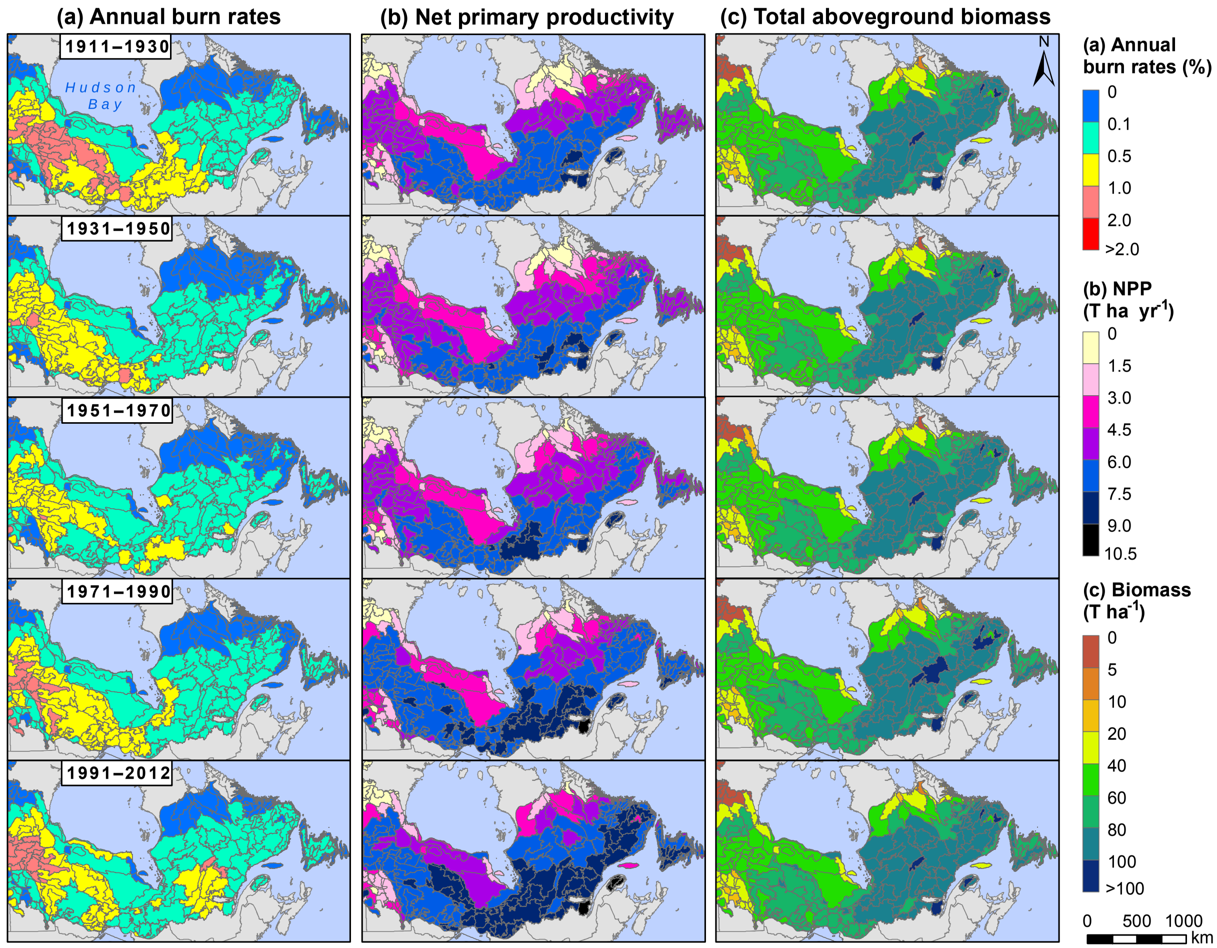

Figure 2.5. (a) LPJ-LMfire-simulated (a) annual burn rates (%), (b) net primary productivity (T ha^{-1} yr^{-1}), and (c) total aboveground biomass (T ha^{-1}) across eastern boreal Canada for five periods between 1911 and 2012.

1.3.2.2 Fuels

For the "Climate + CO_2" experiment, the simulated annual NPP averaged over the entire study region and the whole period was 5.4 T ha^{-1}, with a minimum of 4.2 T ha^{-1} in 1907 and a maximum of 7.1 T ha^{-1} in 2003 (Figure 2.5b). Both sequential t-test analysis and temporal time series showed that NPP has increased since the 1970s (Figure 2.6a and b), mostly in southern areas of Québec and in eastern Ontario (Figure 2.5b). This constant increase in NPP since the 1970s was not observed in Manitoba and western Ontario, where a significant increase in annual burn rates was observed (Figure 2.5a). Some regions in south-central Ontario showed a decline in NPP during the early 20th century, and the same trend has been observed in south-central Québec since the 1980s. The proportion of cells recording a decline in NPP was particularly noteworthy in 2004 and 2006 (Figure 2.6a and b). Differences in NPP between the simulated "Climate + CO_2" and "Climate-only" experiments highlighted that annual simulated NPP, averaged over the whole area, was positively correlated with annual atmospheric CO_2 concentration (r^2 = 0.767, P < 0.001). Mean percentage of increase in NPP that was incurred by rising CO_2 concentration for our five time periods was 2.7, 5.5, 8.9, 16.7, and 27.6% (Figure S2.6 in Supplement S2.7), while it was 18% for the entire period. An even larger effect of CO_2 fertilization was simulated in the extreme southern and northern parts of the study region (Figure S2.6C in Supplement S2.7).

Mean total aboveground biomass averaged 66.4 T ha^{-1} in eastern boreal Canada over the 1901-2012 period. Mean total aboveground biomass decreased slightly from the beginning of the 20th century until the 1930s and then increased until 1995, after which it reached a stable level (Figure 2.5c). Periods of total aboveground biomass loss that were recorded at the beginning of the 20th century correspond to high fire activity, as previously mentioned (Figure 2.5a). Sequential t-test analysis of total aboveground biomass time series showed that biomass increase and reduction followed the same trends that were observed for growth releases and declines, respectively, until the year 2000 (Figure 2.6c and d). Genus-specific aboveground biomass of the *Picea*, *Pinus*, and *Populus* PFTs showed the same increasing trends over the past century, whereas *Abies* PFT aboveground biomass decreased until the year 1960, before regaining the value it had at the beginning of the 20th century (Figure S2.8A in Supplement S2.8). The strongest variation in total aboveground biomass occurred for the *Picea* PFT; it varied from a minimum of 27.8 T ha^{-1} in 1910 to a maximum of 36.7 T ha^{-1} in 2003 (Figure S2.8A in Supplement S2.8). Conversely, genus-specific aboveground biomass of *Abies*, *Pinus*, and *Populus* PFTs varied by less than 1, 2, and 3 T ha^{-1} , respectively, over the same period (Figure S2.8A in Supplement S2.8). The ratio of mean genus-specific aboveground biomass in the recent 1991-2012 period, when compared with the past period of 1911-1930, was 1.23, 1.04, 1.13, and 1.31 for the *Picea*, *Abies*, *Pinus*, and *Populus* PFTs, respectively. The highest ratios for each PFT were found in the northern areas (Figure S2.8B in Supplement S2.8).

1.4 Discussion

1.4.1 Agreements and disagreements in fire activity and forest growth

We used LPJ-LMfire, which was driven by gridded climatology, atmospheric CO_2 concentration, and an estimate of lightning strike density to study the pyrogeography of eastern Canada's boreal forest. Compared with the previous modelling efforts that had been conducted by Pfeiffer et al. (2013) using the original LPJ-LMfire model, the results that are reported here show substantial improvement in the capacity of the DGVM to simulate fire ignition in the Canadian boreal forest. The use of a high-quality lightning strike data set instead of the low-resolution LIS/OTD global data set that was used by Pfeiffer et al. (2013) allowed us to capture the spatial gradient of fire activity in a substantially better manner (Baker et al., 2016). The results confirmed that fire in the study area is strongly ignition limited, while most fire models have simply assumed that fire would always occur under appropriate weather and fuel conditions, e.g. SIMFIRE

(Hantson et al., 2016). LPJ-LMfire simulations confirmed the necessity of simulating fire in a model as the product of the probabilities that are associated with fuel, moisture and ignition.

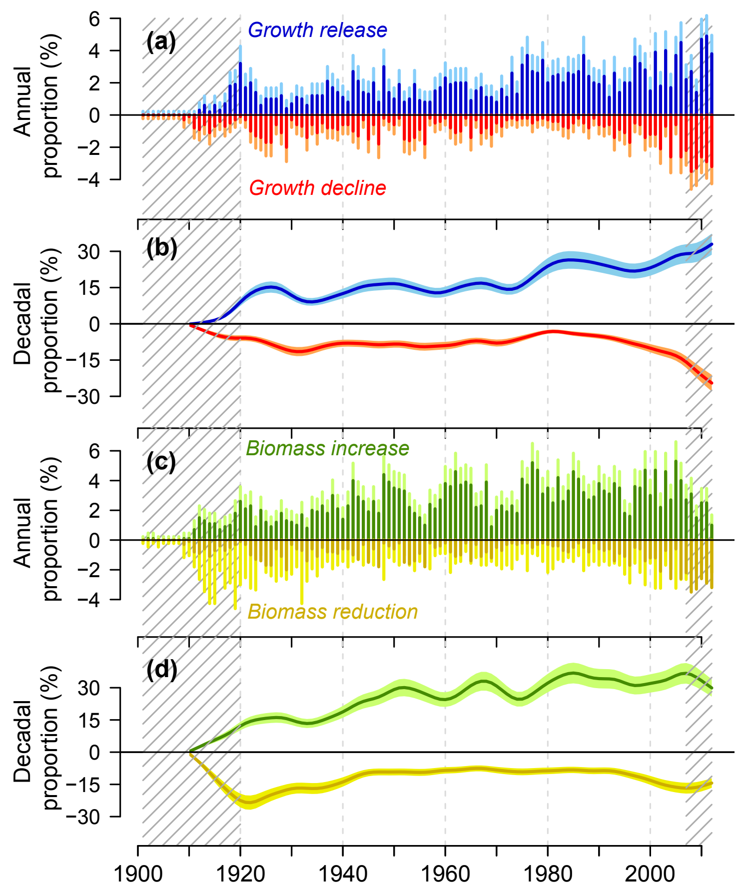

Figure 2.6. (a) Annual and (b) decadal (smoothed over 10-year sums) proportions of cells showing a significant decline or release in net primary productivity (NPP) with 90% confidence intervals (error bars) computed using Bayes method. (c) Annual and (d) decadal (smoothed over 10-year sums) proportions of cells showing a significant reduction or increase in biomass total aboveground with 90% confidence intervals (error bars) computed using the same method.

Interannual variation in lightning strike density was more faithfully reproduced when weighting the mean flash climatology with the CAPE variable to predict lightning-induced fire ignitions and their variability (Peterson et al., 2010). However, this variation is still constrained by the short temporal depth of the years of record in the CLDN lightning strike data set (Orville et al., 2002; Kochtubajda and Burrows, 2010). Synchronicity in major fire activity years across provinces (e.g. 1961, 2005, 2007) was consistent with several studies on fire history, suggesting that changes in forest fire activity have been observed jointly over vast areas since the 1900s (e.g. Bergeron et al., 2004a; Macias Fauria and Johnson, 2008).

Annual burn rates (recent and historical) were underestimated in many areas of northern Québec. It appears that the simulation could not capture the expression of a climate type that is encountered in the Clay Belt of northwestern Québec, where periodic drought is known to occur. This may likely reflect some limitation that is imposed by the low density of weather stations north of 49° N. The lack of station replication can create excessively smoothed climate records, thereby reducing the possibility of correctly emulating the relationship between climate and forest fire activity during extreme drought and fire years (Girardin et al., 2006b, 2009; Xiao and Zhuang, 2007). For example, 1989 is known as a drought year, which was induced by changes in atmospheric circulation that were at the origin of numerous large fires (> 50000 ha) in Manitoba and Québec (Figure S2.4 in Supplement S2.5; Goetz et al., 2006; Xiao and Zhuang, 2007). Other large fires exceeding 50000 ha were observed in northern Québec in 1983 and 2002 (Figure S2.4 in Supplement S2.5). However, these extreme weather conditions were not reproduced in our input data set and, consequently, the model could not simulate these very large fires. These underestimates may also result, in part, from the lack of lightning strike records in these northernmost regions, which prevents fire ignition from being simulated there. Polarity or energy of lightning was not taken into account in our simulations. Positive lightning strikes (transfers of positive charges to the ground) mainly occur in the north and correspond to 10% of all lightning strikes (Morissette and Gauthier, 2008), with the remaining lightning strikes being negative. Positive lightning strikes correspond to an exchange of energy between the highest part of the clouds and the soil, while negative lightning strikes are triggered in a lower part of the clouds. For this reason, positive lightning strikes are more likely to start fires because they carry higher energy owing to the greater travelling distance between the clouds and the soil (Flannigan and Wotton, 1991). As previously mentioned, the number of lightning sensors in northern regions (hatched areas in Figure 2.4) is also limited (Orville et al., 2011), leading to a decrease in detection efficiency at these latitudes (Morissette and Gauthier, 2008). Thus, 10% of positive lightning strikes are not appropriately captured and, consequently, the probability of fire ignition is also likely to be underestimated in these areas. Underestimation of fire activity in northern areas had consequences for the simulation results. Amongst other things, simulated tree mortality was underestimated and, hence, biomass proliferated (as can be noted in Figure 2.4b with the *Picea* PFT).

1.4.2 History of fire in the eastern boreal forest of Canada described by LPJ-LMfire

Based upon the above preliminary agreement and despite some disagreements, the temporal patterns of annual burn rates that were simulated by LPJ-LMfire were strongly consistent with the forest fire histories that have been reconstructed in many studies (e.g. Stocks et al., 2003; Bergeron et al., 2004b; Girardin et al., 2006a). Multidecadal temporal changes in annual burn rates reflect the underlying influence of climate variability and extreme fire weather (Macias Fauria and Johnson, 2008; Girardin et al., 2009); these multidecadal temporal changes were well represented in the input climate data sets. An increase in temperatures and stability in precipitation between 1916 and 1924 (Figure S2.9 in Supplement S2.9) could be at the origin of a high frequency of fire occurrence during those years, marking a pause in the decline of fire activity that had been observed since the 1850s (Bergeron et al., 2004b). Advection of humid air masses over eastern Canada between 1940 and 1970 contributed to the creation of moister conditions, which can lessen the capacity of a fire to spread after a lightning-induced fire ignition (Macias Fauria and Johnson, 2008). Both interannual variation and unsynchronized trends in climatic variables may have brought about changes in fire activity and could have affected the fire season, as it is proposed to have occurred over millennial timescales during the Holocene (Ali et al., 2012). For example, during the years 1977 and 1980, an increase in spring temperatures was observed, whereas spring precipitation decreased, which resulted in the total areas that were burned in spring being 50% greater than in summer (Figure S2.9 in Supplement S2.9).

Correlations between simulated and observed provincial annual burn rates were slightly higher than what has typically been encountered in past studies of fireclimate relationships over the region (e.g. Girardin et al., 2004, 2006a, 2009). For example, Girardin et al. (2009) reported that about 35% of the variance in the annual areas that were burned in the provinces of Ontario and Québec was explained by summer moisture availability. In our modelling experiment, we obtained values between 41 and 50% for these same provinces, without empirical adjustments (e.g. through regression analysis). The improvements that were made here reinforce the idea that aside from "top-down" climate control on fire activity, other factors such as lightning, fuel availability, and composition can influence fire statistics (Podur et al., 2002). This highlights the necessity of reconstructing fire history in a complex system that is related to climate and vegetation by taking into account several feedbacks (Hantson et al., 2016).

LPJ-LMfire simulations provide evidence for the combined influence of fuel conditions and ignition sources on fire within our study area. Indeed, an increase in precipitation around the 1930s constrained fire activity, despite a very high lightning strike density (Figure S2.9 in Supplement S2.9). Conversely, at the end of the century, an increase in lightning strike density and a drier climate (Figure S2.9 in Supplement S2.9) resulted in an increase in annual burn rates. The seasons during which precipitation events and lightning ignitions occur were also found to be important. Notably, LPJ-LMfire did not simulate the core of the fire season between June and August when the highest density of lightning strikes takes place (Morissette and Gauthier, 2008). This phenomenon finds an explanation in that heavy and intense rain events occurring later during the summer decrease the probability of starting fires; weather becomes less conducive to fire due to higher amounts of precipitation between July and September in comparison with April and June. That being said, our simulation was biased with regard to the onset of fire seasonality. LPJ-LMfire simulated the core of the fire season earlier than what is actually observed. LM-fire excludes fire ignition when snow cover is present (Pfeiffer et al., 2013). However, detailed investigations at the grid-cell level in our study area revealed that the fire danger index, which was calculated by the LMfire module, was high as soon as all snow had melted in May and June. This index estimates the probability that an ignition event will start a fire, depending upon both fuel moisture and fire weather conditions (Thonicke et al., 2010). As suggested by Pfeiffer et al. (2013), LPJ-LMfire simulates a very quick drying-out of soils in spring when the snow cover has disappeared or snowmelt has occurred prematurely. This phenomenon may be the reason why it simulated fire season onset earlier than what is observed in Canada's eastern boreal forest.

CO_2-induced enhancement of NPP (Norby et al., 2005; Huang et al., 2007) was clearly emulated in LPJ-LMfire. Our simulated 18% growth enhancement, with a 32.5% increase in CO_2 concentration between 1901 and 2012, was higher than the 15 and 14% growth increases that have been proposed by Hickler et al. (2008) and Girardin et al. (2011), respectively. LPJ-LMfire is highly sensitive to atmospheric CO_2 concentration and interpreting its impacts must be carried out with caution (Girardin et al., 2011). That being said, our results suggest that CO_2-induced enhancement of forest productivity can be offset by fires and climate, which is consistent with the results of Hayes et al. (2011) and Kelly et al. (2016). Despite strong CO_2-induced enhancement of forest productivity in LPJ-LMfire, the total amount of aboveground biomass and forest composition did not change significantly during the course of the simulation period. The CO_2-induced enhancement of NPP had a positive influence on annual burn rates by increasing the availability of fuel. Under very dry conditions, such as in 1971-1990 and 1991-2012, an increase in fire activity led to a decrease in growth and biomass. Drier conditions during the past few decades provided indications for an increase in growth decline events and in biomass reduction related to an increase in fire activity. A similar trend in such conditions was observed around the 1920s, but the range of these negative events during the past decades exceeds the historical range of variability recorded by the simulated forest. Fires had a non-negligible influence on the state of the boreal forest in eastern Canada, especially during the last few decades, but our results also confirm the relative influence of climate alone on the forest in northern regions. Indeed, in northern areas in Québec and Manitoba, biomass has not significantly increased, despite a very strong effect of CO_2-induced enhancement (Figure S2.6 in Supplement S2.7). We hypothesize that with ongoing global warming, growth decline events could increase substantially, given that the positive effect of CO_2 concentration on the growth of forests may not be strong enough to compensate for the loss of biomass to fires and climate change (Kurz et al., 2008), which could lead to the opening up of landscapes.

1.4.3 Uncertainties and future perspectives

The present study demonstrated that LPJ-LMfire is generally able to capture fire history and forest growth trends in the eastern boreal forest of Canada. However, several uncertainties persist. First, forest establishment and the start of growth during the spin-up phase were simulated using a detrended version of modern climate, as is usually performed in DGVM runs (Prentice et al., 2011; Pfeiffer et al., 2013; Yue et al., 2016; Knorr et al., 2016). This initial condition assumes that past relationships between climate, fire, and vegetation have been stationary through time and that variability in modern climate is representative of all variability that has been recorded over the past 1200 years (time of spin-up phase + 112 years of simulation). However, it has been increasingly recognized that such an assumption is invalid and that modern observations are not a good analogue for prehistoric variability (Kelly et al., 2016; Hudiburg et al., 2017). For example, fire activity over much of the Holocene was greater in terms of frequency and fire size than the current levels across broad areas of eastern Canada (Girardin et al., 2013b; Remy et al., 2017). It is likely that not accounting for such variability may introduce biases in forest productivity dynamics and levels, more specifically on soil carbon dynamics (Hudiburg et al., 2017). This may be less problematic when studying fire and forest dynamics over the last century because the mean age of the major part of eastern boreal forest is less than 100 years (Bergeron et al., 2002).

The non-negligible influence of forest composition on fire regimes (Hély et al., 2001) is limited in the model to the representation of three needleleaf PFTs and one broadleaf PFT. Improving LPJ-LMfire's representation of biodiversity with further broadleaf PFT genera could counterbalance or offset overestimates of fire activity in southern areas since these species are less flammable than needleleaf species. Similarly, improving LPJ-LMfire parametrization to account for mosses could reduce overestimation of the quantity of fuel available in northern areas. In the Clay Belt, the poor drainage conditions induced by the presence of an impermeable clay substrate, flat topography, and a cold climate facilitate the accumulation of thick layers of organic soil, an edaphic process that is referred to as paludification (Fenton et al., 2006). Once Sphagnum species increase on the forest floor, the depth of burn varies only slightly in response to changes in weather conditions, owing to very low fluctuations in the degree of water saturation of the organic layer (Fenton et al., 2006).

In the present study, simulations are limited by the relatively low accuracy of soil attributes in databases for Canada's boreal forest (Hengl et al., 2014). The input data set of soil attributes that was used in our simulations tended to underestimate clay and sand percentages in our study area when compared to point observations (Figure S2.10 in Supplement S2.10). These effects add up to other weaknesses in physiological constraints, such as cold climate not being sufficiently restrictive and allowing *Picea* to become overly abundant in the simulation runs. While a previous study showed that the abundance of *Picea* decreases with latitude in the tundra region and is coupled with the occurrence of dwarf shrubs in the *Ericaceae* and herbs (Gajewski et al., 1993), such species were not parametrized in the current version of LPJ-LMfire due to a lack of information on their physiological and biogeographical preferences. Future research could incorporate recently developed parameterizations for boreal shrubs and non-vascular plants into LPJ-LMfire (Druel, 2017; Druel et al., 2017).

Forest stand structure and successional dynamics (age classes), together with processes leading to the formation of peatlands, are not included in the present version of LPJ-LMfire. However, all of these aspects are important determinants of fire ignition and propagation under a given climate (Hély et al., 2001) and can also influence the distinction between crown and surface fires, which affect tree mortality differently (Hély et al., 2003; Yue et al., 2016). Moreover, LPJ-LMfire, like most DGVMs, does not consider constraints on species migrations, phenotypic plasticity, and local adaptation of species (Morin and Thuiller, 2009). The simulation results are surely optimistic in terms of the capacity of southern species to colonize newly available areas in northern regions as the climate warms. As previously mentioned by Morin and Thuiller (2009), species colonization in northern regions could be limited by forest attributes, such as fragmented landscapes or high competition levels from existing species, or through migrational lag (Epstein et al., 2007).

Wildland fires are the most important natural disturbances in Canada's eastern boreal forest, but non-fire and human disturbances also have considerable effects (Price et al., 2013) and may influence fire activity trajectories indirectly. Integrating a range of forest disturbances into a DGVM could improve the accuracy of forecasting and modelling climate change effects on Canadas eastern boreal forest. For instance, insect damage (MacLean, 2016) and outbreaks of eastern spruce budworm (*Choristoneura fumiferana*) in particular (Zhang et al., 2014; James et al., 2017) represent significant forest disturbances by the way they temporarily alter forest structure by affecting specific tree growth, tree survival, regeneration, and succession. These disturbances can also have an important impact on fire activity by modifying fuel distribution and connectivity (James et al., 2017). Additionally, successive fires that take place over a short period before the trees have attained maturity can lead to complete regeneration failure (Girard et al., 2008). Such events in young, unproductive stands can also lead to modified forest composition (Girard et al., 2008) and could exert a strong feedback on ecosystem structure by generating changes in temporal fire patterns over long timescales. Finally, the effects of human activities, such as forest management and active fire suppression efforts, on the composition and distribution of forest fuels were not implemented in the present LPJ-LMfire simulations. Nonetheless, the strong correlation between our simulated annual burn rates and observed data suggests that active fire suppression efforts and forest management since about the 1950s (Le Goff et al., 2008; Lefort et al., 2003) have not contributed much to shifting fire behaviour trajectories in our study region, which admittedly has very low densities of both population and infrastructure in comparison with other populated areas such as in the United States (e.g. Syphard et al., 2017).

1.5 Conclusion

In this study, we used LPJ-LMfire to simulate fire activity from 1901 to 2012 in Canada's eastern boreal forest, at a 10 km resolution. LPJ-LMfire was parametrized for the predominant forest tree genera that are present in our study region, i.e *Picea*, *Abies*, *Pinus*, and *Populus*. The predictive skill of the model to simulate fire activity was determined by comparing our model simulations with published data. LPJ-LMfire was able to simulate interannual- to decadal-scale fire variability from the beginning of the 20th century. However, the low density of weather stations in northern areas likely limited the models ability to capture some extreme fire years. Our study highlights the importance of changes in climate variables on multi-decadal and annual timescales in strongly controlling spatiotemporal patterns of fire that were simulated by LPJ-LMfire. Spatiotemporal patterns were well captured, based upon our climate data inputs. Despite an overarching CO_2-induced enhancement of NPP in LPJ-LMfire, aboveground biomass was relatively stable because of the compensatory effects of increasing fire activity. This study helps reduce uncertainties in our knowledge regarding fire patterns in the recent past and confirms that fires have been a dominant driver of boreal forest in eastern Canada during the last century. We further provide a new tool to refine predictions of future fire risks and effects of ongoing climate change in these forests to better inform management and improve risk mitigation strategies.

Code availability: The source code of LPJ-LMfire is available at https://github.com/ARVE-Research/LPJ-LMfire/tree/v1.3 (Kaplan et al., 2018).

Acknowledgments

This study was made possible thanks to the financial support provided by the European IRSES NEWFOREST project, the Forest Complexity Modelling (FCM) program, and the NSERC Strategic and Discovery programs. Jed Kaplan was supported by the European Research Council (COEVOLVE 313797). This research was conducted as part of the International Associated Laboratory MONTABOR (LIA France, Canada) and the International Research Group on Cold Forests. We thank Melanie Desrochers and Xiao Jing Guo for their help with mapping and computation for this project. We also thank Daniel Stubbs from Calcul Québec and Compute Canada for help with the Fortran language and server space facilities for running LPJ-LMfire. We also thank William F. J. Parsons and Isabelle Lamarre for English language editing of a previous version of the paper and the two anonymous reviewers for comments on an earlier version.

References

Ali, A. A., Blarquez, O., Girardin, M. P., Hely, C., Tinquaut, F., El Guellab, A., Valsecchi, V., Terrier, A., Bremond, L., Genries, A., Gauthier, S., and Bergeron, Y. (2012). Control of the multimillennial wildfire size in boreal North America by spring climatic conditions. *Proceedings of the National Academy of Sciences USA*, 109(51):20966–20970, doi:10.1073/pnas.1203467109.

Ali, A. A., Carcaillet, C., and Bergeron, Y. (2009). Long-term fire frequency variability in the eastern Canadian boreal forest: the influences of climate vs. local factors. *Global Change Biology*, 15(5):1230–1241, doi:10.1111/j.1365-2486.2009.01842.x.

Andrews, P. L., Bevins, C. D., and Seli, R. C. (2008). BehavePlus fire modeling system, version 4.0: User's Guide, available from: https://www.fs.fed.us/rm/pubs/rmrs_gtr106.pdf.

Baker, D. J., Hartley, A. J., Butchart, S. H. M., and Willis, S. G. (2016). Choice of baseline climate data impacts projected species' responses to climate change. *Global Change Biology*, 22(7):2392–2404, doi:10.1111/gcb.13273.

Beaudoin, A., Bernier, P., Guindon, L., Villemaire, P., Guo, X., Stinson, G., Bergeron, T., Magnussen, S., and Hall, R. (2014). Mapping attributes of Canada's forests at moderate resolution through *k*NN and MODIS imagery. *Canadian Journal of Forest Research*, 44(5):521–532, doi:10.1139/cjfr-2013-0401.

Beauregard, F. and de Blois, S. (2014). Beyond a climate-centric view of plant distribution: edaphic variables add value to distribution models. *PLoS one*, 9(3):e92642, doi:10.1371/journal.pone.0092642.

Bergeron, Y., Chen, H. Y., Kenkel, N. C., Leduc, A. L., and Macdonald, S. E. (2014). Boreal mixedwood stand dynamics: ecological processes underlying multiple pathways. *The Forestry Chronicle*, 90(2):202–213, doi:10.5558/tfc2014-039.

Bergeron, Y., Flannigan, M., Gauthier, S., Leduc, A., and Lefort, P. (2004a). Past, current and future fire frequency in the Canadian boreal forest: implications for sustainable forest management. *AMBIO: A Journal of the Human Environment*, 33(6):356–360, doi:10.1579/0044-7447-33.6.356.

Bergeron, Y., Gauthier, S., Flannigan, M., and Kafka, V. (2004b). Fire regimes at the transition between mixedwood and coniferous boreal forest in northwestern Quebec. *Ecology*, 85(7):1916–1932, doi:10.1890/02-0716.

Bergeron, Y., Leduc, A., Harvey, B. D., and Gauthier, S. (2002). Natural fire regime: A guide for sustainable management of the Canadian boreal forest. *Silva Fennica*, 36(1):81–95.

Bergeron, Y., Richard, P. J., Carcaillet, C., Gauthier, S., Flannigan, M., and Prairie, Y. (1998). Variability in fire frequency and forest composition in Canada's southeastern boreal forest: a challenge for sustainable forest management. *Conservation Ecology*, 2(2).

Bond, T. C., Streets, D. G., Yarber, K. F., Nelson, S. M., Woo, J.-H., and Klimont, Z. (2004). A technology-based global inventory of black and organic carbon emissions from combustion. *Journal of Geophysical Research: Atmospheres*, 109:D14203, doi:10.1029/2003JD003697.

Boulanger, Y., Gauthier, S., and Burton, P. J. (2014). A refinement of models projecting future Canadian fire regimes using homogeneous fire regime zones. *Canadian Journal of Forest Research*, 44(4):365–376, doi:10.1139/cjfr-2013-0372.

Boulanger, Y., Gauthier, S., Burton, P. J., and Vaillancourt, M.-A. (2012). An alternative fire regime zonation for Canada. *International Journal of Wildland Fire*, 21(8):1052–1064.

Brandt, J. P. (2009). The extent of the North American boreal zone. *Environmental Reviews*, 17:101–161, doi:10.1139/A09-004.

Canadian Council of Forest Ministers (2017). National Forestry Database. Forest Fire Statistics by Province/Territory/Agency, 1990-2016, available from: http://nfdp.ccfm.org/data/compendium/ html/comp_31e.html,.

Canadian Forest Service (2016). National Fire Database - Agency Fire Data. Natural Resources Canada, Canadian Forest Service, Northern Forestry Centre, Edmonton, Alberta, available from: http://cwfis.cfs.nrcan.gc.ca/ah/nfdb.

Compo, G. P., Whitaker, J. S., Sardeshmukh, P. D., Matsui, N., Allan, R. J., Yin, X., Gleason, B. E., Vose, R. S., Rutledge, G., Bessemoulin, P., Brönnimann, S., Brunet, M., Crouthamel, R. I., Grant, A. N., Groisman, P. Y., Jones, P. D., Kruk, M. C., Kruger, A. C., Marshall, G. J., Maugeri, M., Mok, H. Y., Nordli, Ø., Ross, T. F., Trigo, R. M., Wang, X. L., Woodruff, S. D., and Worley, S. J. (2011). The Twentieth Century Reanalysis Project. *Quarterly Journal of the Royal Meteorological Society*, 137(654):1–28, doi:10.1002/qj.776.

Danneyrolles, V., Arseneault, D., and Bergeron, Y. (2016). Pre-industrial landscape composition patterns and post-industrial changes at the temperate-boreal forest interface in western Quebec, Canada. *Journal of Vegetation Science*, 27(3):470–481, doi:10.1111/jvs.12373.

Druel, A. (2017). *Modélisation de la végétation boréale et de sa dynamique dans le modèle de surface continentale ORCHIDEE*. PhD thesis, Université Grenoble Alpes, Grenoble.

Druel, A., Peylin, P., Krinner, G., Ciais, P., Viovy, N., Peregon, A., Bastrikov, V., Kosykh, N., and Mironycheva-Tokareva, N. (2017). Towards a more detailed representation of high-latitude vegetation in the global land surface model ORCHIDEE (ORC-HL-VEGv1.0). *Geosci. Model Dev. Discuss.*, 2017:1–51, doi:10.5194/gmd-2017-65.

Ecological Stratification Working Group (1996). A national ecological framework for Canada, available from: http://sis.agr.gc.ca/cansis/references/1996ew_a.html. Technical report.

Environment Canada (2013). National Climate Data and Information Archive, available from: http://climate.weatheroffice.gc.ca/.

Epstein, H. E., Yu, Q., Kaplan, J. O., and Lischke, H. (2007). Simulating future changes in arctic and subarctic vegetation. *Computing in Science & Engineering*, 9(4):12–23, doi:10.1109/MCSE.2007.84.

Erni, S., Arseneault, D., Parisien, M.-A., and Bégin, Y. (2017). Spatial and temporal dimensions of fire activity in the fire-prone eastern Canadian taiga. *Global Change Biology*, 23(3):1152–1166, doi:10.1111/gcb.13461.

Fenton, N., Légaré, S., Bergeron, Y., Paré, D., and others (2006). Soil oxygen within boreal forests across an age gradient. *Canadian journal of soil science*, 86(1):1–10, doi:10.4141/S05-004.

Flannigan, M., Stocks, B., Turetsky, M., and Wotton, M. (2009). Impacts of climate change on fire activity and fire management in the circumboreal forest. *Global Change Biology*, 15(3):549–560, doi:10.1111/j.1365-2486.2008.01660.x.

Flannigan, M. D., Stocks, B. J., and Wotton, B. M. (2000). Climate change and forest fires. *Science of the total environment*, 262(3):221–229, doi:10.1016/S0048-9697(00)00524-6.

Flannigan, M. D. and Wotton, B. M. (1991). Lightning-ignited forest fires in northwestern Ontario. *Canadian Journal of Forest Research*, 21(3):277–287, doi:10.1139/x91-035.

Flannigan, M. D., Wotton, B. M., Marshall, G. A., Groot, W. J. d., Johnston, J., Jurko, N., and Cantin, A. S. (2016). Fuel moisture sensitivity to temperature and precipitation: climate change implications. *Climatic Change*, 134(1-2):59–71, doi:10.1007/s10584-015-1521-0.

Gajewski, K., Payette, S., and Ritchie, J. C. (1993). Holocene vegetation history at the boreal-forest-shrub-tundra transition in North-Western Quebec. *Journal of Ecology*, 81(3):433–443.

Gauthier, S., Bergeron, Y., and Simon, J.-P. (1996). Effects of fire regime on the serotiny level of jack pine. *The Journal of Ecology*, 84(4):539, doi:10.2307/2261476.

Gauthier, S., Bernier, P., Burton, P. J., Edwards, J., Isaac, K., Isabel, N., Jayen, K., Le Goff, H., and Nelson, E. A. (2014). Climate change vulnerability and adaptation in the managed Canadian boreal forest. *Environmental Reviews*, 22(3):256–285, doi:10.1139/er-2013-0064.

Gewehr, S., Drobyshev, I., Berninger, F., and Bergeron, Y. (2014). Soil characteristics mediate the distribution and response of boreal trees to climatic variability. *Canadian Journal of Forest Research*, 44(5):487–498, doi:10.1139/cjfr-2013-0481.

Girard, F., Payette, S., and Gagnon, R. (2008). Rapid expansion of lichen woodlands within the closed-crown boreal forest zone over the last 50 years caused by stand disturbances in eastern Canada. *Journal of Biogeography*, 35(3):529–537, doi:10.1111/j.1365-2699.2007.01816.x.

Girardin, M. P., Ali, A. A., Carcaillet, C., Blarquez, O., Hély, C., Terrier, A., Genries, A., and Bergeron, Y. (2013a). Vegetation limits the impact of a warm climate on boreal wildfires. *The New Phytologist*, 199(4):1001–1011, doi:10.1111/nph.12322.

Girardin, M. P., Ali, A. A., Carcaillet, C., Gauthier, S., Hély, C., Le Goff, H., Terrier, A., and Bergeron, Y. (2013b). Fire in managed forests of eastern Canada: Risks and options. *Forest ecology and management*, 294:238–249, doi:10.1016/j.foreco.2012.07.005.

Girardin, M. P., Ali, A. A., Carcaillet, C., Mudelsee, M., Drobyshev, I., Hély, C., and Bergeron, Y. (2009). Heterogeneous response of circumboreal wildfire risk to climate change since the early 1900s. *Global Change Biology*, 15(11):2751–2769, doi:10.1111/j.1365-2486.2009.01869.x.

Girardin, M. P., Bergeron, Y., Tardif, J. C., Gauthier, S., Flannigan, M. D., and Mudelsee, M. (2006a). A 229-year dendroclimatic-inferred record of forest fire activity for the Boreal Shield of Canada. *International Journal of Wildland Fire*, 15(3):375–388, doi:10.1071/WF05065.

Girardin, M. P., Bernier, P. Y., Raulier, F., Tardif, J. C., Conciatori, F., and Guo, X. J. (2011). Testing for a CO_2 fertilization effect on growth of Canadian boreal forests. *Journal of Geophysical Research: Biogeosciences*, 116:G01012, doi:10.1029/2010JG001287.

Girardin, M. P. and Mudelsee, M. (2008). Past and future changes in Canadian boreal wildfire activity. *Ecological Applications*, 18(2):391–406, doi:10.1890/07-0747.1.

Girardin, M.-P., Tardif, J., and Bergeron, Y. (2001). Gradient analysis of Larix laricina dominated wetlands in Canada's southeastern boreal forest. *Canadian Journal of Botany*, 79(4):444–456, doi:10.1139/b01-023.

Girardin, M.-P., Tardif, J., Flannigan, M. D., Wotton, B. M., and Bergeron, Y. (2004). Trends and periodicities in the Canadian Drought Code and their relationships with atmospheric circulation for the southern Canadian boreal forest. *Canadian Journal of Forest Research*, 34(1):103–119, doi:10.1139/x03-195.

Girardin, M. P., Tardif, J. C., Flannigan, M. D., and Bergeron, Y. (2006b). Forest fire-conducive drought variability in the southern Canadian boreal forest and associated climatology inferred from tree rings. *Canadian Water Resources Journal*, 31(4):275–296, doi:10.4296/cwrj3104275.

Girardin, M. P. and Terrier, A. (2015). Mitigating risks of future wildfires by management of the forest composition: an analysis of the offsetting potential through boreal Canada. *Climatic Change*, 130(4):587–601, doi:10.1007/s10584-015-1373-7.

Goetz, S. J., Fiske, G. J., and Bunn, A. G. (2006). Using satellite time-series data sets to analyze fire disturbance and forest recovery across Canada. *Remote Sensing of Environment*, 101(3):352–365, doi:10.1016/j.rse.2006.01.011.

Hantson, S., Arneth, A., Harrison, S. P., Kelley, D. I., Prentice, I. C., Rabin, S. S., Archibald, S., Mouillot, F., Arnold, S. R., Artaxo, P., and others (2016). The status and challenge of global fire modelling. *Biogeosciences*, 13(11):3359–3375, doi:10.5194/bg-13-3359-2016.

Hayes, D. J., McGuire, A. D., Kicklighter, D. W., Gurney, K. R., Burnside, T. J., and Melillo, J. M. (2011). Is the northern high-latitude land-based CO_2 sink weakening? *Global Biogeochemical Cycles*, 25(3):GB3018, doi:10.1029/2010GB003813.

Hély, C., Flannigan, M., and Bergeron, Y. (2003). Modeling tree mortality following wildfire in the southeastern Canadian mixed-wood boreal forest. *Forest Science*, 49(4):566–576.

Hély, C., Flannigan, M., Bergeron, Y., and McRae, D. (2001). Role of vegetation and weather on fire behavior in the Canadian mixedwood boreal forest using two fire behavior prediction systems. *Canadian Journal of Forest Research*, 31(3):430–441, doi:10.1139/cjfr-31-3-430.

Hengl, T., de Jesus, J. M., MacMillan, R. A., Batjes, N. H., Heuvelink, G. B. M., Ribeiro, E., Samuel-Rosa, A., Kempen, B., Leenaars, J. G. B., Walsh, M. G., and Gonzalez, M. R. (2014). SoilGrids1km – Global soil information based on automated mapping. *PLoS One*, 9(8):e105992, doi:10.1371/journal.pone.0105992.

Héon, J., Arseneault, D., and Parisien, M.-A. (2014). Resistance of the boreal forest to high burn rates. *Proceedings of the National Academy of Sciences*, 111(38):13888–13893, doi:10.1073/pnas.1409316111.

Hessl, A. E. (2011). Pathways for climate change effects on fire: Models, data, and uncertainties. *Progress in Physical Geography*, 35(3):393–407, doi:10.1177/0309133311407654.

Hickler, T., Smith, B., Prentice, I. C., Mjöfors, K., Miller, P., Arneth, A., and Sykes, M. T. (2008). CO_2 fertilization in temperate FACE experiments not representative of boreal and tropical forests. *Global Change Biology*, 14(7):1531–1542, doi:10.1111/j.1365-2486.2008.01598.x.

Huang, J.-G., Bergeron, Y., Denneler, B., Berninger, F., and Tardif, J. (2007). Response of forest trees to increased atmospheric CO_2. *Critical Reviews in Plant Sciences*, 26(5-6):265–283, doi:10.1080/07352680701626978.

Hudiburg, T. W., Higuera, P. E., and Hicke, J. A. (2017). Fire-regime variability impacts forest carbon dynamics for centuries to millennia. *Biogeosciences Discussions*, pages 1–24, doi:10.5194/bg-2017-42.

IPCC (2013). *Climate Change 2013 - The Physical Science Basis: Working Group I Contribution to the Fifth Assessment Report of the Intergovernmental Panel on Climate Change*. [Stocker, T.F., D. Qin, G.-K. Plattner, M. Tignor, S.K. Allen, J. Boschung, A. Nauels, Y. Xia, V. Bex and P.M. Midgley (eds.)]. Cambridge University Press, Cambridge, United Kingdom and New York, NY, USA., Cambridge.

James, P. M. A., Robert, L.-E., Wotton, B. M., Martell, D. L., and Fleming, R. A. (2017). Lagged cumulative spruce budworm defoliation affects the risk of fire ignition in Ontario, Canada. *Ecological Applications*, 27(2):532–544, doi:10.1002/eap.1463.

Kaplan, J. O., Pfeiffer, M., and Chaste, E. (2018). ARVE-Research/LPJ-LMfire: LPJ-LMfire (version v1.3), Zenodo. doi:10.5281/zenodo.1184589.

Kasischke, E. S. and Turetsky, M. R. (2006). Recent changes in the fire regime across the North American boreal regionâSpatial and temporal patterns of burning across Canada and Alaska. *Geophysical Research Letters*, 33(9):L09703, doi:10.1029/2006GL025677.

Keeley, J. E. (2009). Fire intensity, fire severity and burn severity: a brief review and suggested usage. *International Journal of Wildland Fire*, 18(1):116, doi:10.1071/WF07049.

Keeling, R., Piper, S., Bollenbacher, A., and Walker, J. (2009). Atmospheric CO_2 records from sites in the SIO air sampling network. In Trends: A Compendium of Data on Global Change. Carbon Dioxide Information Analysis Center, Oak Ridge National Laboratory, U.S. Department of Energy, Oak Ridge, TN, U.S.A. Technical report, doi:10.3334/CDIAC/atg.035.

Kelly, R., Genet, H., McGuire, A. D., and Hu, F. S. (2016). Palaeodata-informed modelling of large carbon losses from recent burning of boreal forests. *Nature Climate Change*, 6(1):79–82, doi:10.1038/nclimate2832.

Knorr, W., Arneth, A., and Jiang, L. (2016). Demographic controls of future global fire risk. *Nature Climate Change*, 6(8):781–785, doi:10.1038/nclimate2999.

Kochtubajda, B. and Burrows, W. (2010). Cloud-to-Ground Lightning in Canada: 1999-2008. volume 12, pages 1280, available from: http://adsabs.harvard.edu/abs/2010EGUGA12.1280K.

Kurz, W. A., Shaw, C. H., Boisvenue, C., Stinson, G., Metsaranta, J., Leckie, D., Dyk, A., Smyth, C., and Neilson, E. T. (2013). Carbon in Canada's boreal forest - A synthesis. *Environmental Reviews*, 21(4):260–292, doi:10.1139/er-2013-0041.

Kurz, W. A., Stinson, G., and Rampley, G. (2008). Could increased boreal forest ecosystem productivity offset carbon losses from increased disturbances? *Philosophical Transactions of the Royal Society of London B: Biological Sciences*, 363(1501):2259–2268, doi:10.1098/rstb.2007.2198.

Le Goff, H., Girardin, M. P., Flannigan, M. D., and Bergeron, Y. (2008). Dendroclimatic inference of wildfire activity in quebec over the 20th century and implications for natural disturbance-based forest management at the northern limit of the commercial forest. *International journal of wildland fire*, 17(3):348–362, doi:10.1071/WF07080.

Lefort, P., Gauthier, S., and Bergeron, Y. (2003). The influence of fire weather and land use on the fire activity of the Lake Abitibi area, eastern Canada. *Forest Science*, 49(4):509–521.

Macias Fauria, M. and Johnson, E. A. (2008). Climate and wildfires in the North American boreal forest. *Philosophical Transactions of the Royal Society B: Biological Sciences*, 363(1501):2315–2327, doi:10.1098/rstb.2007.2202.

MacLean, D. A. (2016). Impacts of insect outbreaks on tree mortality, productivity, and stand development. *The Canadian Entomologist*, 148:S138 – S159, doi:10.4039/tce.2015.24.

Mansuy, N., Gauthier, S., Robitaille, A., and Bergeron, Y. (2011). The effects of surficial deposit-drainage combinations on spatial variations of fire cycles in the boreal forest of eastern Canada. *International Journal of Wildland Fire*, 19(8):1083–1098, doi:10.1071/WF09144.

Margolis, H. A., Nelson, R. F., Montesano, P. M., Beaudoin, A., Sun, G., Andersen, H.-E., and Wulder, M. A. (2015). Combining satellite lidar, airborne lidar, and ground plots to estimate the amount and distribution of aboveground biomass in the boreal forest of North America 1. *Canadian Journal of Forest Research*, 45(7):838–855, doi:10.1139/cjfr-2015-0006.

Messaoud, Y., Bergeron, Y., and Asselin, H. (2007). Reproductive potential of balsam fir (*Abies balsamea*), white spruce (*Picea glauca*), and black spruce (*P. mariana*) at the ecotone between mixedwood and coniferous forests in the boreal zone of western Quebec. *American Journal of Botany*, 94(5):746–754, doi:10.3732/ajb.94.5.746.

Molinari, C., Lehsten, V., Bradshaw, R. H. W., Power, M. J., Harmand, P., Arneth, A., Kaplan, J. O., Vannière, B., and Sykes, M. T. (2013). Exploring potential drivers of European biomass burning over the Holocene: a data-model analysis. *Global Ecology and Biogeography*, 22(12):1248–1260, doi:10.1111/geb.12090.

Morin, X. and Thuiller, W. (2009). Comparing niche- and process-based models to reduce prediction uncertainty in species range shifts under climate change. *Ecology*, 90(5):1301–1313, doi:10.1890/08-0134.1.

Morissette, J. and Gauthier, S. (2008). Study of cloud-to-ground lightning in Quebec: 1996-2005. *Atmosphere-ocean*, 46(4):443–454, doi:10.3137/AO919.2008.

Moritz, M. A., Krawchuk, M. A., and Parisien, M.-A. (2010). Pyrogeography: Understanding the ecological niche of fire. *PAGES News*, 18:83–85.

Natural Resources Canada (2007). Geobase - Canadian digital elevation data, geogratis, available from: http://ftp.geogratis.gc.ca/pub/nrcan_rncan/elevation/canada3d/.

Natural Resources Canada (2010). Geobase - National hydro network, geogratis, available from: http://ftp.geogratis.gc.ca/pub/nrcan_rncan/vector/geobase_nhn_rhn/.

Natural Resources Canada (2017). The State of Canada's Forests. Annual Report 2017, available from http://cfs.nrcan.gc.ca/pubwarehouse/pdfs/38871.pdf.

Norby, R. J., DeLucia, E. H., Gielen, B., Calfapietra, C., Giardina, C. P., King, J. S., Ledford, J., McCarthy, H. R., Moore, D. J. P., Ceulemans, R., De Angelis, P., Finzi, A. C., Karnosky, D. F., Kubiske, M. E., Lukac, M., Pregitzer, K. S., Scarascia-Mugnozza, G. E., Schlesinger, W. H., and Oren, R. (2005). Forest response to elevated CO_2 is conserved across a broad range of productivity. *Proceedings of the National Academy of Sciences, USA*, 102(50):18052–18056, doi:10.1073/pnas.0509478102.

Orville, R. E., Huffines, G. R., Burrows, W. R., and Cummins, K. L. (2011). The North American Lightning Detection Network (NALDN) - Analysis of flash data: 2001â09. *Monthly Weather Review*, 139(5):1305–1322, doi:10.1175/2010MWR3452.1.

Orville, R. E., Huffines, G. R., Burrows, W. R., Holle, R. L., and Cummins, K. L. (2002). The North American lightning detection network (NALDN) - First results: 1998â2000. *Monthly Weather Review*, 130(8):2098–2109, doi:10.1175/1520-0493(2002)130<2098:TNALDN>2.0.CO;2.

Pan, Y., Birdsey, R. A., Fang, J., Houghton, R., Kauppi, P. E., Kurz, W. A., Phillips, O. L., Shvidenko, A., Lewis, S. L., Canadell, J. G., Ciais, P., Jackson, R. B., Pacala, S. W., McGuire, A. D., Piao, S., Rautiainen, A., Sitch, S., and Hayes, D. (2011). A large and persistent carbon sink in the world's forests. *Science*, 333(6045):988–993, doi:10.1126/science.1201609.

Payette, S., Filion, L., and Delwaide, A. (2008). Spatially explicit fire-climate history of the boreal forest-tundra (Eastern Canada) over the last 2000 years. *Philosophical Transactions of the Royal Society of London B: Biological Sciences*, 363(1501):2299–2314, doi:10.1098/rstb.2007.2201.

Peterson, D., Wang, J., Ichoku, C., and Remer, L. A. (2010). Effects of lightning and other meteorological factors on fire activity in the North American boreal forest: implications for fire weather forecasting. *Atmospheric Chemistry and Physics*, 10(14):6873–6888, doi:10.5194/acp-10-6873-2010.

Pfeiffer, M., Spessa, A., and Kaplan, J. O. (2013). A model for global biomass burning in preindustrial time: LPJ-LMfire (v1. 0). *Geoscientific Model Development*, 6(3):643–685, doi:10.5194/gmd-6-643-2013.

Podur, J., Martell, D. L., and Knight, K. (2002). Statistical quality control analysis of forest fire activity in Canada. *Canadian Journal of Forest Research*, 32(2):195–205, doi:10.1139/X01-183.

Portier, J., Gauthier, S., Leduc, A., Arseneault, D., and Bergeron, Y. (2016). Fire regime along latitudinal gradients of continuous to discontinuous coniferous boreal forests in eastern Canada. *Forests*, 7(10):211, doi:10.3390/f7100211.

Prentice, I. C., Kelley, D. I., Foster, P. N., Friedlingstein, P., Harrison, S. P., and Bartlein, P. J. (2011). Modeling fire and the terrestrial carbon balance. *Global Biogeochemical Cycles*, 25(3):GB3005, doi:10.1029/2010GB003906.

Price, D. T., Alfaro, R. I., Brown, K. J., Flannigan, M. D., Fleming, R. A., Hogg, E. H., Girardin, M. P., Lakusta, T., Johnston, M., McKenney, D. W., Pedlar, J. H., Stratton, T., Sturrock, R. N., Thompson, I. D., Trofymow, J. A., and Venier, L. A. (2013). Anticipating the consequences of climate change for Canada's boreal forest ecosystems. *Environmental Reviews*, 21(4):322–365, doi:10.1139/er-2013-0042.

Rabin, S. S., Melton, J. R., Lasslop, G., Bachelet, D., Forrest, M., Hantson, S., Kaplan, J. O., Li, F., Mangeon, S., Ward, D. S., Yue, C., Arora, V. K., Hickler, T., Kloster, S., Knorr, W., Nieradzik, L., Spessa, A., Folberth, G. A., Sheehan, T., Voulgarakis, A., Kelley, D. I., Prentice, I. C., Sitch, S., Harrison, S., and Arneth, A. (2017). The Fire Modeling Intercomparison Project (FireMIP), phase 1: experimental and analytical protocols with detailed model descriptions. *Geosci. Model Dev.*, 10(3):1175–1197, doi:10.5194/gmd-10-1175-2017.

Régnière, J., Saint-Amant, R., and Béchard, A. (2014). *BioSIM 10 - Guide de l'utilisateur.* Number LAU-X-137. Ressour. Nat. Can., Serv. can. for., Cent. for. Laurentides, Québec (Québec), available from: http://www.cfs.nrcan.gc.ca/publications/?id=34817.

Remy, C. C., Hély, C., Blarquez, O., Magnan, G., Bergeron, Y., Lavoie, M., and Ali, A. A. (2017). Different regional climatic drivers of Holocene large wildfires in boreal forests of northeastern America. *Environmental Research Letters*, 12(3):035005, doi:10.1088/1748-9326/aa5aff.

Rodionov, S. N. (2004). A sequential algorithm for testing climate regime shifts. *Geophysical Research Letters*, 31(9):L09204, doi:10.1029/2004GL019448.

Rodionov, S. N. (2006). Use of prewhitening in climate regime shift detection. *Geophysical Research Letters*, 33(12):L12707, doi:10.1029/2006GL025904.

Rogers, B. M., Randerson, J. T., and Bonan, G. B. (2013). High-latitude cooling associated with landscape changes from North American boreal forest fires. *Biogeosciences*, 10(2):699–718, doi:10.5194/bg-10-699-2013.

Romps, D. M., Seeley, J. T., Vollaro, D., and Molinari, J. (2014). Projected increase in lightning strikes in the United States due to global warming. *Science*, 346(6211):851–854, doi:10.1126/science.1259100.

Rothermel, R. C. (1972). A Mathematical Model for Predicting Fire Spread in Wildland Fuels, Intermountain Forest and Range Experiment Station, Forest Service, U.S. Department of Agriculture, Ogden, Utah. Technical report.

Shorohova, E., Kneeshaw, D., Kuuluvainen, T., and Gauthier, S. (2011). Variability and dynamics of old-growth forests in the circumboreal zone: implications for conservation, restoration and management. *Silva Fennica*, 45(5):785–806.

Sitch, S., Smith, B., Prentice, I. C., Arneth, A., Bondeau, A., Cramer, W., Kaplan, J. O., Levis, S., Lucht, W., Sykes, M. T., Thonicke, K., and Venevsky, S. (2003). Evaluation of ecosystem dynamics, plant geography and terrestrial carbon cycling in the LPJ dynamic global vegetation model. *Global Change Biology*, 9(2):161–185, doi:10.1046/j.1365-2486.2003.00569.x.

Smith, B., Prentice, I. C., and Sykes, M. T. (2001). Representation of vegetation dynamics in the modelling of terrestrial ecosystems: comparing two contrasting approaches within European climate space. *Global Ecology and Biogeography*, 10(6):621–637, doi:10.1046/j.1466-822X.2001.t01-1-00256.x.

Stocks, B. J., Mason, J. A., Todd, J. B., Bosch, E. M., Wotton, B. M., Amiro, B. D., Flannigan, M. D., Hirsch, K. G., Logan, K. A., Martell, D. L., and Skinner, W. R. (2003). Large forest fires in Canada, 1959-1997. *Journal of Geophysical Research: Atmospheres*, 107(D1):8149, doi:10.1029/2001JD000484.

Syphard, A. D., Keeley, J. E., Pfaff, A. H., and Ferschweiler, K. (2017). Human presence diminishes the importance of climate in driving fire activity across the United States. *Proceedings of the National Academy of Sciences*, 114(52):13750–13755, doi:10.1073/pnas.1713885114.

Tang, G., Beckage, B., Smith, B., and Miller, P. A. (2010). Estimating potential forest NPP, biomass and their climatic sensitivity in New England using a dynamic ecosystem model. *Ecosphere*, 1(6):1–20, doi:10.1890/ES10-00087.1.

Thonicke, K., Spessa, A., Prentice, I. C., Harrison, S. P., Dong, L., and Carmona-Moreno, C. (2010). The influence of vegetation, fire spread and fire behaviour on biomass burning and trace gas emissions: results from a process-based model. *Biogeosciences*, 7(6):1991–2011, doi:10.5194/bg-7-1991-2010.

Van Wagner, C. E. (1987). *Development and structure of the Canadian Forest Fire Weather Index System*. available from: https://cfs.nrcan.gc.ca/publications?id=19927.

Wang, X., Thompson, D. K., Marshall, G. A., Tymstra, C., Carr, R., and Flannigan, M. D. (2015). Increasing frequency of extreme fire weather in Canada with climate change. *Climatic Change*, 130(4):573–586, doi:10.1007/s10584-015-1375-5.

Xiao, J. and Zhuang, Q. (2007). Drought effects on large fire activity in Canadian and Alaskan forests. *Environmental Research Letters*, 2(4):044003, doi:10.1088/1748-9326/2/4/044003.

Yue, C., Ciais, P., Zhu, D., Wang, T., Peng, S. S., and Piao, S. L. (2016). How past fire disturbances have contributed to the current carbon balance of boreal ecosystems? *Biogeosciences Discussions*, 12:14833–14867, doi:10.5194/bgd-12-14833-2015.

Zhang, X., Lei, Y., Ma, Z., Kneeshaw, D., and Peng, C. (2014). Insect-induced tree mortality of boreal forests in eastern Canada under a changing climate. *Ecology and evolution*, 4(12):2384–2394, doi:10.1002/ece3.988.

Supplementary materials

Supplement S2.1

Reconstruction of the density of monthly lightning flashes (Lm) (n/day/km^2) from 1901 to 2012.

$$[1]\quad coef = max(\mid max(\int_t CAPEano), \mid min(\int_t CAPEano) \mid)$$

$$[2]\quad CAPEano_N = CAPEano \ / \ coef$$

$$[3]\quad Lm = \begin{cases} CLDNm * (1 + 7.5 * CAPEano_N), CAPEano_N \geq 0 \\ CLDNm * (1 + 0.1 * CAPEano_N), CAPEano_N < 0 \end{cases}$$

CAPE anomalies ($CAPEano$) correspond to monthly differences at the grid cell level at time t compared with the average of monthly CAPE from 1961 to 1990. For each grid cell, the time-series of $CAPEano$ was normalized to a range between -1 and 1 ($CAPEano_N$) by dividing $CAPEano$ by the maximum value between the absolute value of the largest positive and negative CAPE anomalies of the time-series (eq. [1] and [2]). Monthly flash density (/km^2/month) between 1901 and 2012 was calculated on the base of monthly flash climatology between 1999 and 2010 ($CLDNm$), but interannual flash variability was applied using $CAPEano_N$ and min-to-mean and max-to-mean ratios (eq. [3]). We determined min-to-mean and max-to-mean ratios (0.1 and 7.5, respectively; Figure S1B) by compiling grid cell values of the CLDN database with more than 5 years of observations in July between 1999 and 2010 across Canada within our study area (Figure S1A).

Figure S2.1. (A) Total number of monthly flashes in Canada and eastern Canada (our study area) from 1999 to 2010. (B) Box plots of minimum-to-mean and maximum-to-mean ratios for flashes in July from 1999 to 2010 based on 60,747 grid cells in Canada with more than 5 years of observations.

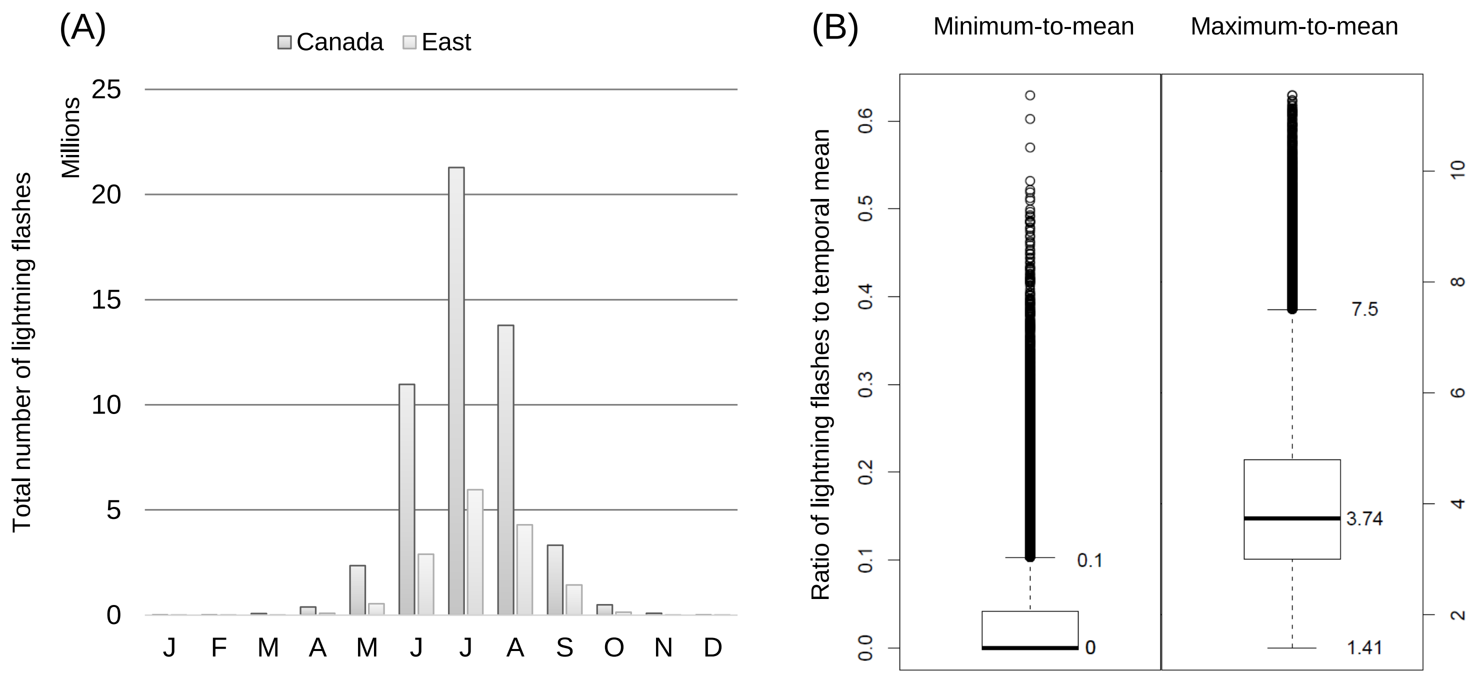

Supplement S2.2

Table S2.1. LPJ-LMfire PFT parameter values used in this study (boreal needleleaf and broadleaf tree parameters values from Pfeiffer et al. (2013) were assigned for the others parameters not presented in this table).

	Parameters	Genus-specific PFT				References
		Picea	*Abies*	*Pinus*	*Populus*	
Growth form and phenology	Fraction of roots in upper soil layer (50 cm)	0.9	0.5	0.5	0.3	Natural Resources Canada 2017 and US Forest Service
	Sapwood turnover period	20	40	20	30	
	Leaf to root ratio under non water-stressed conditions	0.190	0.165	0.165	0.14	Poorter et al. (2012)
	Broadleaf phenology ramp GDD5 requirement to grow to full-leaf canopy	800	1400	766	180	Girardin et al. (2011)
	Sapling (or grass on initialization) LAI	3.4	9.3	4.4	3.2	Calculated from Iio et al. (2014)
Bioclimatic limits and climatic preferences	Min./Max. temperature of the coldest month for establishment (°C day)	-31.65/ -6.80	-25.25/ -4.85	-29.25/ -9.15	-29.30/ 3.70	
	Min GDD5 for establishment (°C day)	300	400	550	345	Thompson et al. (1999)
	Max. temperature of the warmest month to persist (°C day)	20.70	20.65	20.60	24.85	
Individual parameters	Crown length	1	1	0.4	0.5	Derived from Groot and Schneider (2011) and Hély et al. (2003)
	Bark thickness	0.032	0.031	0.040	0.027	Andrews et al. (2008)
Fire resistance	Crown damage parameter	1	3	2	0.2	*Personal communications*

Supplement S2.3

Figure S2.2. (A) Local polynomial regression (with 95% confidence interval (CI)) between genus-specific cover percentage from Beaudoin et al. (2014) and clay percentage from Hengl et al. (2014) in eastern boreal Canada. Only grid cells with a total cover greater than 10% for the four species studied were taken into account in these analyses. (B) Clay percentage distribution in eastern boreal Canada. Each vertical red line corresponds to the upper limit of the 90% CI of the clay percentage distribution for each PFT. (C) Map of clay percentage in eastern boreal Canada with threshold of the upper limit of the 90% CI of the distribution of clay percentage for the *Abies* and *Picea* PFTs.

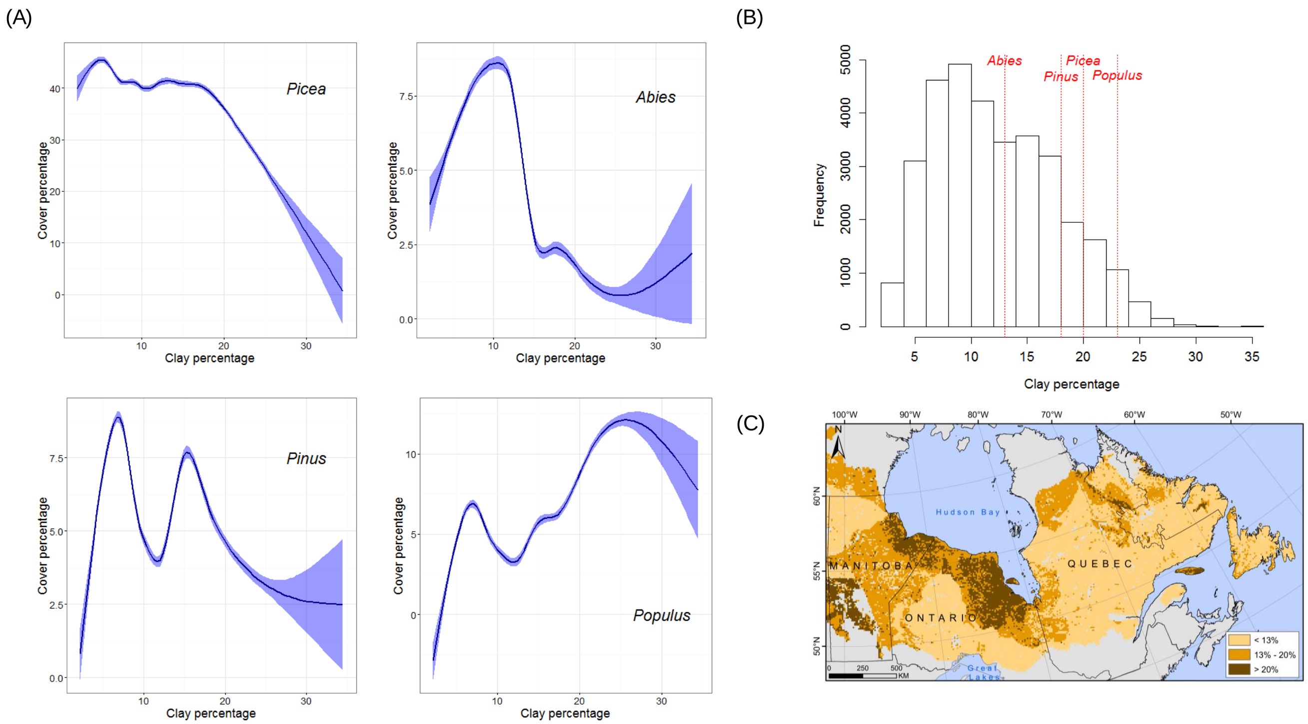

Supplement S2.4

Figure S2.3. Location of stand-replacing fire history studies in eastern Canada with correspondence ID number to Table S2.

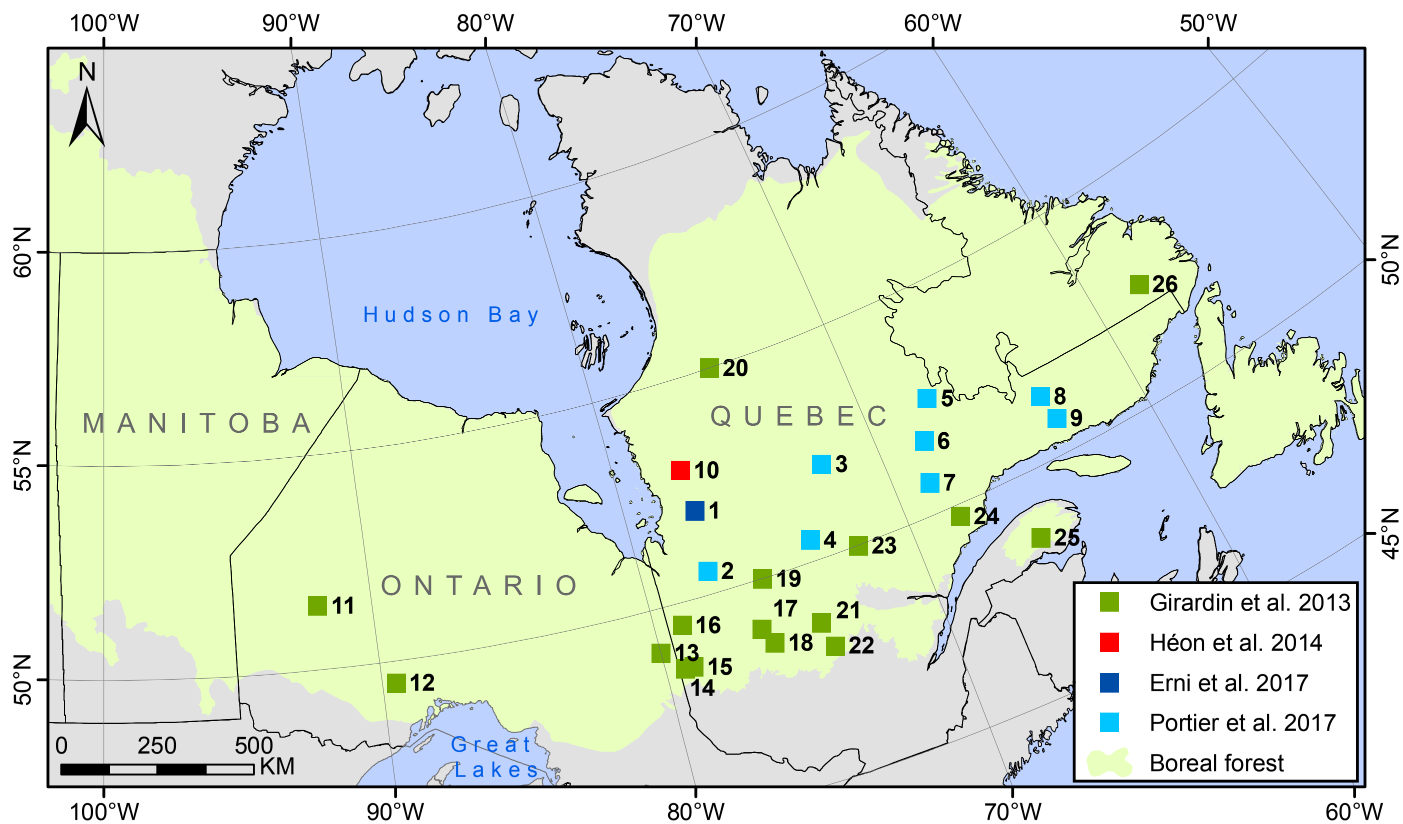

Table S2.2. Observed versus LPJ-LMfire-simulated annual burn rates (with 2.5 and 97.5 percentiles) from stand-replacing fire history studies from 1911 to 2012. Significant differences are underlined.

ID	Time	Localization		Observed	Simulated	References
1	1911-2012	A	North	4.875 (3.119-10.642)	0.384 (0.175-0.773)	Portier et al. (2016) (originated from Erni et al. (2017))
2			South	0.637 (0.410-1.030)	0.427 (0.211-0.768)	Portier et al. (2016)
3		B	North	3.190 (1.462-11.151)	0.345 (0.069-0.752)	
4			South	0.477 (0.323-0.762)	0.484 (0.231-0.879)	
5		C	North	2.859 (2.110-4.827)	0.186 (0.043-0.373)	
6			Center	0.354 (0.177-0.791)	0.199 (0.042-0.458)	
7			South	0.146 (0.070-0.326)	0.262 (0.054 0.597)	
8		D	North	1.761 (0.923-3.800)	0.163 (0.026-0.373)	
9			South	0.129 (0.052-0.386)	0.151 (0.025-0.362)	
10	1910-2013	James Bay		2.400	0.415 (0.164-0.835)	Héon et al. (2014)
11	~1870-1974	Northern Ontario		1.920	0.648 (0.335-1.164)	Girardin et al. (2013)
12	unknown -2000	Lake Nipigon		0.711	0.689 (0.379-1.116)	
13	1740-1998	LAMF		0.580	0.466 (0.000-0.855)	
14	~1750-1988	Western Quebec		0.720	0.414 (0.000-0.726)	
15	1580-2000	Western Abitibi South		0.334	0.415 (0.000-0.753)	
16	1530-1996	Western Abitibi North		0.604	0.531 (0.297-0.892)	
17	1770-1995	Eastern Abitibi		0.708	0.435 (0.226-0.746)	
18	1760-1998	Abitibi East		0.900	0.441 (0.241-0.747)	
19	1720-2000	Waswanipi		0.812	0.439 (0.238-0.788)	
20	1920-1984	Northern boreal		1.000	0.196 (0.074-0.378)	
21	1720-1998	Central Quebec 2		0.665	0.513 (0.224-1.067)	
22	1720-1998	Central Quebec		0.790	0.505 (0.192-0.930)	
23	unknown-2000	Lac-Saint-Jean		0.286	0.411 (0.093-0.791)	
24	1640-2000	North Shore		0.367	0.272 (0.048-0.555)	
25	1680-2000	Gaspésie		0.643	0.150 (0.000-0.419)	
26	1870-1975	Southeastern Labrador		0.200	0.124 (0.000-0.272)	

Supplement S2.5

Figure S2.4. Location of fires exceeding 50,000 ha in eastern Canada for three years of extreme fire activity.

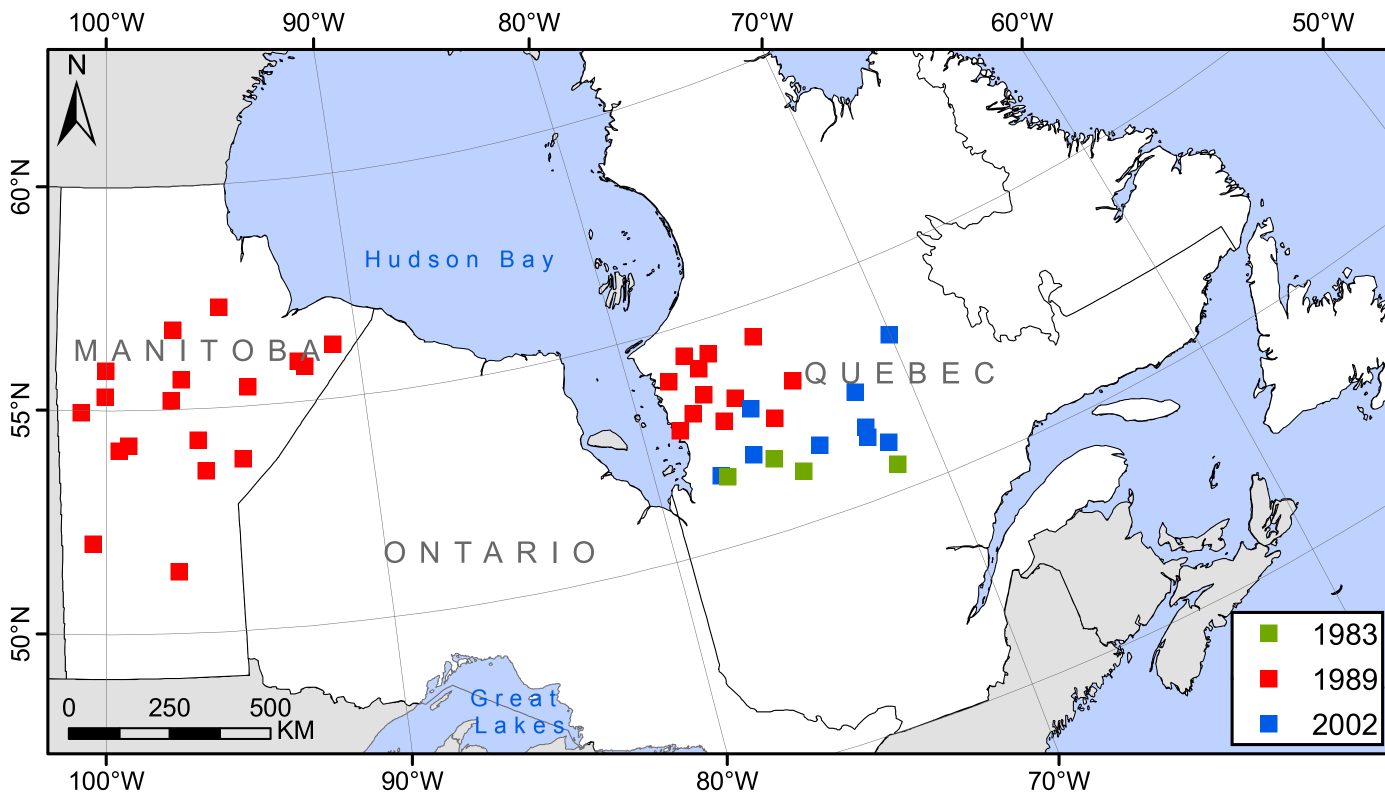

Supplement S2.6

Figure S2.5. (A) Time-series of total annual area burned from 1901 to 2012. Gray blocks correspond to periods with at least three years of annual area burned above the mean annual burn rates for the 1901-2012 period. Orange line corresponds to smoothing values using a LOESS function (span = 0.15). Black dashed line corresponds to the weighed means of the regimes obtained by the sequential application of Student's t-test. (B) Percentage of differences between spring and summer total area burned (called fire seasonality index; FSI) from 1901 to 2012. Black dashed line corresponds to FSI equal to 50%.

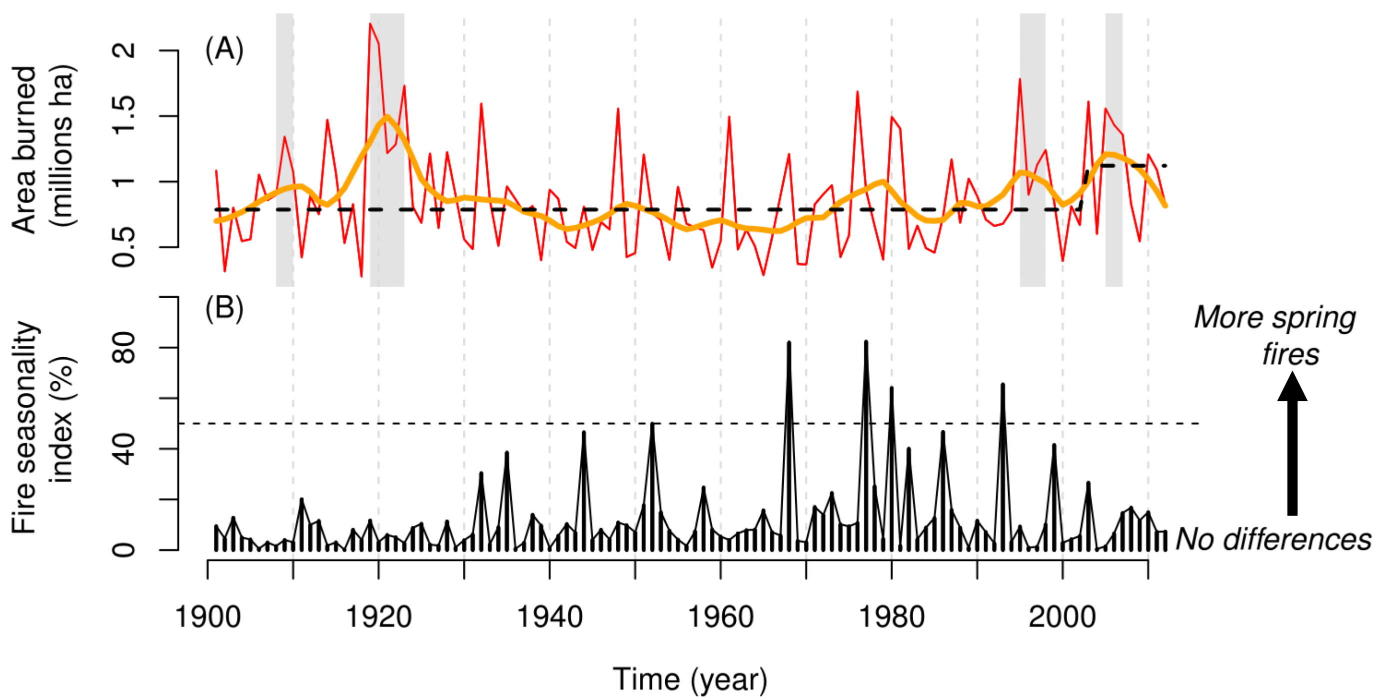

Supplement S2.7

Figure S2.6. LPJ-LMfire NPP (T/ha/yr) simulated across eastern boreal Canada with (A) "Climate + CO_2" and (B) "Climate-only" experiments through five periods from 1911 to 2012. (C) Percentage of increase in NPP due to the CO_2 effect.

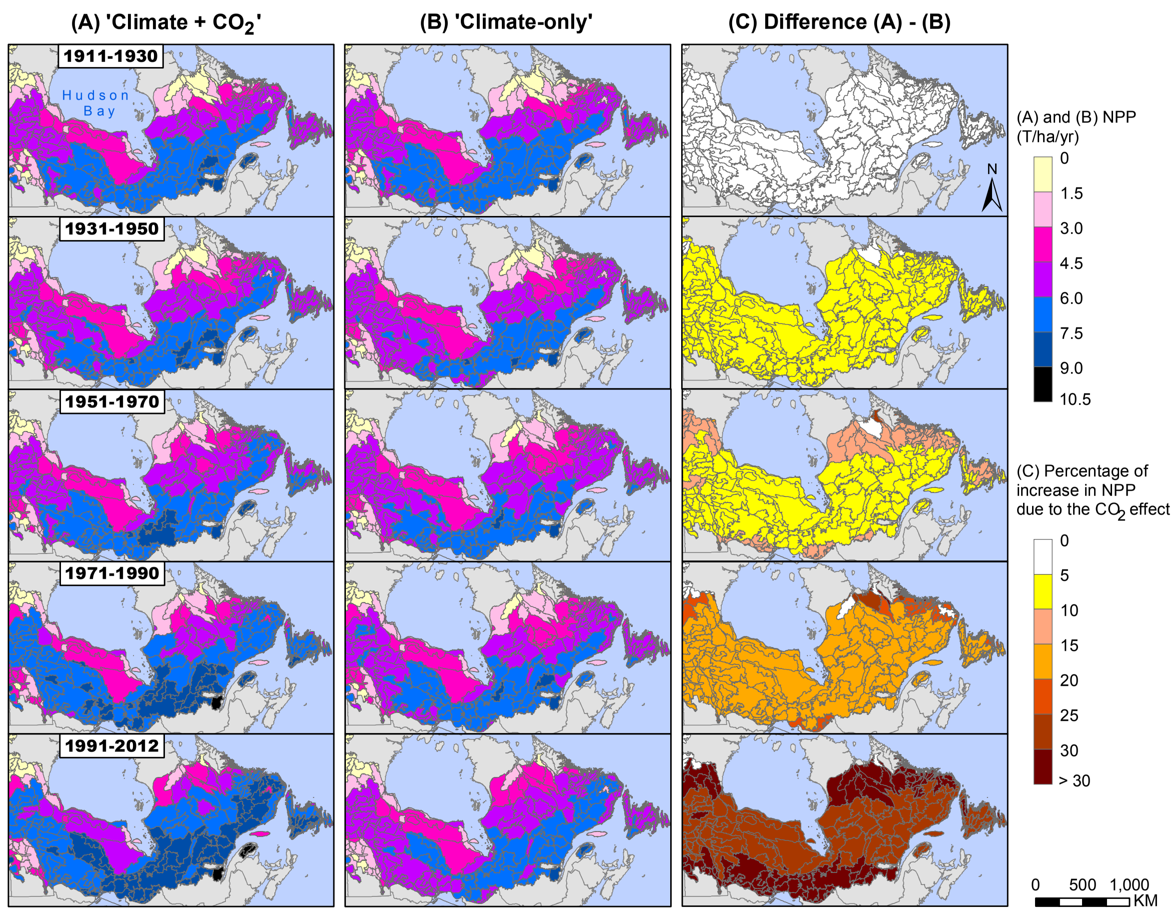

Figure S2.7. LPJ-LMfire annual burn rates (%) simulated across eastern boreal Canada with "Climate + CO_2" and "Climate-only" experiments through five periods from 1911 to 2012.

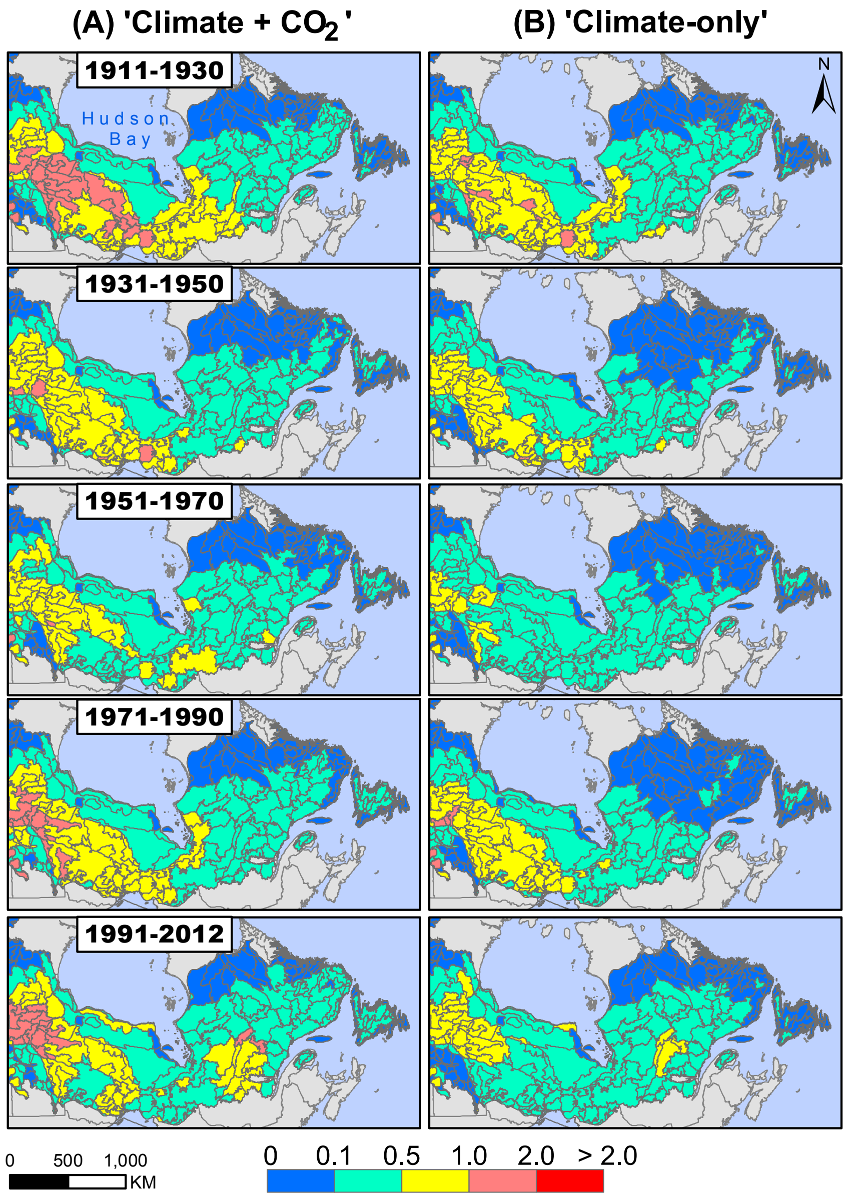

Supplement S2.8

Figure S2.8. (A) Average of cover percentage for each PFT in eastern boreal Canada from 1901 to 2012. Red line corresponds to smoothing values using a LOESS function (span = 0.15). (B) Ratio of cover percentage between a recent period (1911-1930) and a past period (1991-2012). The two periods correspond to the grey background on (A).

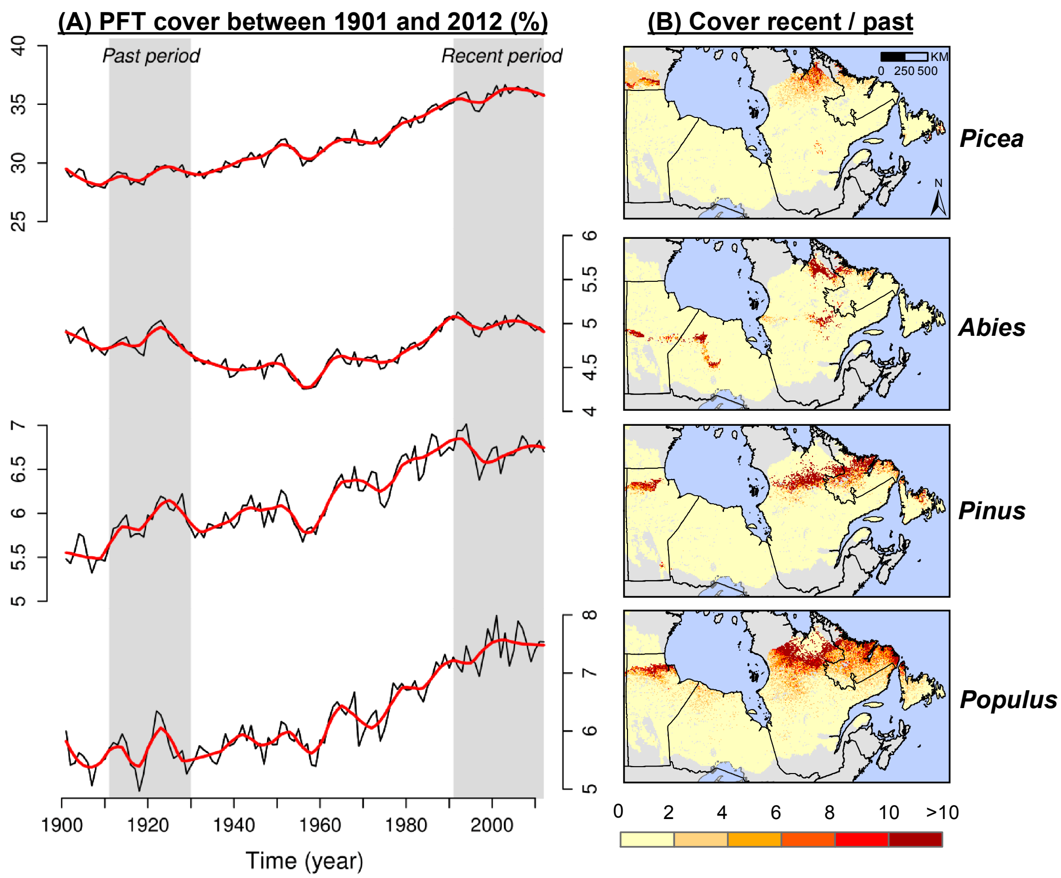

Supplement S2.9

Figure S2.9. Temporal series of (A) spring and (B) summer mean temperatures, (C) spring and (D) summer mean precipitation, and (E) mean flash density. Black dashed lines, black full lines and orange lines correspond to the mean, regression lines, and smoothing values using a LOESS function (span = 0.15), respectively, for each time-series.

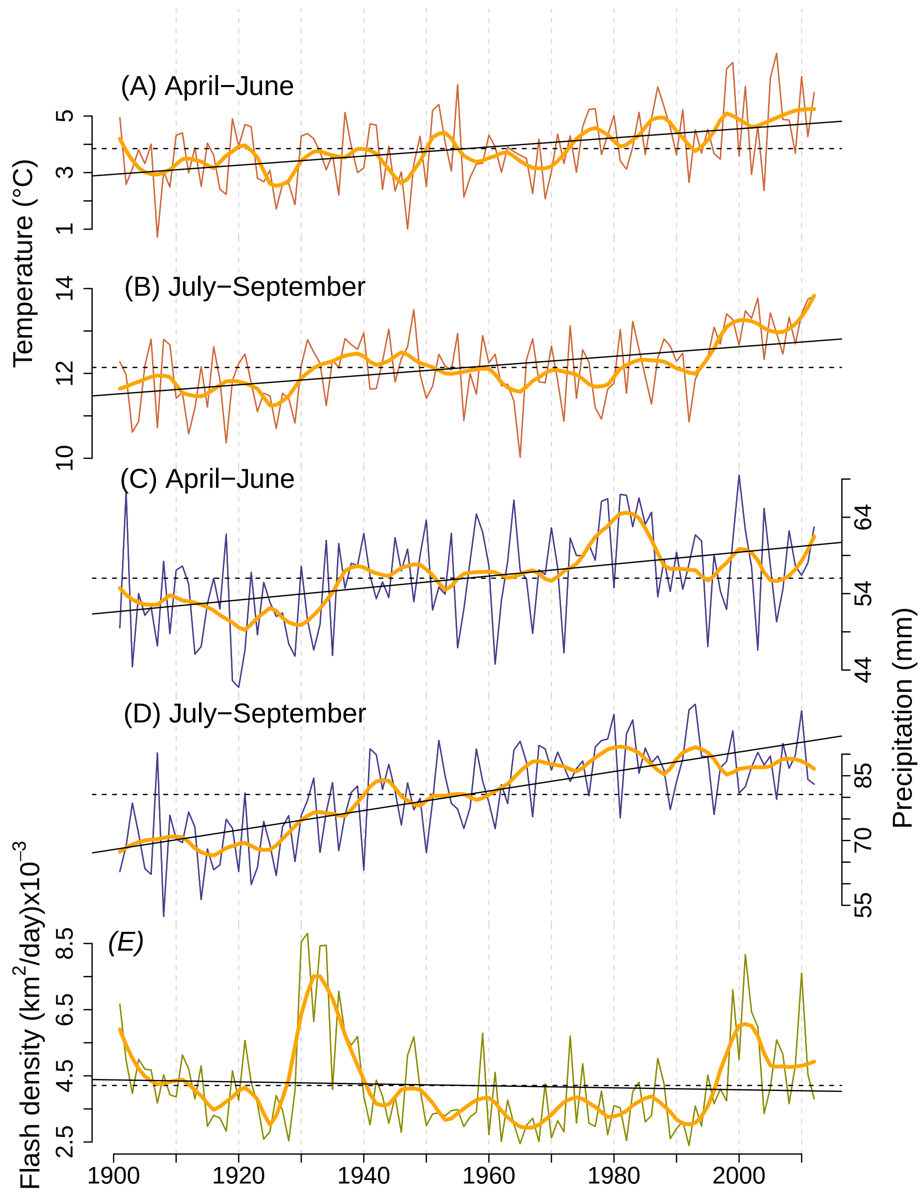

Supplement S2.10

Figure S2.10. Percentage of clay and sand in the mineral horizons across eastern boreal Canada at a 10-km resolution from (A) Hengl et al. (2014) (0-30 cm depth) and (B) Mansuy et al. (2014) (0-15 cm depth).

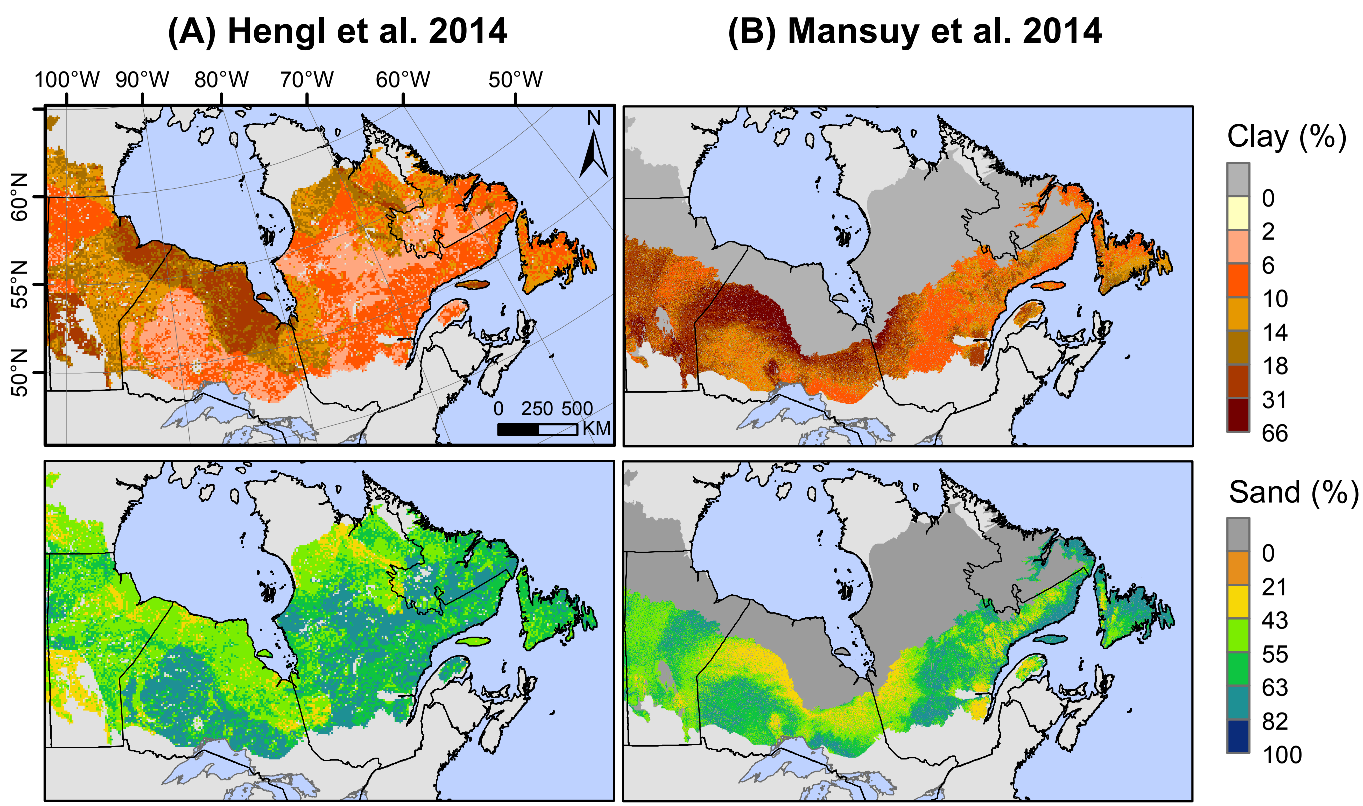

References

Andrews, P. L., Bevins, C. D., and Seli, R. C. (2008). BehavePlus fire modeling system, version 4.0: User's Guide, available from: https://www.fs.fed.us/rm/pubs/rmrs_gtr106.pdf.

Beaudoin, A., Bernier, P., Guindon, L., Villemaire, P., Guo, X., Stinson, G., Bergeron, T., Magnussen, S., and Hall, R. (2014). Mapping attributes of Canada's forests at moderate resolution through *k*NN and MODIS imagery. *Canadian Journal of Forest Research*, 44(5):521–532, doi:10.1139/cjfr-2013-0401.

Erni, S., Arseneault, D., Parisien, M.-A., and Bégin, Y. (2017). Spatial and temporal dimensions of fire activity in the fire-prone eastern Canadian taiga. *Global Change Biology*, 23(3):1152–1166, doi:10.1111/gcb.13461.

Girardin, M. P., Ali, A. A., Carcaillet, C., Gauthier, S., Hély, C., Le Goff, H., Terrier, A., and Bergeron, Y. (2013). Fire in managed forests of eastern Canada: Risks and options. *Forest ecology and management*, 294:238–249, doi:10.1016/j.foreco.2012.07.005.

Girardin, M. P., Bernier, P. Y., Raulier, F., Tardif, J. C., Conciatori, F., and Guo, X. J. (2011). Testing for a CO_2 fertilization effect on growth of Canadian boreal forests. *Journal of Geophysical Research: Biogeosciences*, 116:G01012, doi:10.1029/2010JG001287.

Groot, A. and Schneider, R. (2011). Predicting maximum branch diameter from crown dimensions, stand characteristics and tree species. *The Forestry Chronicle*, 87(4):542–551, doi:10.5558/tfc2011-053.

Hély, C., Flannigan, M., and Bergeron, Y. (2003). Modeling tree mortality following wildfire in the southeastern Canadian mixed-wood boreal forest. *Forest Science*, 49(4):566–576.

Hengl, T., de Jesus, J. M., MacMillan, R. A., Batjes, N. H., Heuvelink, G. B. M., Ribeiro, E., Samuel-Rosa, A., Kempen, B., Leenaars, J. G. B., Walsh, M. G., and Gonzalez, M. R. (2014). SoilGrids1km – Global soil information based on automated mapping. *PLoS One*, 9(8):e105992, doi:10.1371/journal.pone.0105992.

Héon, J., Arseneault, D., and Parisien, M.-A. (2014). Resistance of the boreal forest to high burn rates. *Proceedings of the National Academy of Sciences*, 111(38):13888–13893, doi:10.1073/pnas.1409316111.

Iio, A., Hikosaka, K., Anten, N. P., Nakagawa, Y., and Ito, A. (2014). Global dependence of field-observed leaf area index in woody species on climate: a systematic review. *Global Ecology and Biogeography*, 23(3):274–285, doi:10.1111/geb.12133.

Mansuy, N., Thiffault, E., Paré, D., Bernier, P., Guindon, L., Villemaire, P., Poirier, V., and Beaudoin, A. (2014). Digital mapping of soil properties in Canadian managed forests at 250 m of resolution using the k-nearest neighbor method. *Geoderma*, 235â236:59–73, doi:10.1016/j.geoderma.2014.06.032.

Pfeiffer, M., Spessa, A., and Kaplan, J. O. (2013). A model for global biomass burning in preindustrial time: LPJ-LMfire (v1. 0). *Geoscientific Model Development*, 6(3):643–685, doi:10.5194/gmd-6-643-2013.

Poorter, H., Niklas, K. J., Reich, P. B., Oleksyn, J., Poot, P., and Mommer, L. (2012). Biomass allocation to leaves, stems and roots: meta-analyses of interspecific variation and environmental control. *New Phytologist*, 193(1):30–50, doi:10.1111/j.1469-8137.2011.03952.x.

Portier, J., Gauthier, S., Leduc, A., Arseneault, D., and Bergeron, Y. (2016). Fire regime along latitudinal gradients of continuous to discontinuous coniferous boreal forests in eastern Canada. *Forests*, 7(10):211, doi:10.3390/f7100211.

Thompson, R. S., Anderson, K. H., and Bartlein, P. J. (1999). *Atlas of relations between climatic parameters and distributions of important trees and shrubs in North America*. US Department of the Interior, US Geological Survey.

Chapitre II

Increases in heat-induced tree mortality could drive reductions of biomass resources in Canada's managed boreal forest

Chaste, E., Girardin, M.P., Kaplan, J.O., Bergeron, Y., Hély, C. (2019) Increases in heat-induced tree mortality could drive reductions of biomass resources in Canada's managed boreal forest. *Landscape Ecology*, (), 1-24.

Résumé

Au Canada, la forêt boréale fournit de nombreux services écosystémiques qui constituent une part importante de l'économie régionale et mondiale. Malgré son importance, l'avenir de la forêt boréale canadienne est très incertain car les impacts potentiels des changements climatiques futurs sur les processus écosystémiques et les stocks de biomasse sont actuellement mal compris. Le but de cette étude est d'évaluer comment les changements climatiques prévus pour les prochaines décennies pourraient entrainer des modifications brusques de la biomasse des espèces dominantes de la forêt boréale de l'Est du Canada. En utilisant le modèle de la dynamique globale de végétation LPJ-LMfire paramétré pour les principaux genres d'espèces d'arbres dominants la forêt boréale de l'Est Canadien (*Picea*, *Abies*, *Pinus*, *Populus*) et piloté par un large éventail de scénarios climatiques regroupés selon deux scénarios de forçage (RCP 4.5 et 8.5), nous simulons la composition de la forêt, la biomasse et la fréquence des perturbations, incluant les feux de forêt. Nos simulations couvrent la forêt boréale de l'Est du Canada, du Manitoba à Terre-Neuve. Les résultats suggèrent que les effets du réchauffement climatique seront très importants dans cette région, en particulier dans les scénarios de forçage RCP 8.5 et dans les régions du sud. Dans ces zones, l'effet fertilisant de l'augmentation des concentrations en CO_2 atmosphériques sur la productivité forestière ne compensera pas les pertes de biomasse causées par les feux de forêt et les épisodes de mortalité attribuables aux sécheresses. La diminution des stocks forestiers sera vraisemblablement associée à une ouverture du paysage et à un changement de la composition de la forêt, en particulier des taxons de résineux vers des taxons de feuillus. La réduction de la biomasse résineuse suggère que les stratégies d'aménagement forestier devront s'adapter pour maintenir un niveau durable d'exploitation forestière et une densité d'arbres suffisante pour répondre à la demande en produits ligneux.

Mots-clés

Changements climatiques, Forêt boréale, LPJ-LMfire, Biomasse, Mortalité à la sécheresse.

Abstract

The Canadian boreal forest provides valuable ecosystem services that are regionally and globally significant. Despite its importance, the future of the Canadian boreal forest is highly uncertain because potential impacts of future climate change on ecosystem processes and biomass stocks are poorly understood. We investigate how anticipated climatic changes in coming decades could trigger abrupt changes in the biomass of dominant species in Canada's boreal forests. Using the dynamic global vegetation model LPJ-LMfire, which was parameterized for the dominant tree genera in Canada's boreal forests (*Picea*, *Abies*, *Pinus*, *Populus*) and driven by a large range of climate scenarios grouped by two forcing scenarios (RCP 4.5 and 8.5), we simulated forest composition, biomass, and the frequency of disturbance, including wildfire, from Manitoba to Newfoundland. Results suggest that responses of this region to a warmer future climate will be very important, especially in southern boreal areas and under the RCP 8.5 forcing scenario. In these areas, reductions of total aboveground biomass incurred by fire and heat-induced tree mortality events are projected; the fertilizing effect of increasing atmospheric CO_2 on forest productivity is unlikely to compensate for these losses. Decreases in total forest stocks would likely be associated with forest cover loss and a shift in composition in particular from needleleaf evergreen (softwood) to broadleaf deciduous (hardwood) taxa. The simulated future reduction in softwood biomass suggests that forest management strategies will have to be adapted to maintain a sustainable level of forest harvest and tree density that meets demands for wood products, while maintaining other ecosystem services.

Keywords

Climate change, Boreal forest, LPJ-LMfire, Biomass, Heat-induced mortality.

2.1 Introduction

Boreal forests account for about one-third of the world's forested area (Brandt et al., 2013) and provide a range of highly valuable ecosystem goods and services for regional and global populations, including timber and forest products, recreation, carbon sequestration and regulation of water (Gauthier et al., 2014). Canada is the world's largest producer of forest products and, consequently, forestry is important to the Canadian economy, accounting for more than 1% of the country's gross domestic product. Timber harvesting is particularly important in the boreal forest of eastern Canada (Manitoba, Ontario, Quebec and the Maritime Provinces). This region generated $475M CDN in revenue in 2015, more than 80% of which was needleleaf evergreen trees (softwood) from mixed and coniferous forests (Canadian Council of Forest Ministers, 2017). These two forest types are distributed along a latitudinal gradient from south to north, respectively, with tree cover ranging from closed- to open-canopy forests (Ecological Stratification Working Group, 1996). Climate shapes the structure and composition of these forests directly through the effects of temperature and precipitation that are imposed upon site conditions, physiological processes and the availability of resources required by trees, and indirectly through effects on disturbances (Gauthier et al., 2014).

There is a growing consensus that the increase in temperatures since the beginning of the Industrial Revolution has caused changes in Canadian boreal forests (e.g. Danneyrolles et al., 2016; Boucher et al., 2017), altering physiological processes and natural disturbance regimes (e.g. Girardin et al., 2013a, 2014; Wang et al., 2015; Zhang et al., 2015; Chaste et al., 2018). Observations of climate change effects on these forests (e.g. Girardin et al., 2016b; Hember et al., 2017; Hogg et al., 2017; Rogers et al., 2018) have raised concerns about the impacts of ongoing and future climate change on Canada's boreal forest resources. The boreal forest is notably expected to experience large increases in temperature over the course of the 21st century, accompanied by modest increases in precipitation for some regions (IPCC, 2014). These changes are unprecedented and may lead to an increase in frequency and magnitude of extreme drought events in Canada (Price et al., 2013), which could amplify tree mortality rates (Allen et al., 2010) and the frequency and sizes of wildfires (Flannigan et al., 2009, 2016; Girardin and Mudelsee, 2008; Girardin et al., 2013a; Krause et al., 2014). As a consequence, one might anticipate reductions in tree biomass and mean forest age, and subsequent changes in tree species composition (Gauthier et al., 2014; Bergeron et al., 2017). Yet negative feedbacks on wildfire also may be expected, as a result of changes in fuel type and loading, thereby attenuating some of the effects of a generally warmer climate on wildfire size and frequency. On one hand, studies have suggested that in terms of ecophysiological responses, future climate change may lead to a decrease in tree growth due to increasing stress from summer drought and heat (Girardin et al., 2016b). On the other hand, increasing atmospheric concentrations and an earlier spring could lead to growth enhancement (Norby et al., 2005; Girardin et al., 2011; Richardson et al., 2010), albeit temporarily, and perhaps not with sufficient magnitude to offset decreases that are caused by drought and heat effects. Lower regeneration rates of coniferous tree species under a warmer climate are also likely (e.g. Boiffin and Munson, 2013). Moreover, a northwards shift of the boreal treeline and forest composition is anticipated (Fisichelli et al., 2014; Fei et al., 2017), even though the speed of colonization by new genotypes or species is slower than the rate at which the climate is changing (Epstein et al., 2007; Gauthier et al., 2015b), leading to divergences in species responses to climate change (Fei et al., 2017).

Because of its importance to planetary systems, regional livelihoods and the global economy, improving our understanding of potential future impacts of climate change on Canada's boreal forests is essential (Gauthier et al., 2015b). Forest management strategies require better scenarios of current and future trajectories of forest growth and composition in order to maintain sustainable yields under a warmer climate and increasing disturbances (Gauthier et al., 2015a; Bergeron et al., 2017). Current methods for predicting potential impacts of climate change on the natural distribution of species include correlative descriptions of the current environment and species distributions, such as bioclimate envelope-based models (e.g. Terrier et al., 2013). It is now well recognized that such correlative models may provide a useful first approximation regarding the effects of climate change on species distributions (Pearson and Dawson, 2003), but they do not incorporate important biotic interactions and processes governing the natural distribution of species (e.g. Shafer et al., 2015). These limitations may be overcome using process-based ecosystem models, which have undergone significant development over the past few decades. Yet, these process-based models also have their limitations, given that they rarely take into account the whole range of ecophysiological and feedback processes that occur between vegetation, disturbances and the atmosphere. For instance, the process-based model StandLEAP has been successfully employed to determine the response of tree productivity to climate change, but it does not consider the effects of disturbances on vegetation (Girardin et al., 2016b). In contrast, other process-based models such as LANDIS II and CanFIRE integrate the effects of natural disturbances such as wildland fires on vegetation (Terrier et al., 2014; Boulanger et al., 2017b). However, despite several new modules implemented to better include primary processes such as the CO_2 concentration and its temporal changes (De Bruijn et al., 2014) and fire occurrences based on climate conditions (Perera et al., 2008), none of these model versions has yet been used over eastern Canada's boreal forest. Rather, the frequency of landscape fires has been prescribed in the versions used and, therefore, it does not respond dynamically to changes in climate. Conversely, CO_2 fertilization effects on tree growth, the effects of disturbances on vegetation, and feedback effects of vegetation on disturbances are all included in most process-based dynamic global vegetation models (DGVMs). These integrate mechanistic representations of physiological and biogeochemical processes that lead to simulations of interactions and feedbacks among vegetation, disturbances and the atmosphere (Kucharik et al., 2000; Smith et al., 2001; Krinner et al., 2005).

In this study, we used one of these DGVMs, the LPJ-LMfire model (Pfeiffer et al., 2013), to evaluate the potential for changes in climate, atmospheric CO_2 concentrations, and wildfires in the coming decades to trigger abrupt changes in the biomass of dominant species in Canada's boreal forests. The LPJ-LMfire model was developed from the LPJ DGVM, which was designed to simulate the global terrestrial carbon cycle and the response of carbon and vegetation patterns under climate change (Sitch et al., 2003). The model version employed here includes an extension that dynamically links climate, fire, and vegetation, allowing us to assess the spatial heterogeneity in climate change impacts, notably along temperature (e.g. north to south) and precipitation (e.g. west to east) gradients. Specifically, in this study we examined how gains in productivity resulting from a warmer climate and increasing CO_2 concentrations may be offset by losses in biomass that are induced by fires and heat and drought stresses across an area extending from provinces of Manitoba to Newfoundland in eastern Canada. We further provided detailed analyses focused on regions where timber harvesting is currently an important contribution to the economy. In a series of factorial experiments, we both isolated the individual importance of CO_2 and fire on biomass and quantified the synergies between these driving factors. The strength of the modeling approach proposed here is supported by the good performance of LPJ-LMfire when benchmarking its simulation results with empirically-derived fire and stand attribute studies (Chaste et al., 2018).

2.2 Model, experimental set-up, and methods

2.2.1 Study area

The study domain encompasses the boreal forest regions of eastern Canada (Brandt, 2009) that spans the provinces from Manitoba to Newfoundland (102-53° W; 46-65° N), and which covers an area of ca. 2.9 million km^2 (Figure 3.1). We divided the study area into four ecozones (Figure 3.1) as defined by the National Ecological Framework of Canada (NFEC; Ecological Stratification Working Group, 1996). These large biogeographical units are, from south to north, the Boreal Shield (BS), the Boreal Plain (BP), the Hudson Plain (HP), and the Taiga Shield (TS). The BS ecozone, covering most of the study area, was subdivided at 80° W (corresponds to boundary between Ontario and Quebec) into the Boreal Shield West (BSW) and the Boreal Shield East (BSE) sub-ecozones; the division was based on clear climate and fire regime differences between west and east (Zhang et al., 2000; Lemprière et al., 2008; Boulanger et al., 2013). The TS ecozone was likewise subdivided into two sub-ecozones, i.e., the Taiga Shield West (TSW) and the Taiga Shield East (TSE), respectively, because locations were widely spaced in the study area.

2.2.2 LPJ-LMfire model

We used the LPJ-LMfire dynamic global vegetation model (Pfeiffer et al., 2013), which is a modified version of the LPJ-SPITFIRE model that combines the dynamic global vegetation model LPJ-DGVM (Sitch et al., 2003) and the process-based fire regime model SPITFIRE (Thonicke et al., 2010). The model is designed to simulate vegetation dynamics and fire events in response to changes in climate, CO_2 concentrations, and lightning events (Pfeiffer et al., 2013). LPJ-LMfire is made up of a number of modules (containing one or several submodels) that are interconnected, each containing formulations of a relatively well-defined annual or daily ecosystem process(es). Daily pro-

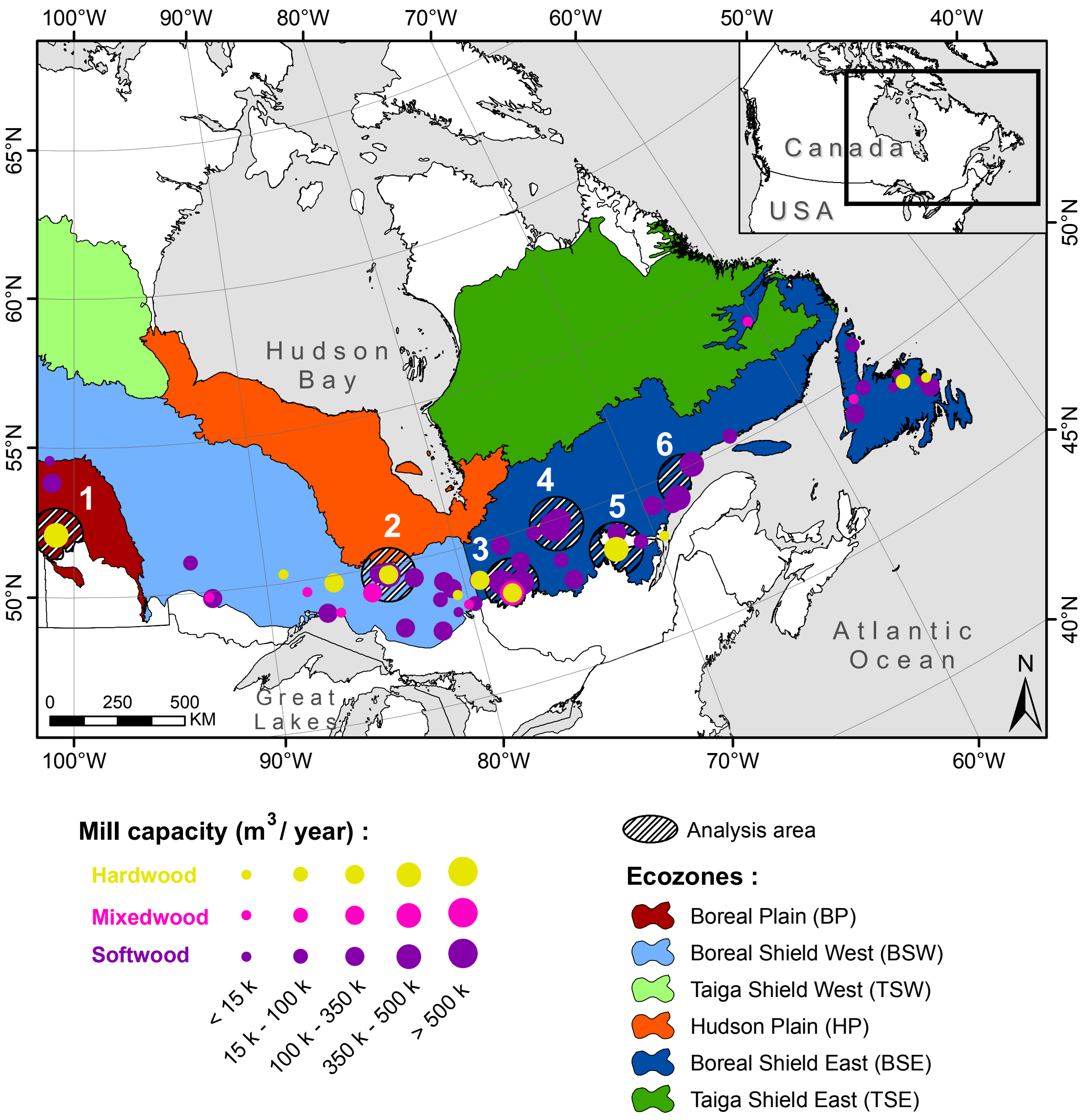

Figure 3.1. Location map of six sub-ecozones in eastern Canada's boreal forest and six analysis areas that were selected next to high-capacity forest mills (100-km radius around mills with capacities > 3.50 x 105 m^3/year). Points represent the 2015 updated version of the forest mill capacities from McKenney et al. (2016). One analysis area is located in the BP ecozone, one is located both in the BSW and HP ecozones, and the remaining areas are located in the BSE ecozone.

cesses are defined in terms of photosynthesis, stomatal regulation, soil hydrology, autotrophic respiration, leaf and root phenology, and decomposition (see Supplement S3.1 for further details). Annual processes are defined in terms of several sources of mortality, seedling establishment, reproduction, allocation, and tissue turnover (Smith et al., 2001; Sitch et al., 2003, see Supplement S3.1 for further details). Carbon dynamic is calculated for four tissue pools (leaf, root, sapwood and heartwood) and is updated annually based on the simulation of daily and annual processes. It is worth noting that we assume that all PFT simulated LPJ-LMfire are present in the 'seed bank' in every gridcell in the simulation domain. This implies that migrational lag is not considered in the model, although it could be important, particularly in the northernmost parts of our study domain (Epstein et al., 2007). The LMfire module simulates processes of natural wildfire and their implications for vegetation mortality and fire emissions that are driven by lightning ignitions, fuel bulk density and fuel moisture, which in turn are used to calculate fire rate of spread, fire intensity, and fire-induced tree mortality (Pfeiffer et al., 2013; Chaste et al., 2018) (Figure S3.2B in Supplement S3.1).

In LPJ-LMfire, each pixel is simulated independently of its neighbors, leading to a high simple representation of the reality because adjacent areas might be affected by species dispersal for example. Vegetation simulated by LPJ-LMfire in a grid cell is described in terms of the fractional coverage of populations of different Plant Functional Types (PFTs; Figure S3.1 in Supplement S3.1). PFTs corresponds to classes of species groups sharing similar roles in an ecosystem, responding in a comparable manner to environmental conditions (e.g. same physiology and dynamics) and constrained by common bioclimatic limits (Nock et al., 2016; Verheijen et al., 2013). The use of PFTs concept to represent vegetation is useful to represent as an easy way the complexity of nature in simulations of plant distribution and climate change research at regional to global scales (Wullschleger et al., 2014). However, it does not take into account intra-specific variability and adaptations (Verheijen et al., 2013). LPJ-LMfire was reparameterized and adapted by Chaste et al. (2018) for the predominant tree genera that are currently present in the Canadian boreal forest and defined according to four PFTs (*Picea*, *Abies*, *Pinus* and *Populus*). LPJ-LMfire describes the state of an ecosystem in terms of annual carbon stocks (living biomass, litter, and soil), net primary productivity (NPP), net biome productivity, evapotranspiration, heterotrophic respiration, soil moisture fraction, and forest structure and vertical profile (cover fraction, individual density, crown area, leaf area index; see Supplement S3.1 for further details).

Here, we ran LPJ-LMfire with pseudo-daily temporal resolution from 1950 to 2099 on a 10 x 10 km equal-area grid covering the study area. Data that were used to run LPJ-LMfire include scenarios of changing climate (see sections 3.2.3 and 3.2.4) and atmospheric CO_2 concentrations (see section 3.2.5), together with static maps of soil particle size distribution (%), volume fraction of coarse fragments (%), elevation (meters), slope (degrees), and water fraction (see section 3.2.6). Climate data were compiled at a monthly time-step, while CO_2 concentrations were provided to the model at an annual time-step based upon IPCC AR5 emission scenarios that are referred to as Representative Concentration Pathways (hereafter, RCP; Vuuren et al., 2011).

2.2.3 Climate scenarios and future climate trends

Climate scenarios are simulations of future climates that have been generated to investigate the potential impacts of anthropogenic greenhouse gas emissions and land cover changes on global and regional climate (Mearns et al., 2001). In the present study, each climate scenario refers to a global climate model (GCM) that is combined with a regional climate model (RCM) and a RCP (Giorgi et al., 2009). A multi-model ensemble of six climate scenarios that combined two GCMs, two RCMs, and two RCPs was used to simulate a broad range of variability in the response of vegetation and fires to climate change (Table 3.1). The GCMs that were provided by the Coupled Model Intercomparison Project phase 5 (CMIP5) were (1) the second generation of the Canadian

Earth System Model (CanESM2; Arora et al., 2011; Chylek et al., 2011) and (2) the European Consortium Earth System Model (EC-EARTH; Hazeleger et al., 2010). The two RCMs were (1) the recent new Canadian Regional Climate Model (CanRCM4; Scinocca et al., 2015) and (2) the Rossby Centre Regional Climate model version 4 (RCA4; Samuelsson et al., 2011). The two RCPs represent (1) the medium-low (RCP 4.5) and (2) high (RCP 8.5) emission scenarios with respective radiative forcing values of 4.5 W/m^2 ($\sim$650 ppm CO_2 eq.) and 8.5 W/m^2 ($\sim$1300 ppm CO_2 eq.) at the end of the 21st century (Meinshausen et al., 2011). As detailed in Table 3.1, shortened names were attributed to each climate scenario used in this study, and correspond to a combination of the RCP used (RCP 4.5 or RCP 8.5) coupled with the GCM-RCM-Center information (i.e., CCC, CRS or ERS, respectively).

Monthly mean temperature (°C), diurnal temperature range (°C), precipitation (mm), number of days per month with precipitation, wind velocities (m.s^{-1}), total cloud cover percentage and daily lightning flashes densities (number.day^{-1}.km^{-2}) were used for running the LPJ-LMfire model. Except for the last variable (see section 3.2.4), daily values for each variable and climate scenario were directly obtained from the coordinated regional climate downscaling experiment website (CORDEX; Giorgi et al., 2009, https://na-cordex.org/; see Table 3.1 for further details) for the historical baseline period 1950-2006 and for the future 2007-2099 period under RCPs 4.5 and 8.5, respectively. Monthly mean values were obtained by averaging daily values or by summing number of days with precipitation. Monthly mean diurnal temperature range was calculated as the average difference between maximum and minimum daily temperatures. The number of days per month with precipitation was calculated as days with > 1 mm of total precipitation (solid and liquid combined). Monthly values for each variable were then bilinearly interpolated onto the 10-km grid using Matlab software. To remove bias from each internal climate scenario that would allow scenario comparisons, we calculated their anomalies, which are the differences between the modeled and present climate for each climate scenario over the overlapping period 1951-2010. Monthly means of present climate were calculated from the Environment Canada's historical climate database (Environment Canada, 2013) interpolated to a 100-km^2 resolution grid (for further details, see Chaste et al., 2018). The computed monthly anomalies were then added (for temperature, relative humidity and wind velocity) or multiplied (for precipitation) to the modeled climate at each time step.

The multi-model average of annual mean temperature and precipitation for the historical baseline period 1951-1980 are equal to -2.6°C and 645 mm, respectively, and decrease along a latitudinal gradient from south to north and from east to west, respectively. The multi-model ensemble projects an increase in mean temperature and precipitation over the 1950-2099 period across the entire study area (Figure 3.2). Temperature and precipitation are projected to increase from +3.7 to +8.1 °C and from +16.9 to +31.5%, respectively, by the end of the 21st century relative to the late 20th century baseline (Table S3.1 in Supplement S3.2). The smallest and largest increases in mean temperature from 2011 to 2099 occur in the BSE and TSW ecozones (Figure 3.2 and Table S3.1 in Supplement S3.2). The greatest increases in precipitation from 2011 to 2099 are projected for the northern ecozones (TSW, HP and TSE; Figure 3.2 and Table S3.1 in Supplement S3.2). The RCP 4.5- and RCP 8.5-ERS climate scenarios exhibit the smallest magnitude of warming, while greater warming is simulated in the RCP 4.5- and RCP 8.5-CRS climate scenarios (Figure 3.2 and Table S3.1 in Supplement S3.2). Monthly frequency of days with precipitation is projected to increase by the end of the 21st century compared to the baseline, but projections are highly variable among climate scenarios and ecozones (Figure 3.2). The greatest increase in the monthly frequency of days with precipitation over 1950-2099 is projected for the HP ecozone by the RCP 8.5-ERS climate scenario (+9 days), whereas the smallest increase (+1 day) is projected to occur in the BP and BSW ecozones according to the RCP 4.5-CCC scenario and in the TSW ecozone according to the RCP 4.5-CRS scenario

(Figure 3.2).

Although monthly mean temperature and precipitation totals were given directly as inputs into LPJ-LMfire, we derived the July Monthly Drought Code (MDC; Girardin and Wotton, 2009). The MDC is an estimate of the net effect of changes in evapotranspiration (related to temperatures) and precipitation on cumulative moisture depletion in deep organic layers, and is well correlated with annual fire statistics across the circumboreal regions (Girardin et al., 2009). The calculation of the MDC was done here in order to have a sub-continental portrait of the spatiotemporal evolution of the water availability projected by the multi-model ensemble and thus to guide the elaboration of hypotheses; in no case does the MDC enter the simulation performed by LPJ-LMfire. The multi-model ensemble means of July MDC suggest that increased precipitation in the boreal forest of eastern Canada would not compensate for increasing atmospheric moisture demand that is caused by warmer temperatures. The study region is thus projected to become increasingly dry, particularly in southwestern areas (Figure 3.3). This response will be stronger and faster under the RCP 8.5 forcing scenario (Figure 3.3). Only the north of Quebec would experience a slight decrease in the July MDC, indicative of generally wetter conditions (Figure 3.3). Consequently, and consistent with previous studies (Wang et al., 2017; Wotton et al., 2017), we postulated that the annual area burned simulated by LPJ-LMfire would also increase over time.

Table 3.1. List of eight climate scenarios (ensemble climate scenarios in white and sensitivity analysis scenarios in grey) that were used in this paper. Information regarding the combination of RCP-GCM-RCM is mentioned (and the abbreviation attributed). RCM information is also described. RCP 8.5-CCO_1 and RCP 8.5-CCO_2 corresponds to two separate runs of the same climate scenario.

	Climate scenarios					**RCM information**		
	GCM	RCM	RCP	Centre	Name attributed	Data Source	Native resolution (°)	Time period
Ensemble climate scenarios	CANESM2	CANRCM4	4.5	CCCMA	RCP45-CCC	CORDEX	0.44	1950-2100
	CANESM2	CANRCM4	4.5	CCCMA	RCP45-CCC	CORDEX	0.44	1950-2100
	CANESM2	CANRCM4	8.5	CCCMA	RCP85-CCC	CORDEX	0.44	1950-2100
	CANESM2	RCA4	4.5	SMHI	RCP45-CRS	CORDEX	0.44	1950-2099
	CANESM2	RCA4	8.5	SMHI	RCP85-CRS	CORDEX	0.44	1950-2099
	EC-EARTH	RCA4	4.5	SMHI	RCP45-ERS	CORDEX	0.44	1950-2099
	EC-EARTH	RCA4	8.5	SMHI	RCP85-ERS	CORDEX	0.44	1950-2099
Sensitivity analysis scenarios	CANESM2	CRCM5	8.5	Ouranos	RCP85-CCO_1	Ouranos (run 1)	0.22	1950-2100
	CANESM2	CRCM5	8.5	Ouranos	RCP85-CCO_2	Ouranos (run 2)	0.22	1950-2100

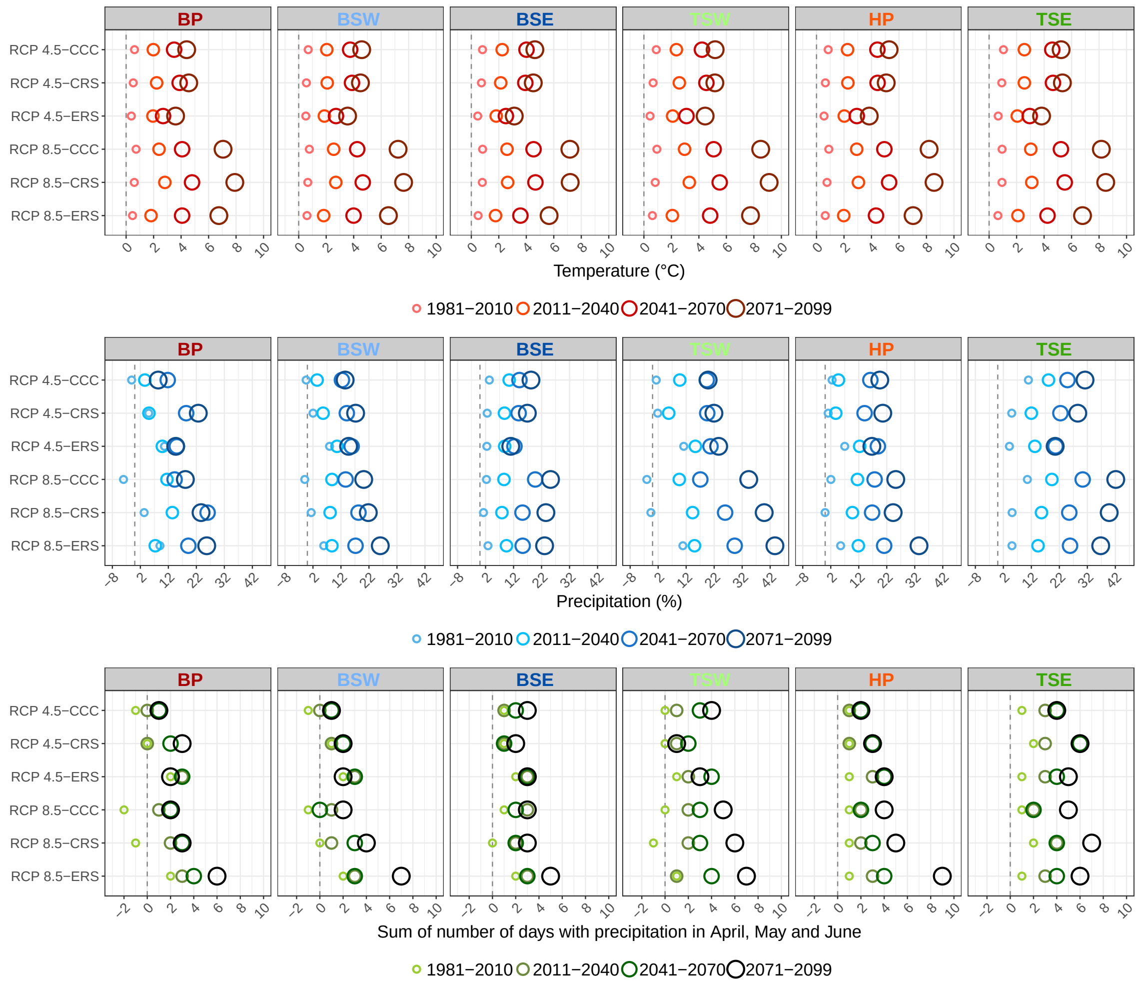

Figure 3.2. Mean changes in temperature (°C), precipitation (%) and mean number of days with precipitation in April, May and June in 1981-2010, 2011-2040, 2041-2070 and 2071-2099 compared to the baseline climate 1951-1980 across six ecozones of eastern Canada's boreal forest, under each climate scenario of the multi-model ensemble. Shortened names (RCP45-CCC; RCP45-CRS; RCP45-ERS; RCP85-CCC; RCP85-CRS; RCP85-ERS) were attributed to each climate scenario and correspond to a combination of the RCP used (RCP 4.5 or RCP 8.5) coupled with the GCM-RCM-Center information (see Table 3.1 for further details). Ecozones are, from south to north, the Boreal Plain (BP), the Boreal Shield West (BSW), the Boreal Shield East (BSE), the Taiga Shield West (TSW), the Hudson Plain (HP), and the Taiga Shield East (TSE) (Ecological Stratification Working Group, 1996).

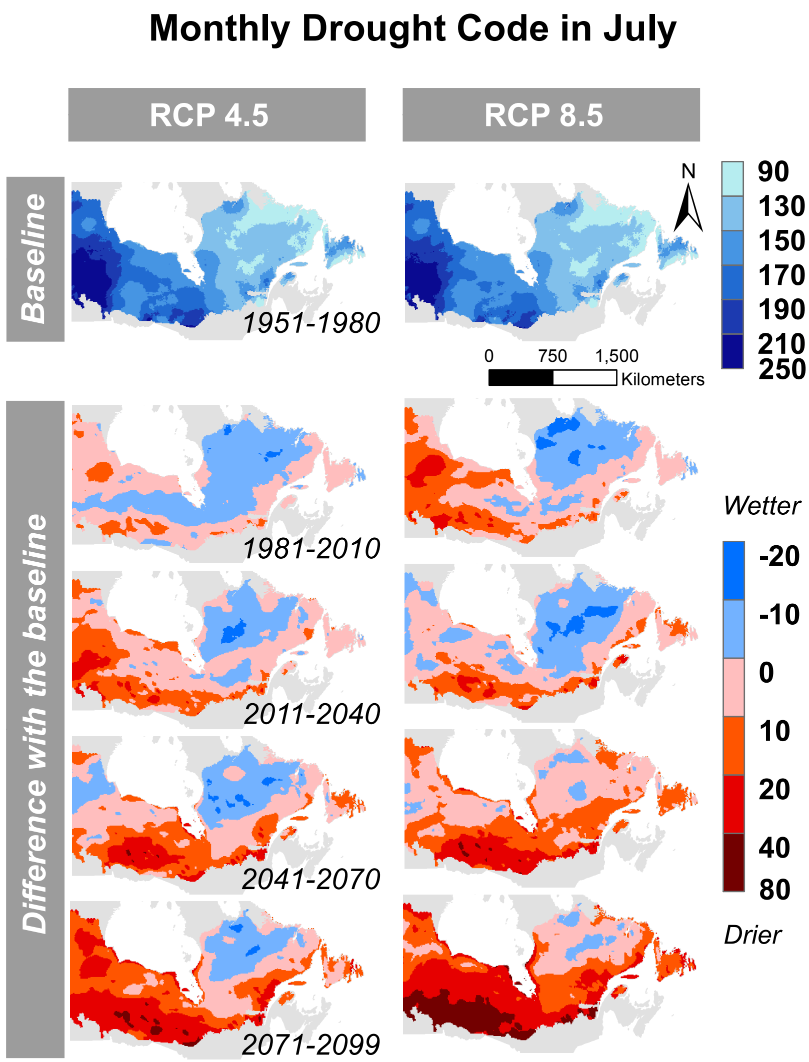

Figure 3.3. Predicted changes in the July Monthly Drought Code (MDC) across eastern boreal Canada for four periods from 1981 to 2099 compared to the baseline 1951-1980 for the RCP averages (RCP 4.5 and RCP 8.5). The MDC calculation that was used was developed by Girardin and Wotton (2009) and is a generalized version of the daily Drought Code that is widely used across Canada by forest fire management agencies in their monitoring of wildfire risk. This index represents the net effect of changes in evapotranspiration and precipitation on soil moisture storage. Daily MDC values below 200 are considered low, whereas values around 400 or higher indicate that fire could involve burning of deep subsurface and heavy fuels (Bergeron et al., 2010).

2.2.4 Lightning flash density data

LPJ-LMfire requires as input the monthly density of lightning flashes in the calculation of the fire ignition probability but these data, as is the case for many climate models, were unavailable for the climate scenarios that were constructed and implemented in this study. We addressed this lack of data by developing two very different lightning flash density experiments to cover a large range of variability in future lightning conditions.

In the first lightning flash density experiment (hereafter, $\text{Flashes}_{\text{constant}}$), we applied a constant lightning flash density from 1950 to 2099 that varied spatially through time. In this case, the Canadian lightning detection network (CLDN) dataset, which covers the period 1999-2010 (Orville et al., 2011), was used to construct time-series of monthly lightning flash densities (number.day^{-1}.km^{-2}) from 1950 to 2099. The time-series were constructed by randomly selecting monthly values from the 12 years of monthly CLDN time-series. Monthly lightning flash densities were then converted to daily lightning flash densities before being set as input to the model. The LPJ-LMfire model distributes lightning flash occurrence only on rainy days disaggregated from monthly sums of precipitation by the weather generator (see Supplement S3.1 for further details). This redistribution of lightning flash occurrence on rainy days was based on previous observations showing that lightning flash activity and precipitation are strongly correlated in the North American boreal forest, with only 20% of the total lightning flash activity in boreal Canada corresponding to dry lightning flash (Peterson et al., 2010; Romps et al., 2014; Veraverbeke et al., 2017).

In the second lightning flash density experiment (hereafter, $\text{Flashes}_{\text{increase}}$), we applied an increase in lightning flash density during the 21$^{\text{st}}$ century. This experiment is consistent with the expectation that lightning flash density would increase until the end of the 21$^{\text{st}}$ century (Krause et al., 2014; Romps et al., 2014), given that it is correlated with increases in temperature and moisture (Krause et al., 2014; Wang et al., 2017). Given the strong correlations between lightning flash density and the convective available potential energy (CAPE) that is an indicator of atmospheric instability (Peterson et al., 2010; Romps et al., 2014), we used daily values of CAPE that were available from a climate scenario developed by the Ouranos Consortium (Separovic et al., 2013) to develop the $\text{Flashes}_{\text{increase}}$ experiment. The Ouranos Consortium climate scenario combines the CanESM2 GCM with the Canadian Regional Climate Model version 5 (CRCM5; Martynov et al., 2013; Separovic et al., 2013) and the RCP 8.5. Two runs of this climate scenario were available (RCP 8.5-CCO_1 and RCP 8.5-CCO_2; see Table 3.1 for further details). However, as these climate scenario runs were available for the RCP 8.5 only, they were not used as inputs in LPJ-LMfire; rather, they were used to develop the lightning flash density experiment. The RCP 8.5-CCO_1 projected the highest monthly increase in CAPE for the 1950-2099 period (Figure S3.3A in Supplement S3.3). Consequently, we applied daily CAPE values from the RCP 8.5-CCO_1 on the daily lightning flash density from the CLDN dataset using the methodology that was described in Chaste et al. (2018): (i) calculate monthly CAPE anomalies compared to the average of monthly CAPE from 1961 to 1990, (ii) normalize these to a range between -1 and 1, and find the largest positive or negative CAPE anomaly value within the time series for a specific grid cell to estimate the total magnitude of the range of observed lightning strikes, and then (iii) applying the normalized CAPE anomaly with scaling factors on the monthly CLDN time-series to generate a time-variant scenario. The resulting $\text{Flashes}_{\text{increase}}$ experiment projected an increase in monthly lightning flash density over the 1950-2099 period with highest monthly lightning flash density occurring between June and September, with a maximum in July (Figure S3.3B in Supplement S3.3). Monthly mean lightning flash density was projected to increase by 342% between June and September for the period 2071-2099 relative to the 1951-1980 baseline period.

These two lightning flash density experiments ($Flashes_{constant}$ and $Flashes_{increase}$) were separately paired with each climate scenario that has been previously described in section 3.2.3 and lead to generate twelve climate scenarios in total.

2.2.5 Atmospheric CO_2 concentrations

Monthly mean concentrations of atmospheric carbon dioxide (CO_2) covering the 1951-1980 and 1981-2099 periods were obtained from Pfeiffer et al. (2013) and from Meinshausen et al. (2011), respectively. For the latter period, values were directly obtained from IPCC (IPCC, 2013) for RCP 4.5 and RCP 8.5. Mean annual atmospheric CO_2 concentrations varied from 310.7 ppm in 1950 to 537.8 ppm in 2099 for the RCP 4.5, and to 926.7 ppm in 2099 for RCP 8.5. It should be noted that CO_2 concentrations from both RCP forcing scenarios started to diverge in 2008.

2.2.6 Other model input datasets

We used the methodology of Chaste et al. (2018) to construct the biophysical layers that are required as inputs in LPJ-LMfire. Soil texture fractions were extracted from the SoilGrids1km dataset (Hengl et al., 2014) and interpolated to our 10-km resolution grid. Lithology was unchanged from Pfeiffer et al. (2013). The 30 arc-second gridded digital elevation model (DEM) of Canada was interpolated to our 10-km grid and used to calculate slopes in degrees using ArcGIS 10.4.1. The land fraction, which is defined as the inverse of the water fraction (lake and watercourse areas), was calculated from the National Hydro Network (NHN) dataset at 100-m resolution (Natural Resources Canada, 2010). We calculated the water fraction at 10-km resolution from grid cells at 100-m resolution that had a percentage of water fraction > 50%. Roads, power lines, dams, mines, and other anthropogenic structures were not considered in this study. Impacts of human activities, including forest management and active fire suppression efforts, on characteristics of forest fuels were also not considered in the present LPJ-LMfire simulations.

2.2.7 Modeling and simulation protocol

A 1120-year spin-up period was prescribed to equilibrate vegetation and carbon pools with climate at the beginning of the study period (Smith et al., 2001), and to ensure that forest biomass was in equilibrium with climate and fire (Tang et al., 2010). This spin-up run was unchanged from Chaste et al. (2018) and corresponds to a linearly detrended version of the observed climate data covering the 1901-2012 period, which was repeated 10 times. After the spin-up period concluded, transient period were performed using as input each climate scenarios describe above in section 3.2.3 and 3.2.4. For each of those twelve independent simulations, we analyzed the outputs of LPJ-LMfire in terms of annual area burned, annual net primary productivity (ANPP), total aboveground biomass and PFT cover percentages. We summarized simulated results using moving 30-year periods covering 1951-1980, 1981-2010, 2011-2040, 2041-2070 and 2071-2099 in each ecozone and for all zones that were grouped together. These results are presented by RCP averages (mean of simulated results for RCP 4.5 and RCP 8.5 distinctly) in the manuscript and separately for each climate scenarios in the supplementary materials. In addition, we also performed twelve others simulations that corresponds to two sensitivity analyses describe below (CO_2 fertilization and fires) and performed under simulations using the six climate scenarios paired with the '$\text{Flashes}_{\text{increase}}$' experiment.

2.2.7.1 Sensitivity analysis to CO_2 fertilization

Like many vegetation and earth system models, LPJ-LMfire is particularly sensitive to changes in atmospheric CO_2 concentrations (Chaste et al., 2018). Some of the effects may reflect an under-representation of climatic feedbacks or a lack of representation of nutrient constraints on vegetation (e.g. Smith et al., 2016). We explored the potential implication of CO_2 fertilization effect on our conclusions by running LPJ-LMfire with two sets of CO_2 experiments that were combined with each climate scenario. In the first set of simulations, we tested an increase in the CO_2 concentration, 'Climate + CO_2' experiment, as described in the section 3.2.5. This experiment was used throughout our evaluation of LPJ-LMfire projections. In the second set of simulations, we used constant CO_2 concentrations from 1950 to 2099, 'Climate - CO_2', where CO_2 was fixed at the 2008 level, i.e., the last year for which CO_2 concentration was equal in both RCPs (384.8 ppm). In the latter case, there was no response of vegetation gross primary productivity (GPP) to direct changes in CO_2 concentrations, but we recognize that the indirect effect of the CO_2 concentration increase in terms of climate response cannot be fully removed. The direct effect of CO_2 fertilization on vegetation, therefore, was determined by the difference of ANPP between simulations 'Climate + CO_2' and 'Climate - CO_2'.

2.2.7.2 Influence of climate change with and without fires on forest biomass

To assess the role of future climate and fire on vegetation separately, we simulated vegetation with and without fire in two distinctive sets of LPJ-LMfire experiments. In the first experiment of simulations, we ran LPJ-LMfire with each climate scenario, coupled with the possibility that lightning flash density could start fires if conditions for fire propagation and fuel availability were conducive (hereafter, the 'Climate + fires' experiment). This experiment was used throughout our evaluation of LPJ-LMfire projections. In the second set of simulations, we ran LPJ-LMfire with each climate scenario, coupled with a forcing rule that none of the fires could occur, regardless of the lightning density (i.e., the 'Climate - fires' experiment). Note that these two experiments might not be directly comparable owing to postfire establishment rules of fire-adapted genera that were included in LPJ-LMfire (for further details, see Chaste et al., 2018). Thus, the effect of fires on vegetation was determined by analyzed the outputs of LPJ-LMfire in terms of total aboveground biomass under each experiment.

2.2.7.3 Detailed analyses

We performed detailed analyses at six locations in the study area where important forest industries are located (Figure 3.1). We analyzed the outputs of LPJ-LMfire in terms of annual area burned, tree cover percentage (sum of all PFTs), establishment rate and heat-induced mortality rate. These detailed analyses are only reported for the RCP 4.5-CCC climate scenario, which represents the medium climate scenario between the six climate scenarios that were used in this study (see section 3.2.3). We refer to forest cover gain and loss when the tree cover percentage increases and decreases, respectively. Here, heat-induced mortality refers to heat damage mortality induced by stress during prolonged periods with high temperatures and that could lead to forest dieback (Sitch et al., 2003). Heat-induced mortality rate increases linearly with the number of growing degree days above a PFT-specific temperature base (Sitch et al., 2003).

2.3 Results

2.3.1 Annual area burned

As outlined in section 3.2.3, we postulated that the amount of area that was burned would increase over time across the study area, given that drought severity (July MDC, Figure 3.3) was projected to substantially increase over time by the multi-model ensemble of climate scenarios. Contrary to expectation, our model simulations showed a general decrease in annual area burned regardless of the climate scenario that was used (Figures 3.4). LPJ-LMfire simulations projected decreases in mean annual area burned from 1951 to 2099 in both the RCP 4.5 and 8.5 forcing scenarios, except in the TSE ecozone, where a 12% increase was projected under the RCP 8.5 (Table S3.2 in Supplement S3.4). The smallest decrease in mean annual area burned was simulated in the northwestern ecozones and southeastern ecozone, while the greatest decline in mean annual area burned was simulated in the southwestern ecozones (Figures 3.4; Table S3.2 in Supplement S3.4). It is noteworthy that the rate of change in the decline in annual area burned was not constant, and in many instances, a brief increase in burned area was simulated before the onset of the decline. Under the RCP 8.5 forcing scenario and starting at 2011-2041, mean annual area burned was projected to decrease in the BP, BSW and TSW ecozones; in other ecozones, they were projected to increase up to 2041-2070 and then to decline afterwards (Figures 3.4). Simulations performed with climate scenarios that was paired with the two experiments of lightning flash density ('$\text{Flashes}_{\text{constant}}$' or '$\text{Flashes}_{\text{increase}}$'; see section 3.2.4) did not project significant differences in annual area burned (Figure S3.9 in Supplement S3.5).

2.3.2 Net primary productivity

Mean annual net primary productivity (ANPP) that was simulated by LPJ-LMfire under the 'Climate + CO_2' experiment was projected to increase from 1951 to 2099 for all ecozones (Figures 3.4), except in the BSW where decreases of 19% and 34% were projected under the RCP 4.5 and RCP 8.5, respectively (Figures 3.4; Table S3.2 in Supplement S3.4). The smallest and largest increases in mean ANPP were simulated respectively in the BP and TSW ecozones, and were equivalent to less than 15% and more than 80% (Figures 3.4; Table S3.2 in Supplement S3.4). The increase in mean ANPP from 1951 to 2099 was relatively constant under RCP 4.5 (Figure 3.4). However, an increase in mean ANPP from 1951 to 2070, followed by a decrease in mean ANPP until the end of the 21st century, was projected under RCP 8.5 for the BP and BSE ecozones (Figure 3.4). A similar trend was observed in the BSW ecozone, but the decrease in mean ANPP started earlier in the simulation period (Figures 3.4; Table S3.2 in Supplement S3.4). Thus, ANPP was projected to increase with climate change, except in the southwestern part of our study area.

Results from the 'Climate - CO_2' experiment suggested a decrease in mean ANPP from 1951 to 2099 for all ecozones (Figure S3.10 in Supplement S3.5), except for the TSW

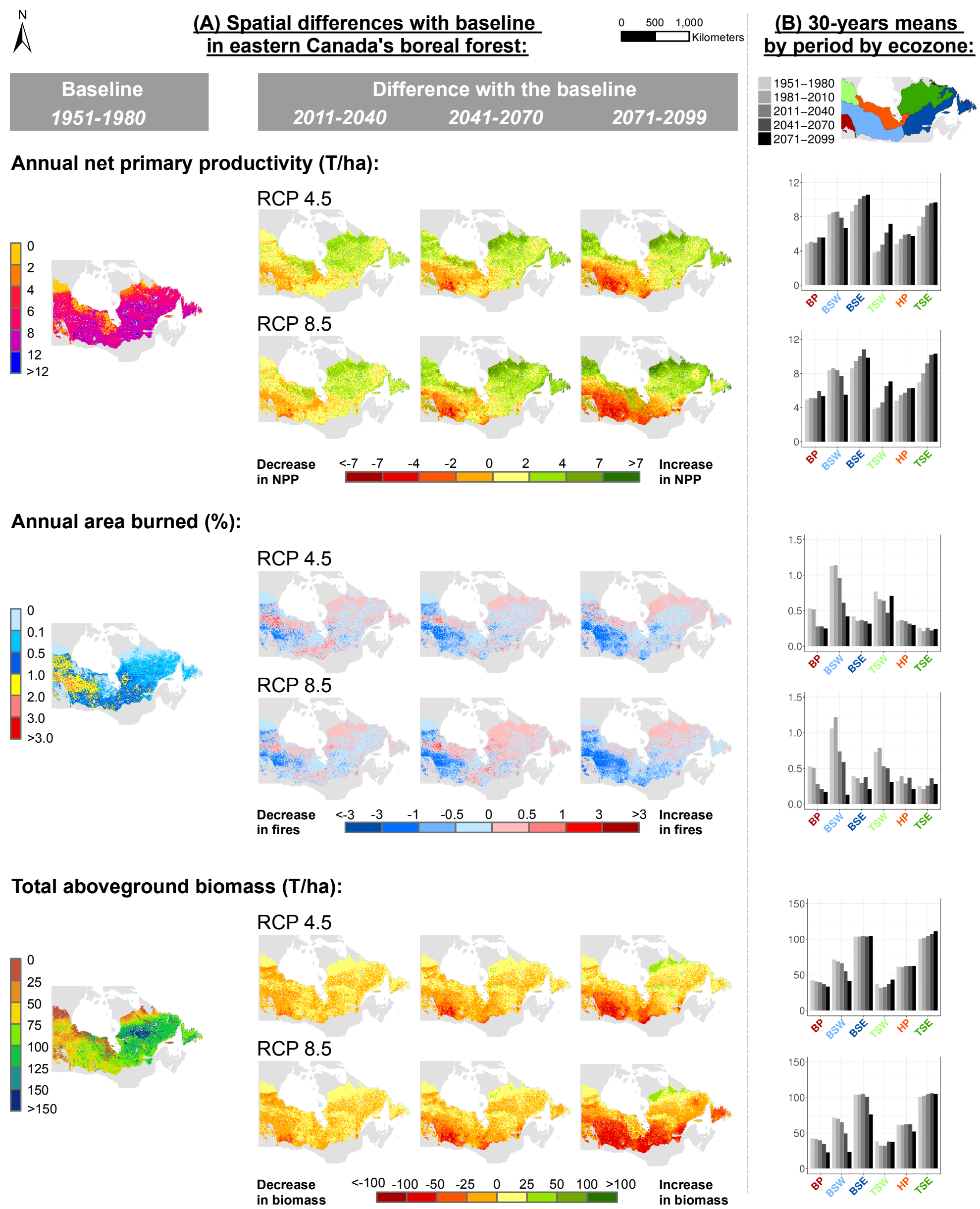

Figure 3.4. RCP averages (RCP 4.5 and RCP 8.5) of mean annual net primary productivity ($T.ha^{-1}.yr^{-1}$), mean annual area burned ($\%.yr^{-1}$) and mean total aboveground biomass ($T.ha^{-1}$) that were simulated by LPJ-LMfire under the 'Flashes$_{increase}$' lightning, 'Climate + CO_2' and 'Climate + fires' experiments. (A) Changes in the 2011-2040, 2041-2071, and 2071-2099 periods compared to the baseline 1951-1980 across eastern Canada's boreal forest (100 km^2-resolution). (B) Changes simulated for 30-year periods in each ecozone. T refers to tonnes.

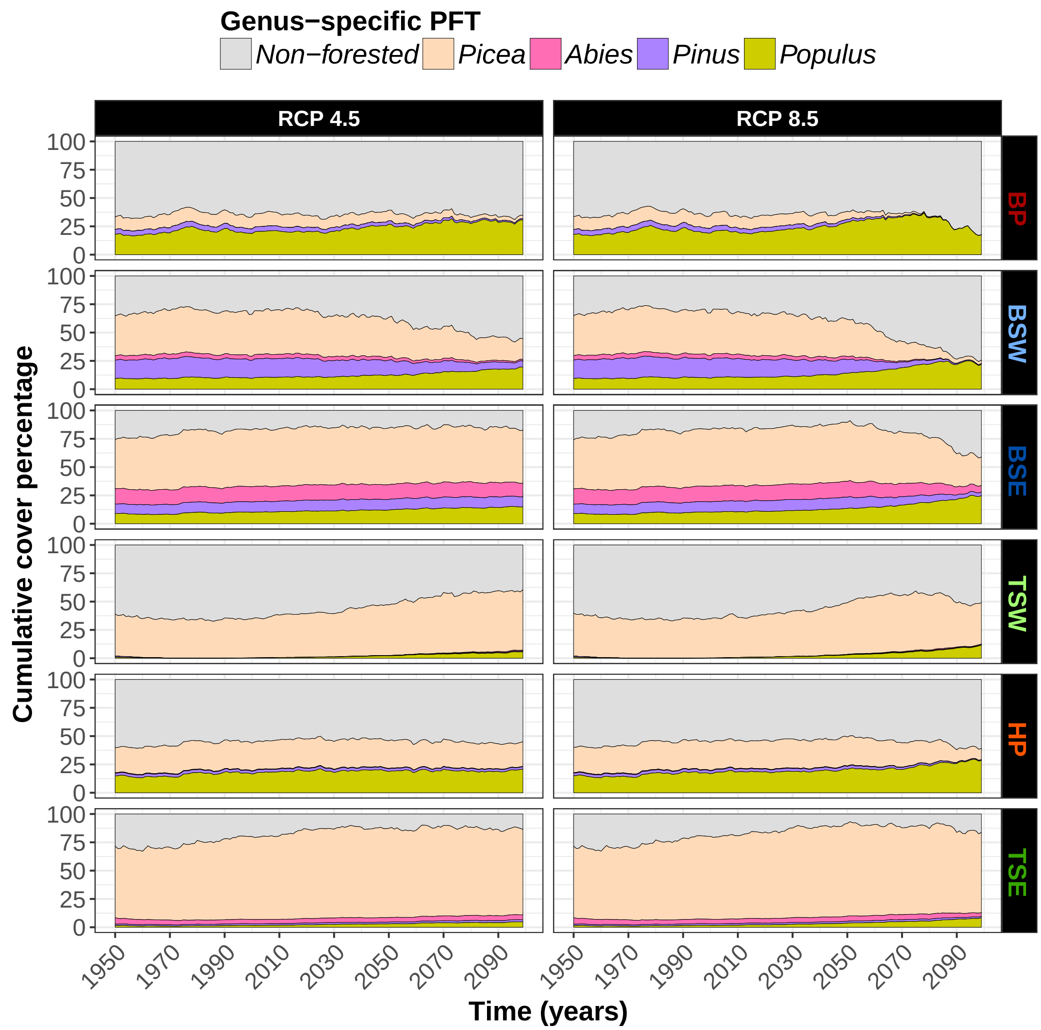

Figure 3.5. RCP averages (RCP 4.5 and RCP 8.5) of mean cumulative percentage tree cover for the four genus-specific PFTs (*Picea*, *Abies*, *Pinus* and *Populus*) and for the percentage of non-forested areas in each ecozone that were simulated by LPJ-LMfire under the 'Flashes$_{increase}$' lightning, 'Climate + CO_2' and 'Climate + fires' experiments. In the main text, we refer to forest cover gain (loss) when the cumulative percentage tree cover increases (decreases) relative to a baseline period.

and TSE ecozones under RCP 4.5, where respective increases of 41% and 10% were projected (Table S3.3 in Supplement S3.5).The highest decrease in mean ANPP was simulated in the BSW and BP ecozones (Figure S3.10 in Supplement S3.5). Percentages of differences in mean ANPP that were simulated by LPJ-LMfire between the

'Climate + CO_2' experiment and the 'Climate - CO_2' experiments were 9% in 2011-2040, 26% in 2041-2070, and 35% for the 2071-2099 period under RCP 4.5. These percentages of differences were higher under RCP 8.5 (equal to 11.5%, 43.4% and 96.8%, respectively). Thus, the increase in ANPP that was simulated by LPJ-LMfire with the 'Climate + CO_2' experiment was associated with increasing CO_2 concentrations, especially in the southwestern parts of the study area (Figure S3.10 in Supplement S3.5). The higher the CO_2 concentration, the stronger was the fertilization effect.

2.3.3 Total aboveground biomass

Broadly, mean total aboveground biomass was projected to decrease from 1951 to 2099 in southern areas (with a maximum decrease in the BSW ecozone) and increase in northern areas (with a maximum increase in the TSE ecozone, followed by TSW (Figures 3.4; Table S3.2 in Supplement S3.4). The range of increases or reductions in total aboveground biomass showed regional variation. Some differences were apparent between the two RCP scenarios, although the responses were stronger under the RCP 8.5 scenarios compared to RCP 4.5 (Figures 3.4; Table S3.2 in Supplement S3.4). For instance, in the HP and BSE ecozones, mean total aboveground biomass was projected to remain relatively stable during the entire period under RCP 4.5, whereas it was projected to decrease from 2041-2070 until the end of the century under RCP 8.5 (Figures 3.4; Table S3.2 in Supplement S3.4). Overall, total aboveground biomass was closely tied to mean annual area burned and net primary productivity (Figure S3.7 in Supplement S3.4).

Results from the 'Climate - fires' experiment showed trends in aboveground biomass that were similar to the 'Climate + fires' experiment (Figure S3.11 in Supplement S3.5). In the southern ecozones, simulated biomass was higher in the 'Climate - fires' experiment, whereas it was similar in the northern ecozones for both experiments (Figure S3.11 in Supplement S3.5). The percentage decreases in mean total aboveground biomass between the 1951-1980 and 2071-2099 periods were relatively similar under both experiments in the southern ecozones (Table S3.4 in Supplement S3.5).

2.3.4 Forest composition

Simultaneous to the biomass decline that was simulated in the southern ecozones, forest composition and forest covered areas changed significantly, particularly in the second half of the 21st century (Figure 3.5). LPJ-LMfire simulations projected a significant decrease in the cover percentage of *Picea* and *Pinus* by the end of the century compared to the baseline under both emission scenarios (Figure 3.5). Changes in forest composition in the southern ecozones were strongly driven by a shift in dominance to *Populus* under RCP 8.5, while co-dominance of *Picea* and *Populus* was projected in the BSW and HP ecozones under RCP 4.5 (Figure 3.5). A decrease of the tree cover percentage (i.e. a forest cover loss) in the southern ecozones was also simulated by LPJ-LMfire at the end of the century under RCP 8.5 (Figure 3.5; Figure S3.8 in Supplement S3.4); this trend was slightly limited in the BSW ecozone under RCP 4.5 (Figure 3.5; Figure S3.8 in Supplement S3.4). In contrast, no significant change in forest composition was simulated in the northern ecozones over the simulation period (Figure 3.5): *Picea* remained dominant despite a slight increase in *Populus* cover percentage at the end of the century (Figure 3.5). Overall, forest cover gains were simulated in the northern ecozones (i.e., TSW and TSE) in both the RCP 4.5 and 8.5 scenarios, followed by forest cover losses during the 2071-2099 period under RCP 8.5. This pattern of gain and loss was also simulated in the HP ecozone with greater amplitude and earlier onset in the 21st century (Figure 3.5).

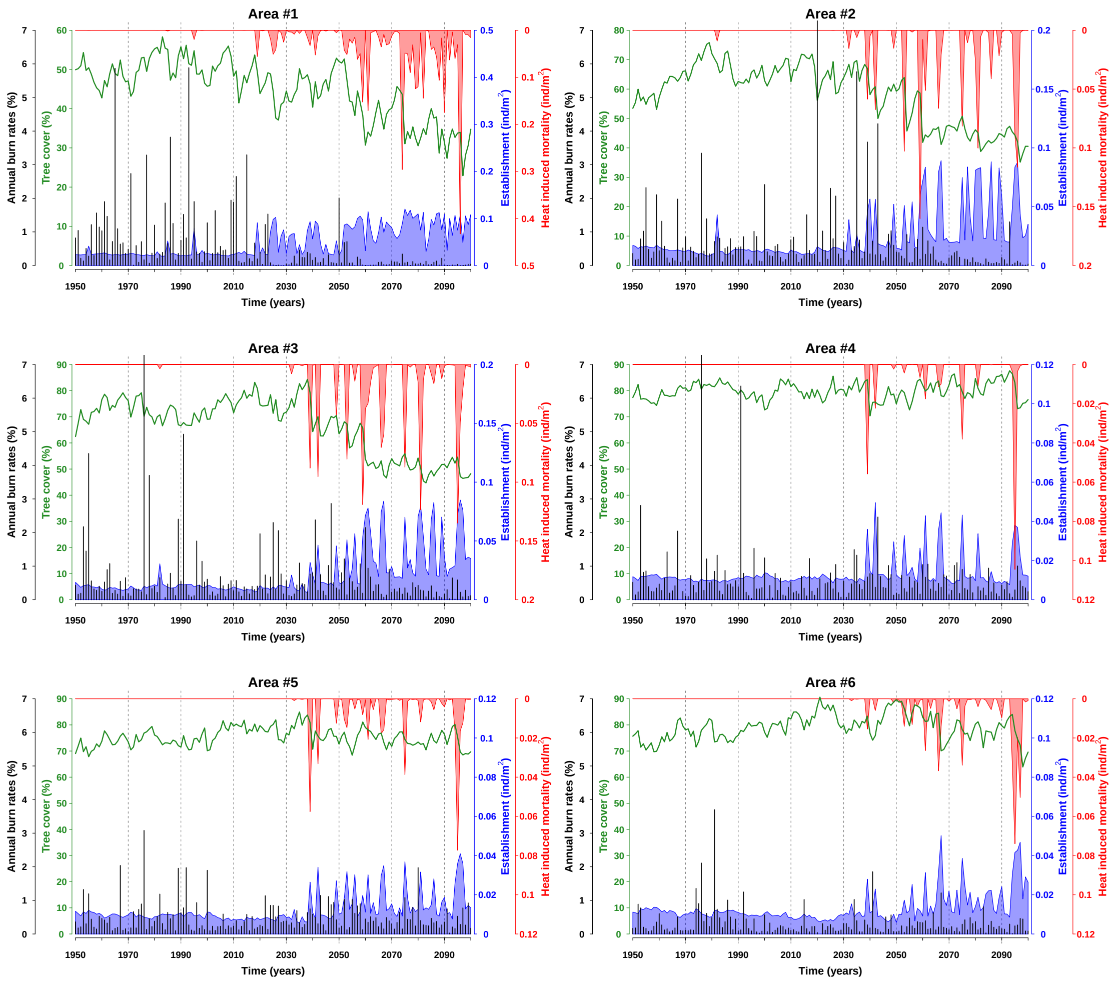

Figure 3.6. Mean annual area burned (%, in black), tree cover (%, in green; sum of the four PFTs), establishment (in blue), and heat-induced mortality rates (ind.m^{-2}, in red) in six mill areas of eastern Canada's boreal forest (see locations in Figure 3.1) that were simulated by LPJ-LMfire under the RCP 4.5-CCC climate scenario paired with the 'Flashes$_{increase}$' lightning, 'Climate + CO_2' and 'Climate + fires' experiments. Except for annual area burned, note that scales differ among areas.

2.3.5 Heat-induced mortality rates vs establishment rates

The detailed analysis of heat-induced mortality and recruitment patterns at six locations that were co-located with the largest sawmills suggested an increase in both establishment rates and heat-induced mortality rates during the second half of the 21st century, with decreasing variability along a longitudinal gradient from west to east (Figure 3.6). Variability in forest cover was closely related to heat-induced mortality rates, especially during the second half of the 21st century and in the western areas (Figure 3.7). While fires have played a role in the reduction of total aboveground biomass in southern ecozones, the upstream effect of heat-induced mortality brought with climate warming has likely been more important. Therein, forest cover losses paralleled the increase in heat-induced mortality rates that exceeded tree establishment rates (Figure 3.6). In the three eastern areas, a relatively constant forest cover was simulated in association with low establishment rates and low heat-induced mortality; annual areas burned remained relatively constant throughout the 21st century (Figure 3.6). Noteworthy, in the westernmost areas we noted that the simulated decrease in annual area burned was closely tied to the tree cover percentage: a large decline in annual area burned was simulated when the tree cover percentage was less than 50% (Figure 3.6). The highest decrease in annual area burned was simulated at site #1 (in the BP ecozone), where it declined to almost 0% of the land area by the end of the 21st century (Figure 3.6). This decline in annual area burned is synchronous with the forest cover loss noted at the ecozone level (Figure 3.5).

2.4 Discussion

2.4.1 Changes in fire regimes and forest dynamics

Our study indicates that impacts of climate change will be very significant throughout the boreal forest of eastern Canada by the end of the 21st century, but they will vary greatly across the study region. In the southernmost ecozones (BP, BSW, and BSE), a decrease in annual area burned and total aboveground biomass associated with a regression of forested areas (forest cover losses) and a northward migration of needleleaf tree types are expected. Conversely, in the northern ecozones (HP, TSW, and TSE), a significant increase in ANPP for the first half of the 21st century is expected and will

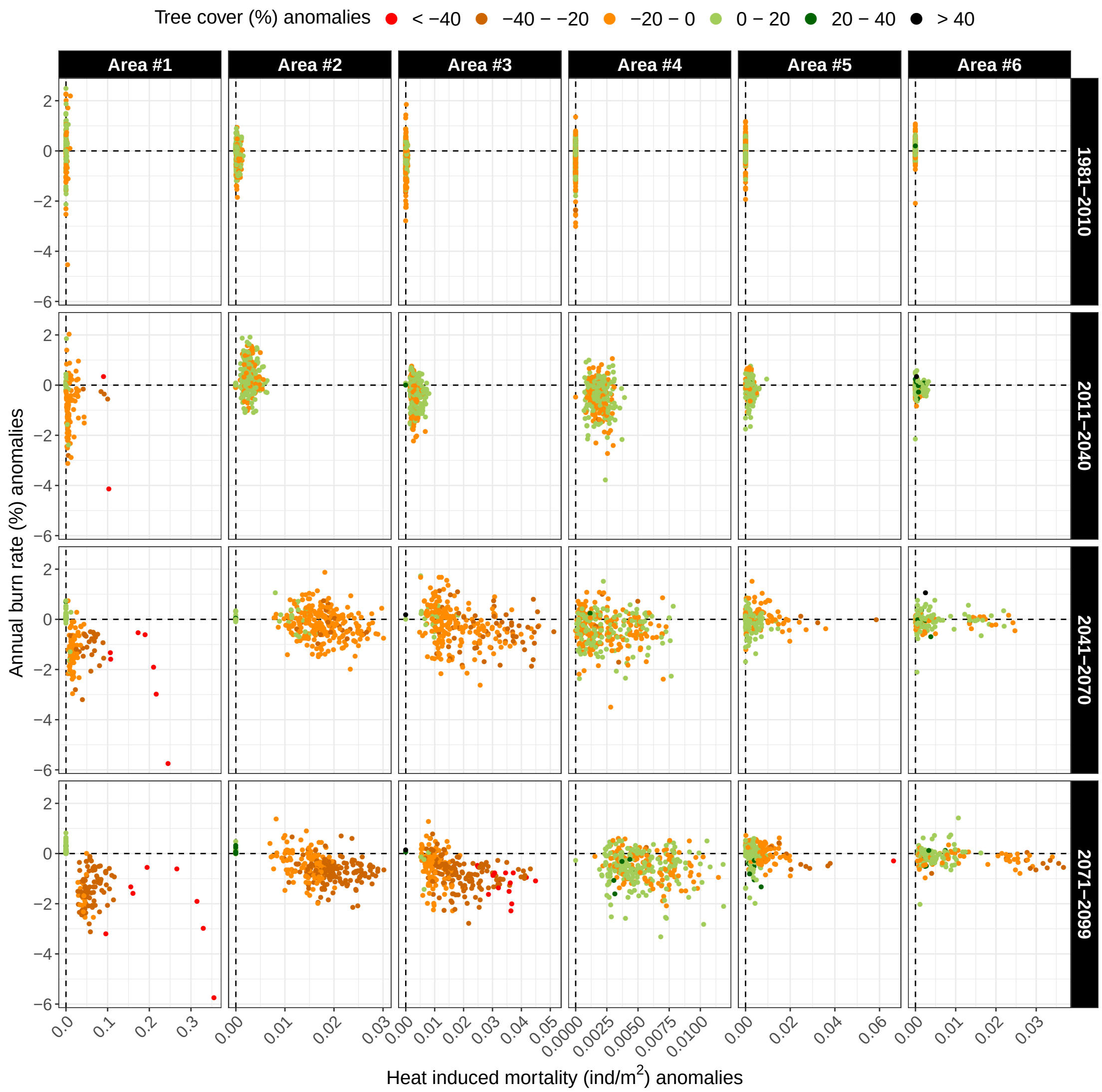

Figure 3.7. LPJ-LMfire's simulated tree cover (%) anomalies expressed as functions of heat induced mortality (ind.m^{-2}) anomalies and annual (%) burn rates anomalies for moving 30-year periods in six mill areas of eastern Canada's boreal forest (see locations in Figure 3.1). Anomalies were calculated with the baseline period 1951-1980. Results corresponds to the RCP 4.5-CCC climate scenario paired with the 'Flashes$_{increase}$' lightning, 'Climate + CO_2' and 'Climate + fires' experiments. Note the different x-scale from one area to another. A positive tree cover anomaly here denotes a forest cover gain; a positive tree cover anomaly denotes a forest cover loss.

be associated with an expansion of forested areas (forest cover gains) mainly dominated by *Picea* PFT. Yet, these trends were simulated to reverse by the end of the 21st century under RCP 8.5 and follow trends to those that were projected for the southern ecozones. Differences in the speed of responses, in terms of productivity, annual area burned and total aboveground biomass, to climate change were projected, depending upon the climate scenarios that were used: projections are anticipated to occur faster and more strongly under RCP 8.5 than under RCP 4.5 (Figures S3.4, S3.5 and S3.6 in Supplement S3.4).

The simulated increase in annual area burned in western ecozones for the 1950-2010 period is supported by independent observations (e.g. Stocks et al., 2003), and appears to have been driven mainly by an increase in extreme fire weather events that were conducive to fires, which is reflected here by an increase in the July MDC (Figure 3.3). In the southeastern ecozone, simulated annual area burned remained stationary over this same period; this phenomenon is echoed in observed annual area burned data and may be the continuation of atmospheric moistening that began more than a century ago (Drobyshev et al., 2017). Atmospheric moistening could act on the annual area burned as long as precipitation compensates for the increase in temperature (Flannigan et al., 2016). Yet, several studies have projected that annual area burned is likely to increase until the end of the 21st century in eastern Canada's boreal forest in response to ongoing climate warming (e.g. Ali et al., 2012; Boulanger et al., 2014; Wotton et al., 2017). Our simulations contradict these previous conclusions and project a decrease in annual area burned for the upcoming century in southernmost areas; the discrepancy is likely because previous studies did not include fire-vegetation feedbacks (Girardin et al., 2013b), which are a key feature of process-based vegetation models. Increases in the frequency of heat-induced mortality events will lead to forest cover loss in the southern ecozones, which in turn has the potential of inducing a negative feedback on the annual area burned. Warming leads to an increase in evapotranspiration that depletes soil moisture (Girardin et al., 2016a), and it also increases the frequency of heat-induced mortality events (Figure 3.6). These results concur with previous studies that have highlighted that the enhancement of vegetation growth by climate change would not be unlimited and may be counteracted by the negative effects of climate change on other plant processes (Silva et al., 2010; Price et al., 2013; Girardin et al., 2016a), such as tree mortality events (Forkel et al., 2016) or nutrient limitation (Norby et al., 2010). This being said, the stimulating effects of increasing temperatures and atmospheric CO_2 concentrations on boreal forest productivity (Norby et al., 2005; Girardin et al., 2011) were well captured by our simulations in northern ecozones (Figure 3.4). The contrasting trends in NPP between the northern (enhancement) and southern (declining) portions of our study domain agree with previous studies, which suggested that future responses of forest productivity will show considerable spatial variation associated with the latitudinal gradient of climate factors (Friend et al., 2014; Girardin et al., 2016a; Forkel et al., 2016).

Although heat-induced tree mortality events seems to play a significant role on the decrease in annual area burned during the second half of the 21st century, fires play a role on simulated forest composition changes. Within our simulations, high annual area burned in southwestern areas from 1950 to 2010 induced a decrease of the coverage of the needleleaf evergreen PFT to the benefit of the broadleaf deciduous PFT (Figure 3.5), which likely imposed a negative feedback on fires up until the end of the century. Recent preindustrial reconstructions of vegetation composition have already shown that landscapes where large fires occurred have undergone a shift in dominance from needleleaf evergreen species (e.g., *Picea* spp.) to broadleaf deciduous species, such as *Populus* spp. or *Betula* spp. (Danneyrolles et al., 2016; Boucher et al., 2017). Broadleaf deciduous stands are less flammable than needleleaf coniferous stands due to lower fuel quantity and quality to ignite fires and sustain propagation. Moreover, they are characterized by higher moisture in the understory compartment (Hély et al., 2001), and deciduous crown trees do not contain the highly flammable oils and resins that are common in needleleaf species (Van Wagner, 1987; Terrier et al., 2013). Consequently, the change in vegetation composition, which is anticipated to accelerate during the mid-twentieth century within our simulations, leads to a reduction in both ignition efficiency and fire spread, which in turn reduces fire size and total annual area burned (Figures 3.4 ; Hély et al., 2010; Terrier et al., 2013; Bernier et al., 2016). The present study, therefore, highlights the 'bottom-up' controls of fuel composition and availability on future fire risk in a warmer climate, especially in southwestern ecozones of the study area, as has been previously suggested for the current conditions (Hély et al., 2000, 2001).

Our study indicates that an increase in establishment rates in southern ecozones would not compensate for the loss of biomass that is induced by heat-induced mortality events. The decrease in total aboveground biomass in southern ecozones was more strongly influenced by the increase in heat-induced mortality, which killed young needleleaf seedlings, than by the negative effects of fires on mature tree biomass.

2.4.2 Forest management implications

The impacts of future climate change on the boreal forest of eastern Canada are likely to be a decrease in the proportion of needleleaf evergreen (softwood) species in southern regions, particularly *Picea* and *Pinus*, which would be partially replaced by an increase in the proportion of *Populus* PFT (Figure 3.5). This shift to broadleaf deciduous (hardwood) species dominance could be also translated into an increase in *Betula* spp., which were not included in the LPJ-LMfire parameterization. In reality, *Populus* spp. are species more restricted to fine-textured upland soils (Gower et al., 1997) that are only abundant in some parts of the study area (Chaste et al., 2018). Changes in species composition could also be concurrent with an overall reduction in forest density and the development of unforested areas. A major change in softwood stocks and productivity in the commercially important boreal forests of eastern Canada could have considerable impacts on the forest industry, since these are the main commercial timber species that are harvested in the country (Canadian Council of Forest Ministers, 2017). As previously mentioned in recent studies (McKenney et al., 2016; Taylor et al., 2017), our results suggest that traditional commercial reliance on softwood species in eastern Canada's boreal forests may become unsustainable in subsequent decades. Changes in management strategies focusing on harvest substitutions from softwood to hardwood species would need to be considered (Boulanger et al., 2017a). Some intensive silvicultural scenarios could help to increase forest productivity and maintain a sufficient level of softwood species in landscape mosaic, such as partial cutting or pre-commercial thinning (Bureau du forestier en chef, 2013). These silvicultural practices could favor young stands that are more productive than old stands, and decrease competition for space and light between species. Thus, they could facilitate regeneration of pre-established coniferous species and accelerate the transition from hardwood species dominance to softwood species dominance in the boreal forest (Bose et al., 2014; Prévost et al., 2010). Enrichment plantings of softwood species in natural forest or forest gaps could also be implemented (Bose et al., 2014; Prévost et al., 2010). It should be noted that these activities would also contribute to an increase in conductive forest fuel. This implies an additive hazard risk of wildfire in a context where the climate will become more favorable to their ignition and spread. It is to be understood that such land use planning must be coordinated with sectoral stakeholders, including communities and fire suppression agencies.

2.4.3 Uncertainties and limitations

Our results imply that climate change may have significant effects on the biomass of dominant species in eastern Canada's boreal forest, but it is important to recognise that these results are limited and should be interpreted carefully. Indeed, the changes that are expected in future climate and CO_2 concentrations that have been projected under both RCP scenarios still include a range of uncertainties that cannot be quantified by this present study, and the main trends of which may not be borne out in reality. Simulations that were performed with a multi-model ensemble of climate scenarios are considered to be more robust than with one climate scenario only, but the ensemble still does not guarantee that the mean state is realistic (Tebaldi and Knutti, 2007). Climate projections that were used in the present study had been corrected with observed data that were recorded by meteorological stations from 1951 to 2010 using an anomaly method to reduce bias in modeled climate data. However, this method is based upon the assumption that model biases are stationary over the entire period of simulations (Ivanov and Kotlarski, 2017), and that the frequency and magnitude of extreme weather events relative to baseline would remain constant through time (Terrier et al., 2013). Yet, it has been increasingly recognized that such an assumption is invalid. Indeed, some changes in extreme weather events have already been observed globally (Easterling et al., 2000). Moreover, in Canada, an increase in the frequency of extreme drought years is expected to occur, due to more frequent and persistent high-pressure blocking systems (Girardin and Mudelsee, 2008).

Although simulations of future fire activity in response to climate change include the feedback effects of vegetation changes on fire behavior, two important limitations must be noted. First, regeneration failures that are due to two successive fires in immature stands are not represented in LPJ-LMfire. The inclusion of such natural disturbance events in our simulations could further amplify the simulated trends in forest cover loss, biomass resource reduction and changes in forest composition. Also, LPJ-LMfire is not parameterized for ericaceous shrub species, which could potentially establish in areas where tree cover percentages would decrease following fire (Shafer et al., 2015). Shrub encroachment and expansion within a landscape ('shrubification') inhibits the regeneration of tree species and can retard the development of forests for up to a decade (Hewitt et al., 2016). Dense shrubs and grasses covers between tree stands are flammable ecosystems. They also would further influence the connectivity of fuel in tree stands available for burning and, therefore, increase the propagation of fires (Higuera et al., 2009). Thus, the increasing importance of shrubs and grasses could further delay forest regeneration and lead to increases in burned areas. Net biomass losses will occur across successive fire cycles (Kettridge et al., 2015) and progressively lead to the formation of stable non-forest ecosystems that will burn periodically. Consequently, the future decrease in annual area burned simulated by LPJ-LMfire is uncertain and may not be borne out in reality.

Further, it should be noted that feedbacks between land cover change and climate are not included in these simulations; given the large area and substantial changes that are simulated by LPJ-LMfire, important climate feedbacks could occur. It has been well documented that changes in boreal vegetation (e.g., tree density and species composition) can create feedbacks that influence the climate system (mitigating or exacerbating the climate warming trend) through changes in surface albedo and energy fluxes between land and atmosphere (Price et al., 2013; Euskirchen et al., 2016). Reduced tree cover could lead to an increase in albedo by exposing more snow-covered ground, which could ultimately reduce local warming trends (Loranty et al., 2013; Druel et al., 2017; Mykleby et al., 2017). Moreover, landscape shrubification could act as a positive feedback to climate warming because shrub species exhibit low albedo than snow-covered ground (Loranty et al., 2013). Conversely, an increase in proportion of young deciduous trees, which characteristically have a greater albedo than mature coniferous forests, could result in a negative biogeophysical feedback to climate warming (Euskirchen et al., 2016). The snow- and vegetation cover-albedo feedbacks on the climate system at high latitudes are often poorly represented in the current generation of global climate models (Loranty et al., 2013; Druel et al., 2017) and leads to uncertainties in projections of future climate change impacts on high latitude forests including those in Canada.

There are several processes that affect vegetation composition and distribution in Canadian boreal forests that are not simulated in LPJ-LMfire. These include, for example, peatland processes (Schneider et al., 2016), the regulation of successional dynamics by nitrogen availability (Trugman et al., 2016), and local adaptation of tree species to future climate (Housset et al., 2018). Other processes are simulated by the current version of LPJ-LMfire (Chaste et al., 2018), but in a simplified form: for instance, the requirement of fire heat to release seeds from serotinous cones of *Pinus* PFT was simulated by LPJ-LMfire by inhibiting seedling establishment during years without fire whereas seedling establishment of others PFT was not constrained by fire occurrence. Moreover, a number of key parameters that serve as inputs to LPJ-LMfire have strong effects on the establishment, growth, and mortality of PFTs. It has been demonstrated that uncertainties in these parameters contribute most to the total uncertainties of projections compared to climate uncertainties (Zaehle et al., 2005; Jiang et al., 2012).

The aforementioned model limitations are not unique to LPJ-LMfire (e.g. Prentice et al., 2011; Terrier et al., 2013; Shafer et al., 2015). Substantial efforts have been devoted worldwide to the parameterization of more complete processes or other factors (Fisher et al., 2018), including efforts to integrate biotic disturbances into DGVMs, such as those imposed by insect herbivory (e.g. Landry et al., 2015) or forest harvesting and management prescriptions (e.g. Bondeau et al., 2007). That being said, and in view of the uncertainties that are described above, our results are indicative of the impacts of future climate change on the boreal forests of eastern Canada, but they should not be seen as definitive statements. There is an urgent necessity for ensemble-based simulations so as to reduce uncertainties in predictions and to provide a solid basis for guiding forest management strategies.

2.5 Conclusions

In this study, we used the LPJ-LMfire dynamic vegetation model to simulate changes in biomass, composition, and fire frequency in the boreal forests of eastern Canada in response to climate change from 1950 to 2099. Two emission-forcing scenarios that were coupled with a large set of climate scenarios were used to simulate a broad range of variability in the response of vegetation and fires to climate change. While our study cannot directly quantify the role of wildfire on forest resources, we argue that the negative effects of warming temperatures on tree recruitment and mortality would be more important than the positive effects of warming and increasing atmospheric CO_2 concentrations and precipitation, especially in the southern ecozones. The impacts of climate change may lead to a shift in composition from softwood (coniferous needleleaf) to hardwood (deciduous broadleaf) species or even, to important forest cover losses in southern ecozones. This study helps to reduce uncertainties in our knowledge regarding the impacts of climate change and fire, and provides additional support for deployment of management strategies focusing on hardwood species.

Code availability: The source code of LPJ-LMfire is available at https://github.com/ARVE-Research/LPJ-LMfire/tree/v1.3 (Kaplan et al., 2018).

Acknowledgments

The study was made possible thanks to financial support that was provided by the European NEWFOREST project (PIRSES-GA-2013-612645), the Forest Complexity Modelling (FCM) program, and the NSERC Strategic and Discovery programs. Jed Kaplan was supported by the European Research Council (COEVOLVE 313797). This research was conducted as part of the International Associated Laboratory MONTABOR (LIA France-Canada) and the International Research Group on Cold Forests (CNRS). We thank NSERC (Natural Sciences and Engineering Research Council of Canada) and CFCAS for the funding of the development of the CRCM5. The authors are particularly grateful to Travis Logan of the Ouranos Consortium for help with computation of climatic models, Daniel Stubbs from Calcul Quebec and Compute Canada for help with the Fortran programming and server space facilities for running LPJ-LMfire, and Xiao Jing Guo for help with mapping and computation for this project. We also thank W.F.J. Parsons for English-language editing of the manuscript, and David Price and the two anonymous reviewers for comments on an earlier version.

References

Ali, A. A., Blarquez, O., Girardin, M. P., Hely, C., Tinquaut, F., El Guellab, A., Valsecchi, V., Terrier, A., Bremond, L., Genries, A., Gauthier, S., and Bergeron, Y. (2012). Control of the multimillennial wildfire size in boreal North America by spring climatic conditions. *Proceedings of the National Academy of Sciences USA*, 109(51):20966–20970, doi:10.1073/pnas.1203467109.

Allen, C. D., Macalady, A. K., Chenchouni, H., Bachelet, D., McDowell, N., Vennetier, M., Kitzberger, T., Rigling, A., Breshears, D. D., Hogg, E. H. T., Gonzalez, P., Fensham, R., Zhang, Z., Castro, J., Demidova, N., Lim, J.-H., Allard, G., Running, S. W., Semerci, A., and Cobb, N. (2010). A global overview of drought and heat-induced tree mortality reveals emerging climate change risks for forests. *Forest Ecology and Management*, 259(4):660–684, doi:10.1016/j.foreco.2009.09.001.

Arora, V. K., Scinocca, J. F., Boer, G. J., Christian, J. R., Denman, K. L., Flato, G. M., Kharin, V. V., Lee, W. G., and Merryfield, W. J. (2011). Carbon emission limits required to satisfy future representative concentration pathways of greenhouse gases. *Geophysical Research Letters*, 38(5):L05805, doi:10.1029/2010GL046270.

Bergeron, Y., Cyr, D., Girardin, M. P., and Carcaillet, C. (2010). Will climate change drive 21st century burn rates in Canadian boreal forest outside of its natural variability: collating global climate model experiments with sedimentary charcoal data. *International Journal of Wildland Fire*, 19(8):1127–1139, doi:10.1071/WF09092.

Bergeron, Y., Vijayakumar, D. B. I. P., Ouzennou, H., Raulier, F., Leduc, A., and Gauthier, S. (2017). Projections of future forest age class structure under the influence of fire and harvesting: implications for forest management in the boreal forest of eastern Canada. *Forestry: An International Journal of Forest Research*, 90:485–495, doi:10.1093/forestry/cpx022.

Bernier, P. Y., Gauthier, S., Jean, P.-O., Manka, F., Boulanger, Y., Beaudoin, A., and Guindon, L. (2016). Mapping local effects of forest properties on fire risk across Canada. *Forests*, 7(8):157.

Boiffin, J. and Munson, A. D. (2013). Three large fire years threaten resilience of closed crown black spruce forests in eastern Canada. *Ecosphere*, 4(5):1–20, doi:10.1890/ES13-00038.1.

Bondeau, A., Smith, P. C., Zaehle, S., Schaphoff, S., Lucht, W., Cramer, W., Gerten, D., Lotze-Campen, H., Müller, C., and Reichstein, M. (2007). Modelling the role of agriculture for the 20th century global terrestrial carbon balance. *Global Change Biology*, 13(3):679–706, doi:10.1111/j.1365-2486.2006.01305.x.

Bose, A. K., Harvey, B. D., and Brais, S. (2014). Sapling recruitment and mortality dynamics following partial harvesting in aspen-dominated mixedwoods in eastern Canada. *Forest ecology and management*, 329:37–48, doi:10.1016/j.foreco.2014.06.004.

Boucher, Y., Auger, I., Noël, J., Grondin, P., and Arseneault, D. (2017). Fire is a stronger driver of forest composition than logging in the boreal forest of eastern Canada. *Journal of Vegetation Science*, 28(1):57–68, doi:10.1111/jvs.12466.

Boulanger, Y., Gauthier, S., and Burton, P. J. (2014). A refinement of models projecting future Canadian fire regimes using homogeneous fire regime zones. *Canadian Journal of Forest Research*, 44(4):365–376, doi:10.1139/cjfr-2013-0372.

Boulanger, Y., Gauthier, S., Gray, D. R., Le Goff, H., Lefort, P., and Morissette, J. (2013). Fire regime zonation under current and future climate over eastern Canada. *Ecological applications*, 23(4):904–923.

Boulanger, Y., Girardin, M., Bernier, P. Y., Gauthier, S., Beaudoin, A., and Guindon, L. (2017a). Changes in mean forest age in Canada's forests could limit future increases in area burned but compromise potential harvestable conifer volumes. *Canadian Journal of Forest Research*, 47(6):755–764, doi:10.1139/cjfr-2016-0445.

Boulanger, Y., Taylor, A. R., Price, D. T., Cyr, D., McGarrigle, E., Rammer, W., Sainte-Marie, G., Beaudoin, A., Guindon, L., and Mansuy, N. (2017b). Climate change impacts on forest landscapes along the Canadian southern boreal forest transition zone. *Landscape Ecology*, 32(7):1415–1431, doi:10.1007/s10980-016-0421-7.

Brandt, J., Flannigan, M., Maynard, D., Thompson, I., and Volney, W. (2013). An introduction to Canada's boreal zone: ecosystem processes, health, sustainability, and environmental issues. *Environmental Reviews*, 21(4):207–226, doi:10.1139/er-2013-0040.

Brandt, J. P. (2009). The extent of the North American boreal zone. *Environmental Reviews*, 17:101–161, doi:10.1139/A09-004.

Bureau du forestier en chef (2013). Manuel de détermination des possibilités forestières 2013-2018. *Gouvernement du Québec, Roberval, Qc*, page 247.

Canadian Council of Forest Ministers (2017). National Forestry Database. Forest Fire Statistics by Province/Territory/Agency, 1990-2016, available from: http://nfdp.ccfm.org/data/compendium/ html/comp_31e.html,.

Chaste, E., Girardin, M. P., Kaplan, J. O., Portier, J., Bergeron, Y., and Hély, C. (2018). The pyrogeography of eastern boreal Canada from 1901 to 2012 simulated with the LPJ-LMfire model. *Biogeosciences*, 15(5):1273–1292, doi:10.5194/bg-15-1273-2018.

Chylek, P., Li, J., Dubey, M. K., Wang, M., and Lesins, G. (2011). Observed and model simulated 20th century Arctic temperature variability: Canadian Earth System Model CanESM2. *Atmos. Chem. Phys. Discuss.*, 2011:22893–22907, doi:10.5194/acpd-11-22893-2011.

Danneyrolles, V., Arseneault, D., and Bergeron, Y. (2016). Pre-industrial landscape composition patterns and post-industrial changes at the temperate-boreal forest interface in western Quebec, Canada. *Journal of Vegetation Science*, 27(3):470–481, doi:10.1111/jvs.12373.

De Bruijn, A., Gustafson, E. J., Sturtevant, B. R., Foster, J. R., Miranda, B. R., Lichti, N. I., and Jacobs, D. F. (2014). Toward more robust projections of forest landscape dynamics under novel environmental conditions: embedding PnET within LANDIS-II. *Ecological Modelling*, 287:44–57.

Drobyshev, I., Bergeron, Y., Girardin, M. P., Gauthier, S., Ols, C., and Ojal, J. (2017). Strong gradients in forest sensitivity to climate change revealed by dynamics of forest fire cycles in the post Little Ice Age era. *Journal of Geophysical Research: Biogeosciences*, 122(10):2605–2616, doi:10.1002/2017JG003826.

Druel, A., Peylin, P., Krinner, G., Ciais, P., Viovy, N., Peregon, A., Bastrikov, V., Kosykh, N., and Mironycheva-Tokareva, N. (2017). Towards a more detailed representation of high-latitude vegetation in the global land surface model ORCHIDEE (ORC-HL-VEGv1.0). *Geosci. Model Dev. Discuss.*, 2017:1–51, doi:10.5194/gmd-2017-65.

Easterling, D. R., Evans, J. L., Groisman, P. Y., Karl, T. R., Kunkel, K. E., and Ambenje, P. (2000). Observed Variability and Trends in Extreme Climate Events: A Brief Review. *Bulletin of the American Meteorological Society*, 81(3):417–425, doi:10.1175/1520-0477(2000)081<0417:OVATIE>2.3.CO;2.

Ecological Stratification Working Group (1996). A national ecological framework for Canada, available from: http://sis.agr.gc.ca/cansis/references/1996ew_a.html. Technical report.

Environment Canada (2013). National Climate Data and Information Archive, available from: http://climate.weatheroffice.gc.ca/.

Epstein, H. E., Yu, Q., Kaplan, J. O., and Lischke, H. (2007). Simulating future changes in arctic and subarctic vegetation. *Computing in Science & Engineering*, 9(4):12–23, doi:10.1109/MCSE.2007.84.

Euskirchen, E. S., Bennett, A. P., Breen, A. L., Genet, H., Lindgren, M. A., Kurkowski, T. A., McGuire, A. D., and Rupp, T. S. (2016). Consequences of changes in vegetation and snow cover for climate feedbacks in Alaska and northwest Canada. *Environmental Research Letters*, 11(10):105003, doi:10.1088/1748-9326/11/10/105003.

Fei, S., Desprez, J. M., Potter, K. M., Jo, I., Knott, J. A., and Oswalt, C. M. (2017). Divergence of species responses to climate change. *Science Advances*, 3(5):e1603055, doi:10.1126/sciadv.1603055.

Fisher, R. A., Koven, C. D., Anderegg, W. R. L., Christoffersen, B. O., Dietze, M. C., Farrior, C. E., Holm, J. A., Hurtt, G. C., Knox, R. G., Lawrence, P. J., Lichstein, J. W., Longo, M., Matheny, A. M., Medvigy, D., Muller-Landau, H. C., Powell, T. L., Serbin, S. P., Sato, H., Shuman, J. K., Smith, B., Trugman, A. T., Viskari, T., Verbeeck, H., Weng, E., Xu, C., Xu, X., Zhang, T., and Moorcroft, P. R. (2018). Vegetation demographics in Earth System Models: A review of progress and priorities. *Global Change Biology*, 24(1):35–54, doi:10.1111/gcb.13910.

Fisichelli, N. A., Frelich, L. E., and Reich, P. B. (2014). Temperate tree expansion into adjacent boreal forest patches facilitated by warmer temperatures. *Ecography*, 37(2):152–161, doi:10.1111/j.1600-0587.2013.00197.x.

Flannigan, M., Stocks, B., Turetsky, M., and Wotton, M. (2009). Impacts of climate change on fire activity and fire management in the circumboreal forest. *Global Change Biology*, 15(3):549–560, doi:10.1111/j.1365-2486.2008.01660.x.

Flannigan, M. D., Wotton, B. M., Marshall, G. A., Groot, W. J. d., Johnston, J., Jurko, N., and Cantin, A. S. (2016). Fuel moisture sensitivity to temperature and precipitation: climate change implications. *Climatic Change*, 134(1-2):59–71, doi:10.1007/s10584-015-1521-0.

Forkel, M., Carvalhais, N., Rodenbeck, C., Keeling, R., Heimann, M., Thonicke, K., Zaehle, S., and Reichstein, M. (2016). Enhanced seasonal CO_2 exchange caused by amplified plant productivity in northern ecosystems. *Science*, 351(6274):696–699, doi:10.1126/science.aac4971.

Friend, A. D., Lucht, W., Rademacher, T. T., Keribin, R., Betts, R., Cadule, P., Ciais, P., Clark, D. B., Dankers, R., Falloon, P. D., Ito, A., Kahana, R., Kleidon, A., Lomas, M. R., Nishina, K., Ostberg, S., Pavlick, R., Peylin, P., Schaphoff, S., Vuichard, N., Warszawski, L., Wiltshire, A., and Woodward, F. I. (2014). Carbon residence time dominates uncertainty in terrestrial vegetation responses to future climate and atmospheric CO_2. *Proceedings of the National Academy of Sciences*, 111(9):3280–3285, doi:10.1073/pnas.1222477110.

Gauthier, S., Bernier, P., Boulanger, Y., Guo, J., Guindon, L., Beaudoin, A., and Boucher, D. (2015a). Vulnerability of timber supply to projected changes in fire regime in Canada's managed forests. *Canadian Journal of Forest Research*, 45(11):1439–1447, doi:10.1139/cjfr-2015-0079.

Gauthier, S., Bernier, P., Burton, P. J., Edwards, J., Isaac, K., Isabel, N., Jayen, K., Le Goff, H., and Nelson, E. A. (2014). Climate change vulnerability and adaptation in the managed Canadian boreal forest. *Environmental Reviews*, 22(3):256–285, doi:10.1139/er-2013-0064.

Gauthier, S., Bernier, P., Kuuluvainen, T., Shvidenko, A. Z., and Schepaschenko, D. G. (2015b). Boreal forest health and global change. *Science*, 349(6250):819–822, doi:10.1126/science.aaa9092.

Giorgi, F., Jones, C., Asrar, G. R., and others (2009). Addressing climate information needs at the regional level: the CORDEX framework. *World Meteorological Organization (WMO) Bulletin*, 58(3):175.

Girardin, M. P., Ali, A. A., Carcaillet, C., Blarquez, O., Hély, C., Terrier, A., Genries, A., and Bergeron, Y. (2013a). Vegetation limits the impact of a warm climate on boreal wildfires. *The New Phytologist*, 199(4):1001–1011, doi:10.1111/nph.12322.

Girardin, M. P., Ali, A. A., Carcaillet, C., Gauthier, S., Hély, C., Le Goff, H., Terrier, A., and Bergeron, Y. (2013b). Fire in managed forests of eastern Canada: Risks and options. *Forest ecology and management*, 294:238–249, doi:10.1016/j.foreco.2012.07.005.

Girardin, M. P., Ali, A. A., Carcaillet, C., Mudelsee, M., Drobyshev, I., Hély, C., and Bergeron, Y. (2009). Heterogeneous response of circumboreal wildfire risk to climate change since the early 1900s. *Global Change Biology*, 15(11):2751–2769, doi:10.1111/j.1365-2486.2009.01869.x.

Girardin, M. P., Bernier, P. Y., Raulier, F., Tardif, J. C., Conciatori, F., and Guo, X. J. (2011). Testing for a CO_2 fertilization effect on growth of Canadian boreal forests. *Journal of Geophysical Research: Biogeosciences*, 116:G01012, doi:10.1029/2010JG001287.

Girardin, M. P., Bouriaud, O., Hogg, E. H., Kurz, W., Zimmermann, N. E., Metsaranta, J. M., Jong, R. d., Frank, D. C., Esper, J., Büntgen, U., Guo, X. J., and Bhatti, J. (2016a). No growth stimulation of Canada's boreal forest under half-century of combined warming and CO_2 fertilization. *Proceedings of the National Academy of Sciences*, 113(52):E8406–E8414, doi:10.1073/pnas.1610156113.

Girardin, M. P., Guo, X. J., De Jong, R., Kinnard, C., Bernier, P., and Raulier, F. (2014). Unusual forest growth decline in boreal North America covaries with the retreat of Arctic sea ice. *Global change biology*, 20(3):851–866, doi:10.1111/gcb.12400.

Girardin, M. P., Hogg, E. H., Bernier, P. Y., Kurz, W. A., Guo, X. J., and Cyr, G. (2016b). Negative impacts of high temperatures on growth of black spruce forests intensify with the anticipated climate warming. *Global change biology*, 22(2):627–643, doi:10.1111/gcb.13072.

Girardin, M. P. and Mudelsee, M. (2008). Past and future changes in Canadian boreal wildfire activity. *Ecological Applications*, 18(2):391–406, doi:10.1890/07-0747.1.

Girardin, M. P. and Wotton, B. M. (2009). Summer moisture and wildfire risks across Canada. *Journal of Applied Meteorology and Climatology*, 48(3):517–533, doi:10.1175/2008JAMC1996.1.

Gower, S. T., Vogel, J. G., Norman, J. M., Kucharik, C. J., Steele, S. J., and Stow, T. K. (1997). Carbon distribution and aboveground net primary production in aspen, jack pine, and black spruce stands in Saskatchewan and Manitoba, Canada. *Journal of Geophysical Research: Atmospheres*, 102(D24):29029–29041, doi:10.1029/97JD02317.

Hazeleger, W., Severijns, C., Semmler, T., Stefanescu, S., Yang, S., Wang, X., Wyser, K., Dutra, E., Baldasano, J. M., Bintanja, R., Bougeault, P., Caballero, R., Ekman, A. M. L., Christensen, J. H., van den Hurk, B., Jimenez, P., Jones, C., Kallberg, P., Koenigk, T., McGrath, R., Miranda, P., Van Noije, T., Palmer, T., Parodi, J. A., Schmith, T., Selten, F., Storelvmo, T., Sterl, A., Tapamo, H., Vancoppenolle, M., Viterbo, P., and Willén, U. (2010). EC-Earth: A Seamless Earth-System Prediction Approach in Action. *Bulletin of the American Meteorological Society*, 91(10):1357–1363, doi:10.1175/2010BAMS2877.1.

Hély, C., Bergeron, Y., and Flannigan, M. D. (2000). Effects of stand composition on fire hazard in mixed-wood Canadian boreal forest. *Journal of Vegetation Science*, 11(6):813–824, doi:10.2307/3236551.

Hély, C., Flannigan, M., Bergeron, Y., and McRae, D. (2001). Role of vegetation and weather on fire behavior in the Canadian mixedwood boreal forest using two fire behavior prediction systems. *Canadian Journal of Forest Research*, 31(3):430–441, doi:10.1139/cjfr-31-3-430.

Hély, C., Fortin, C. M.-J., Anderson, K. R., and Bergeron, Y. (2010). Landscape composition influences local pattern of fire size in the eastern Canadian boreal forest: role of weather and landscape mosaic on fire size distribution in mixedwood boreal forest using the Prescribed Fire Analysis System. *International Journal of Wildland Fire*, 19(8):1099–1109, doi:10.1071/WF09112.

Hember, R. A., Kurz, W. A., and Coops, N. C. (2017). Relationships between individual-tree mortality and water-balance variables indicate positive trends in water stress-induced tree mortality across North America. *Global change biology*, 23(4):1691–1710, doi:10.1111/gcb.13428.

Hengl, T., de Jesus, J. M., MacMillan, R. A., Batjes, N. H., Heuvelink, G. B. M., Ribeiro, E., Samuel-Rosa, A., Kempen, B., Leenaars, J. G. B., Walsh, M. G., and Gonzalez, M. R. (2014). SoilGrids1km – Global soil information based on automated mapping. *PLoS One*, 9(8):e105992, doi:10.1371/journal.pone.0105992.

Hewitt, R. E., Hollingsworth, T. N., Stuart Chapin III, F., and Lee Taylor, D. (2016). Fire-severity effects on plantâfungal interactions after a novel tundra wildfire disturbance: implications for arctic shrub and tree migration. *BMC Ecology*, 16:25, doi:10.1186/s12898-016-0075-y.

Higuera, P. E., Brubaker, L. B., Anderson, P. M., Hu Feng Sheng, and Brown Thomas A. (2009). Vegetation mediated the impacts of postglacial climate change on fire regimes in the south-central Brooks Range, Alaska. *Ecological Monographs*, 79(2):201–219, doi:10.1890/07-2019.1.

Hogg, E. H., Michaelian, M., Hook, T. I., and Undershultz, M. E. (2017). Recent climatic drying leads to age-independent growth reductions of white spruce stands in western Canada. *Global change biology*, doi:10.1111/gcb.13795.

Housset, J. M., Nadeau, S., Isabel, N., Depardieu, C., Duchesne, I., Lenz, P., and Girardin, M. P. (2018). Tree rings provide a new class of phenotypes for genetic associations that foster insights into adaptation of conifers to climate change. *New Phytologist*, doi:10.1111/nph.14968.

IPCC (2013). *Climate Change 2013 - The Physical Science Basis: Working Group I Contribution to the Fifth Assessment Report of the Intergovernmental Panel on Climate Change*. [Stocker, T.F., D. Qin, G.-K. Plattner, M. Tignor, S.K. Allen, J. Boschung, A. Nauels, Y. Xia, V. Bex and P.M. Midgley (eds.)]. Cambridge University Press, Cambridge, United Kingdom and New York, NY, USA., Cambridge.

IPCC (2014). *Climate Change 2014: Synthesis Report . Contribution of Working Groups I, II and III to the Fifth Assessment Report of the Intergovernmental Panel on Climate Change*. [Core Writing Team, R.K. Pachauri and L.A. Meyer (eds.)]. IPCC, Geneva, Switzerland.

Ivanov, M. A. and Kotlarski, S. (2017). Assessing distribution-based climate model bias correction methods over an alpine domain: added value and limitations. *International Journal of Climatology*, 37(5):2633–2653, doi:10.1002/joc.4870.

Jiang, Y., Zhuang, Q., Schaphoff, S., Sitch, S., Sokolov, A., Kicklighter, D., and Melillo, J. (2012). Uncertainty analysis of vegetation distribution in the northern high latitudes during the 21st century with a dynamic vegetation model. *Ecology and Evolution*, 2(3):593–614, doi:10.1002/ece3.85.

Kaplan, J. O., Pfeiffer, M., and Chaste, E. (2018). ARVE-Research/LPJ-LMfire: LPJ-LMfire (version v1.3), Zenodo. doi:10.5281/zenodo.1184589.

Kettridge, N., Turetsky, M. R., Sherwood, J. H., Thompson, D. K., Miller, C., Benscoter, B. W., Flannigan, M. D., Wotton, B., and Waddington, J. M. (2015). Moderate drop in water table increases peatland vulnerability to post-fire regime shift. *Scientific Reports*, 5:8063.

Krause, A., Kloster, S., Wilkenskjeld, S., and Paeth, H. (2014). The sensitivity of global wildfires to simulated past, present, and future lightning frequency. *Journal of Geophysical Research: Biogeosciences*, 119(3):312–322, doi:10.1002/2013JG002502.

Krinner, G., Viovy, N., de Noblet-Ducoudré, N., Ogée, J., Polcher, J., Friedlingstein, P., Ciais, P., Sitch, S., and Prentice, I. C. (2005). A dynamic global vegetation model for studies of the coupled atmosphere-biosphere system. *Global Biogeochemical Cycles*, 19(1), doi:10.1029/2003GB002199.

Kucharik, C. J., Foley, J. A., Delire, C., Fisher, V. A., Coe, M. T., Lenters, J. D., Young-Molling, C., Ramankutty, N., Norman, J. M., and Gower, S. T. (2000). Testing the performance of a dynamic global ecosystem model: water balance, carbon balance, and vegetation structure. *Global Biogeochemical Cycles*, 14(3):795–825, doi:10.1029/1999GB001138.

Landry, J.-S., Price, D. T., Ramankutty, N., Parrott, L., and Matthews, H. D. (2015). Implementation of a Marauding Insect Module (MIM, version 1.0) in the Integrated BIosphere Simulator (IBIS, version 2.6 b4) Dynamic Vegetation-Land Surface Model. *Geoscientific Model Development Discussions*, 8(12), doi:10.5194/gmd-9-1243-2016.

Lemprière, T., Bernier, P., Carroll, A., Flannigan, M., Gilsenan, R., McKenney, D., Hogg, E., Pedlar, J., Blain, D., et al. (2008). The importance of forest sector adaptation to climate change. *Natural Resources Canada, Canadian Forest Service, Northern Forestry Centre. Edmonton, Alta. Inf. Rep. NOR-X-416E.*

Loranty, M. M., Berner, L. T., Goetz, S. J., Jin, Y., and Randerson, J. T. (2013). Vegetation controls on northern high latitude snow-albedo feedback: observations and CMIP5 model simulations. *Global Change Biology*, 20(2):594–606, doi:10.1111/gcb.12391.

Martynov, A., Laprise, R., Sushama, L., Winger, K., Separovic, L., and Dugas, B. (2013). Reanalysis-driven climate simulation over CORDEX North America domain using the Canadian Regional Climate Model, version 5: model performance evaluation. *Climate dynamics*, 41(11-12):2973–3005, doi:10.1007/s00382-013-1778-9.

McKenney, D. W., Yemshanov, D., Pedlar, J. H., Allen, D. J., Lawrence, K. M., Hope, E., Lu, B., and Eddy, B. (2016). Canada's timber supply: current status and future prospects under a changing climate. Information Report GLC-X-15.

Mearns, L. O., Hulme, M., Carter, T. R., Leemans, R., Lal, M., Whetton, P., Hay, L., Jones, R. N., Kittel, T., Smith, J., and Wilby, R. (2001). Climate scenario development. In *Climate change 2001: the science of climate change*, pages 739–768. Cambrigde University Press, Cambridge.

Meinshausen, M., Smith, S. J., Calvin, K., Daniel, J. S., Kainuma, M. L. T., Lamarque, J.-F., Matsumoto, K., Montzka, S. A., Raper, S. C. B., Riahi, K., Thomson, A., Velders, G. J. M., and Vuuren, D. P. P. v. (2011). The RCP greenhouse gas concentrations and their extensions from 1765 to 2300. *Climatic Change*, 109(1-2):213, doi:10.1007/s10584-011-0156-z.

Mykleby, P. M., Snyder, P. K., and Twine, T. E. (2017). Quantifying the trade-off between carbon sequestration and albedo in midlatitude and high-latitude North American forests. *Geophysical Research Letters*, 44(5):2016GL071459, doi:10.1002/2016GL071459.

Natural Resources Canada (2010). Geobase - National hydro network, geogratis, available from: http://ftp.geogratis.gc.ca/pub/nrcan_rncan/vector/geobase_nhn_rhn/.

Nock, C. A., Vogt, R. J., and Beisner, B. E. (2016). Functional Traits. In *eLS*, Major Reference Works, pages 1–8. John Wiley & Sons, Ltd, Chichester edition.

Norby, R. J., DeLucia, E. H., Gielen, B., Calfapietra, C., Giardina, C. P., King, J. S., Ledford, J., McCarthy, H. R., Moore, D. J. P., Ceulemans, R., De Angelis, P., Finzi, A. C., Karnosky, D. F., Kubiske, M. E., Lukac, M., Pregitzer, K. S., Scarascia-Mugnozza, G. E., Schlesinger, W. H., and Oren, R. (2005). Forest response to elevated CO_2 is conserved across a broad range of productivity. *Proceedings of the National Academy of Sciences, USA*, 102(50):18052–18056, doi:10.1073/pnas.0509478102.

Norby, R. J., Warren, J. M., Iversen, C. M., Medlyn, B. E., and McMurtrie, R. E. (2010). CO_2 enhancement of forest productivity constrained by limited nitrogen availability. *Proceedings of the National Academy of Sciences*, 107(45):19368–19373, doi:10.1073/pnas.1006463107.

Orville, R. E., Huffines, G. R., Burrows, W. R., and Cummins, K. L. (2011). The North American Lightning Detection Network (NALDN) - Analysis of flash data: 2001â09. *Monthly Weather Review*, 139(5):1305–1322, doi:10.1175/2010MWR3452.1.

Pearson, R. G. and Dawson, T. P. (2003). Predicting the impacts of climate change on the distribution of species: are bioclimate envelope models useful? *Global Ecology and Biogeography*, 12(5):361–371, doi:10.1046/j.1466-822X.2003.00042.x.

Perera, A. H., Ouellette, M., Cui, W., Drescher, M., Boychuk, D., et al. (2008). BFOLDS 1.0: a spatial simulation model for exploring large scale fire regimes and succession in boreal forest landscapes. *Forest Research Report-Ontario Forest Research Institute*, (152).

Peterson, D., Wang, J., Ichoku, C., and Remer, L. A. (2010). Effects of lightning and other meteorological factors on fire activity in the North American boreal forest: implications for fire weather forecasting. *Atmospheric Chemistry and Physics*, 10(14):6873–6888, doi:10.5194/acp-10-6873-2010.

Pfeiffer, M., Spessa, A., and Kaplan, J. O. (2013). A model for global biomass burning in preindustrial time: LPJ-LMfire (v1. 0). *Geoscientific Model Development*, 6(3):643–685, doi:10.5194/gmd-6-643-2013.

Prentice, I. C., Kelley, D. I., Foster, P. N., Friedlingstein, P., Harrison, S. P., and Bartlein, P. J. (2011). Modeling fire and the terrestrial carbon balance. *Global Biogeochemical Cycles*, 25(3):GB3005, doi:10.1029/2010GB003906.

Prévost, M., Raymond, P., and Lussier, J.-M. (2010). Regeneration dynamics after patch cutting and scarification in yellow birch-conifer stands. *Canadian journal of forest research*, 40(2):357–369, doi:10.1139/X09-192.

Price, D. T., Alfaro, R. I., Brown, K. J., Flannigan, M. D., Fleming, R. A., Hogg, E. H., Girardin, M. P., Lakusta, T., Johnston, M., McKenney, D. W., Pedlar, J. H., Stratton, T., Sturrock, R. N., Thompson, I. D., Trofymow, J. A., and Venier, L. A. (2013). Anticipating the consequences of climate change for Canada's boreal forest ecosystems. *Environmental Reviews*, 21(4):322–365, doi:10.1139/er-2013-0042.

Richardson, A. D., Andy Black, T., Ciais, P., Delbart, N., Friedl, M. A., Gobron, N., Hollinger, D. Y., Kutsch, W. L., Longdoz, B., Luyssaert, S., et al. (2010). Influence of spring and autumn phenological transitions on forest ecosystem productivity. *Philosophical Transactions of the Royal Society B: Biological Sciences*, 365(1555):3227–3246.

Rogers, B. M., Solvik, K., Hogg, E. H., Ju, J., Masek, J. G., Michaelian, M., Berner, L. T., and Goetz, S. J. (2018). Detecting early warning signals of tree mortality in boreal North America using multi-scale satellite data. *Global change biology*, doi:10.1111/gcb.14107.

Romps, D. M., Seeley, J. T., Vollaro, D., and Molinari, J. (2014). Projected increase in lightning strikes in the United States due to global warming. *Science*, 346(6211):851–854, doi:10.1126/science.1259100.

Samuelsson, P., Jones, C. G., Willén, U., Ullerstig, A., Gollvik, S., Hansson, U. L. F., Jansson, C., Kjellström, E., Nikulin, G., and Wyser, K. (2011). The Rossby Centre Regional Climate model RCA3: model description and performance. *Tellus A*, 63(1):4–23, doi:10.1111/j.1600-0870.2010.00478.x.

Schneider, R. R., Devito, K., Kettridge, N., and Bayne, E. (2016). Moving beyond bioclimatic envelope models: integrating upland forest and peatland processes to predict ecosystem transitions under climate change in the western Canadian boreal plain. *Ecohydrology*, 9(6):899–908, doi:10.1002/eco.1707.

Scinocca, J. F., Kharin, V. V., Jiao, Y., Qian, M. W., Lazare, M., Solheim, L., Flato, G. M., Biner, S., Desgagne, M., and Dugas, B. (2015). Coordinated Global and Regional Climate Modeling. *Journal of Climate*, 29(1):17–35, doi:10.1175/JCLI-D-15-0161.1.

Separovic, L., Alexandru, A., Laprise, R., Martynov, A., Sushama, L., Winger, K., Tete, K., and Valin, M. (2013). Present climate and climate change over North America as simulated by the fifth-generation Canadian regional climate model. *Climate dynamics*, 41(11-12):3167–3201, doi:10.1007/s00382-013-1737-5.

Shafer, S. L., Bartlein, P. J., Gray, E. M., and Pelltier, R. T. (2015). Projected Future Vegetation Changes for the Northwest United States and Southwest Canada at a Fine Spatial Resolution Using a Dynamic Global Vegetation Model. *PLOS ONE*, 10(10):e0138759, doi:10.1371/journal.pone.0138759.

Silva, L. C., Anand, M., and Leithead, M. D. (2010). Recent widespread tree growth decline despite increasing atmospheric CO_2. *PLoS One*, 5(7):e11543, doi:10.1371/journal.pone.0011543.

Sitch, S., Smith, B., Prentice, I. C., Arneth, A., Bondeau, A., Cramer, W., Kaplan, J. O., Levis, S., Lucht, W., Sykes, M. T., Thonicke, K., and Venevsky, S. (2003). Evaluation of ecosystem dynamics, plant geography and terrestrial carbon cycling in the LPJ dynamic global vegetation model. *Global Change Biology*, 9(2):161–185, doi:10.1046/j.1365-2486.2003.00569.x.

Smith, B., Prentice, I. C., and Sykes, M. T. (2001). Representation of vegetation dynamics in the modelling of terrestrial ecosystems: comparing two contrasting approaches within European climate space. *Global Ecology and Biogeography*, 10(6):621–637, doi:10.1046/j.1466-822X.2001.t01-1-00256.x.

Smith, W. K., Reed, S. C., Cleveland, C. C., Ballantyne, A. P., Anderegg, W. R., Wieder, W. R., Liu, Y. Y., and Running, S. W. (2016). Large divergence of satellite and Earth system model estimates of global terrestrial CO_2 fertilization. *Nature Climate Change*, 6(3):306–310, doi:10.1038/nclimate2879.

Stocks, B. J., Mason, J. A., Todd, J. B., Bosch, E. M., Wotton, B. M., Amiro, B. D., Flannigan, M. D., Hirsch, K. G., Logan, K. A., Martell, D. L., and Skinner, W. R. (2003). Large forest fires in Canada, 1959-1997. *Journal of Geophysical Research: Atmospheres*, 107(D1):8149, doi:10.1029/2001JD000484.

Tang, G., Beckage, B., Smith, B., and Miller, P. A. (2010). Estimating potential forest NPP, biomass and their climatic sensitivity in New England using a dynamic ecosystem model. *Ecosphere*, 1(6):1–20, doi:10.1890/ES10-00087.1.

Taylor, A. R., Boulanger, Y., Price, D. T., Cyr, D., McGarrigle, E., Rammer, W., and Kershaw, J. A. (2017). Rapid 21st century climate change projected to shift composition and growth of Canada's Acadian Forest Region. *Forest Ecology and Management*, 405(Supplement C):284–294, doi:10.1016/j.foreco.2017.07.033.

Tebaldi, C. and Knutti, R. (2007). The use of the multi-model ensemble in probabilistic climate projections. *Philosophical Transactions of the Royal Society of London A: Mathematical, Physical and Engineering Sciences*, 365(1857):2053–2075, doi:10.1098/rsta.2007.2076.

Terrier, A., Girardin, M. P., Cantin, A., Groot, W. J., Anyomi, K. A., Gauthier, S., and Bergeron, Y. (2014). Disturbance legacies and paludification mediate the ecological impact of an intensifying wildfire regime in the Clay Belt boreal forest of eastern North America. *Journal of Vegetation Science*, 26(3):588–602, doi:10.1111/jvs.12250/full.

Terrier, A., Girardin, M. P., Périé, C., Legendre, P., and Bergeron, Y. (2013). Potential changes in forest composition could reduce impacts of climate change on boreal wildfires. *Ecological Applications*, 23(1):21–35, doi:10.1890/12-0425.1.

Thonicke, K., Spessa, A., Prentice, I. C., Harrison, S. P., Dong, L., and Carmona-Moreno, C. (2010). The influence of vegetation, fire spread and fire behaviour on biomass burning and trace gas emissions: results from a process-based model. *Biogeosciences*, 7(6):1991–2011, doi:10.5194/bg-7-1991-2010.

Trugman, A. T., Fenton, N. J., Bergeron, Y., Xu, X., Welp, L. R., and Medvigy, D. (2016). Climate, soil organic layer, and nitrogen jointly drive forest development after fire in the North American boreal zone. *Journal of Advances in Modeling Earth Systems*, 8(3):1180–1209, doi:10.1002/2015MS000576.

Van Wagner, C. E. (1987). *Development and structure of the Canadian Forest Fire Weather Index System*. available from: https://cfs.nrcan.gc.ca/publications?id=19927.

Veraverbeke, S., Rogers, B. M., Goulden, M. L., Jandt, R. R., Miller, C. E., Wiggins, E. B., and Randerson, J. T. (2017). Lightning as a major driver of recent large fire years in North American boreal forests. *Nature Climate Change*, 7(7):529.

Verheijen, L., Brövkin, V., Aerts, R., Bonisch, G., Cornelissen, J. H., Kattge, J., Reich, P. B., Wright, I. J., Van Bodegom, P., et al. (2013). Impacts of trait variation through observed trait-climate relationships on performance of an Earth system model: a conceptual analysis. *Biogeosciences*, 10:5497–5515.

Vuuren, D. P. v., Edmonds, J., Kainuma, M., Riahi, K., Thomson, A., Hibbard, K., Hurtt, G. C., Kram, T., Krey, V., Lamarque, J.-F., Masui, T., Meinshausen, M., Nakicenovic, N., Smith, S. J., and Rose, S. K. (2011). The representative concentration pathways: an overview. *Climatic Change*, 109(1-2):5, doi:10.1007/s10584-011-0148-z.

Wang, X., Parisien, M.-A., Taylor, S. W., Candau, J.-N., Stralberg, D., Marshall, G. A., Little, J. M., and Flannigan, M. D. (2017). Projected changes in daily fire spread across Canada over the next century. *Environmental Research Letters*, 12(2):025005, doi:10.1088/1748-9326/aa5835.

Wang, X., Thompson, D. K., Marshall, G. A., Tymstra, C., Carr, R., and Flannigan, M. D. (2015). Increasing frequency of extreme fire weather in Canada with climate change. *Climatic Change*, 130(4):573–586, doi:10.1007/s10584-015-1375-5.

Wotton, B. M., Flannigan, M. D., and Marshall, G. A. (2017). Potential climate change impacts on fire intensity and key wildfire suppression thresholds in Canada. *Environmental Research Letters*, 12(9):095003, doi:10.1088/1748-9326/aa7e6e.

Wullschleger, S. D., Epstein, H. E., Box, E. O., Euskirchen, E. S., Goswami, S., Iversen, C. M., Kattge, J., Norby, R. J., van Bodegom, P. M., and Xu, X. (2014). Plant functional types in Earth system models: past experiences and future directions for application of dynamic vegetation models in high-latitude ecosystems. *Annals of botany*, 114(1):1–16.

Zaehle, S., Sitch, S., Smith, B., and Hatterman, F. (2005). Effects of parameter uncertainties on the modeling of terrestrial biosphere dynamics. *Global Biogeochemical Cycles*, 19(3):GB3020, doi:10.1029/2004GB002395.

Zhang, J., Huang, S., and He, F. (2015). Half-century evidence from western Canada shows forest dynamics are primarily driven by competition followed by climate. *Proceedings of the National Academy of Sciences*, 112(13):4009–4014, doi:10.1073/pnas.1420844112.

Zhang, X., Vincent, L. A., Hogg, W., and Niitsoo, A. (2000). Temperature and precipitation trends in Canada during the 20th century. *Atmosphere-ocean*, 38(3):395–429.

Supplementary materials

Supplement S3.1. The LPJ-LMfire model functioning

This section describes the LPJ-LMfire model functioning. LPJ-LMfire is a modified version of the LPJ-SPITFIRE model that combines the dynamic global vegetation model LPJ-DGVM (Sitch et al., 2003) and the process-based fire regime model SPITFIRE (Thonicke et al., 2010).

1. LPJ-LMfire Plant functional types (PFTs)

Vegetation in a grid cell is described in terms of the fractional coverage of populations of different plant functional types (PFTs). Each PFT is represented by a single average individual (I_m) and is associated to a population density (number of I_m per unit area, *n*; Figure S3.1a) and an area of soil covered by the foliage of an I_m (FPC, 'Foliar projective cover'; Figure S3.1a). This notion of average individual means that all individuals in a given PFT population are represented by the same individual which is defined by a set of key parameters (Figure S3.1b); each one corresponds to the average of this parameter for all individuals regardless of the environment in which they develop and their stages of development (Figure S3.1c).

The total number of PFT-specific parameters is 53. These define the morphology (e.g., maximum crown area), phenology (e.g., evergreen or deciduous leaves), dynamics (e.g., maximum rate establishment of new individuals) and bioclimatic limits (e.g. minimum temperature of the coldest month). PFT-specific parameters of an I_m are scaled to the pixel by multiplying them by the population density *n* and the FPC in some case. For example, the cover percentage of each PFT is obtained by multiplying the FPC by the average crown surface of an average individual and the population density *n* (Figure S3.1a).

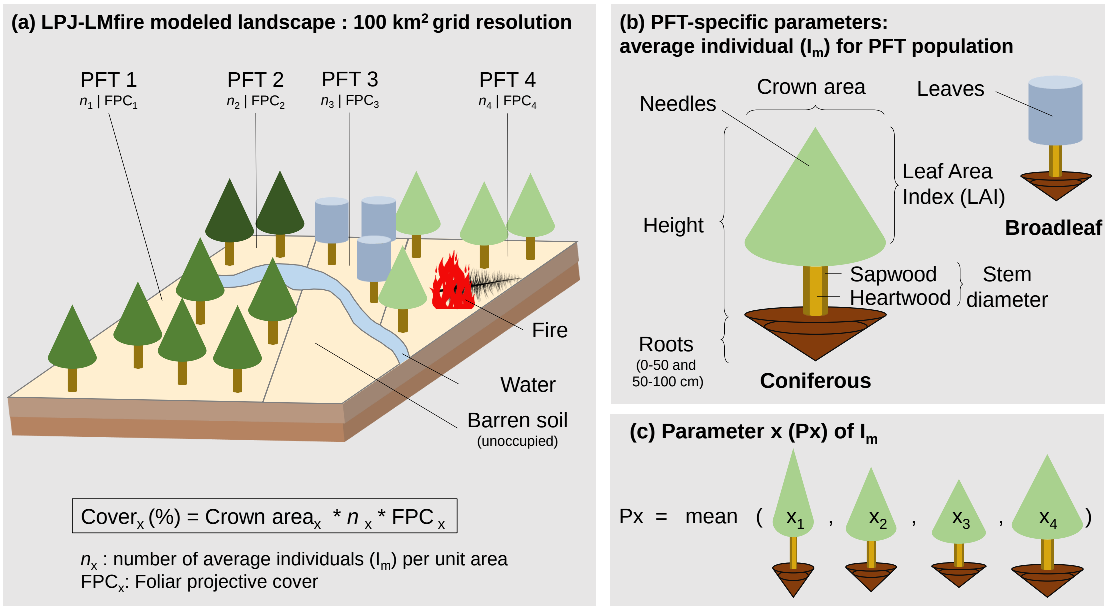

Figure S3.1. Schematic view of the PFT population simulation process in LPJ-LMfire for a given pixel (adapted from Smith (2001)). Leaf Area Index (LAI) is a dimensionless parameter that expresses the leaf area of an average individual (I_m).

A pixel corresponds to a mosaic of PFTs cover percentage, bare ground area percentage and water area percentage (Figure S3.1a); the sum of all of these covers percentages cannot exceed 100% on a given pixel. PFTs covers are distinct from each other on a given pixel which means that there can be no vertical overlap among PFTs. However, all PFTs are not necessarily represented on each pixel and one or more PFTs could be absent on a given pixel.

2. Input data sets (PFTs)

Several suitable input data sets are required to drive the LPJ-LMfire model: (i) monthly maps of climate conditions, (ii) maps of environmental constraints, (iii) annual atmospheric CO_2 concentrations, (iv) a list of PFT-specific parameters values, and if possible, (v) maps for anthropogenic land uses (Figure S3.2a). It should be noted that anthropogenic disturbances were not considered in this study due to lack of spatially explicit data covering a sufficient period in Canada. Monthly maps of climate conditions correspond to monthly mean temperature (°C), diurnal temperature range (°C), precipitation (mm), number of days per month with precipitation, wind velocities ($m.s^{-1}$), total cloud cover percentage and lightning flashes densities ($number.day^{-1}.km^{-2}$) (Figure S3.2a). Monthly maps of climate conditions are given as inputs to the LPJ-LMfire model over the analyzed time period, but also over a spin-up period (approximately equal to 1000 years) in order to fill carbon pools and to simulate vegetation in equilibrium with climate and disturbances (Smith et al. 2001). It should be noted that LPJ-LMfire uses a weather generator to disaggregate monthly climate variables to daily values (Pfeiffer et al., 2013). Maps of environmental constraints correspond to static maps of soil particle size distribution (%), volume fraction of coarse fragments (%), elevation (meters), slope (degrees), and water fraction (Figure S3.2a). Non-spatialized atmospheric CO_2 concentrations are given as input to the LPJ-LMfire model at the annual time step.

3. Simulated processes

This section is a short resume of processes calculated in the LPJ-DGVM model (Figure S3.2b), further details about the equations used to represent each process could be found in Sitch et al. (2003). Daily carbon uptake is through photosynthesis calculated as a function of absorbed active radiation, temperature, day-length and canopy conductance, and derived from the Farquhar photosynthesis model (for furthers details see Sitch et al., 2003; Smith, 2001). Atmospheric CO_2 concentration affects net primary productivity (NPP) through stomatal regulation during photosynthesis (Sitch et al., 2003). Soil maps given as input to the model are used to derive texture-related parameters governing the soil hydrology and thermal diffusivity of the soil. Soil hydrology is calculated for two soil layers with different thickness (constant in time), whose the amount of water is updated daily taking into account rainfall, percolation, evapotranspiration, run off and snowmelt. PFT maintenance respiration is calculated daily based on the tissue specific

Figure S3.2. Schematic view of the LPJ-LMfire model functioning and the input dataset given in the model

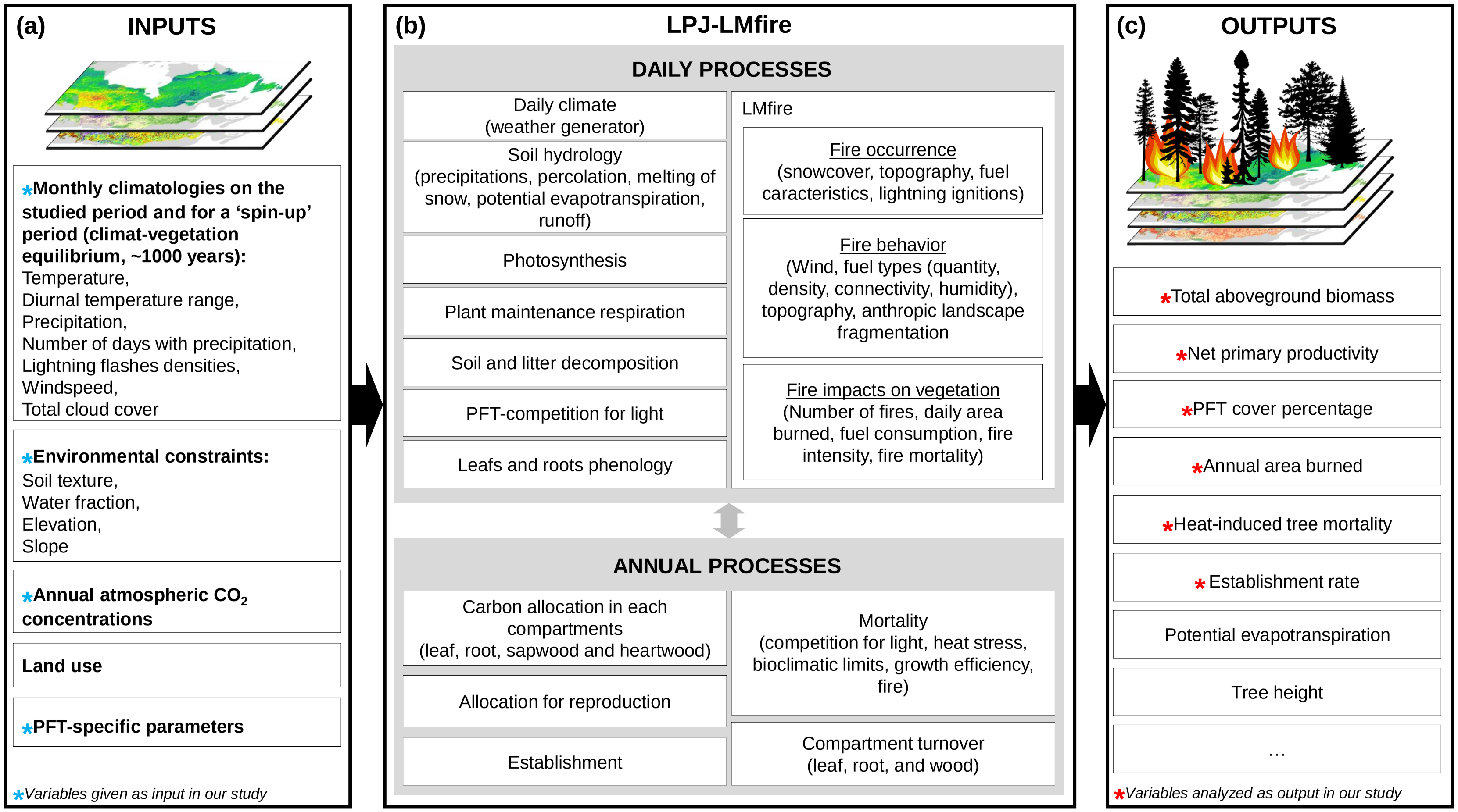

C:N ratio, temperature, phenology and tissue biomass. Net primary productivity of average individuals is calculated at the end of each simulation year and corresponds to the net carbon uptake from photosynthesis minus the carbon costs of maintenance respiration and reproduction. Annual net primary productivity is allocated to three tissues pools (leaves, sapwood and roots) adjusted so that four allometric equations, or 'constraints', which control the structural development of the average individual, remain satisfied (e.g. highest carbon allocation in roots than in leaves during periods of water limitation). At the same time, a proportion of the existing sapwood is transferred to the non-living heartwood pool. Establishment of new individuals in a given PFT is implemented annually by increasing the density of the PFT population and adjusting the mass and structure of Im to reflect the new population state. Density of establishment depends on unoccupied pixel area in order to take into account competition for light and space. PFT population mortality can result from light competition, heat stress, excess of bioclimatic limits, low growth efficiency and fire damage. Biomass of dead individuals is transferred annually to the litter pools according to PFT-specific parameters.

Supplement S3.2. Climate scenarios

Table S3.1. Mean changes in temperature (°C) and precipitation (%) for 1981-2010, 2011-2040, 2041-2070 and 2071-2100 (respectively separated by a slash) compared to the baseline climate of 1951-1980 across six ecozones in eastern Canada under six climate scenarios used in the study. Ecozones are the Boreal Plain (BP), the Boreal Shield West (BSW), the Boreal Shield East (BSE), the Taiga Shield West (TSW), the Hudson Plain (HP), and the Taiga Shield East (TSE).

Climate scenarios			Ecozones						Total average area
RCP	Name attributed		BP	BSW	TSW	HP	BSE	TSE	
RCP 4.5									
	CCC	T°C	0.6 / 2.0 / 3.5 / 4.4	0.7 / 2.0 / 3.7 / 4.6	0.9 / 2.4 / 4.2 / 5.2	0.8 / 2.3 / 4.4 / 5.3	0.8 / 2.2 / 4.0 / 4.6	1.0 / 2.6 / 4.6 / 5.2	0.8 / 2.2 / 4.1 / 4.9
		Pre	-1.1 / 3.6 / 11.8 / 8.4	-0.4 / 3.5 / 12.3 / 13.5	1.3 / 9.7 / 19.3 / 19.8	2.5 / 4.7 / 16.1 / 19.5	3.4 / 10.4 / 14.1 / 18.2	11.0 / 18.1 / 24.9 / 31.2	2.8 / 8.4 / 16.4 / 18.4
	CRS	T°C	0.5/ 2.2 / 3.9 / 4.6	0.6 / 2.1 / 3.9 / 4.5	0.7 / 2.6 / 4.5 / 5.2	0.6 / 2.3 / 4.4 / 5.1	0.7 / 2.1 / 3.9 / 4.5	0.9 / 2.6 / 4.6 / 5.3	0.7 / 2.3 / 4.2 / 4.9
		Pre	5.0 / 5.1 / 18.4 / 22.7	2.0 / 5.6 / 14.1 / 17.2	1.8 / 5.8 / 19.5 / 21.9	1.1 / 3.8 / 14.1 / 20.6	2.6 / 8.7 / 13.8 / 16.9	5.0 / 12.0 / 22.4 / 28.6	2.9 / 6.8 / 17.0 / 21.3
	BRS	T°C	0.4 / 1.9 / 2.7 / 3.6	0.5 / 1.9 / 2.7 / 3.6	0.4 / 2.1 / 3.1 / 4.5	0.5 / 2.0 / 2.9 / 3.8	0.5 / 1.8 / 2.5 / 3.1	0.7 / 2.1 / 3.0 / 3.8	0.5 / 2.0 / 2.8 / 3.7
		Pre	10.6 / 9.8 / 15.0 / 14.6	7.9 / 10.6 / 15.8 / 14.7	11.1 / 15.3 / 20.7 / 23.6	7.0 / 12.3 / 18.8 / 16.7	2.5 / 8.8 / 12.3 / 11.0	4.2 / 13.3 / 20.6 / 20.5	7.2 / 11.7 / 17.2 / 16.9
RCP 8.5									
	CCC	T°C	0.7 / 2.4 / 4.1 / 7.1	0.8 / 2.5 / 4.3 / 7.2	0.9 / 3.0 / 5.1 / 8.5	0.9 / 2.9 / 4.9 / 8.2	0.8 / 2.6 / 4.5 / 7.2	0.9 / 3.0 / 5.2 / 8.2	0.9 / 2.7 / 4.7 / 7.7
		Pre	-4.0 / 11.5 / 14.2 / 18.1	-0.9 / 8.8 / 13.7 / 20.1	-2.0 / 9.5 / 17.0 / 34.3	2.0 / 11.5 / 17.7 / 25.2	2.3 / 8.6 / 19.7 / 25.2	10.6 / 19.3 / 30.3 / 42.2	1.3 / 11.5 / 18.8 / 27.5
	CRS	T°C	0.6 / 2.8 / 4.8 / 7.9	0.7 / 2.7 / 4.7 / 7.6	0.8 / 3.3 / 5.5 / 8.5	0.8 / 3.0 / 5.3 / 8.6	0.8 / 2.6 / 4.7 / 7.2	0.9 / 3.1 / 5.5 / 8.5	0.9 / 3.1 / 5.5 / 8.5
		Pre	3.3 / 13.4 / 26.0 / 23.7	1.4 / 8.1 / 18.3 / 21.8	-0.6 / 14.3 / 25.9 / 39.9	0.0 / 9.8 / 16.8 / 24.3	1.3 / 7.8 / 15.2 / 23.5	5.1 / 15.6 / 25.5 / 39.8	1.7 / 11.5 / 21.3 / 28.8
	BRS	T°C	0.5 / 1.8 / 4.1 / 6.7	0.6 / 1.8 / 4.0 / 6.5	0.6 / 2.1 / 4.8 / 7.8	0.6 / 2.0 / 4.3 / 7.0	0.5 / 1.8 / 3.6 / 5.7	0.6 / 2.1 / 4.2 / 6.8	0.6 / 1.9 / 4.2 / 6.8
		Pre	9.0 / 7.3 / 19.1 / 25.7	5.9 / 8.8 / 17.2 / 26.0	10.8 / 15.0 / 29.3 / 43.7	5.5 / 11.9 / 21.1 / 33.5	2.9 / 9.5 / 15.2 / 23.1	5.1 / 14.4 / 25.8 / 36.8	6.5 / 11.1 / 21.3 / 31.5
	Mean	T°C	0.5 / 2.2 / 3.8 / 5.7	0.6 / 2.2 / 3.9 / 5.7	0.7 / 2.6 / 4.5 / 6.7	0.7 / 2.4 / 4.4 / 6.3	0.7 / 2.2 / 3.9 / 5.4	0.9 / 2.6 / 4.5 / 6.3	
		Pre	3.8 / 8.5 / 17.4 / 18.9	2.6 / 7.6 / 15.2 / 18.9	3.7 / 11.6 / 22.0 / 30.5	3.0 / 9.0 / 17.4 / 23.3	2.5 / 9.0 / 15.1 / 19.7	6.8 / 15.5 / 24.9 / 33.2	

Supplement S3.3. Lightning flash density experiments

Figure S3.3. Figure S3. Mean of (A) convective available potential energy (CAPE; $J.Kg^{-1}$) and (B) monthly lightning flashes density across eastern Canada's boreal forest for 1951-1980, 1981-2010, 2011-2040, 2041-2070 and 2071-2100. Monthly mean of CAPE was calculated for the two scenarios of Ouranos Consortium (RCP85-CCO_1 and RCP85-CCO_2) and monthly lightning flashes density was computed for the two lightning flashes density experiments developed in this study ('$\text{Flashes}_{\text{constant}}$' and '$\text{Flashes}_{\text{increase}}$').

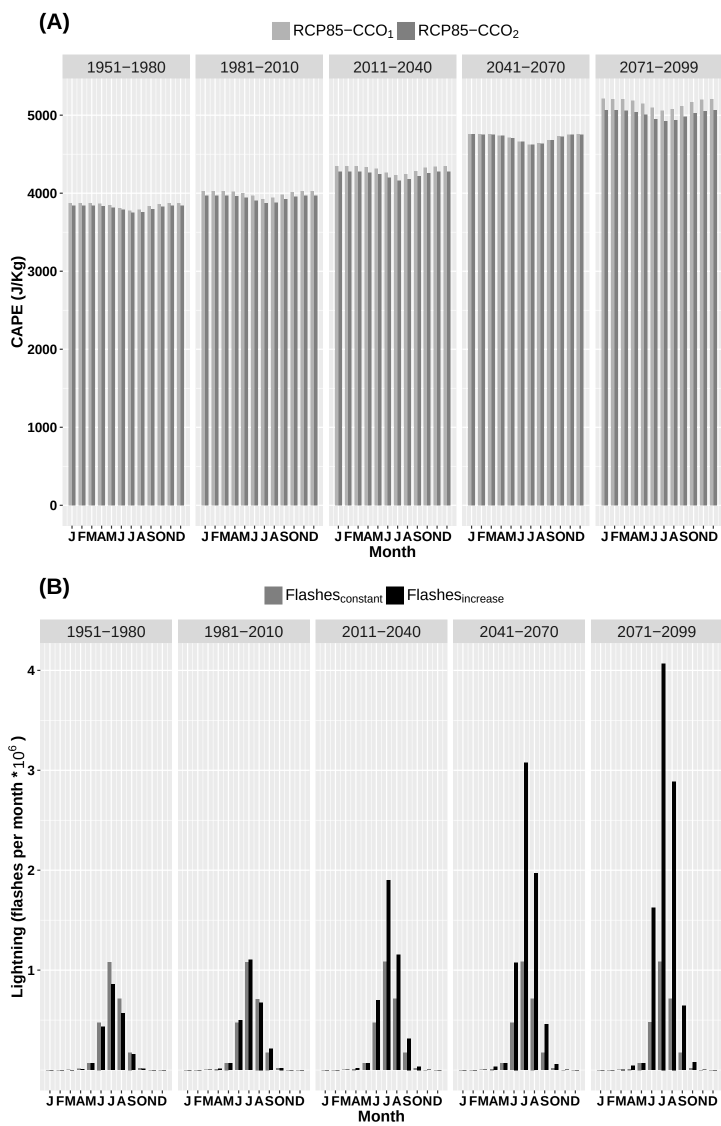

Supplement S3.4. 30-years means of LPJ-LMfire results

Table S3.2. RCP averages of mean annual net primary productivity (T.ha^{-1}.yr^{-1}), mean annual burn rates (%) and mean total aboveground biomass (T.ha^{-1}) that were simulated by LPJ-LMfire under the 'Flashes$_{\text{increase}}$' lightning, 'Climate + CO_2' and 'Climate + fires' experiments for five 30-year periods (1951-1980, 1981-2010, 2011-2040, 2041-2070 and 2071-2099) across six ecozones in eastern Canada. Ecozones are the Boreal Plain (BP), the Boreal Shield West (BSW), the Boreal Shield East (BSE), the Taiga Shield West (TSW), the Hudson Plain (HP), and the Taiga Shield East (TSE).

Variables	Ecozones	RCP	1951-1980	1980-2010	2011-2040	2041-2070	2071-2099
Net primary productivity							
	BP	RCP45	4.86	5.1	5	5.6	5.58
		RCP85	4.95	5.15	5.08	5.95	5.36
	BSW	RCP45	8.32	8.53	8.6	7.89	6.7
		RCP85	8.39	8.62	8.4	7.7	5.53
	TSW	RCP45	3.82	3.95	4.77	6.17	7.19
		RCP85	3.86	4	4.64	6.53	7.07
	HP	RCP45	4.8	5.42	5.92	5.95	5.73
		RCP85	4.81	5.49	5.74	6.27	6.29
	BSE	RCP45	8.64	9.42	10.11	10.41	10.59
		RCP85	8.63	9.48	10.05	10.84	9.86
	TSE	RCP45	6.94	7.99	9.33	9.59	9.68
		RCP85	6.96	8.04	9.19	10.2	10.34
Burn rates							
	BP	RCP45	0.53	0.52	0.28	0.28	0.25
		RCP85	0.53	0.51	0.28	0.21	0.17
	BSW	RCP45	1.13	1.14	0.96	0.61	0.42
		RCP85	1.06	1.22	0.74	0.59	0.13
	TSW	RCP45	0.77	0.66	0.64	0.47	0.71
		RCP85	0.73	0.79	0.53	0.5	0.31
	HP	RCP45	0.35	0.37	0.35	0.32	0.3
		RCP85	0.32	0.39	0.29	0.37	0.21
	BSE	RCP45	0.42	0.36	0.37	0.35	0.32
		RCP85	0.39	0.36	0.3	0.38	0.21
	TSE	RCP45	0.26	0.21	0.26	0.22	0.24
		RCP85	0.25	0.21	0.26	0.36	0.28
Total aboveground biomass							
	BP	RCP45	42.16	40.92	39.41	37.01	33.48
		RCP85	42.4	41.33	39.46	34.66	22.82
	BSW	RCP45	71.54	68.92	66.21	55.06	41.74
		RCP85	72.16	70.02	64.94	49.51	23.11
	TSW	RCP45	37.44	31.8	32.62	37.32	43.17
		RCP85	38.09	32.3	32.05	37.87	37.61
	HP	RCP45	61.34	60.86	62.24	62.26	62.37
		RCP85	61.59	61.45	62.4	62.56	52.13
	BSE	RCP45	103.88	103.88	104.85	103.97	104.55
		RCP85	104.07	104.36	105.01	100.93	76.25
	TSE	RCP45	100.64	102.18	104.62	107.22	111.48
		RCP85	100.86	102.48	104.58	106.1	104.99

Figure S3.4. Mean annual net primary productivity ($T.ha^{-1}.yr^{-1}$) that were simulated by LPJ-LMfire under six climate scenarios paired with the 'Flashes$_{increase}$' lightning, 'Climate + CO_2' and 'Climate + fires' experiments for five 30-year periods (1951-1980, 1981-2010, 2011-2040, 2041-2070 and 2071-2099) across eastern Canada's boreal forest.

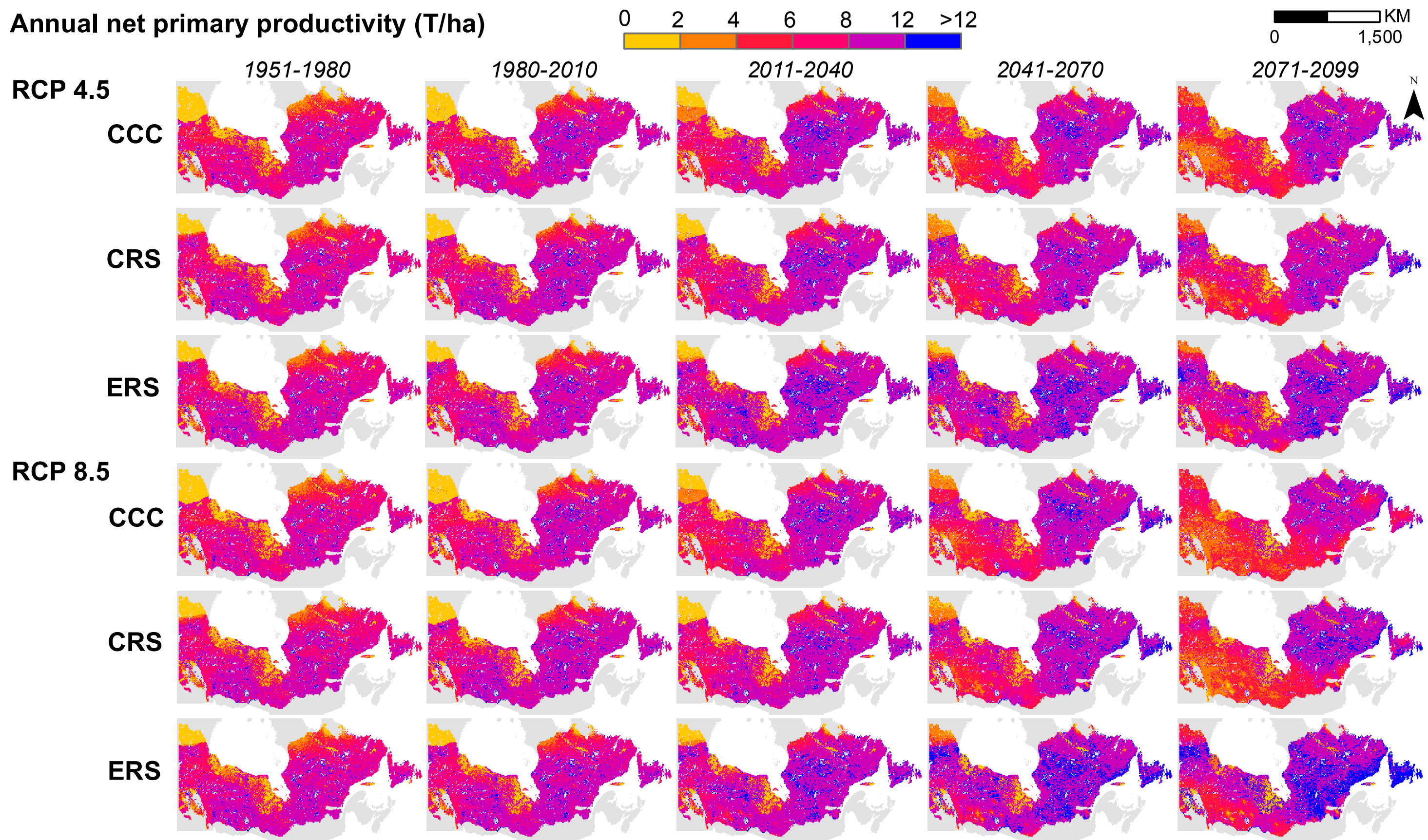

Figure S3.5. Mean annual burn rates (%) that were simulated by LPJ-LMfire under six climate scenarios paired with the 'Flashes$_{increase}$' lightning, 'Climate + CO_2' and 'Climate + fires' experiments for five 30-year periods (1951-1980, 1981-2010, 2011-2040, 2041-2070 and 2071-2099) across eastern Canada's boreal forest.

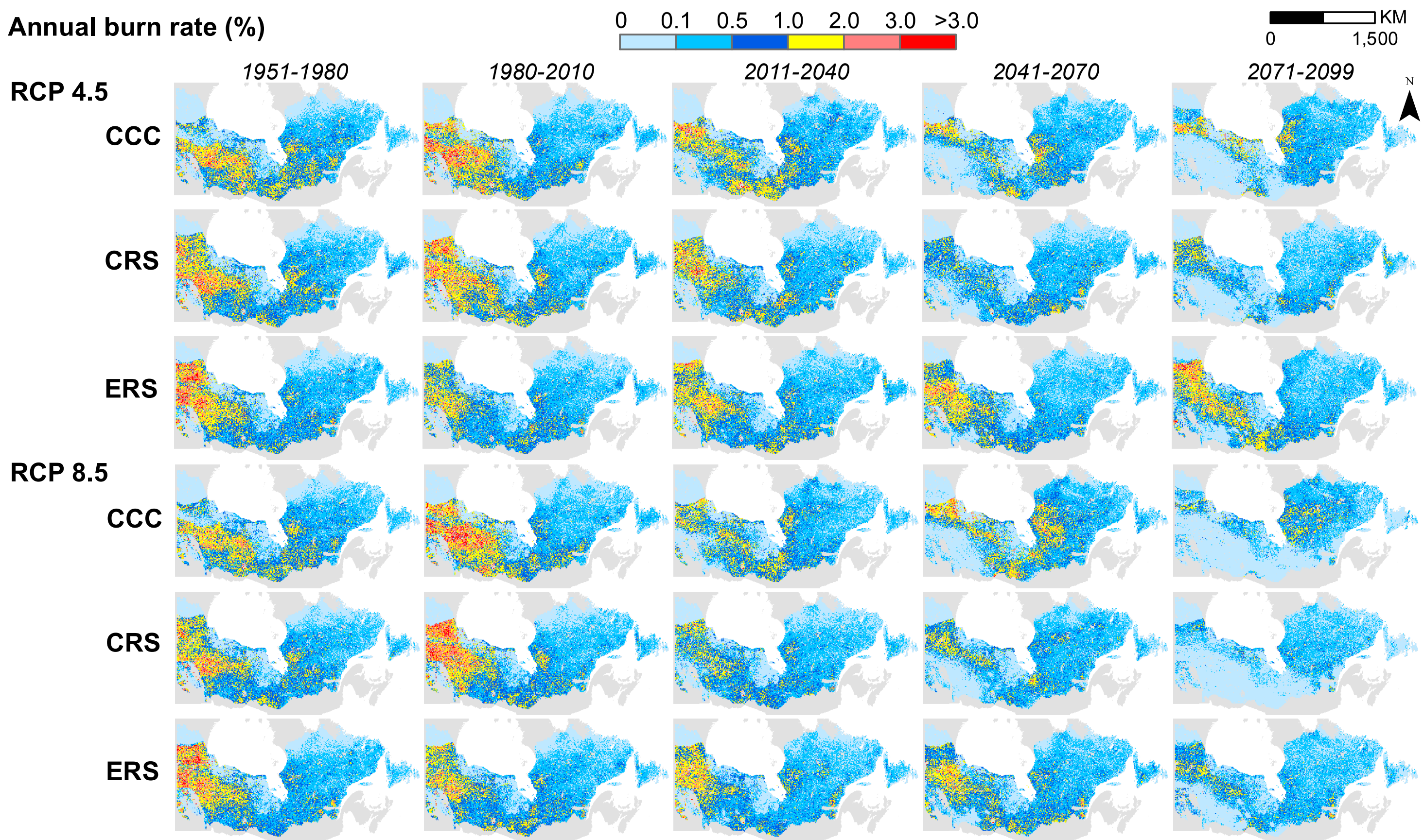

Figure S3.6. Mean total aboveground biomass ($T.ha^{-1}$) that were simulated by LPJ-LMfire under six climate scenarios paired with the 'Flashes$_{increase}$' lightning, 'Climate + CO_2' and 'Climate + fires' experiments for five 30-year periods (1951-1980, 1981-2010, 2011-2040, 2041-2070 and 2071-2099) across eastern Canada's boreal forest.

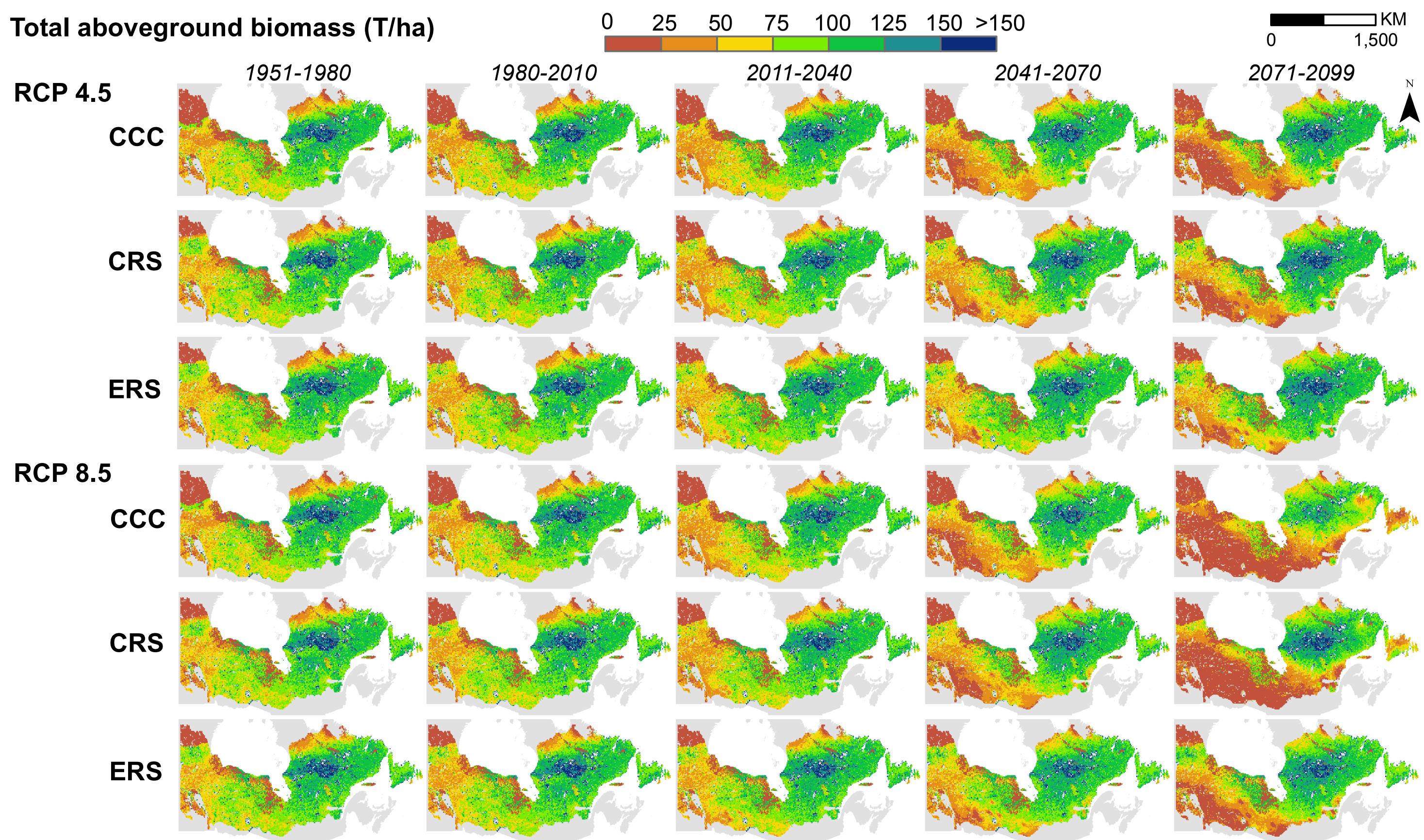

Figure S.3.7. LPJ-LMfire's simulated mean total aboveground biomass anomalies ($T.ha^{-1}$) compared to mean annual net primary productivity (NPP) anomalies ($T.ha^{-1}$) and mean annual burn rates anomalies (%) that were simulated by LPJ-LMfire under the 'Flashes$_{increase}$' lightning, 'Climate + CO_2' and 'Climate + fires' experiments for moving 30-year periods (1951-1980, 1981-2010, 2011-2040, 2041-2070 and 2071-2099) across eastern Canada's boreal forest. Anomalies were calculated with the baseline period 1951-1980.

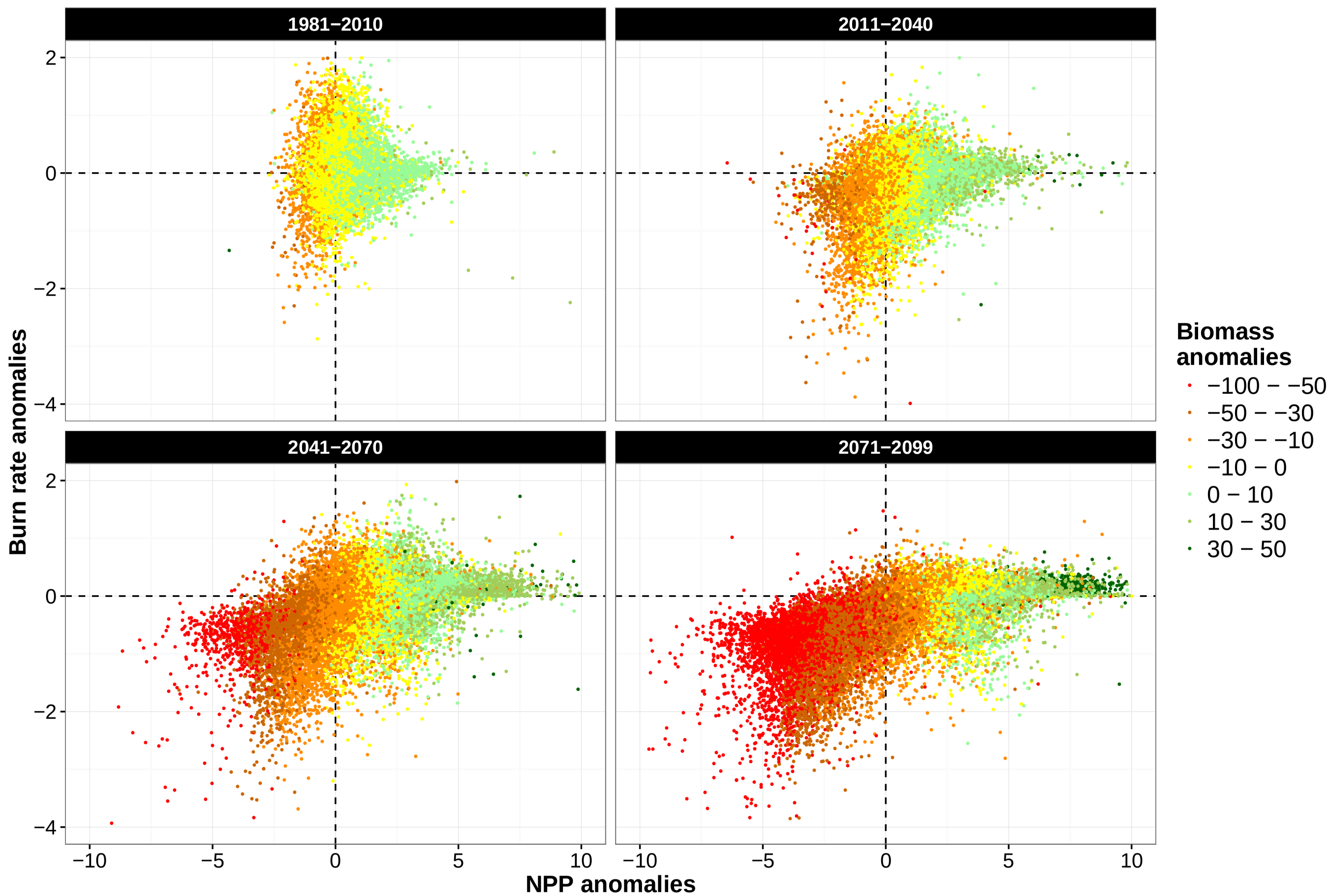

Figure S3.8. RCP averages of mean changes in non-forested areas (unoccupied by the four PFTs) that were simulated by LPJ-LMfire under the 'Flashes$_{increase}$' lightning, 'Climate + CO_2' and 'Climate + fires' experiments between the 1981-2010, 2011-2040, 2041-2071 and 2071-2099 periods compared to the baseline between 1951-1980 across eastern Canada's boreal forest (100 km^2 pixel).

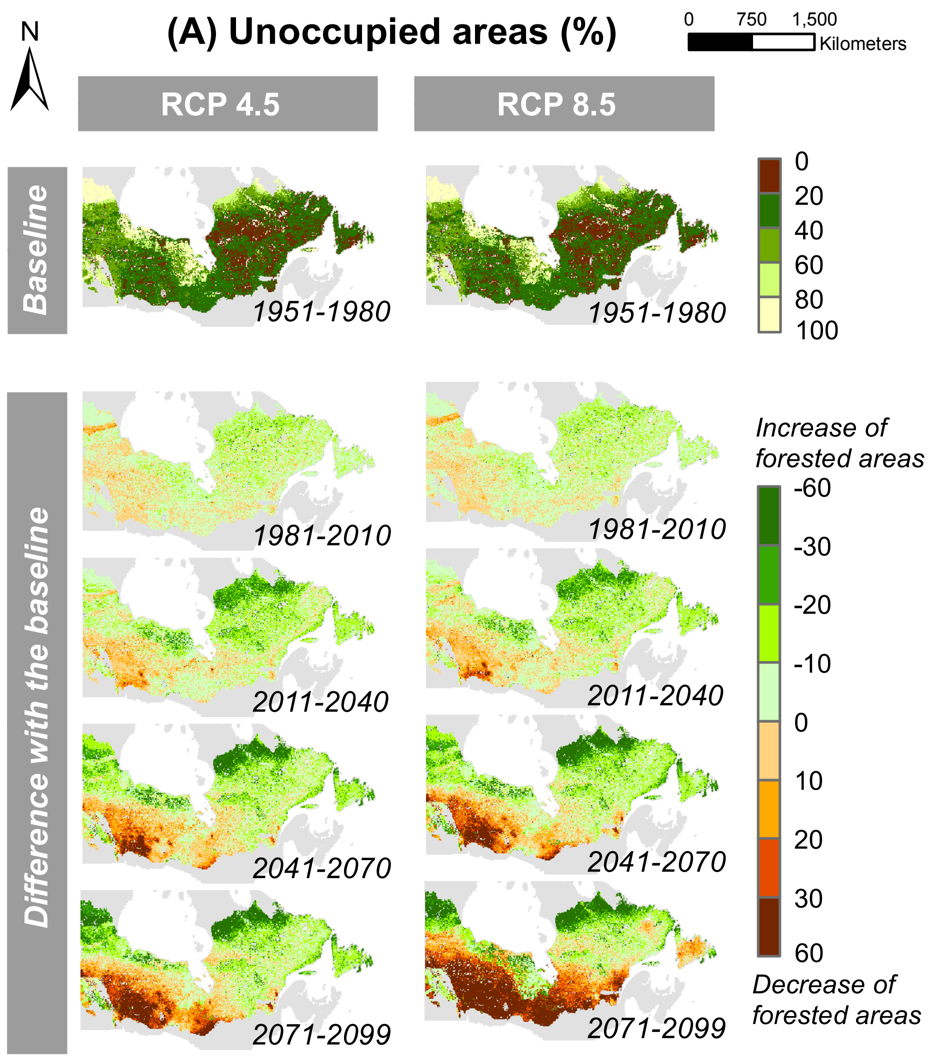

Supplement S3.5. Comparison of LPJ-LMfire results between experiments

Figure S3.9. RCP averages of mean annual net primary productivity (T.ha^{-1}; 'ANPP'), mean annual burn rates (%; 'Burn-Rate') and mean total aboveground biomass (T.ha^{-1}; 'Biomass') that were simulated by LPJ-LMfire under simulations paired with two lighting flashes experiments ('Flashes$_{constant}$' and 'Flashes$_{increase}$') for each 30-years period across eastern Canada's boreal forest (100 km^2 pixel).

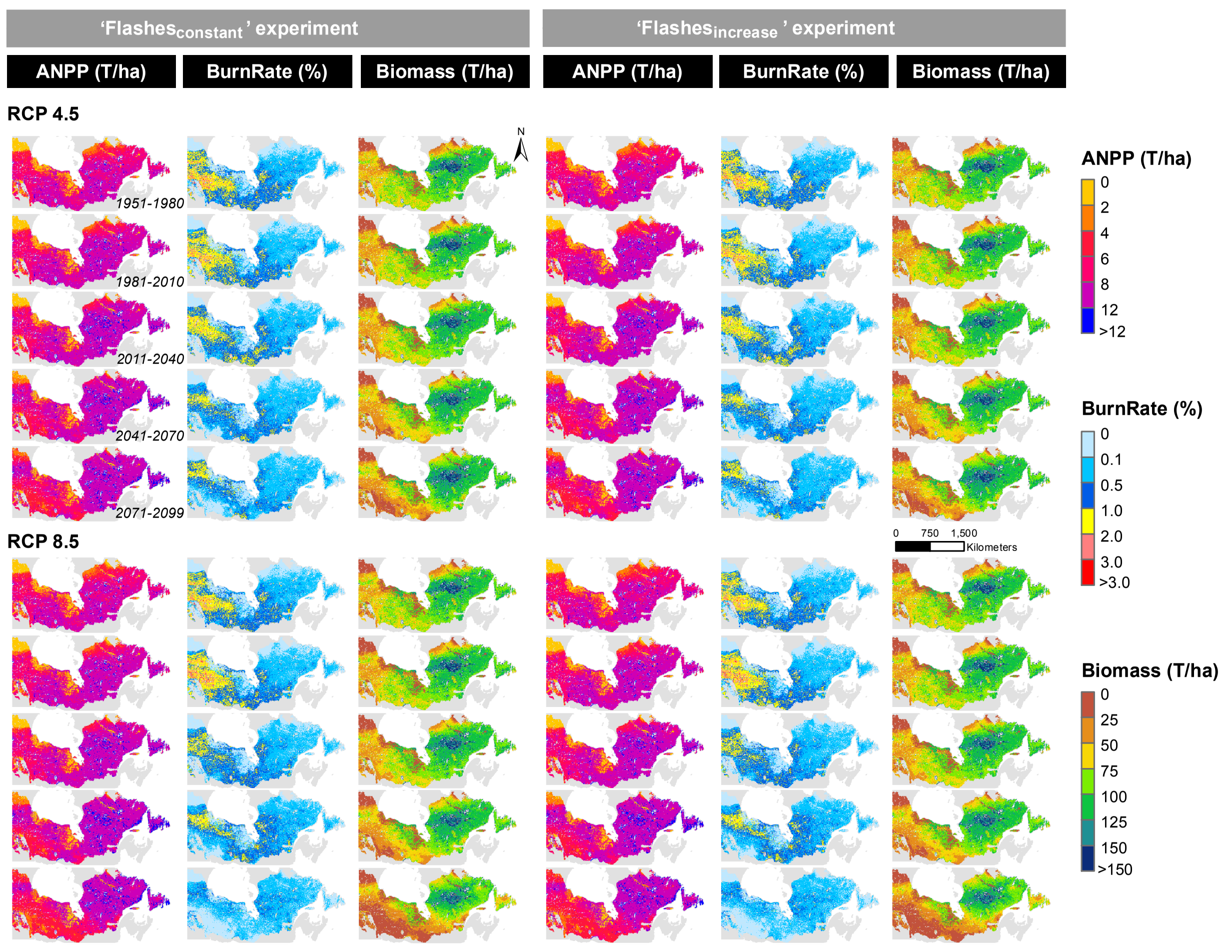

Figure S3.10. RCP averages of mean annual net primary productivity (T.ha^{-1}; 'ANPP') (A) at 100 km^2 resolution and (B) averaged by ecozone, that were simulated by LPJ-LMfire under simulations paired with two sets of CO_2 experiments ('Climate + CO_2' and 'Climate - CO_2') for moving 30-years periods from 1951 to 2099 across eastern Canadaâs boreal forest. The percentage of increase in ANPP by [CO_2] effect correspond to the difference between mean ANPP with the 'Climate + CO_2' experiment and with the 'Climate - CO_2' experiment.

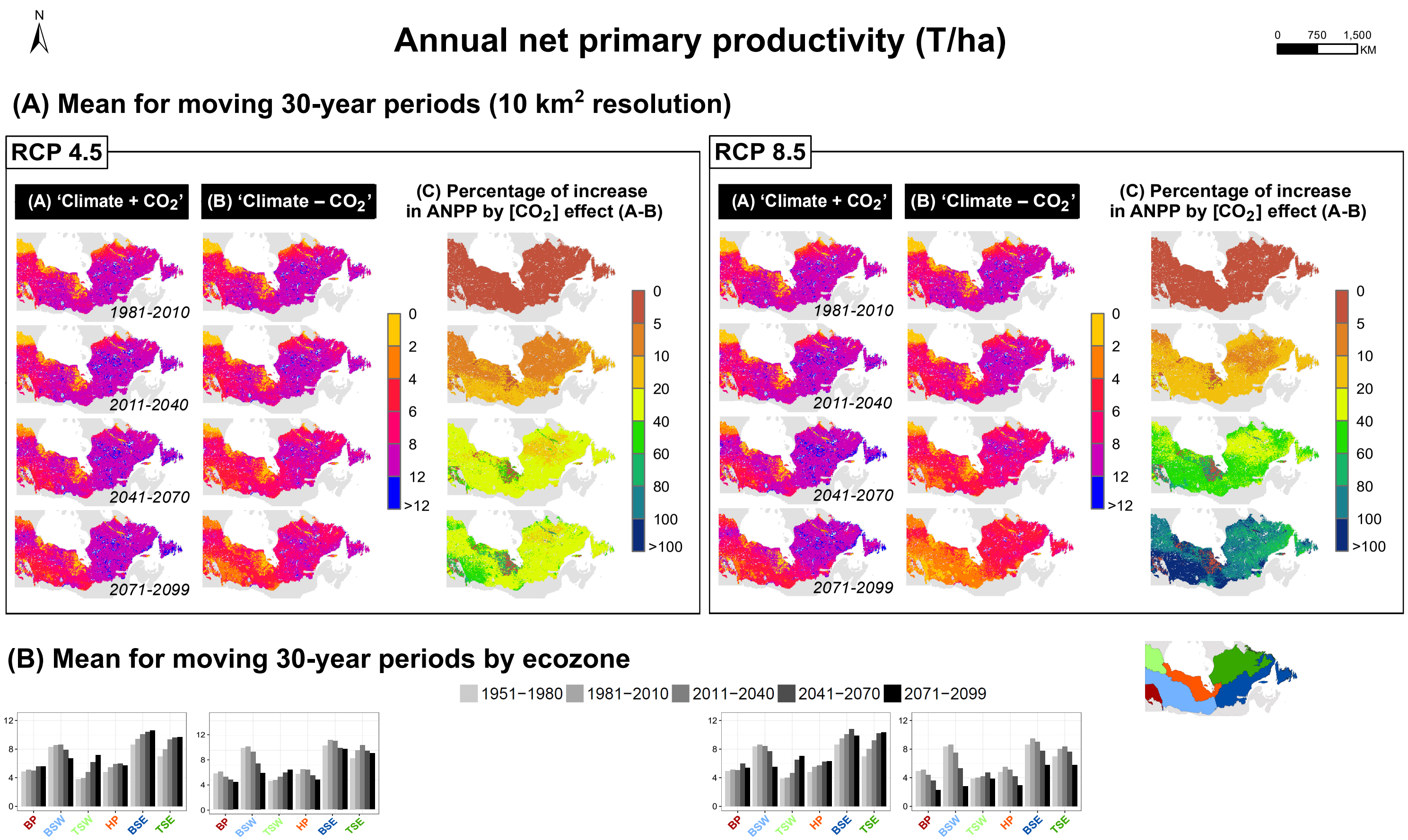

Table S3.3. RCP averages of mean annual net primary productivity (T.ha^{-1}; 'ANPP') that were simulated by LPJ-LMfire under simulations paired with the 'Climate - CO_2' experiment for moving 30-years periods from 1951 to 2099 across six ecozones in eastern Canada. Results of LPJ-LMfire mean annual net primary productivity simulated with the 'Climate + CO_2' are presented in Table S3.2.

Variables	Ecozones	RCP	1951-1980	1980-2010	2011-2040	2041-2070	2071-2099
"Climate - CO_2" experiment							
	BP	RCP45	4.86	5.1	4.42	4.06	3.71
		RCP85	4.95	5.15	4.38	3.62	2.3
	BSW	RCP45	8.32	8.52	7.84	6.22	4.92
		RCP85	8.39	8.61	7.47	5.35	2.8
	TSW	RCP45	3.82	3.95	4.39	4.97	5.4
		RCP85	3.86	4	4.19	4.7	3.86
	HP	RCP45	4.8	5.42	5.38	4.58	4.05
		RCP85	4.81	5.49	5.09	4.2	2.96
	BSE	RCP45	8.64	9.41	9.26	8.34	8.17
		RCP85	8.63	9.48	9	7.76	5.76
	TSE	RCP45	8.32	8.52	7.84	6.22	4.92
		RCP85	8.39	8.61	7.47	5.35	2.8

Figure S3.11. RCP averages of mean total aboveground biomass ($T.ha^{-1}$) (A) at 100 km^2 resolution and (B) averaged by ecozone, that were simulated by LPJ-LMfire under simulations paired with two sets of fires experiments ('Climate + fires' and 'Climate - fires') for moving 30-years periods from 1951 to 2099 across eastern Canada's boreal forest.

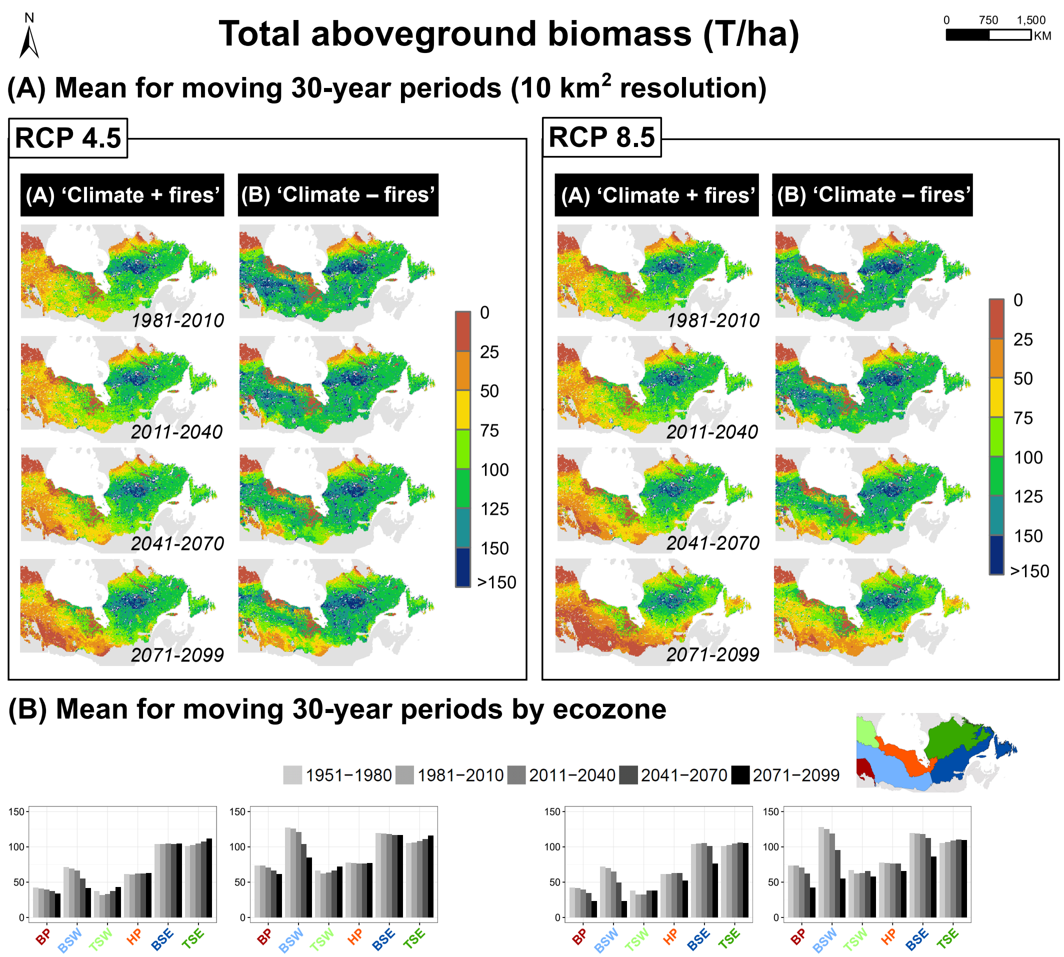

Table S3.4. RCP averages of mean total aboveground biomass (T.ha^{-1}) that were simulated by LPJ-LMfire under simulations paired with the 'Climate - fires' experiment for moving 30-years periods from 1951 to 2099 across six ecozones in eastern Canada. Results of LPJ-LMfire mean total aboveground biomass simulated with the 'Climate + fires' are presented in Table S3.2.

Variables	Ecozones	RCP	1951-1980	1980-2010	2011-2040	2041-2070	2071-2099
"Climate-fires" experiment							
	BP	RCP45	73.46	73.45	70.68	66.36	61.07
		RCP85	73.6	73.52	70.41	62.06	42.47
	BSW	RCP45	127.41	125.44	120.91	104.16	84.81
		RCP85	127.55	125.4	118.85	95.62	54.99
	TSW	RCP45	66.55	62.2	63.39	66.52	71.94
		RCP85	66.98	61.91	63.01	65.76	57.58
	HP	RCP45	77.64	76.73	76.5	76.38	76.84
		RCP85	77.62	76.75	76.45	75.96	65.37
	BSE	RCP45	119.39	118.34	117.83	116.78	116.7
		RCP85	119.44	118.35	117.64	112.27	86.16
	TSE	RCP45	105.07	106.25	108.41	111	115.53
		RCP85	105.3	106.5	108.55	110.31	109.65

CHAPITRE III

HOLOCENE DYNAMICS OF THE BOREAL FOREST OF EASTERN CANADA : UNTANGLING THE DRIVERS OF VEGETATION CHANGE USING PALEOECOLOGICAL DATA AND MODELS

Chaste E., Girardin M. P., Kaplan, J. O., Bergeron Y., Hély C. (2019). Holocene dynamics of the boreal forest of Eastern Canada : Untangling the drivers of vegetation change using paleoecological data and models. In prep.

Résumé

Les forêts boréales Nord-Américaine se sont développées au cours de l'Holocène après le retrait de l'Inlandsis laurentidien. De nos jours, cette région stocke une quantité importante de carbone dans la biomasse vivante, les sols et les tourbières, et influence de fait le climat de l'hémisphere nord via d'importantes rétroactions biogéophysiques. Alors que les forêts se sont rapidement développées sur un terrain nu après le retrait des glaces, les analyses paléoécologiques indiquent que des changements majeurs dans la composition des espèces, les propriétés du sol et la fréquence de perturbation se sont produits en forêt boréale au cours de l'Holocène. Comprendre les facteurs qui influencent la dynamique de ces écosystèmes est essentiel pour prévoir comment cette région forestière d'importance mondiale peut réagir face aux changements climatiques à venir. Nous avons utilisé le modèle LPJ-LMfire paramétré pour les principaux genres d'espèces d'arbres dominants les forêts boréales de l'Est canadien (*Picea*, *Abies*, *Pinus*, *Populus*) et piloté par un scénario climatique de l'Holocène issu des sorties mensuelles du modèle IPSL-CM5A-LR à une résolution décennale. LPJ-LMfire a été éxécuté au pas de temps mensuel entre 6000 et 0 BP sur une grille de résolution de 100 km^2 couvrant la forêt boréale du Manitoba à Terre-Neuve. Les sorties de LPJ-LMfire ont été analysées en termes de fréquence de feu, de productivité primaire nette, de biomasse aérienne des arbres et de pourcentage de couverture spécifique aux genres. Les capacités prédictives de LPJ-LMfire ont été examinées en comparant nos simulations des aires brûlées annuellement et de biomasse arborée avec des reconstructions paléoécologiques obtenues à partir des enregistrements lacustres de charbons et de pollens, respectivement. Nos résultats confirment que les tendances climatiques régionales à long terme influencent en grande partie la dynamique de la végétation qui agit elle-même comme un important contrôle «ascendant» de la fréquence de feu sur de longues échelles de temps. Un climat chaud pendant la saison de croissance au milieu de l'Holocène a permis à la végétation de s'établir rapidement à l'est, tandis que des températures printanières froides ont limité la croissance des arbres à l'ouest. Une biomasse faible et un pourcentage de couverture élevé du genre *Populus* expliquent les faibles surfaces brûlées simulées. Toutefois, les trajectoires simulées de la fréquence de feu et des changements de végétation au cours de l'Holocène n'étaient pas synchrones avec les tendances reconstruites de la fréquence de feu et de la biomasse arborée pour la région, celles-ci étant souvent décalées de plusieurs centaines de kilomètres. À première vue, il semblerait que l'écart entre les trajectoires simulées et observées soit attribuable aux incertitudes des données climatiques IPSL-CM5A-LR données en entrée dans le modèle LPJ-LMfire.

Mots-clés

Forêt boréale, LPJ-LMfire, simulations paléoclimatiques IPSL-CM5A-LR, Végétation, Feu.

Abstract

The boreal forests of Eastern North America developed during the Holocene following the retreat of the Laurentide Ice Sheet. This region now stores a substantial amount of carbon in living biomass, soils, and peat, and has an important biogeophysical feedback to the atmosphere that influences hemispheric climate. While forests developed rapidly on bare ground following ice retreat, the boreal forest was not static over the Holocene. Paleoecological analyses indicate that major changes in species composition, soil properties, and disturbance frequency occurred over the past 6 ka. Understanding the drivers behind these ecosystem dynamics is important for projecting how this globally important forest region may respond to future climate change. Here we present a study simulating the responses of vegetation and fire to changes in climate during the last 6000 years using a dynamic vegetation model, and evaluating the model output at multi-millennial time-scales using paleoecological archives. We used the LPJ-LMfire model, parametrized for the most abundant tree genera in eastern boreal Canada (*Picea*, *Abies*, *Pinus*, *Populus*) and driven by a Holocene scenario of climate derived from the Earth system model IPSL-CM5A-LR at 10-year resolution. LPJ-LMfire was run with a monthly time-step from 6000 to 0 BP on a 100-km^2 resolution grid covering the boreal forest from Manitoba to Newfoundland. LPJ-LMfire output was analyzed in terms of annual burn rates (ABR), net primary productivity, aboveground biomass and genus-specific cover percentage. We compared ABR and tree biomass simulated by LPJ-LMfire results with paleoecological reconstructions obtained from lacustrine-charcoal and pollen records, respectively. Our results support the hypothesis that Holocene climate change had an important influence on the dynamics of the boreal forest of northeastern North America. Forest composition acted as an important "bottom-up" control on fire frequency on multi-centennial time-scales. Warm growing seasons at 6000 BP fostered the rapid establishment of vegetation in the east of our study domain, whereas cold spring temperatures limited biomass growth in the west. Low biomass and high Populus cover percentage contributed to low simulated ABR. Simulated changes in ABR and biomass over time were not entirely synchronous with reconstructions based on charcoal and pollen. Where LPJ-LMfire shows trends similar to the paleoecological reconstructions, these are often offset in space by several 100s of km. We suggest that the discrepancies between simulated and reconstructed vegetation time series are associated with inaccuracies in the climate model output that was used to drive LPJ-LMfire.

Keywords

Boreal forest, LPJ-LMfire, IPSL-CM5A-LR paleoclimate simulations, Vegetation, Fire.

3.1 Introduction

There is growing evidence that climate change will modify fire regimes and forest attributes (e.g. composition, biomass, age) in North America's boreal forests over the next century (e.g. Bergeron et al., 2017; Flannigan et al., 2016; Gauthier et al., 2014; Girardin et al., 2013; Krause et al., 2014; Price et al., 2013). However, these projections are hampered by our limited understanding of the natural variability in climate-vegetation-fire relationships recorded on long (centennial-millennial) timescales (Kelly et al., 2013; Mackay et al., 2003). Indeed, climate-vegetation-fire relationships are complex because of multiple biological and physical controls and feedbacks whose relative importance may vary across a wide range of spatial and temporal scales (Archibald et al., 2018; Harris et al., 2016; Hu et al., 2006). Moreover, most studies focusing on these relationships are confounded by human influences because most observations are available only for the last century, i.e. a period of intensive forest management and active fire suppression (Kelly et al., 2013, 2016; Podur et al., 2002). However, present day-environmental processes have been conditioned by past climate-vegetation-fire relationships (Mackay et al., 2003). These concerns have stimulated paleoecological research aiming at improving our understanding of the natural trajectories in climate-vegetation-fire relationships prior to the onset of the Anthropocene ca. AD 1950 (Lloyd and Winsberg, 2018).

Numerous paleoecological studies have documented the changes in climate drivers (Girardin et al., 2006; Jaume-Santero et al., 2016; Marsicek et al., 2018), forest dynamics (e.g. Carcaillet et al., 2001; Magnan et al., 2014; Senici et al., 2013) and natural disturbance regimes (e.g. Frégeau et al., 2015; Jasinski and Payette, 2005; Oris et al., 2014; Ouarmim et al., 2015; Simard et al., 2006) through the Holocene in eastern Canada's boreal forest. However, these reconstructions made through the use of different proxies preserved in the sedimentary layers of soil, lacustrine or ice cores and in tree rings have several limitations (e.g. Pilon et al., 2018). Generally, proxies do not permit reconstruction of the complete temporal variability of past environments (Power et al., 2008). Indeed, data are often incomplete because paleoecological methods are costl and time-consuming; in some cases, a degradation or loss of proxies occurred in certain conditions (Pilon et al., 2018). Moreover, some proxies reflect only local processes. For instance, reconstructions of fire frequencies using macroscopic charcoals ($\geq$ 2 mm) provide information on "local" fire occurrence (Higuera et al., 2007), whereas microscopic charcoals ($\geq$ 150 µm) likely represent both local and regional fires (Tinner et al., 2006). Although reconstructions with proxy indicators permit comparison of past changes in several environment of compartments that reflect past interactions and processes (Blarquez et al., 2015; Carcaillet et al., 2001), they do not permit explicit determination of the weights of potential drivers associated with these changes. Consequently, the most likely cause is often highlighted by evaluating competing hypotheses between studies (Miller et al., 2008). Reconstructions at high spatio-temporal resolution of vegetation changes in response to climate and fire regimes are possible using dynamic global vegetation models (DGVMs). These models simulate interactions and feedbacks among climate, vegetation and fires using somewhat mechanistic representations of physiological and biogeochemical processes (Krinner et al., 2005; Kucharik et al., 2000; Smith et al., 2001). Thus, DGVM models permit determination of processes at the origin of simulated temporal changes pattern.

The goal of this study is to present advances made in the deployment of a DGVM (Lund-Postdam-Jena Lausanne-Mainz fire, LPJ-LMfire) for research in eastern Canada's boreal forest, and to discuss its performance at multi-millennial time-scales. In a novel approach, simulations with the LPJ-LMfire model parametrized for the dominant tree genera in the boreal forests of Eastern Canada (*Picea*, *Abies*, *Pinus*, *Populus*; Chaste et al., 2018) were performed using a transient (i.e. continuous resolution) climate dataset over the last 6000 years derived from the output of an Earth system model (ESM) which have a 10-year resolution. Assessment of LPJ-LMfire performance for past changes in vegetation and fires was performed by comparing the model's outputs with palaeoecological reconstructions obtained from pollen and lacustrine-charcoal records.

3.2 Model, experimental set-up, and methods

3.2.1 Study area

The study area encompasses the boreal forest in eastern Canada from Manitoba to Newfoundland (Figure 4.1). The study area is currently divided from south to north in four ecozones (Figure 4.1) as defined by the National Ecological Framework of Canada (NFEC; Ecological Stratification Working Group, 1996). These large biogeographical units are, from south to north, the Boreal Shield (BS), the Boreal Plain (BP), the Hudson Plain (HP) and the Taiga Shield (TS). The BS and TS ecozones were each subdivided into two sub-ecozones: (1) the Boreal Shield West (BSW) and the Boreal Shield East (BSE) sub-ecozones separated by the arbitrary 80° W gradient, and (2) the Taiga Shield West (TSW) and the Taiga Shield East (TSE) sub-ecozones separated by their actual widely spaced locations in the study area.

3.2.2 LPJ-LMfire model

Simulations of the terrestrial ecosystem were carried out using the dynamic global vegetation model LPJ-LMfire, which includes updates of both LPJ and the SPread and InTensity of FIRE (SPITFIRE) wildfire module (Thonicke et al., 2010). LPJ-LMfire is designed to simulate regional ecosystem dynamics, structure, and composition, with vegetation and fire events as responses to changes in climate and carbon dioxide (CO_2) concentration (Sitch et al., 2003). The model has been developed and evaluated for

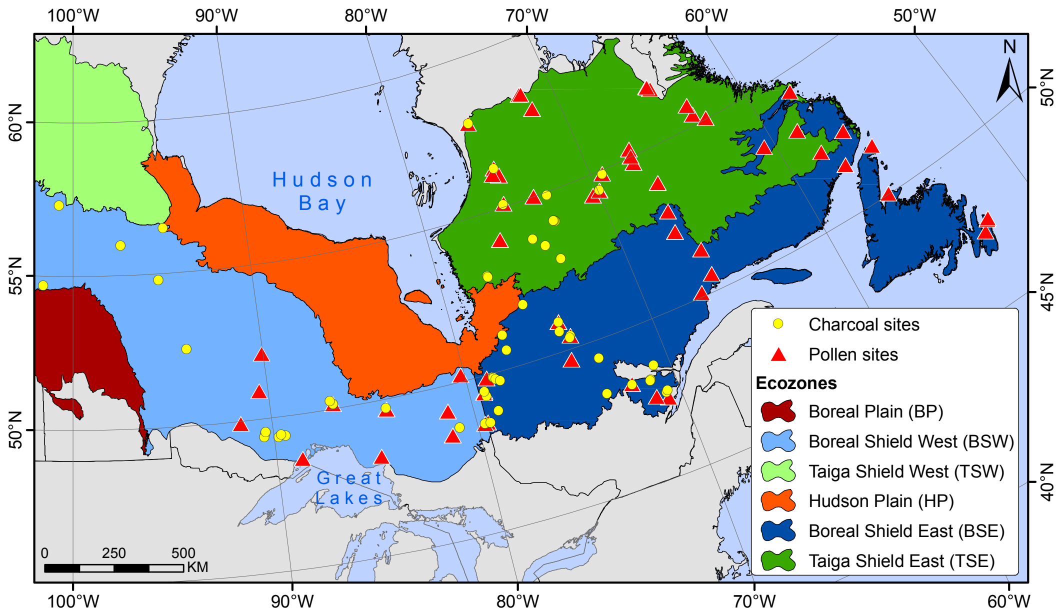

Figure 4.1. Location maps of six sub-ecozones in eastern Canada's boreal forest (Brandt, 2009) and selected pollen and lacustrine-charcoal records sites. The study area ranges from 102° W to 53° W in longitude and from 46° N to 65° N in latitude and covers an area of ca. 2.9 million km^2.

boreal forests (Pfeiffer et al., 2013). LPJ-LMfire describes the state of an ecosystem in terms of annual carbon stocks (living biomass, litter, and soil), NPP, net biome productivity, evapotranspiration, heterotrophic respiration, soil moisture fraction, and forest structure and vertical profile (cover fraction, individual density, crown area, leaf area index). In the present study, changes in the vegetation state are described in terms of NPP and total carbon stocks in living aboveground biomass. In LPJ-LMfire, vegetation is defined by up to nine plant functional types (PFTs). Each PFT represents one or several species sharing the same physiology and dynamics, governed by a short list of vital attributes, and constrained by bioclimatic limits (Sitch et al., 2003). Vegetation dynamics are updated annually based on the simulation of daily and annual processes. Daily processes are defined in terms of photosynthesis, stomatal regulation, soil hydrology, autotrophic respiration, leaf and root phenology, and decomposition. Annual processes are defined in terms of several sources of mortality, seedling establishment, reproduction, allocation, and tissue turnover (Smith et al., 2001; Sitch et al., 2003). The computational core of SPITFIRE is based upon Rothermel-type surface fire behaviour models (Rothermel, 1972; Andrews et al., 2008) and is designed to simulate processes of natural fires and their impacts on vegetation mortality and fire emissions (Thonicke et al., 2010). The LMfire module simulates lightning ignitions based upon a daily time step and uses fuel bulk density and fuel moisture to calculate the fire's rate of spread, intensity, and fire-related mortality. It allows fires to burn over multiple days and simulates fire extinction from changes in weather and fuel (Pfeiffer et al., 2013). As in the original version of SPITFIRE and nearly all other large-scale fire models, LMfire does not simulate the cell-to-cell spread of fire (Hantson et al., 2016; Pfeiffer et al., 2013; Rabin et al., 2017).

3.2.3 Holocene climate data

Monthly mean temperature (°C), diurnal temperature range (°C), precipitation total amount (mm), number of days per month with precipitation, mean wind velocity (m s^{-1}), cloud cover (%) and daily density of lightning flashes (number day^{-1} km^{-2}) were required to run the LPJ-LMfire model. Except for the latter variable, monthly decadal mean values of each variable between 6000-0 calibrated years Before Present (hereafter BP, present being assumed here to be equivalent to 1950 i.e. 0 BP) were obtained from the French Pierre-Simon-Laplace Institute Earth system model IPSL-CM5A using a low resolution version (IPSL-CM5A-LR; 1.875°x3.75°) that has been sped-up at 10-years. This means that the complete run of IPSL-CM5A-LR over the 6000 years, taking into account changes in orbital forcing parameters and green-house gas concentrations, was performed in 600 simulated year, that was then interpolated over 6000 years before it could be used as LPJ-LMfire input. IPSL-CM5A is one of two configurations of the IPSL-CM5 model used in the Coupled Model Intercomparison Project phase 5 (CMIP5, Taylor et al., 2012). It is built around a physical core that includes atmosphere (LMDZ5A model), ocean and sea ice components (NEMOv3.2), land-surface (ORCHIDEE) and atmospheric chemistry (INCA). The OASIS coupler is used to interpolate and exchange the variables, and to synchronize the models (Dufresne et al., 2013). An ensemble of two runs of this climate model version was available (LR1 and LR2) and previously analyzed in the context of Africa (Lézine et al., 2017). We applied the same approach to run two separate LPJ-LMfire simulations although we followed the same protocol for the two runs.

The decadal IPSL-CM5A-LR values were bilinearly interpolated to a 100-km^2 resolution grid covering the study area. Anomalies at decadal time step relative to the preindustrial control period (PI, equal to the 1901-1950 period) were calculated and then linearly interpolated to the annual time step. Next, we used Environment Canada's historical climate database (Environment Canada, 2013) to prescribe interannual variability for our IPSL-CM5A-LR simulations. For each climate variable, monthly means for the 1951-2010 period were extracted at 100-km^2 resolution using the BioSIM software (v.10.3.2; Régnière et al., 2014; see Chaste et al., 2018 for further details). These monthly values were detendred using a robust loess regression filter (bandwidth of 30 years). Four 30-year blocks were selected corresponding to detendred values between 1951-1980, 1961-1990, 1971-2000 and 1981-2010 respectively. Then we created a 6030-year time-series of these detrended data using a pseudo-random sampling of the 30-year blocks that were merge one after the other. The pseudo-random sampling, similar to the "shuffle" function in a digital music player, means blocks were selected at random, but once chosen, were not selected again until all of the remaining had been selected. Finally, this 6030-year time-series of anomalies was applied to the 6030-year baseline climatology to estimate Holocene climatology in an appropriate format to run the LPJ-LMfire model.

Monthly lightning flash density data were unavailable for the IPSL-CM5A-LR model.

Given the strong correlations between lightning flash density and the convective available potential energy (CAPE; Peterson et al., 2010; Romps et al., 2014), we used monthly means of CAPE at decadal time steps available from the IPSL-CM5A-LR model, to estimate monthly lightning flash density (number day^{-1} km^{-2}) from 6000 to 0 BP on an annual time step. Four steps were carried out to perform this reconstruction. First, decadal monthly means of CAPE were bilinearly interpolated to a 100-km^2 resolution grid covering the study area, and monthly means of CAPE anomalies at decadal time steps relative to the PI were calculated. Then, we estimated decadal values of monthly lightning flash density using the methodology described in Chaste et al. (2018), based on the use of decadal monthly means of CAPE anomalies and the Canadian lightning detection network (CLDN) dataset covering the period 1999-2010 (Orville et al., 2011). Thirdly, the decadal values were linearly interpolated to an annual time step and a 6030-year time-series of monthly lightning flash density anomalies was calculated following the aforementioned anomaly approach. Finally, this 6030-year time-series of lightning flash density anomalies was applied to the monthly climatology of lightning flash density reported in Chaste et al. (2018).

Climate trajectories, averaged for the two runs of the IPSL-CM5-LR model, and reported in terms of annual and seasonal (spring and summer) mean anomalies of temperatures (°C) and precipitation (%) relative to PI show a 2°C-decrease in summer temperatures during the studied period and over the entire study area (Figure 4.2 and Table S4.1 in Supplement S4.1), which is consistent with the decrease in solar radiation since 6000 BP (Berger and Loutre, 1991). However, the decline is more pronounced and with higher variability in eastern ecozones of the studied area (Figure 4.2). Simulated spring temperatures show more dissimilarities along a longitudinal gradient from west to east (Figure 4.2). In eastern ecozones (BSE and TSE) spring temperatures are relatively constant from 6000 to 2000 BP, followed by warming up to present-day conditions (Figure 4.2). Similarly, simulated spring temperatures in western ecozones

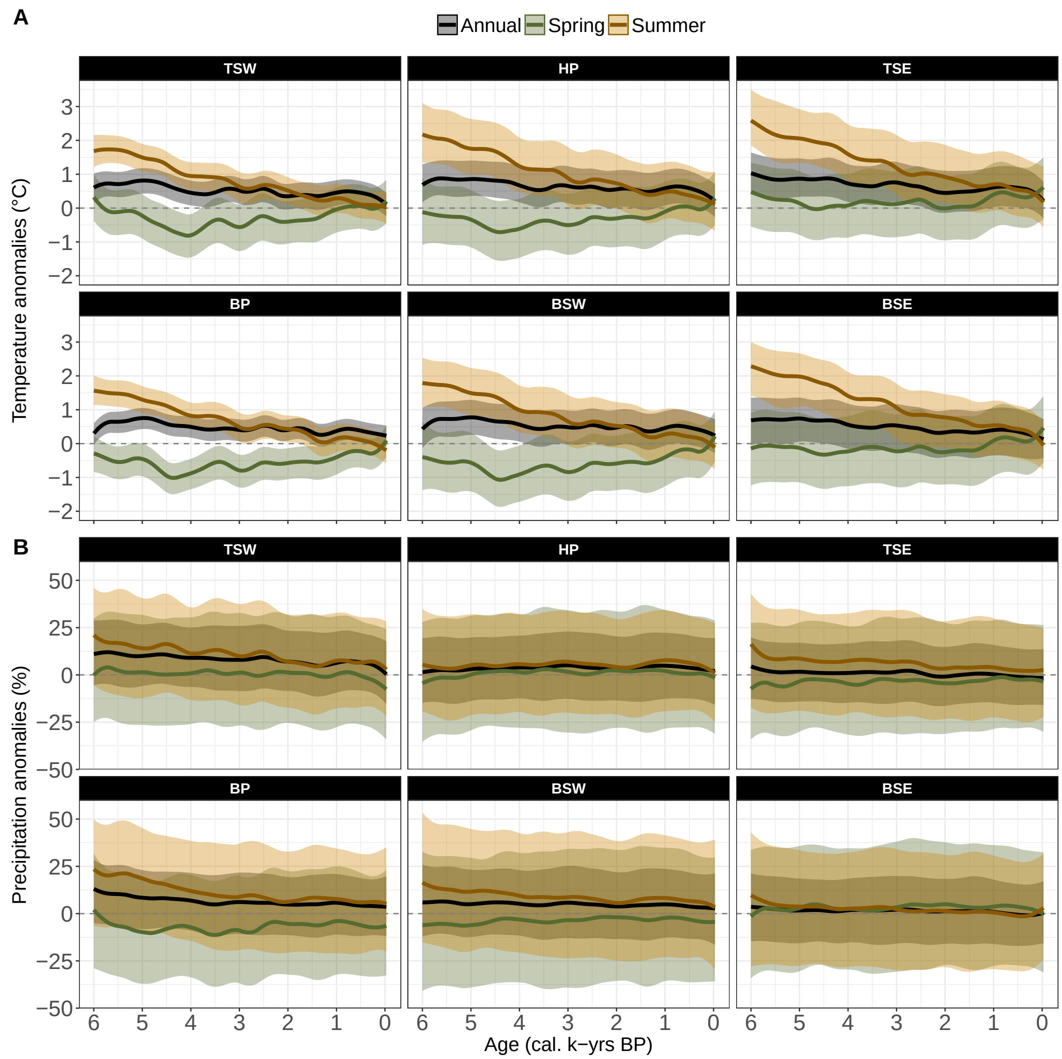

Figure 4.2. Annual and seasonal (A) temperature anomalies (°C) and (B) precipitation anomalies (%) over the last 6000 years expressed as anomalies from the 1901-1950 average temperatures for each ecozone. Lines and color areas corresponds to the mean and the 95% confidence interval of the scatter plot smoother calculated using a 500 year window half width, respectively.

(BP, BSW, TSW) Similarly, simulated spring temperatures in western ecozones (BP, BSW, TSW) show a trend of colder springs from mid-Holocene (6000 BP) to late-Holocene (∼4000 BP) with a decrease of -1°C, and then warming until the PI (Figure 4.2). Spring temperatures in the HP ecozone show similar trends, albeit less pronounced and with greater variability (Figure 4.2). Trends in precipitation anomalies relative to the PI are unclear and show very high variability (Figure 4.2 and Table S4.1 in Supplement S4.1). Simulated summer precipitations averaged for the study area show drier summers between 6000-2000 BP, more pronounced in the southwestern areas followed by an increase in summer precipitation between 2000-0 BP (Figure 4.2 and Table S4.1 in Supplement S4.1).

3.2.4 Atmospheric CO_2 concentration

Monthly mean atmospheric CO_2 concentrations covering the period from 6000 to 0 BP were obtained from Pfeiffer et al. (2013). Annual mean atmospheric CO_2 concentration varied from 266.03 ppm in 6000 BP to 312.11 ppm in 0 BP (Figure S4.1 in Supplement S4.2).

3.2.5 Environmental constraints data

We applied the same method as Chaste et al. (2018) to prepare other biophysical layers for LPJ-LMfire inputs. The soil texture fractions were obtained from the 1-km resolution ISRIC - World Soil Information dataset (Hengl et al., 2014) and interpolated at 10-km resolution. Lithology soil codes were unchanged from Pfeiffer et al. (2013). Elevation and slopes were interpolated at 10-km resolution from the 30 arc-second gridded digital elevation model (DEM) of Canada. The land fraction was calculated from the National Hydro Network (NHN) dataset at 100 m resolution (Natural Resources Canada, 2010). We defined the land fraction as the inverse of the water fraction (lakes and water courses areas). We calculated water fraction at 10-km resolution from grid cells at 100 m resolution with water fraction > 50%. Roads, power lines, dams, mines, and other human-made structures were not considered in this study.

3.2.6 Modeling and simulation protocol

As with many DGVMs, LPJ-LMfire requires a spin-up period to equilibrate C and N pools with climate, ecosystem properties, and fire regime (Hudiburg et al., 2017; Smith et al., 2001). A 1080-year spin-up period was prescribed for the vegetation to grow on original bare soil and to reach an equilibrium state. This spin-up period was made using the IPSL-CM5-LR's monthly anomalies (section 4.2.2) calculated for the year 6000 BP and repeated 1080 times. This 1080-year time-series of anomalies was applied to a 1080-year long climatology time-series, created with the aforementioned pseudo-random sampling method and based on the monthly means of the baseline climatology for 1951-2010.

We analyzed the outputs of LPJ-LMfire after the spinup period end, in terms of annual area burned, annual net primary productivity (ANPP), total aboveground biomass and cover percentage for each genus-specific PFT. An average of each output variable was calculated as the mean of the two LPJ-LMfire simulations. We summarized simulated results of the first three variables for six 1000-year periods at 100-km^2 resolution. The cumulative cover percentage for the four genus-specific PFTs was averaged for each ecozone in eastern Canada's boreal forest over the last 6000 years.

3.2.7 Model evaluation

We assessed LPJ-LMfire's efficiency in simulating past fires and aboveground biomass by comparing simulation results with previously published paleoecological datasets on past fire and vegetation biomass reconstructions. Holocene fire histories were reconstructed from 56 charcoal records in the forests of eastern Canada (Blarquez et al., 2015), classified into three of the six sub-ecozones (Figure 4.1); a total of 17, 25 and 14 charcoal sites were assigned in the BSW, BSE and TSE ecozones, respectively. Regional averages of charcoal records (composite series of biomass burning) were calculated for each ecozone using the same methodology developed in Blarquez et al. (2015). Site locations of pollen records available in the North American Surface Sample Dataset (Whitmore et al., 2005) were also extracted for eastern Canada's boreal forest and classified into the same three of the six sub-ecozones (Figure 4.1). Holocene total tree biomass, inferred from pollen records and published by Blarquez and Aleman (2016), were extracted for these site locations and averaged by ecozone.

3.3 Results

3.3.1 Holocene trajectories of forest dynamics simulated by LPJ-LMfire

Simulated mean total aboveground biomass, mean annual area burned and mean annual net primary productivity increased from 6000 BP to present, except in the TSE ecozone where these components remained at a constant level (Figure 4.3 and Figure S4.2 in Supplement S4.3). Largest increases were simulated in southern ecozones BP, BSW and BSE, but these trends were not widespread across the study area and were not continuous over the 6000 years (Figure 4.3 and Figure S4.2 in Supplement S4.3). For instance, the increase in total aboveground biomass was small and not spatially uniform during the first two millennia in the BP and BSE ecozones (Figure 4.3). Furthermore, a very large increase in total aboveground biomass from 6000-5000 BP to 5000-4000 BP was simulated, followed by a decrease during the 4000-3000 BP period, before increasing again (Figure S4.2 in Supplement S4.3). Similar trends were observed for the mean annual area burned and mean annual primary productivity (Figure S4.2 in Supplement S4.3). The highest increase in mean annual area burned was simulated in the BSW ecozone (238%, Figure S4.2 in Supplement S4.3). Although a general trend of annual net primary productivity increase was simulated, this response was three times larger in southern ecozones compared to northern ecozones (average of 29% and 10%, respectively; Figure S4.2 in Supplement S4.3).

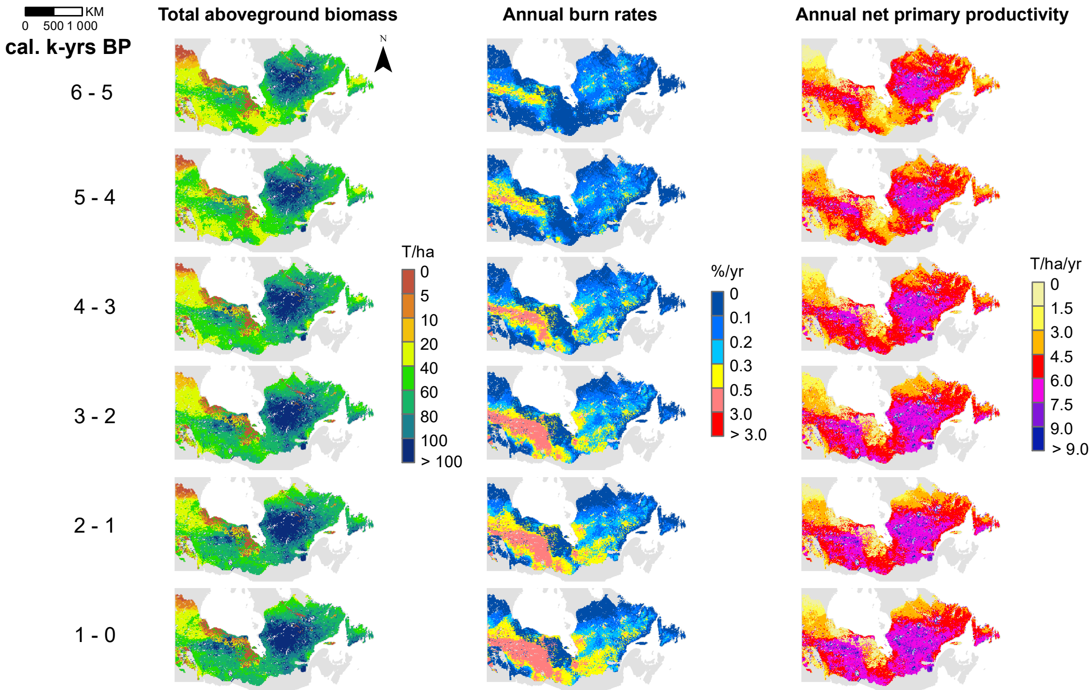

Figure 4.3. 1000-year's mean LPJ-LMfire's simulated total aboveground biomass (T.ha^{-1}), annual area burned (%.yr^{-1}) and annual net primary productivity (T.ha^{-1}.yr^{-1}) between 6000-0 cal. years BP across eastern Canada's boreal forest (100km^2-resolution).

Simulations showed that genus-specific *Picea*, *Pinus* and *Populus* PFTs were present within all ecozones and throughout the 6000 years (Figure 4.4). Overall, biomass was dominated by coniferous PFT (*Picea*, *Abies* and *Pinus*) from 6000 to 0 BP, notably by *Picea* PFT; except in the BP ecozone, where *Populus* PFT was predominant (Figure 4.4). Needleleaf and broadleaf cover percentages were relatively equal during the first two millennia (from 6000 to 4000 BP) in the HP ecozone (Figure 4.4), and then PFT cover percentages of *Picea* and *Pinus* slightly increase until 0 BP at the expense of a decrease in the *Populus* PFT. The same patterns between 4000-0 BP were simulated in BSW, BSE and TSE ecozones (Figure 4.4). Minimum and maximum forested areas (sum of all PFTs cover percentages) were simulated in the western (BP and TSW) and eastern (BSE and TSE) ecozones, respectively (Figure 4.4). Except for the TSW ecozone, forested areas were simulated to increase during the last six millennia, with rapid rises simulated at the end of the simulation period, especially in all three southern ecozones (BP, BSW and BSE) and in the HP ecozone (Figure 4.4).

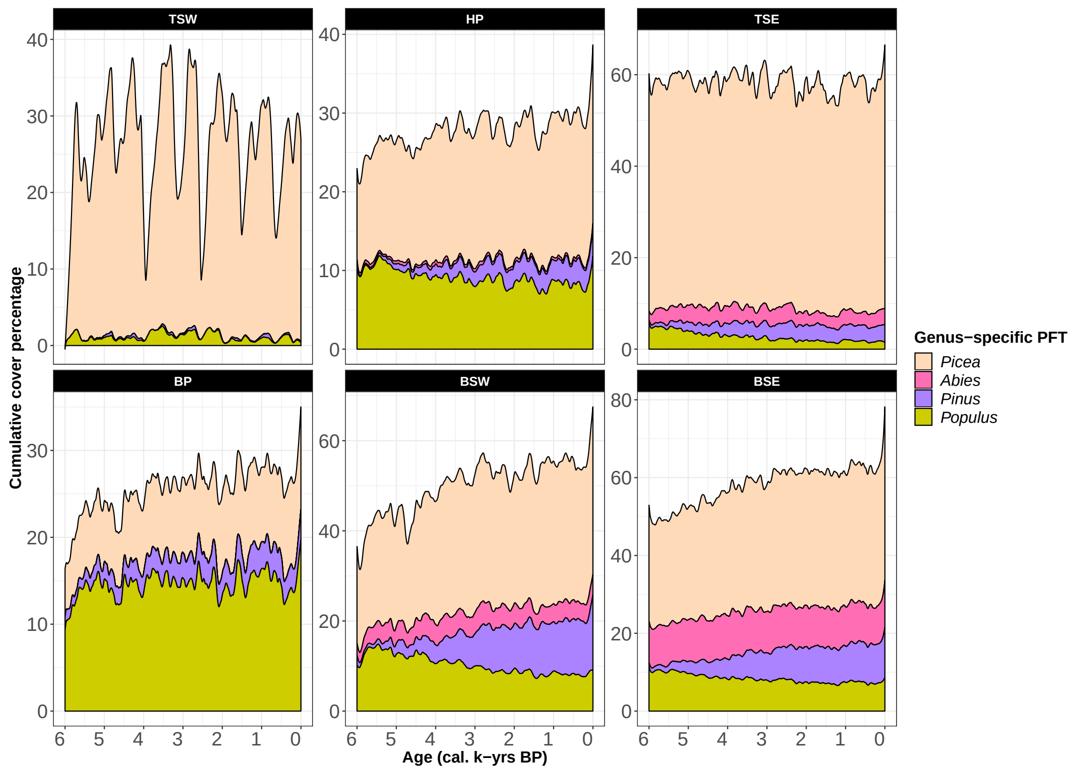

Figure 4.4. LPJ-LMfire's simulated cumulative cover percentage for four genus-specific PFTs (*Picea*, *Abies*, *Pinus* and *Populus*) for each ecozone in eastern Canada's boreal forest over the last 6000 years.

3.3.2 Comparison of LPJ-LMfire model simulations with reconstructions obtained from pollen and lacustrine-charcoal records

Changes in annual area burned and total tree biomass simulated by LPJ-LMfire during the last 6000 years were not synchronous with changes in biomass burning activity nor total tree biomass reconstructions obtained from lacustrine-charcoal and pollen records, respectively (Figure 4.5A), especially in the southern ecozones (BSW and BSE). Biomass burning activity reconstructions obtained from lacustrine-charcoal showed that the long-term fire regime at regional scale fluctuated during the last 6000 years with greater biomass burning prevailing from 6000 to 3000 BP and then declining toward the present day (Figure 4.5A; Figure S4.3 in Supplement S4.4). In contrast, simulated annual area burned increased continuously until today in the BSW and BSE ecozones with a rapid increase simulated approximately at the end of the simulation period (Figure 4.5A). Observed biomass burning increased only from 6000 to 5000 BP and then declined continuously until today in the TSE ecozone (Figure 4.5A; Figure S4.3 in Supplement S4.4), whereas simulated annual areas burned were relatively constant during the entire period (Figure 4.5A). The paleofire history representative of reconstructions pooled at the subcontinental-scale (i.e. "All" reconstruction) was very similar to those trends observed and simulated in southern ecozones (BSW and BSE; Figure 4.5A). The reconstructed increase in fire frequency is likely inherent to the fact that southern charcoal sites were more numerous than the northern ones (41 versus 14, respectively); hence the "All" reconstruction is weighted more strongly toward the southern regions (Figure 4.1).

Overall, the total tree biomass from pollen-based reconstructions was relatively constant in the three ecozones and at the subcontinental-scale (Figure 4.5B). Maximum and minimum observed total tree biomass, equal to $\sim$58 and $\sim$24 T.ha^{-1}, were in the BSW and TSE ecozones, respectively. Simulated total tree biomass decreased slightly until 5000 BP, and then increased continuously until today in the BSW and BSE ecozones (Figure 4.5B). Simulated total tree biomass in the TSE showed fewer variations during the entire period and agreed more closely with observed trend (Figure 4.5B). However, simulated total tree biomass was higher than observed all over the study area during the entire period, except in the BSW ecozone from 6000 to 4000 BP (Figure 4.5B).

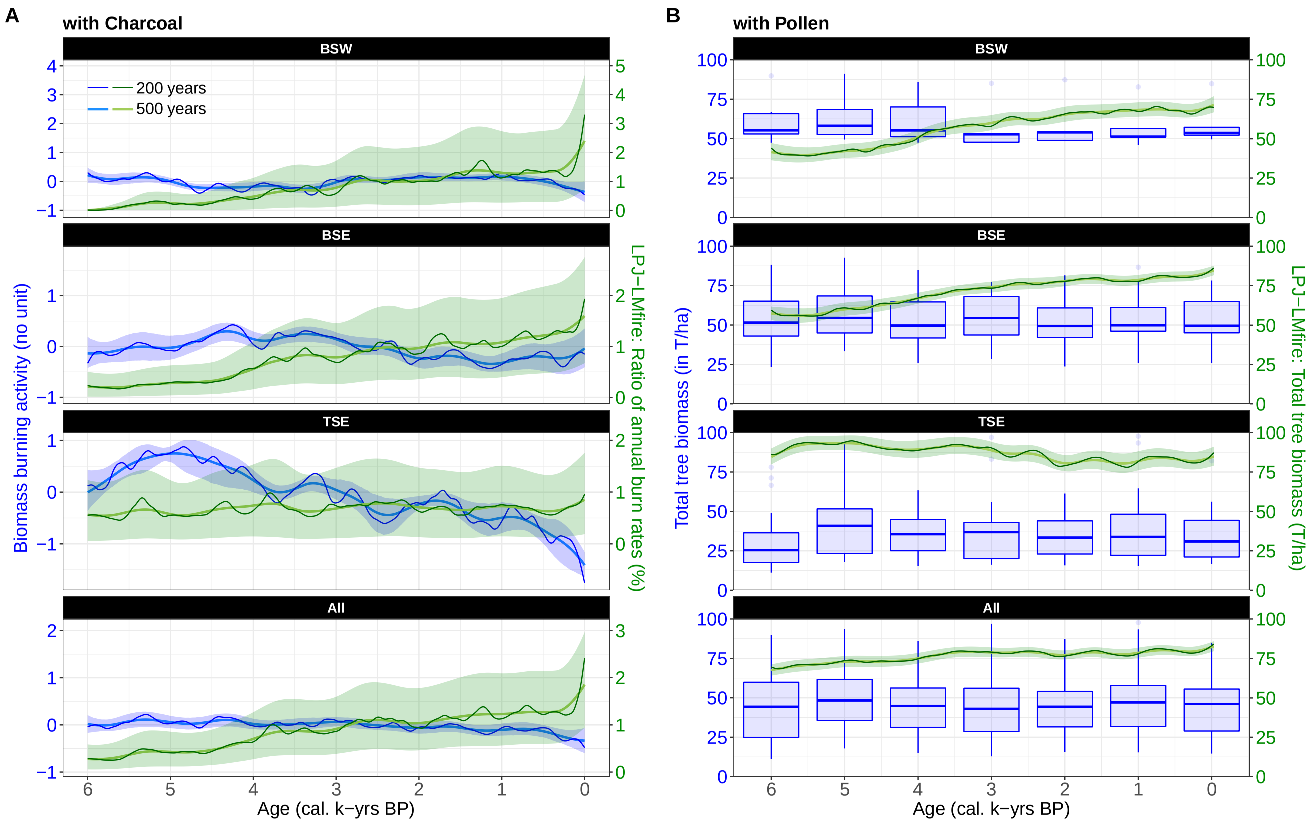

Figure 4.5. Observed (blue) versus LPJ-LMfire-simulated (green) (A) fire activity and (B) total tree biomass (T.ha^{-1}) in three ecozones in eastern Canada's boreal forest and all over the study area during the last 6000 years. Observed fire activity corresponds to biomass burning activity reconstructed from the composite charcoal records, while observed total tree biomass were reconstructed by applying the Modern Analogue Technique (MAT) transfer function to pollen records. Simulated fire activity and total tree biomass correspond to the ratio of mean annual area burned and total aboveground biomass, respectively, compared to the average between 6000-0 cal. years BP period. Transparent color areas represent the 95% confidence interval smoothed using a 500-year window half width.

Reconstruction of vegetation history with pollen records pooled at the subcontinental-scale showed constant level of tree biomass, whereas simulations showed a continuous increase from 6000 to 0 BP (Figure 4.5B).

3.4 Discussion

We presented advances made in the deployment of the LPJ-LMfire DGVM in eastern Canada's boreal forest, and evaluated the performance of the model at multi-millennial time-scales in a comparison of its simulations against lacustrine sedimentary charcoal records and pollen-based aboveground biomass records. Our model simulations showed a continuous increase in annual area burned from 6000 to 0 BP (Figures 4.3 and 4.5A), with a corresponding increase in the proportion of needleleaf stands in the BSW, HP and BSE ecozones (Figure 4.4). An increase of fire susceptibility in needleaf stands comes from the fact that needles contain highly flammable oils and resin that favor the growth and propagation of fires (Terrier et al., 2013; Van Wagner, 1987; Hély et al., Submitted). The present results highlight the "bottom-up" controls of fuel composition and availability on fire risk within the simulation (Hély et al., 2000, 2001). In contrast, biomass burning activity reconstructions obtained from lacustrine-charcoal showed that, except for the BSW ecozone, the long-term fire histories at regional scale fluctuated during the last 6000 years with higher biomass burning prevailing from 6000 to 3000 BP and then declining toward the present day (Figure 4.5A; Figure S4.3 in Supplement S4.4). This long-term fire trajectory is now firmly established by paleoecological studies from eastern Canada, which also showed that declines in biomass burning activity from 3000 BP were driven by changes toward less fire-conducive regional climates (the so-called Neoglacial period; e.g. Ali et al., 2012; Carcaillet et al., 2001; Couillard et al., 2013; El-Guellab et al., 2015; Girardin et al., 2013; Hély et al., 2010a; Moos and Cumming, 2012). Hence, there is a mismatch between simulations and observations at multi-millennial time-scales.

Albeit the trends in LPJ-LMfire simulated annual areas burned are in contradiction with the trends observed from paleoecological records, the simulated trends do find echoes in more specific regional paleoecological studies originating from the boreal mixedwood forest that is located further south. Based on charcoal analyses, Blarquez et al. (2015) have reconstructed an increase in biomass burning activity from 6000 BP to 2000 BP, followed by high and stable biomass burning activity over the last 2000 years. The high biomass burning activity from 2000 to 0 BP was associated with a decrease in broadleaf tree biomass recorded from pollen-based proxy records. These changes observed in the annual area burned and in the forest composition of the boreal mixedwood forest in Quebec are very similar to the patterns simulated by LPJ-LMfire in the Boreal Shield East. It is likely that the mismatch between simulated and observed forest biomass and fire trajectories in eastern ecozones results from vegetation zones simulated too far north by LPJ-LMfire compared to their actual distribution. Moreover, since the processes associated with post-fire regeneration failures are not included in LPJ-LMfire, compositional conditions remained favorable to fire propagation within the simulations whereas in reality, a decline of forest cover has taken place (Girard et al., 2008; Payette et al., 2008). The absence of post-fire regeneration failures may explain why annual area burned remained at a constant level from 6000 to 0 BP in the TSE ecozone (Figure S4.2 in Supplement S4.3) where the treeless areas did not decrease (Figure 4.4).

Discrepancies between model simulations and observations can inform climate modellers about representativeness of past climate simulated globally and the importance of considering indirect responses of the environment at regional scale. It was not the aim of this study to evaluate the IPSL-CM5-LR output used to force LPJ-LMfire, but rather to use it as a possible Holocene scenario of climate and investigate its impact on the vegetation in relation to fires. However, the disagreement between simulated and observed changes in annual area burned and total tree biomass during the last 6000 years (Figure 4.5) could imply that some climate processes are not well represented in the IPSL-CM5-LR climate model. Orbital parameters prescribed in IPSL-CM5-LR for the mid-Holocene period (6000 BP) could result in an amplification of the seasonal heating in the Northern Hemisphere (Kageyama et al., 2013) and lead to warmer summers and colder winters in Northern Hemisphere (Chevalier et al., 2017). In eastern ecozones, high summer temperatures during the mid-Holocene period (6000 BP) associated with spring temperatures relatively similar to those during the PI (Figure 4.2), led to simulated high net primary productivity soon after the deglaciation (Figure S4.2 in Supplement S4.3) and consequently, simulated vegetation was established quickly (Figure S4.2 in Supplement S4.3). The high mean total aboveground biomass in the TSE ecozone after the deglaciation is unrepresentative of the long-term vegetation history reconstructed for northern Quebec (Gajewski et al., 1993; Richard et al., 1982) but is more similar to the one reconstructed for the southernmost areas (Blarquez and Aleman, 2016; Carcaillet et al., 2001). In the western ecozones, high summer temperatures were associated with cold spring temperatures from 6000 to 2000 BP. (Figure 4.2). It has been demonstrated that the amplitude of the warming between seasons during the growing season (April to September) influences tree productivity (Girardin et al., 2014). For instance, a negative response of vegetation productivity could appear if summer warming exceeds spring warming (Girardin et al., 2014). By following this reasoning, we can speculate that colder springs simulated by IPSL-CM5-LR from mid-Holocene to late-Holocene (∼4000 BP) in western ecozones have limited simulated tree growth and resulted in low total aboveground biomass (Figure S4.2 in Supplement S4.3) and smaller forested areas (Figure 4.4) and hence less annual area burned (Figure 4.3). Moreover, colder temperatures in spring can lead to small fire years due to shorter snow free periods and shortening of the fire seasons (Ali et al., 2012; Girardin and Terrier, 2015; Hély et al., 2010a). Consequently, the discrepancy between simulated and observed trajectories may be due to uncertainty in the IPSL-CM5A-LR climate data that were used as input to the LPJ-LMfire model. We speculate that this seasonal heating amplification could result in the displacement of vegetation zones simulated too far north in the east and too far south in the west.

An evaluation of IPSL-CM5-LR's paleoclimate simulations at regional scale in eastern Canada is essential to test this hypothesis; to our knowledge, the performance of these transient simulations has only been evaluated for Africa (Chevalier et al., 2017; Lézine et al., 2017). Generally, paleoclimate simulations show difficulties in predicting the magnitude of shifting regional climates although the direction of these shifts are often correct. There is a growing necessity to continue the evaluation of paleoclimate simulations carried out by the PMIP5 group at regional scales to determine with higher resolution the causes of persistent mismatches (Harrison et al., 2015). Additional transient climate simulations are needed to further understand millennial-to centennial-scale interactions among climate, vegetation and fire (Marsicek et al., 2018). Moreover, we have added uncertainties in the climate data because we had no means to estimate how interannual climatic variability had changed during the Holocene, so we applied the observed variability between 1951 and 2010 to the full Holocene record (see section 4.2.3). However, it is increasingly recognized that recent past variability of climate observations are not a good analogue for Holocene variability (Kelly et al., 2016; Hudiburg et al., 2017). For instance, Miller et al. (2008) have shown that a DGVM simulation forced by a doubling of the level of interannual climatic variability during the Holocene in Fennoscandia led to the absence of species close to their bioclimatic distribution limits, although pollen reconstructions showed their presence in the past.

Climate projections indicate that an increase in temperature and in frequency and magnitude of extreme drought events over the course of the 21st century in Canada (IPCC, 2014; Price et al., 2013) will result in an increase in frequency and sizes of wildfires (Flannigan et al., 2009, 2016; Girardin et al., 2013; Girardin and Mudelsee, 2008; Krause et al., 2014; Bergeron et al., 2010). However, these projections are commonly based on studies that do not include the negative feedbacks of vegetation changes (fuel composition, availability and connectivity) on wildfire and processes associated with post-fire regeneration failures. Although a possible spatial shift of vegetation zones was simulated by LPJ-LMfire, our results supports previous conclusions that vegetation dynamics are driven in large part by long-term regional climate (Miller et al., 2008) and vegetation could act as an important "bottom-up" control to attenuate some of the impacts of a generally warmer climate on the future fire risk (Chaste et al., 2019; Hély et al., 2010b; Héon et al., 2014).

3.5 Conclusions

In this study, past changes in fire frequency, vegetation (composition and biomass) and primary productivity, as well as their interactions and feedbacks, were simulated using the LPJ-LMfire dynamic vegetation model driven by two transient climate datasets representing the last 6000 years and compared with palaeoecological reconstructions obtained from pollen and lacustrine-charcoal records. Disagreements between simulation outputs and paleoecological reconstructions that often reflect local processes, provide evidence that some local processes, not included in LPJ-LMfire, have influenced Holocene trajectories of forest dynamics. Moreover, the comparison revealed that spatial distributions of vegetation zones were not simulated very well, perhaps because some climate processes are not well represented in the IPSL-CM5-LR climate model. This study may help the climate modelling community to target the gaps in paleoclimate simulations and thus provide information for future directions to improve paleoclimate simulations to further understand millennial-to-centennial-scale interactions among climate, vegetation and fire.

Code availability: The source code of LPJ-LMfire is available at https://github.com/ARVE-Research/LPJ-LMfire/tree/v1.3 (Kaplan et al., 2018).

Acknowledgments

The study was made possible thanks to financial supports provided by the European European IRSES NEWFOREST project, the Forest Complexity Modelling (FCM) program and the NSERC Strategic and Discovery programs. Jed Kaplan was supported by the European Research Council (COEVOLVE 313797). This research was conducted as part of the International Associated Laboratory MONTABOR (LIA France-Canada) and the International Research Group on Cold Forests. The authors are particularly grateful to Olivier Marti and Pascale Braconnot for datas sharing of the French Pierre-Simon-Laplace Institute Earth system model IPSL-CM5A-LR; to Olivier Blarquez for help with charcoal records calculations; to Calcul Quebec and Compute Canada for server space facilities for running LPJ-LMfire; to Xiao Jing Guo for help with computation for this project.

References

Ali, A. A., Blarquez, O., Girardin, M. P., Hely, C., Tinquaut, F., El Guellab, A., Valsecchi, V., Terrier, A., Bremond, L., Genries, A., Gauthier, S., and Bergeron, Y. (2012). Control of the multimillennial wildfire size in boreal North America by spring climatic conditions. *Proceedings of the National Academy of Sciences USA*, 109(51):20966–20970, doi:10.1073/pnas.1203467109.

Andrews, P. L., Bevins, C. D., and Seli, R. C. (2008). BehavePlus fire modeling system, version 4.0: User's Guide, available from: https://www.fs.fed.us/rm/pubs/rmrs_gtr106.pdf.

Archibald, S., Lehmann, C. E. R., Belcher, C. M., Bond, W. J., Bradstock, R. A., Daniau, A. L., Dexter, K. G., Forrestel, E. J., Greve, M., and He, T. (2018). Biological and geophysical feedbacks with fire in the Earth system. *Environmental Research Letters*, 13(3):033003, doi:10.1088/1748-9326/aa9ead.

Berger, A. and Loutre, M.-F. (1991). Insolation values for the climate of the last 10 million years. *Quaternary Science Reviews*, 10(4):297–317, doi:10.1016/0277-3791(91)90033-Q.

Bergeron, Y., Cyr, D., Girardin, M. P., and Carcaillet, C. (2010). Will climate change drive 21st century burn rates in Canadian boreal forest outside of its natural variability: collating global climate model experiments with sedimentary charcoal data. *International Journal of Wildland Fire*, 19(8):1127–1139, doi:10.1071/WF09092.

Bergeron, Y., Vijayakumar, D. B. I. P., Ouzennou, H., Raulier, F., Leduc, A., and Gauthier, S. (2017). Projections of future forest age class structure under the influence of fire and harvesting: implications for forest management in the boreal forest of eastern Canada. *Forestry: An International Journal of Forest Research*, 90:485–495, doi:10.1093/forestry/cpx022.

Blarquez, O. and Aleman, J. C. (2016). Tree biomass reconstruction shows no lag in postglacial afforestation of eastern Canada. *Canadian Journal of Forest Research*, 46(4):485–498, doi:10.1139/cjfr-2015-0201.

Blarquez, O., Ali, A. A., Girardin, M. P., Grondin, P., Fréchette, B., Bergeron, Y., and Hély, C. (2015). Regional paleofire regimes affected by non-uniform climate, vegetation and human drivers. *Scientific Reports*, 5(1), doi:10.1038/srep13356.

Brandt, J. P. (2009). The extent of the North American boreal zone. *Environmental Reviews*, 17:101–161, doi:10.1139/A09-004.

Carcaillet, C., Bergeron, Y., Richard, P. J., Fréchette, B., Gauthier, S., and Prairie, Y. T. (2001). Change of fire frequency in the eastern Canadian boreal forests during the Holocene: does vegetation composition or climate trigger the fire regime? *Journal of Ecology*, 89(6):930–946, doi:10.1111/j.1365-2745.2001.00614.x.

Chaste, E., Girardin, M. P., Kaplan, J. O., Bergeron, Y., and Hély, C. (2019). Increases in heat-induced tree mortality could drive reductions of biomass resources in Canada's managed boreal forest. *Landscape Ecology*, pages 1–24, doi:10.1007/s10980-019-00780-4.

Chaste, E., Girardin, M. P., Kaplan, J. O., Portier, J., Bergeron, Y., and Hély, C. (2018). The pyrogeography of eastern boreal Canada from 1901 to 2012 simulated with the LPJ-LMfire model. *Biogeosciences*, 15(5):1273–1292, doi:10.5194/bg-15-1273-2018.

Chevalier, M., Brewer, S., and Chase, B. M. (2017). Qualitative assessment of PMIP3 rainfall simulations across the eastern African monsoon domains during the mid-Holocene and the Last Glacial Maximum. *Quaternary Science Reviews*, 156:107–120, doi:10.1016/j.quascirev.2016.11.028.

Couillard, P.-L., Payette, S., and Grondin, P. (2013). Long-term impact of fire on high-altitude balsam fir (*Abies balsamea*) forests in south-central Quebec deduced from soil charcoal. *Canadian Journal of Forest Research*, 43(2):188–199, doi:10.1139/cjfr-2012-0414.

Dufresne, J.-L., Foujols, M.-A., Denvil, S., Caubel, A., Marti, O., Aumont, O., Balkanski, Y., Bekki, S., Bellenger, H., Benshila, R., Bony, S., Bopp, L., Braconnot, P., Brockmann, P., Cadule, P., Cheruy, F., Codron, F., Cozic, A., Cugnet, D., Noblet, N. d., Duvel, J.-P., Ethé, C., Fairhead, L., Fichefet, T., Flavoni, S., Friedlingstein, P., Grandpeix, J.-Y., Guez, L., Guilyardi, E., Hauglustaine, D., Hourdin, F., Idelkadi, A., Ghattas, J., Joussaume, S., Kageyama, M., Krinner, G., Labetoulle, S., Lahellec, A., Lefebvre, M.-P., Lefevre, F., Levy, C., Li, Z. X., Lloyd, J., Lott, F., Madec, G., Mancip, M., Marchand, M., Masson, S., Meurdesoif, Y., Mignot, J., Musat, I., Parouty, S., Polcher, J., Rio, C., Schulz, M., Swingedouw, D., Szopa, S., Talandier, C., Terray, P., Viovy, N., and Vuichard, N. (2013). Climate change projections using the IPSL-CM5 Earth System Model: from CMIP3 to CMIP5. *Climate Dynamics*, 40(9-10):2123–2165, doi:10.1007/s00382-012-1636-1.

Ecological Stratification Working Group (1996). A national ecological framework for Canada, available from: http://sis.agr.gc.ca/cansis/references/1996ew_a.html. Technical report.

El-Guellab, A., Asselin, H., Gauthier, S., Bergeron, Y., and Ali, A. A. (2015). Holocene variations of wildfire occurrence as a guide for sustainable management of the north-eastern Canadian boreal forest. *Forest Ecosystems*, 2(1):15, doi:10.1186/s40663-015-0039-2.

Environment Canada (2013). National Climate Data and Information Archive, available from: http://climate.weatheroffice.gc.ca/.

Flannigan, M., Stocks, B., Turetsky, M., and Wotton, M. (2009). Impacts of climate change on fire activity and fire management in the circumboreal forest. *Global Change Biology*, 15(3):549–560, doi:10.1111/j.1365-2486.2008.01660.x.

Flannigan, M. D., Wotton, B. M., Marshall, G. A., Groot, W. J. d., Johnston, J., Jurko, N., and Cantin, A. S. (2016). Fuel moisture sensitivity to temperature and precipitation: climate change implications. *Climatic Change*, 134(1-2):59–71, doi:10.1007/s10584-015-1521-0.

Frégeau, M., Payette, S., and Grondin, P. (2015). Fire history of the central boreal forest in eastern North America reveals stability since the mid-Holocene. *The Holocene*, 25(12):1912–1922, doi:0.1177/0959683615591361.

Gajewski, K., Payette, S., and Ritchie, J. C. (1993). Holocene vegetation history at the boreal-forest-shrub-tundra transition in North-Western Quebec. *Journal of Ecology*, 81(3):433–443, doi:10.2307/2261522.

Gauthier, S., Bernier, P., Burton, P. J., Edwards, J., Isaac, K., Isabel, N., Jayen, K., Le Goff, H., and Nelson, E. A. (2014). Climate change vulnerability and adaptation in the managed Canadian boreal forest. *Environmental Reviews*, 22(3):256–285, doi:10.1139/er-2013-0064.

Girard, F., Payette, S., and Gagnon, R. (2008). Rapid expansion of lichen woodlands within the closed-crown boreal forest zone over the last 50 years caused by stand disturbances in eastern Canada. *Journal of Biogeography*, 35(3):529–537, doi:10.1111/j.1365-2699.2007.01816.x.

Girardin, M. P., Ali, A. A., Carcaillet, C., Gauthier, S., Hély, C., Le Goff, H., Terrier, A., and Bergeron, Y. (2013). Fire in managed forests of eastern Canada: Risks and options. *Forest ecology and management*, 294:238–249, doi:10.1016/j.foreco.2012.07.005.

Girardin, M. P., Bergeron, Y., Tardif, J. C., Gauthier, S., Flannigan, M. D., and Mudelsee, M. (2006). A 229-year dendroclimatic-inferred record of forest fire activity for the Boreal Shield of Canada. *International Journal of Wildland Fire*, 15(3):375–388, doi:10.1071/WF05065.

Girardin, M. P., Guo, X. J., De Jong, R., Kinnard, C., Bernier, P., and Raulier, F. (2014). Unusual forest growth decline in boreal North America covaries with the retreat of Arctic sea ice. *Global change biology*, 20(3):851–866, doi:10.1111/gcb.12400.

Girardin, M. P. and Mudelsee, M. (2008). Past and future changes in Canadian boreal wildfire activity. *Ecological Applications*, 18(2):391–406, doi:10.1890/07-0747.1.

Girardin, M. P. and Terrier, A. (2015). Mitigating risks of future wildfires by management of the forest composition: an analysis of the offsetting potential through boreal Canada. *Climatic Change*, 130(4):587–601, doi:10.1007/s10584-015-1373-7.

Hantson, S., Arneth, A., Harrison, S. P., Kelley, D. I., Prentice, I. C., Rabin, S. S., Archibald, S., Mouillot, F., Arnold, S. R., Artaxo, P., and others (2016). The status and challenge of global fire modelling. *Biogeosciences*, 13(11):3359–3375, doi:10.5194/bg-13-3359-2016.

Harris, R. M. B., Remenyi, T. A., Williamson, G. J., Bindoff, N. L., and Bowman, D. M. J. S. (2016). Climate-vegetation-fire interactions and feedbacks: trivial detail or major barrier to projecting the future of the Earth system? *Wiley Interdisciplinary Reviews: Climate Change*, 7(6):910–931, doi:10.1002/wcc.428.

Harrison, S. P., Bartlein, P., Izumi, K., Li, G., Annan, J., Hargreaves, J., Braconnot, P., and Kageyama, M. (2015). Evaluation of CMIP5 palaeo-simulations to improve climate projections. *Nature Climate Change*, 5(8):735, doi:10.1038/nclimate2649.

Hély, C., Bergeron, Y., and Flannigan, M. D. (2000). Effects of stand composition on fire hazard in mixed-wood Canadian boreal forest. *Journal of Vegetation Science*, 11(6):813–824, doi:10.2307/3236551.

Hély, C., Flannigan, M., Bergeron, Y., and McRae, D. (2001). Role of vegetation and weather on fire behavior in the Canadian mixedwood boreal forest using two fire behavior prediction systems. *Canadian Journal of Forest Research*, 31(3):430–441, doi:10.1139/cjfr-31-3-430.

Hély, C., Fortin, C. M.-J., Anderson, K. R., and Bergeron, Y. (2010a). Landscape composition influences local pattern of fire size in the eastern Canadian boreal forest: role of weather and landscape mosaic on fire size distribution in mixedwood boreal forest using the Prescribed Fire Analysis System. *International Journal of Wildland Fire*, 33(6):356–360, doi:10.1579/0044-7447-33.6.356.

Hély, C., Girardin, M. P., Ali, A. A., Carcaillet, C., Brewer, S., and Bergeron, Y. (2010b). Eastern boreal North American wildfire risk of the past 7000 years: A model-data comparison. *Geophysical Research Letters*, 85(7):1916–1932, doi:10.1890/02-0716.

Hély, C., Remy, C. C., Chaste, E., Girardin, M.-P., Blarquez, O., Bergeron, Y., and Ali, A. A. (Submitted). Fire models serving paleoecology: fire size and spring fires as key processes in differentiating the mixedwood from the coniferous boreal forests.

Hengl, T., de Jesus, J. M., MacMillan, R. A., Batjes, N. H., Heuvelink, G. B. M., Ribeiro, E., Samuel-Rosa, A., Kempen, B., Leenaars, J. G. B., Walsh, M. G., and Gonzalez, M. R. (2014). SoilGrids1km – Global soil information based on automated mapping. *PLoS One*, 9(8):e105992, doi:10.1371/journal.pone.0105992.

Héon, J., Arseneault, D., and Parisien, M.-A. (2014). Resistance of the boreal forest to high burn rates. *Proceedings of the National Academy of Sciences*, 111(38):13888–13893, doi:10.1073/pnas.1409316111.

Higuera, P. E., Peters, M. E., Brubaker, L. B., and Gavin, D. G. (2007). Understanding the origin and analysis of sediment-charcoal records with a simulation model. *Quaternary Science Reviews*, 26(13):1790–1809, doi:10.1016/j.quascirev.2007.03.010.

Hu, F. S., Brubaker, L. B., Gavin, D. G., Higuera, P. E., Lynch, J. A., Rupp, T. S., and Tinner, W. (2006). How Climate and Vegetation Influence the fire Regime of the Alaskan Boreal Biome: The Holocene Perspective. *Mitigation and Adaptation Strategies for Global Change*, 11(4):829–846, doi:10.1007/s11027-005-9015-4.

Hudiburg, T. W., Higuera, P. E., and Hicke, J. A. (2017). Fire-regime variability impacts forest carbon dynamics for centuries to millennia. *Biogeosciences Discussions*, pages 1–24, doi:10.5194/bg-2017-42.

IPCC (2014). *Climate Change 2014: Synthesis Report . Contribution of Working Groups I, II and III to the Fifth Assessment Report of the Intergovernmental Panel on Climate Change*. [Core Writing Team, R.K. Pachauri and L.A. Meyer (eds.)]. IPCC, Geneva, Switzerland.

Jasinski, J. P. and Payette, S. (2005). The creation of alternative stable states in the southern boreal forest, Quebec, Canada. *Ecological Monographs*, 75(4):561–583, doi:10.1890/04-1621.

Jaume-Santero, F., Pickler, C., Beltrami, H., and Mareschal, J.-C. (2016). North American regional climate reconstruction from ground surface temperature histories. *Climate of the Past*, 12(12):2181, doi:10.5194/cp-12-2181-2016.

Kageyama, M., Braconnot, P., Bopp, L., Caubel, A., Foujols, M.-A., Guilyardi, E., Khodri, M., Lloyd, J., Lombard, F., Mariotti, V., Marti, O., Roy, T., and Woillez, M.-N. (2013). Mid-Holocene and Last Glacial Maximum climate simulations with the IPSL model - part I: comparing IPSL_cm5a to IPSL_cm4. *Climate Dynamics*, 40(9-10):2447–2468, doi:10.1007/s00382-012-1488-8.

Kaplan, J. O., Pfeiffer, M., and Chaste, E. (2018). ARVE-Research/LPJ-LMfire: LPJ-LMfire (version v1.3), Zenodo. doi:10.5281/zenodo.1184589.

Kelly, R., Chipman, M. L., Higuera, P. E., Stefanova, I., Brubaker, L. B., and Hu, F. S. (2013). Recent burning of boreal forests exceeds fire regime limits of the past 10,000 years. *Proceedings of the National Academy of Sciences*, 110(32):13055–13060, doi:10.1073/pnas.1305069110.

Kelly, R., Genet, H., McGuire, A. D., and Hu, F. S. (2016). Palaeodata-informed modelling of large carbon losses from recent burning of boreal forests. *Nature Climate Change*, 6(1):79–82, doi:10.1038/nclimate2832.

Krause, A., Kloster, S., Wilkenskjeld, S., and Paeth, H. (2014). The sensitivity of global wildfires to simulated past, present, and future lightning frequency. *Journal of Geophysical Research: Biogeosciences*, 119(3):312–322, doi:10.1002/2013JG002502.

Krinner, G., Viovy, N., de Noblet-Ducoudré, N., Ogée, J., Polcher, J., Friedlingstein, P., Ciais, P., Sitch, S., and Prentice, I. C. (2005). A dynamic global vegetation model for studies of the coupled atmosphere-biosphere system. *Global Biogeochemical Cycles*, 19(1), doi:10.1029/2003GB002199.

Kucharik, C. J., Foley, J. A., Delire, C., Fisher, V. A., Coe, M. T., Lenters, J. D., Young-Molling, C., Ramankutty, N., Norman, J. M., and Gower, S. T. (2000). Testing the performance of a dynamic global ecosystem model: water balance, carbon balance, and vegetation structure. *Global Biogeochemical Cycles*, 14(3):795–825, doi:10.1029/1999GB001138.

Lézine, A.-M., Ivory, S. J., Braconnot, P., and Marti, O. (2017). Timing of the southward retreat of the ITCZ at the end of the Holocene Humid Period in Southern Arabia: Data-model comparison. *Quaternary Science Reviews*, 164:68–76, doi:10.1016/j.quascirev.2017.03.019.

Lloyd, E. A. and Winsberg, E. (2018). *Climate Modelling: Philosophical and Conceptual Issues*. Springer.

Mackay, A., Battarbee, R., Birks, J., and Oldfield, F. E. (2003). *Global change in the Holocene.* Arnold, Hodder Headline Group.

Magnan, G., Garneau, M., and Payette, S. (2014). Holocene development of maritime ombrotrophic peatlands of the St. Lawrence North Shore in eastern Canada. *Quaternary Research*, 82(1):96–106, doi:10.1016/j.yqres.2014.04.016.

Marsicek, J., Shuman, B. N., Bartlein, P. J., Shafer, S. L., and Brewer, S. (2018). Reconciling divergent trends and millennial variations in Holocene temperatures. *Nature*, 554(7690):92, doi:10.1038/nature25464.

Miller, P. A., Giesecke, T., Hickler, T., Bradshaw, R. H., Smith, B., Seppä, H., Valdes, P. J., and Sykes, M. T. (2008). Exploring climatic and biotic controls on Holocene vegetation change in Fennoscandia. *Journal of Ecology*, 96(2):247–259, doi:10.1111/j.1365-2745.2007.01342.x.

Moos, M. T. and Cumming, B. F. (2012). Climate-fire interactions during the Holocene: a test of the utility of charcoal morphotypes in a sediment core from the boreal region of north-western Ontario (Canada). *International Journal of Wildland Fire*, 21(6):640–652, doi:10.1071/WF10117.

Natural Resources Canada (2010). Geobase - National hydro network, geogratis, available from: http://ftp.geogratis.gc.ca/pub/nrcan_rncan/vector/geobase_nhn_rhn/.

Oris, F., Asselin, H., Finsinger, W., Hely, C., Blarquez, O., Ferland, M.-E., Bergeron, Y., and Ali, A. A. (2014). Long-term fire history in northern Quebec: implications for the northern limit of commercial forests. *Journal of applied ecology*, 51(3):675–683, doi:10.1111/1365-2664.12240.

Orville, R. E., Huffines, G. R., Burrows, W. R., and Cummins, K. L. (2011). The North American Lightning Detection Network (NALDN) - Analysis of flash data: 2001â09. *Monthly Weather Review*, 139(5):1305–1322, doi:10.1175/2010MWR3452.1.

Ouarmim, S., Ali, A. A., Asselin, H., Hély, C., and Bergeron, Y. (2015). Evaluating the persistence of post-fire residual patches in the eastern Canadian boreal mixedwood forest. *Boreas*, 44(1):230–239, doi:10.1111/bor.12087.

Payette, S., Filion, L., and Delwaide, A. (2008). Spatially explicit fire-climate history of the boreal forest-tundra (Eastern Canada) over the last 2000 years. *Philosophical Transactions of the Royal Society of London B: Biological Sciences*, 363(1501):2299–2314, doi:10.1098/rstb.2007.2201.

Peterson, D., Wang, J., Ichoku, C., and Remer, L. A. (2010). Effects of lightning and other meteorological factors on fire activity in the North American boreal forest: implications for fire weather forecasting. *Atmospheric Chemistry and Physics*, 10(14):6873–6888, doi:10.5194/acp-10-6873-2010.

Pfeiffer, M., Spessa, A., and Kaplan, J. O. (2013). A model for global biomass burning in preindustrial time: LPJ-LMfire (v1. 0). *Geoscientific Model Development*, 6(3):643–685, doi:10.5194/gmd-6-643-2013.

Pilon, V., Payette, S., Couillard, P.-L., and Laflamme, J. (2018). Surface analysis as a method to reconstruct past and recent dynamics of forest ecosystems. *Forest Ecology and Management*, 407:84–94, doi:10.1016/j.foreco.2017.09.064.

Podur, J., Martell, D. L., and Knight, K. (2002). Statistical quality control analysis of forest fire activity in Canada. *Canadian Journal of Forest Research*, 32(2):195–205, doi:10.1139/X01-183.

Power, M. J., Marlon, J., Ortiz, N., Bartlein, P. J., Harrison, S. P., Mayle, F. E., Ballouche, A., Bradshaw, R. H., Carcaillet, C., and Cordova, C. (2008). Changes in fire regimes since the Last Glacial Maximum: an assessment based on a global synthesis and analysis of charcoal data. *Climate dynamics*, 30(7-8):887–907, doi:10.1007/s00382-007-0334-x.

Price, D. T., Alfaro, R. I., Brown, K. J., Flannigan, M. D., Fleming, R. A., Hogg, E. H., Girardin, M. P., Lakusta, T., Johnston, M., McKenney, D. W., Pedlar, J. H., Stratton, T., Sturrock, R. N., Thompson, I. D., Trofymow, J. A., and Venier, L. A. (2013). Anticipating the consequences of climate change for Canada's boreal forest ecosystems. *Environmental Reviews*, 21(4):322–365, doi:10.1139/er-2013-0042.

Rabin, S. S., Melton, J. R., Lasslop, G., Bachelet, D., Forrest, M., Hantson, S., Kaplan, J. O., Li, F., Mangeon, S., Ward, D. S., Yue, C., Arora, V. K., Hickler, T., Kloster, S., Knorr, W., Nieradzik, L., Spessa, A., Folberth, G. A., Sheehan, T., Voulgarakis, A., Kelley, D. I., Prentice, I. C., Sitch, S., Harrison, S., and Arneth, A. (2017). The Fire Modeling Intercomparison Project (FireMIP), phase 1: experimental and analytical protocols with detailed model descriptions. *Geosci. Model Dev.*, 10(3):1175–1197, doi:10.5194/gmd-10-1175-2017.

Régnière, J., Saint-Amant, R., and Béchard, A. (2014). *BioSIM 10 - Guide de l'utilisateur.* Number LAU-X-137. Ressour. Nat. Can., Serv. can. for., Cent. for. Laurentides, Québec (Québec), available from: http://www.cfs.nrcan.gc.ca/publications/?id=34817.

Richard, P., Larouche, A., and Bouchard, M. (1982). Âge de la déglaciation finale et histoire postglaciaire de la végétation dans la partie centrale du Nouveau-Québec. *Géographie physique et Quaternaire*, 36(1-2):63–90, doi:10.7202/032470ar.

Romps, D. M., Seeley, J. T., Vollaro, D., and Molinari, J. (2014). Projected increase in lightning strikes in the United States due to global warming. *Science*, 346(6211):851–854, doi:10.1126/science.1259100.

Rothermel, R. C. (1972). A Mathematical Model for Predicting Fire Spread in Wildland Fuels, Intermountain Forest and Range Experiment Station, Forest Service, U.S. Department of Agriculture, Ogden, Utah. Technical report.

Senici, D., Lucas, A., Chen, H. Y., Bergeron, Y., Larouche, A., Brossier, B., Blarquez, O., and Ali, A. A. (2013). Multi-millennial fire frequency and tree abundance differ between xeric and mesic boreal forests in central Canada. *Journal of Ecology*, 101(2):356–367, doi:10.1111/1365-2745.12047.

Simard, I., Morin, H., and Lavoie, C. (2006). A millennial-scale reconstruction of spruce budworm abundance in Saguenay, Québec, Canada. *The Holocene*, 16(1):31–37, doi:10.1191/0959683606hl904rp.

Sitch, S., Smith, B., Prentice, I. C., Arneth, A., Bondeau, A., Cramer, W., Kaplan, J. O., Levis, S., Lucht, W., Sykes, M. T., Thonicke, K., and Venevsky, S. (2003). Evaluation of ecosystem dynamics, plant geography and terrestrial carbon cycling in the LPJ dynamic global vegetation model. *Global Change Biology*, 9(2):161–185, doi:10.1046/j.1365-2486.2003.00569.x.

Smith, B., Prentice, I. C., and Sykes, M. T. (2001). Representation of vegetation dynamics in the modelling of terrestrial ecosystems: comparing two contrasting approaches within European climate space. *Global Ecology and Biogeography*, 10(6):621–637, doi:10.1046/j.1466-822X.2001.t01-1-00256.x.

Taylor, K. E., Stouffer, R. J., and Meehl, G. A. (2012). An Overview of CMIP5 and the Experiment Design. *Bulletin of the American Meteorological Society*, 93(4):485–498, doi:10.1175/BAMS-D-11-00094.1.

Terrier, A., Girardin, M. P., Périé, C., Legendre, P., and Bergeron, Y. (2013). Potential changes in forest composition could reduce impacts of climate change on boreal wildfires. *Ecological Applications*, 23(1):21–35, doi:10.1890/12-0425.1.

Thonicke, K., Spessa, A., Prentice, I. C., Harrison, S. P., Dong, L., and Carmona-Moreno, C. (2010). The influence of vegetation, fire spread and fire behaviour on biomass burning and trace gas emissions: results from a process-based model. *Biogeosciences*, 7(6):1991–2011, doi:10.5194/bg-7-1991-2010.

Tinner, W., Hofstetter, S., Zeugin, F., Conedera, M., Wohlgemuth, T., Zimmermann, L., and Zweifel, R. (2006). Long-distance transport of macroscopic charcoal by an intensive crown fire in the Swiss Alps - implications for fire history reconstruction. *The Holocene*, 16(2):287–292, doi:10.1191/0959683606hl925rr.

Van Wagner, C. E. (1987). *Development and structure of the Canadian Forest Fire Weather Index System*. available from: https://cfs.nrcan.gc.ca/publications?id=19927.

Whitmore, J., Gajewski, K., Sawada, M., Williams, J. W., Shuman, B., Bartlein, P. J., Minckley, T., Viau, A. E., Webb, T., and Shafer, S. (2005). Modern pollen data from North America and Greenland for multi-scale paleoenvironmental applications. *Quaternary Science Reviews*, 24(16):1828–1848, doi:10.1016/j.quascirev.2005.03.005.

Supplementary materials

Supplement S4.1

Table S4.1. Annual and seasonal temperature (°C) and precipitation (%) anomalies over the last 6000 years relative to the preindustrial control period averages (equal to the 1901-1950 period).

		Mean anomalies relative to preindustrial control period average (°C and %)						Preindustrial control period average (°C and mm)
50-years time period (cal. years BP)		6000	5000	4000	3000	2000	1000	0 (1901-1950)
Temperature								
	Annual	0.8	0.6	0.6	0.5	0.4	0.8	-2.0
	Spring	0.2	0.1	-0.6	-0.7	-0.4	0.1	4.2
	Summer	2.1	1.6	1.2	0.8	0.5	0.8	12.4
Precipitation								
	Annual	5.3	2.4	4.2	3.5	1.5	4.6	732.8
	Spring	-3.0	-6.6	-2.4	1.9	-3.5	3.5	177.0
	Summer	12.4	10.1	6.6	5.6	4.9	8.1	261.3

Supplement S4.2

Figure S4.1. Carbon dioxide concentration over the last 6000 years used to run LPJ-LMfire.

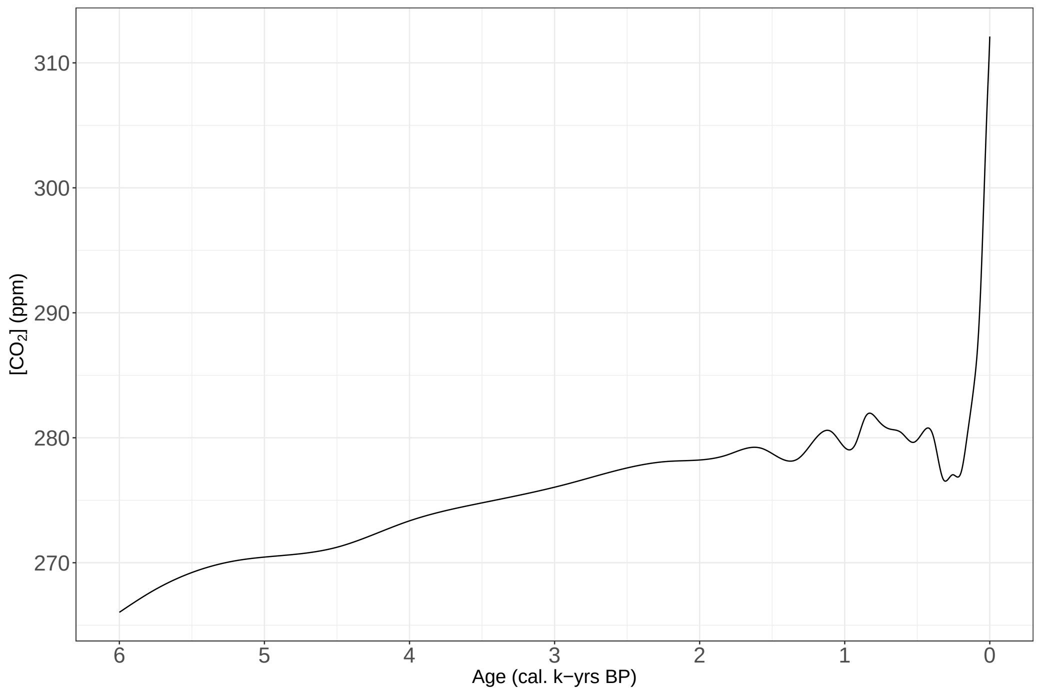

Supplement S4.3

Figure S4.2. Mean total aboveground biomass ($T.ha^{-1}$), annual area burned ($\%.yr^{-1}$) and annual net primary productivity ($T.ha^{-1}.yr^{-1}$) for six 1000-year periods between 6000-0 BP across six ecozones in eastern Canada.

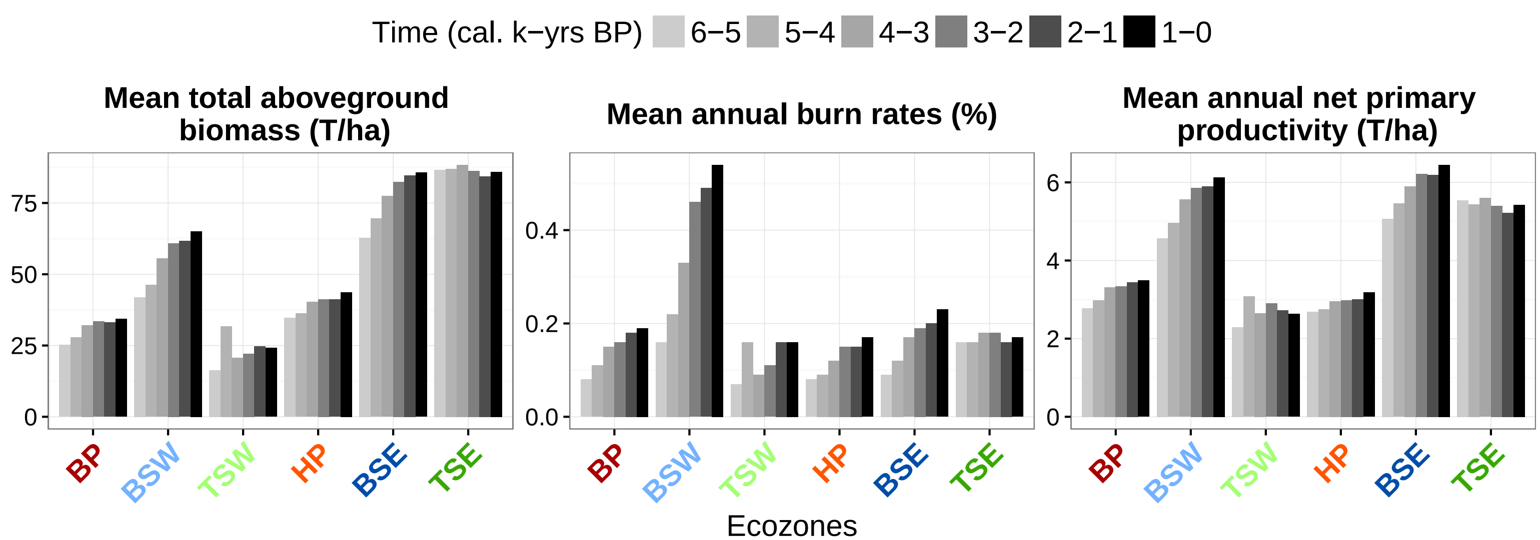

Supplement S4.4

Figure S4.3. Biomass burning activity from the compositing of charcoal records for three ecozones in eastern Canada's boreal forest and all sites (sub-continental average). The black and red lines correspond to the scatter plot smoothing calculated using a 500 and 200 year window half width, respectively. The grey coloured areas represent the 95% confidence interval calculated using the bootstrap procedure (calculated on the 500-yr trend).

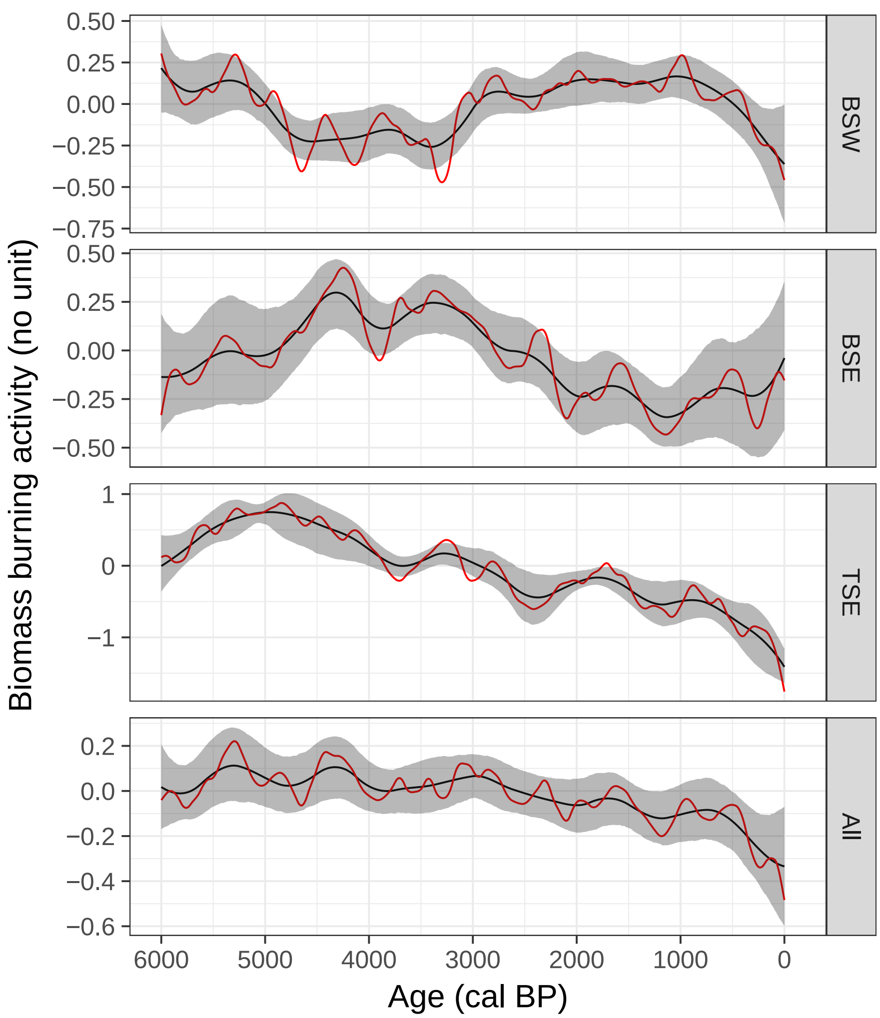

Conclusion générale

Cette thèse de doctorat s'inscrit dans un contexte d'aménagement adaptatif des ressources forestières boréales à l'Est du Canada en prévision des changements climatiques. Le principal objectif de ce travail était d'approfondir les connaissances actuelles des effets potentiels des changements climatiques sur la dynamique de végétation et des incendies, et de caractériser leurs effets conjoints sur la résilience de la forêt boréale de l'Est canadien de part et d'autre de la limite nordique des forêts sous aménagement. Pour rappel, la résilience est définie comme la capacité de la forêt à se rétablir suite à des perturbations. Déterminer les zones forestières où la résilience de la forêt sera amoindrie par les changements climatiques est essentiel afin d'adapter les pratiques sylvicoles en vue de respecter les enjeux écologiques et socio-économiques de l'aménagement forestier durable.

Ce travail de recherche propose pour la première fois des simulations effectuées avec le modèle LPJ-LMfire sur une longue échelle temporelle (passé, présent, futur) et à haute résolution spatiale (100 km^2) sur la forêt boréale de l'Est canadien, afin de déterminer les relations étroites entre le climat, les feux et la végétation qui ont existé sur une longue échelle de temps dans le passé (chapitres 1 et 3) et qui sont projetées jusqu'en 2100 (chapitre 2). Cette conclusion expose de manière synthétique les nouvelles connaissances apportées par ce travail de doctorat concernant (i) la variabilité temporelle des relations climat-feux-végétation, (ii) l'hétérogénéité spatiale de la réponse de la forêt boréale de l'Est canadien aux changements climatiques et les implications pour l'aménagement forestier, et (iii) les pistes de recherche future.

4.1 Variabilité temporelle des relations climat-feux-végétation

Ce travail a tout d'abord montré que la variabilité climatique est un facteur déterminant des tendances spatio-temporelles de la fréquence des feux au cours du dernier siècle (chapitre 1). Bien qu'il ait été démontré que ces relations ont existé au cours de l'Holocène, l'utilisation de données climatiques passées, qui semble amplifier les tendances temporelles des températures et entrainer un possible déplacement trop au nord de la forêt coniférienne dans nos simulations, a entravé notre compréhension des relations entre le climat et les feux au cours de l'Holocène (chapitre 3). Généralement, les projections du risque de feux futur sont obtenues en utilisant des modèles empiriques s'appuyant soit sur des variables décrivant les processus d'assèchement des couches du sol, soit sur le produit de fonctions représentant l'occurrence des impacts de foudre et la disponibilité et l'humidité du combustible. Ces projections s'accordent sur une tendance d'augmentation de la fréquence et de la taille des feux en réponse à la hausse prévue des températures, et de la fréquence et de l'amplitude des évènements météorologiques extrêmes tels que les sécheresses. Nos résultats vont à l'encontre de ces projections et suggèrent au contraire une diminution de la fréquence des feux d'ici 2100, particulièrement dans les régions sud de notre zone d'étude, bien que l'occurrence des impacts de foudre soit plus importante et que les conditions climatiques futures soient plus propices aux feux (chapitre 2). Cette diminution sera en fait associée à un changement de composition des forêts, en particulier des taxons résineux remplacés par des taxons feuillus, et à une ouverture/fragmentation des paysages via l'augmentation du couvert non boisé qui devrait limiter les allumages et la propagation des feux (chapitre 2). Par conséquent, nos résultats révèlent que la fréquence de feu future sera vraisemblablement limitée par la végétation (composition, disponibilité et fragmentation) dans ces régions. L'influence de la végétation sur la fréquence des feux existe depuis l'Holocène (chapitre 3), mais devrait jouer un rôle prépondérant sur l'activité de feu dans le futur, notamment dans la deuxième moitié du 21[ème] siècle dans les régions du sud de la forêt boréale de l'Est canadien (chapitre 2). Nos résultats confirment l'importance des rétroactions des changements de végétation, particulièrement la composition, sur la fréquence des feux (chapitres 2 et 3) et montrent la nécessité de les inclure dans les projections futures du risque de feux, ce que ne faisaient généralement pas les études précédentes. Bien que les effets de rétroactions des changements de végétation sur la fréquence des feux pourraient atténuer les effets d'un climat plus chaud et sec sur l'activité de feux, il est à noter que ces changements seront également en partie le résultat de l'influence du climat passé sur l'activité des feux (chapitre 1). En effet, une augmentation des événements météorologiques extrêmes propices aux feux entre 1950 et 2010 a déjà entrainé une hausse de la fréquence des feux dans les régions sud-ouest (chapitres 1 et 2), favorisant ainsi l'expansion des feuillus moins propices aux feux (chapitre 2). Il semble que cette tendance va s'amplifier dans le futur et s'étendre vers le nord.

Nos résultats démontrent également que les tendances spatio-temporelles récentes des feux n'ont pas été influencées par les allumages d'origine anthropique (chapitre 1) bien que ceux-ci soient nombreux en zone boréale malgré de faibles densités de population (Parisien et al., 2016). Par ailleurs, nos résultats suggèrent que les efforts de lutte contre les incendies mis en place par les agences de suppression des feux n'ont pas contribué à altérer les tendances spatio-temporelles « naturelles » des feux (Cumming, 2005; Martell and Sun, 2008; Parisien et al., 2011). Nos résultats montrent également l'influence de la variabilité interannuelle de l'occurrence des impacts de foudre sur les tendances spatio-temporelles récentes des feux en forêt boréale de l'Est canadien (chapitre 1). Cependant, une hausse de l'occurrence des impacts de foudre dans le futur ne devrait pas causer une augmentation des superficies brûlées en raison de l'influence limitante (rétroaction négative) de la végétation (chapitre 2). Ainsi, ce travail de recherche confirme que la variabilité interannuelle des aires brûlées s'explique par un effet conjoint de l'occurrence des impacts de foudre, des conditions climatiques et météorologiques, et des caractéristiques du combustible (type, disponibilité, humidité, fragmentation) (chapitres 1 et 2).

Ces recherches ont également mis en cause l'influence de la hausse des températures et des concentrations en CO_2 atmosphérique sur l'augmentation de la productivité des forêts (chapitre 1 et 2). Toutefois cet accroissement de productivité ne sera pas illimité et pourrait être contraint par les effets des sécheresses sur la mortalité des arbres, particulièrement dans les régions sud (chapitre 2). À noter que, bien que cela n'ait pas été démontré dans notre travail, les changements climatiques pourront en outre limiter la disponibilité des nutriments, ce qui aura un effet négatif sur la productivité de la végétation (Norby et al., 2010). L'influence négative des changements climatiques sur la productivité ne sera pas un phénomène nouveau puisque des évènements de déclin de la productivité forestière ont déjà été observés dans le passé (chapitre 1), et notamment proche de la limite nordique des forêts sous aménagement (Girardin et al., 2016).

4.2 Hétérogénéité spatiale de la réponse de la forêt boréale de l'Est canadien aux changements climatiques et implications pour l'aménagement forestier

Les simulations réalisées dans cette thèse de doctorat mettent en évidence la variabilité temporelle des relations climat-feux-végétation et confirment l'hétérogénéité spatiale de la réponse de la végétation aux changements climatiques au sein d'un même biome. Les gains de productivité induits par l'augmentation des concentrations en CO_2 atmosphérique ont compensé les pertes de biomasse causées par les feux au cours du dernier siècle sur l'ensemble de la forêt boréale de l'Est canadien (chapitre 1). Cependant, ces effets compensatoires ne devraient pas perdurer dans les régions au sud de la limite nordique des forêts sous aménagement, particulièrement à l'ouest de la zone d'étude (chapitre 2). Ce déséquilibre serait notamment le résultat de l'augmentation des conditions météorologiques sèches qui entraînerait un accroissement des épisodes de mortalité des arbres. À court terme, cette augmentation des événements de mortalité engendrerait une hausse du combustible disponible pour les feux dans la première moitié du 21ème siècle (chapitre 2). Cependant à moyen et long terme, cette baisse de productivité pourrait induire une diminution importante de la productivité et des stocks de bois, en particulier des espèces résineuses, limitant ainsi l'activité de feux (chapitre 2). Ainsi, les espèces adaptées voire dépendantes du passage de feux (p. ex. le pin gris et l'épinette noire) auront des difficultés à se maintenir dans les paysages forestiers. La résilience de la forêt boréale pourrait ainsi être amoindrie au sud de la limite nordique des forêts sous aménagement dans l'Est canadien et cette réponse sera d'autant plus rapide que les conditions climatiques dans le futur seront chaudes et sèches (chapitre 2).

Une diminution des stocks de bois des espèces résineuses au profit des feuillus au sud de la limite nordique des forêts sous aménagement pourrait engendrer des retombées économiques importantes sur le secteur forestier. En effet, les espèces résineuses sont majoritairement ciblées par l'industrie forestière au Canada en raison de la grande force de résistance mécanique de leur bois et de leur haute valeur ajoutée (Bureau du forestier en chef, 2013; McKenney et al., 2016). Par ailleurs, la pérennité de l'aménagement forestier durable qui vise une résilience des écosystèmes suffisante pour maintenir des forêts de densité et de productivité adéquate risque d'être compromise si aucune mesure n'est prise. Des stratégies d'aménagement doivent être mises en place afin d'anticiper cette perte de résilience et d'assurer une pérennité de l'aménagement forestier durable. Certains scénarios sylvicoles plus intensifs pourraient permettre d'augmenter la productivité et orienter la composition des peuplements vers des espèces résineuses ciblées, tels que les coupes partielles ou les éclaircies précommerciales (Bureau du forestier en chef, 2013). En effet, ces pratiques sylvicoles pourraient redynamiser la croissance végétale en favorisant les peuplements jeunes, plus productifs que les peuplements vieux, et en enlevant certains compétiteurs (comme les arbres coupés) permettant aux arbres en place de profiter d'un maximum d'espace et de nutriments. Ainsi, elles pourraient permettent de faciliter la régénération des espèces résineuses préétablies et de limiter l'effeuillement de la forêt boréale (Bose et al., 2014; Prévost and Pothier, 2003). Des plantations d'enrichissement d'espèces résineuses dans les trouées forestières d'origine naturelle ou sylvicole pourraient également être mises en œuvre (Bose et al., 2014; Prévost et al., 2010).

Bien que les espèces résineuses soient d'importance économique pour le secteur forestier, plusieurs d'entre elles pourraient devenir non-adaptées aux nouvelles conditions climatiques dans la partie sud de leurs aires de répartition (p. ex. le pin gris, l'épinette blanche, le sapin baumier ; McKenney et al., 2014; Périé et al., 2014). Cela pourrait menacer l'existence même de la forêt boréale mixte. Néanmoins, il est important de noter que la grande diversité génétique intraspécifique des arbres boréaux (Verta et al., 2013) pourrait permettre à ces espèces de survivre, même dans des zones où les conditions futures seront très différentes des conditions actuelles (Housset et al., 2018). Par ailleurs, nos recherches ne prennent pas en compte l'ensemble des perturbations naturelles et anthropiques qui pourraient avoir des effets cumulatifs négatifs sur la résilience des forêts. Au regard de ces incertitudes, axer majoritairement les stratégies sylvicoles sur le maintien de la composition actuelle en espèces résineuses pourrait ne pas suffire pour assurer une pérennité de l'aménagement forestier durable. Ainsi, des pratiques sylvicoles orientées vers un aménagement de peuplements mixtes pourraient déjà être envisagées afin de maintenir un niveau de résilience suffisant à plus long terme. Il a d'ailleurs été démontré que ce type d'aménagement pourrait être intéressant économiquement tout en maintenant une certaine diversité de paysages et en favorisant ainsi les multiples usagers de la forêt (Légaré et al., 2005). Pour conserver un niveau de résilience suffisant sur le long terme, il pourrait être également envisageable d'avoir recours à la migration assistée des espèces arborées à haute valeur ajoutée très tolérantes à la sécheresse que l'on retrouve actuellement plus au sud (Duveneck and Scheller, 2015).

Les régions au nord et au sud-est de la limite nordique des forêts sous aménagement dans l'Est canadien devraient répondre moins négativement aux changements climatiques que celles situées au sud-ouest. Nos simulations montrent que l'équilibre devrait perdurer entre les gains de productivité induits par le CO_2 et le climat, et les pertes associées aux feux et aux sécheresses (chapitre 2). Néanmoins, ces conclusions ne prennent pas en compte le fait que la résilience de la forêt boréale dans ces régions pourrait être amoindrie par des effets négatifs cumulatifs de plusieurs perturbations naturelles et processus écosystémiques. Un maintien de la fréquence des feux dans les régions les plus septentrionales associé à des accidents de régénération diminuerait la disponibilité des banques de graines viables et la présence d'individus matures pour les produire, ce qui diminuerait du même coup la régénération des peuplements. Ainsi, une ouverture des paysages forestiers au profit d'un couvert de lichens est à envisager afin de limiter l'établissement des espèces résineuses (Splawinski et al., In press). Les épidémies de la tordeuse des bourgeons de l'épinette (TBE) qui constituent une importante perturbation naturelle en Amérique du Nord entraînent actuellement une forte mortalité des espèces de conifères (p. ex. le sapin baumier et l'épinette blanche) dans les régions les plus méridionales (Gray, 2013; Pureswaran et al., 2015). La dynamique des populations de la TBE est principalement régie par le climat qui a une influence directe sur le cycle de vie de l'insecte, et indirecte sur la distribution de ses hôtes, à savoir le sapin baumier et les épinettes. Des températures estivales plus chaudes pourraient favoriser la croissance, la survie et la reproduction de la TBE. Par ailleurs, des printemps plus précoces pourraient entrainer un synchronisme plus rapide entre le développement des larves au printemps et le débourrement des hôtes, augmentant ainsi la durée des épidémies. Un déplacement vers le nord des aires de répartition des espèces d'arbres hôtes pourrait également entrainer une migration de la limite nord de la défoliation vers des latitudes plus septentrionales (Logan et al., 2003; Pureswaran et al., 2015). Ainsi, une augmentation globale de la superficie et de la durée de défoliation est envisagée et pourrait avoir des répercussions considérables sur la biomasse forestière. De plus, la prise en compte des processus de paludification dans LPJ-LMfire contribuerait également à diminuer la productivité des arbres au sein de la forêt boréale de la Ceinture d'Argile (Terrier et al., 2014). Ainsi, au regard de l'impact potentiel de tous ces effets négatifs cumulatifs sur la résilience de la forêt boréale septentrionale et de sa répartition spatiale actuelle, il serait prudent de conserver la position actuelle de la limite nordique des forêts sous aménagement (Jobidon et al., 2015).

4.3 Pistes de recherche

Ce travail de doctorat a apporté de nouveaux éléments de réponse sur les impacts potentiels des changements climatiques sur la résilience de la forêt boréale de l'Est Canadien. Ce faisant, il a également contribué à mettre en lumière des limites concernant les données et les outils actuels, ainsi que des verrous que la recherche scientifique devra tenter de résoudre à l'avenir. Tout d'abord, une réduction de l'incertitude associée à la modélisation de la résilience de la forêt pourrait être effectuée en paramétrisant LPJ-LMfire pour une liste d'espèces arborées plus diversifiée, notamment celles présentes actuellement plus au Sud. Par ailleurs, l'incorporation des paramétrisations récemment développées pour les arbustes boréaux et les plantes non-vasculaires (Druel, 2017) permettrait notamment de mieux représenter les conditions nordiques. Une amélioration des simulations effectuées sur l'Holocène (chapitre 3) est nécessaire pour mieux comprendre les relations qui ont existé entre le climat, le feu et la végétation. Pour ce faire, des simulations LPJ-LMfire réalisées avec d'autres données paléo-climatiques disponibles (p. ex. HadCM3BL-M1 ; Valdes et al., 2017) permettraient d'améliorer la robustesse des reconstructions passées. Les futurs travaux devront aussi se concentrer sur l'intégration de nouveaux modules dans LPJ-LMfire qui reflètent les processus d'autres perturbations naturelles susceptibles d'impacter significativement la forêt boréale de l'Est canadien. C'est dans ce cadre que cette recherche avait également comme objectif initial d'intégrer un module de TBE dans LPJ-LMfire. Ce module, principalement basé sur les travaux de Régnière et al. (p. ex. 1989; 2012; 2014), devait avoir pour fonction de calculer (i) une probabilité de présence de populations de larves de TBE en réponse aux températures saisonnières, et (ii) l'impact potentiel de ces populations sur la biomasse forestière des principales espèces d'arbres hôtes. Pour des raisons pratiques liées au fonctionnement même du modèle, ce module initialement écrit en langage R a été correctement traduit en Fortran 90 mais son intégration complète n'a finalement pas pu voir le jour dans le cadre de cette thèse. Des travaux à venir sont cependant prévus pour achever son développement et son intégration dans LPJ-LMfire. Ainsi, des résultats à venir prochainement nous permettront d'apporter de nouveaux éléments de réponse sur la résilience de la forêt boréale de l'Est canadien en réponse aux changements climatiques et à la dynamique des deux plus grandes perturbations en forêt boréale au Canada. Les efforts déployés par la communauté scientifique au cours des dernières années pour améliorer les modèles de la dynamique globale de végétation ont été considérables. Les projections futures ont été affinées et les incertitudes réduites, ce qui est encourageant pour continuer le développement des modèles de prédictions. Par ailleurs, cette thèse a montré la nécessité d'avoir à disposition des données observées multi-proxies afin de déterminer la robustesse des modèles utilisés pour les projections. C'est pourquoi, continuer l'acquisition de données observées sur des zones encore peu échantillonnées et à haute résolution temporelle est à encourager même si ces démarches sont longues et coûteuses.

BIBLIOGRAPHIE GÉNÉRALE

Ali, A. A., Blarquez, O., Girardin, M. P., Hély, C., Tinquaut, F., El Guellab, A., Valsecchi, V., Terrier, A., Bremond, L., Genries, A., Gauthier, S., and Bergeron, Y. (2012). Control of the multimillennial wildfire size in boreal North America by spring climatic conditions. *Proceedings of the National Academy of Sciences USA*, 109(51) :20966–20970, doi :10.1073/pnas.1203467109.

Allen, C. D., Macalady, A. K., Chenchouni, H., Bachelet, D., McDowell, N., Vennetier, M., Kitzberger, T., Rigling, A., Breshears, D. D., Hogg, E. H. T., Gonzalez, P., Fensham, R., Zhang, Z., Castro, J., Demidova, N., Lim, J.-H., Allard, G., Running, S. W., Semerci, A., and Cobb, N. (2010). A global overview of drought and heat-induced tree mortality reveals emerging climate change risks for forests. *Forest Ecology and Management*, 259(4) :660–684, doi :10.1016/j.foreco.2009.09.001.

Anyomi, K. A., Raulier, F., Bergeron, Y., Mailly, D., and Girardin, M. P. (2014). Spatial and temporal heterogeneity of forest site productivity drivers : a case study within the eastern boreal forests of canada. *Landscape ecology*, 29(5) :905–918, doi :10.1007/s10980-014-0026-y.

Arseneault, D. (2001). Impact of fire behavior on postfire forest development in a homogeneous boreal landscape. *Canadian Journal of Forest Research*, 31(8) :1367–1374, doi :10.1139/cjfr-31-8-1367.

Baudena, M., Dekker, S. C., van Bodegom, P. M., Cuesta, B., Higgins, S. I., Lehsten, V., Reick, C. H., Rietkerk, M., Scheiter, S., Yin, Z., et al. (2015). Forests, savannas and grasslands : bridging the knowledge gap between ecology and Dynamic Global Vegetation Models. *Biogeosciences*, 12 :1833–1848, doi :10.5194/bg-12-1833-2015.

Beaudoin, A., Bernier, P., Guindon, L., Villemaire, P., Guo, X., Stinson, G., Bergeron, T., Magnussen, S., and Hall, R. (2014). Mapping attributes of Canada's forests at moderate resolution through *k*NN and MODIS imagery. *Canadian Journal of Forest Research*, 44(5) :521–532, doi :10.1139/cjfr-2013-0401.

Bergeron, Y., Chen, H. Y., Kenkel, N. C., Leduc, A. L., and Macdonald, S. E. (2014). Boreal mixedwood stand dynamics : ecological processes underlying multiple pathways. *The Forestry Chronicle*, 90(2) :202–213, doi :10.5558/tfc2014-039.

Bernier, P. Y., Gauthier, S., Jean, P.-O., Manka, F., Boulanger, Y., Beaudoin, A., and Guindon, L. (2016). Mapping local effects of forest properties on fire risk across Canada. *Forests*, 7(8) :157, doi :10.3390/f7080157.

Bonsai, B. R. and Wheaton, E. E. (2005). Atmospheric circulation comparisons between the 2001 and 2002 and the 1961 and 1988 Canadian prairie droughts. *Atmosphere-Ocean*, 43(2) :163–172, doi :10.3137/ao.430204.

Bose, A. K., Harvey, B. D., and Brais, S. (2014). Sapling recruitment and mortality dynamics following partial harvesting in aspen-dominated mixedwoods in eastern Canada. *Forest ecology and management*, 329 :37–48, doi :10.1016/j.foreco.2014.06.004.

Boucher, D., Boulanger, Y., Aubin, I., Bernier, P. Y., Beaudoin, A., Guindon, L., and Gauthier, S. (2018). Current and projected cumulative impacts of fire, drought, and insects on timber volumes across canada. *Ecological applications*, 28(5) :1245–1259.

Boucher, Y., Auger, I., Noël, J., Grondin, P., and Arseneault, D. (2017). Fire is a stronger driver of forest composition than logging in the boreal forest of eastern Canada. *Journal of Vegetation Science*, 28(1) :57–68, doi :10.1111/jvs.12466.

Boulanger, Y., Gauthier, S., and Burton, P. J. (2014). A refinement of models projecting future Canadian fire regimes using homogeneous fire regime zones. *Canadian Journal of Forest Research*, 44(4) :365–376, doi :10.1139/cjfr-2013-0372.

Boulanger, Y., Gauthier, S., Burton, P. J., and Vaillancourt, M.-A. (2012). An alternative fire regime zonation for Canada. *International Journal of Wildland Fire*, 21(8) :1052–1064, doi :10.1071/WF11073.

Boulanger, Y., Taylor, A. R., Price, D. T., Cyr, D., McGarrigle, E., Rammer, W., Sainte-Marie, G., Beaudoin, A., Guindon, L., and Mansuy, N. (2017). Climate change impacts on forest landscapes along the Canadian southern boreal forest transition zone. *Landscape Ecology*, 32(7) :1415–1431, doi :10.1007/s10980-016-0421-7.

Bradshaw, R. H. and Sykes, M. T. (2014). *Ecosystem dynamics : from the past to the future*. John Wiley & Sons.

Brandt, J., Flannigan, M., Maynard, D., Thompson, I., and Volney, W. (2013). An introduction to Canada's boreal zone : ecosystem processes, health, sustainability, and environmental issues. *Environmental Reviews*, 21(4) :207–226, doi :10.1139/er-2013-0040.

Brandt, J. P. (2009). The extent of the North American boreal zone. *Environmental Reviews*, 17 :101–161, doi :10.1139/A09-004.

Bureau du forestier en chef (2013). Manuel de détermination des possibilités forestières 2013-2018. *Gouvernement du Québec, Roberval, Qc*, page 247.

Canadian Council of Forest Ministers (2017). National Forestry Database. Forest Fire Statistics by Province/Territory/Agency, 1990-2016, available from : http ://nfdp.ccfm.org/data/compendium/ html/comp_31e.html,.

Charney, N. D., Babst, F., Poulter, B., Record, S., Trouet, V. M., Frank, D., Enquist, B. J., and Evans, M. E. (2016). Observed forest sensitivity to climate implies large changes in 21st century North American forest growth. *Ecology letters*, 19(9) :1119–1128.

Cook, J., Oreskes, N., Doran, P. T., Anderegg, W. R., Verheggen, B., Maibach, E. W., Carlton, J. S., Lewandowsky, S., Skuce, A. G., Green, S. A., et al. (2016). Consensus on consensus : a synthesis of consensus estimates on human-caused global warming. *Environmental Research Letters*, 11(4) :048002, doi :10.1088/1748-9326/11/4/048002.

Cox, P. M. (2001). Description of the triffid dynamic global vegetation model. *Hadley Centre technical note*, 24 :1–16.

Cumming, S. G. (2005). Effective fire suppression in boreal forests. *Canadian Journal of Forest Research*, 35(4) :772–786, doi :10.1139/X04-174.

Danneyrolles, V., Arseneault, D., and Bergeron, Y. (2016). Pre-industrial landscape composition patterns and post-industrial changes at the temperate-boreal forest interface in western Quebec, Canada. *Journal of Vegetation Science*, 27(3) :470–481, doi :10.1111/jvs.12373.

Deluca, T. H. and Boisvenue, C. (2012). Boreal forest soil carbon : distribution, function and modelling. *Forestry : An International Journal of Forest Research*, 85(2) :161–184, doi :10.1093/forestry/cps003.

D'orangeville, L., Duchesne, L., Houle, D., Kneeshaw, D., Côté, B., and Pederson, N. (2016). Northeastern North America as a potential refugium for boreal forests in a warming climate. *Science*, 352(6292) :1452–1455, doi :10.1126/science.aaf4951.

Druel, A. (2017). *Modélisation de la végétation boréale et de sa dynamique dans le modèle de surface continentale ORCHIDEE*. PhD thesis, Université Grenoble Alpes, Grenoble.

Duveneck, M. J. and Scheller, R. M. (2015). Climate-suitable planting as a strategy for maintaining forest productivity and functional diversity. *Ecological Applications*, 25(6) :1653–1668, doi :10.1890/14-0738.1.

Epstein, H. E., Yu, Q., Kaplan, J. O., and Lischke, H. (2007). Simulating future changes in arctic and subarctic vegetation. *Computing in Science & Engineering*, 9(4) :12–23, doi :10.1109/MCSE.2007.84.

Erni, S., Arseneault, D., Parisien, M.-A., and Bégin, Y. (2017). Spatial and temporal dimensions of fire activity in the fire-prone eastern Canadian taiga. *Global Change Biology*, 23(3) :1152–1166, doi :10.1111/gcb.13461.

Fei, S., Desprez, J. M., Potter, K. M., Jo, I., Knott, J. A., and Oswalt, C. M. (2017). Divergence of species responses to climate change. *Science Advances*, 3(5) :e1603055, doi :10.1126/sciadv.1603055.

Fenton, N., Lecomte, N., Légaré, S., and Bergeron, Y. (2005). Paludification in black spruce (Piceamariana) forests of eastern Canada : Potential factors and management implications. *Forest Ecology and Management*, 213(1) :151–159, doi :10.1016/j.foreco.2005.03.017.

Fisher, R. A., Koven, C. D., Anderegg, W. R. L., Christoffersen, B. O., Dietze, M. C., Farrior, C. E., Holm, J. A., Hurtt, G. C., Knox, R. G., Lawrence, P. J., Lichstein, J. W., Longo, M., Matheny, A. M., Medvigy, D., Muller-Landau, H. C., Powell, T. L., Serbin, S. P., Sato, H., Shuman, J. K., Smith, B., Trugman, A. T., Viskari, T., Verbeeck, H., Weng, E., Xu, C., Xu, X., Zhang, T., and Moorcroft, P. R. (2018). Vegetation demographics in Earth System Models : A review of progress and priorities. *Global Change Biology*, 24(1) :35–54, doi :10.1111/gcb.13910.

Fisichelli, N. A., Frelich, L. E., and Reich, P. B. (2014). Temperate tree expansion into adjacent boreal forest patches facilitated by warmer temperatures. *Ecography*, 37(2) :152–161, doi :10.1111/j.1600-0587.2013.00197.x.

Flannigan, M., Stocks, B., Turetsky, M., and Wotton, M. (2009). Impacts of climate change on fire activity and fire management in the circumboreal forest. *Global Change Biology*, 15(3) :549–560, doi :10.1111/j.1365-2486.2008.01660.x.

Flannigan, M. D., Logan, K. A., Amiro, B. D., Skinner, W. R., and Stocks, B. (2005). Future area burned in canada. *Climatic change*, 72(1-2) :1–16, doi :10.1007/s10584-005-5935-y.

Flannigan, M. D., Stocks, B. J., and Wotton, B. M. (2000). Climate change and forest fires. *Science of the total environment*, 262(3) :221–229, doi :10.1016/S0048-9697(00)00524-6.

Flannigan, M. D. and Wotton, B. M. (2001). Climate, weather and area burned. *Forest fires*, 351 :73, doi :10.1016/B978-012386660-8/50012-X.

Flannigan, M. D., Wotton, B. M., Marshall, G. A., Groot, W. J. d., Johnston, J., Jurko, N., and Cantin, A. S. (2016). Fuel moisture sensitivity to temperature and precipitation : climate change implications. *Climatic Change*, 134(1-2) :59–71, doi :10.1007/s10584-015-1521-0.

Foley, J. A., Prentice, I. C., Ramankutty, N., Levis, S., Pollard, D., Sitch, S., and Haxeltine, A. (1996). An integrated biosphere model of land surface processes, terrestrial carbon balance, and vegetation dynamics. *Global Biogeochemical Cycles*, 10(4) :603–628, doi :10.1029/96GB02692.

Gauthier, S., Bergeron, Y., and Simon, J.-P. (1996). Effects of fire regime on the serotiny level of jack pine. *The Journal of Ecology*, 84(4) :539, doi :10.2307/2261476.

Gauthier, S., Bernier, P., Kuuluvainen, T., Shvidenko, A. Z., and Schepaschenko, D. G. (2015). Boreal forest health and global change. *Science*, 349(6250) :819–822, doi :10.1126/science.aaa9092.

Gauthier, S., De Grandpré, L., and Bergeron, Y. (2000). Differences in forest composition in two boreal forest ecoregions of Quebec. *Journal of Vegetation Science*, 11(6) :781–790, doi :10.2307/3236548.

Girard, F., Payette, S., and Gagnon, R. (2008). Rapid expansion of lichen woodlands within the closed-crown boreal forest zone over the last 50 years caused by stand disturbances in eastern Canada. *Journal of Biogeography*, 35(3) :529–537, doi :10.1111/j.1365-2699.2007.01816.x.

Girardin, M. P., Ali, A. A., Carcaillet, C., Gauthier, S., Hély, C., Le Goff, H., Terrier, A., and Bergeron, Y. (2013). Fire in managed forests of eastern Canada : Risks and options. *Forest ecology and management*, 294 :238–249, doi :10.1016/j.foreco.2012.07.005.

Girardin, M. P., Bouriaud, O., Hogg, E. H., Kurz, W., Zimmermann, N. E., Metsaranta, J. M., Jong, R. d., Frank, D. C., Esper, J., Büntgen, U., Guo, X. J., and Bhatti, J. (2016). No growth stimulation of Canada's boreal forest under half-century of combined warming and CO_2 fertilization. *Proceedings of the National Academy of Sciences*, 113(52) :E8406–E8414, doi :10.1073/pnas.1610156113.

Girardin, M. P., Guo, X. J., De Jong, R., Kinnard, C., Bernier, P., and Raulier, F. (2014). Unusual forest growth decline in boreal North America covaries with the retreat of Arctic sea ice. *Global change biology*, 20(3) :851–866, doi :10.1111/gcb.12400.

Girardin, M. P. and Mudelsee, M. (2008). Past and future changes in Canadian boreal wildfire activity. *Ecological Applications*, 18(2) :391–406, doi :10.1890/07-0747.1.

Government of Canada, N. R. C. (2003). Définir l'aménagement forestier durable au Canada, avaible from : https ://cfs.nrcan.gc.ca/publications ?id=23637.

Gray, D. R. (2013). The influence of forest composition and climate on outbreak characteristics of the spruce budworm in eastern Canada. *Canadian Journal of Forest Research*, 43(12) :1181–1195, doi :10.1139/cjfr-2013-0240.

Hantson, S., Arneth, A., Harrison, S. P., Kelley, D. I., Prentice, I. C., Rabin, S. S., Archibald, S., Mouillot, F., Arnold, S. R., Artaxo, P., and others (2016). The status and challenge of global fire modelling. *Biogeosciences*, 13(11) :3359–3375, doi :10.5194/bg-13-3359-2016.

Harris, D. J. (2015). Generating realistic assemblages with a joint species distribution model. *Methods in Ecology and Evolution*, 6(4) :465–473, doi :10.1111/2041-210X.12332.

Hedwall, P.-O., Skoglund, J., and Linder, S. (2015). Interactions with successional stage and nutrient status determines the life-form-specific effects of increased soil temperature on boreal forest floor vegetation. *Ecology and evolution*, 5(4) :948–960, doi :10.1002/ece3.1412.

Hély, C., Bergeron, Y., and Flannigan, M. D. (2000). Effects of stand composition on fire hazard in mixed-wood Canadian boreal forest. *Journal of Vegetation Science*, 11(6) :813–824, doi :10.2307/3236551.

Hély, C., Flannigan, M., Bergeron, Y., and McRae, D. (2001). Role of vegetation and weather on fire behavior in the Canadian mixedwood boreal forest using two fire behavior prediction systems. *Canadian Journal of Forest Research*, 31(3) :430–441, doi :10.1139/cjfr-31-3-430.

Hobbie, S. E., Schimel, J. P., Trumbore, S. E., and Randerson, J. R. (2000). Controls over carbon storage and turnover in high-latitude soils. *Global Change Biology*, 6(S1) :196–210, doi :10.1046/j.1365-2486.2000.06021.x.

Housset, J. M., Nadeau, S., Isabel, N., Depardieu, C., Duchesne, I., Lenz, P., and Girardin, M. P. (2018). Tree rings provide a new class of phenotypes for genetic associations that foster insights into adaptation of conifers to climate change. *New Phytologist*, doi :10.1111/nph.14968.

IPCC (2013). *Climate Change 2013 - The Physical Science Basis : Working Group I Contribution to the Fifth Assessment Report of the Intergovernmental Panel on Climate Change*. [Stocker, T.F., D. Qin, G.-K. Plattner, M. Tignor, S.K. Allen, J. Boschung, A. Nauels, Y. Xia, V. Bex and P.M. Midgley (eds.)]. Cambridge University Press, Cambridge, United Kingdom and New York, NY, USA., Cambridge.

IPCC (2014). *Climate Change 2014 : Synthesis Report . Contribution of Working Groups I, II and III to the Fifth Assessment Report of the Intergovernmental Panel on Climate Change*. [Core Writing Team, R.K. Pachauri and L.A. Meyer (eds.)]. IPCC, Geneva, Switzerland.

Jobidon, R., Bergeron, Y., Robitaille, A., Raulier, F., Gauthier, S., Imbeau, L., Saucier, J.-P., and Boudreault, C. (2015). A biophysical approach to delineate a northern limit to commercial forestry : the case of Quebec's boreal forest. *Canadian Journal of Forest Research*, 45(5) :515–528.

Keeley, J. E. (2009). Fire intensity, fire severity and burn severity : a brief review and suggested usage. *International Journal of Wildland Fire*, 18(1) :116, doi :10.1071/WF07049.

Kelley, D. I., Harrison, S. P., and Prentice, I. C. (2014). Improved simulation of fire-vegetation interactions in the Land surface Processes and eXchanges dynamic global vegetation model (LPX-Mv1). *Geoscientific Model Development*, 7(5) :2411–2433, doi :10.5194/gmd-7-2411-2014.

Kerns, B. and Perterson, D. (2014). An Overview of Vegetation Models for Climate Change Impacts. U.S. Department of Agriculture, Forest Service, Climate Change Resource Center.

Krause, A., Kloster, S., Wilkenskjeld, S., and Paeth, H. (2014). The sensitivity of global wildfires to simulated past, present, and future lightning frequency. *Journal of Geophysical Research : Biogeosciences*, 119(3) :312–322, doi :10.1002/2013JG002502.

Krawchuk, M., Lisgo, K., Leroux, S., Vernier, P., Cumming, S., and Schmiegelow, F. (2012). Boreal Forest, Canada. In *Climate and Conservation*, pages 69–79. Springer.

Krinner, G., Viovy, N., de Noblet-Ducoudré, N., Ogée, J., Polcher, J., Friedlingstein, P., Ciais, P., Sitch, S., and Prentice, I. C. (2005). A dynamic global vegetation model for studies of the coupled atmosphere-biosphere system. *Global Biogeochemical Cycles*, 19(1), doi :10.1029/2003GB002199.

Kucharik, C. J., Foley, J. A., Delire, C., Fisher, V. A., Coe, M. T., Lenters, J. D., Young-Molling, C., Ramankutty, N., Norman, J. M., and Gower, S. T. (2000). Testing the performance of a dynamic global ecosystem model : water balance, carbon balance, and vegetation structure. *Global Biogeochemical Cycles*, 14(3) :795–825, doi :10.1029/1999GB001138.

Landry, J.-S. and Matthews, H. D. (2016). Non-deforestation fire vs. fossil fuel combustion : the source of CO_2 emissions affects the global carbon cycle and climate responses. *Biogeosciences*, 13(7) :2137–2149, doi :10.5194/bg-13-2137-2016.

Le Goff, H. and Sirois, L. (2004). Black spruce and jack pine dynamics simulated under varying fire cycles in the northern boreal forest of Quebec, canada. *Canadian Journal of Forest Research*, 34(12) :2399–2409, doi :10.1139/x04-121.

Légaré, S., Bergeron, Y., and Paré, D. (2005). Effect of aspen (*Populus tremuloides*) as a companion species on the growth of black spruce (*Picea mariana*) in the southwestern boreal forest of Quebec. *Forest Ecology and Management*, 208(1) :211–222, doi :10.1016/j.foreco.2004.12.004.

Lenihan, J. M. and Bachelet, D. (2015). Historical climate and suppression effects on simulated fire and carbon dynamics in the conterminous United States. *Global Vegetation Dynamics : Concepts and Applications in the MC1 Model*, pages 17–30, doi :10.1002/9781119011705.ch2.

Logan, J. A., Régnière, J., and Powell, J. A. (2003). Assessing the impacts of global warming on forest pest dynamics. *Frontiers in Ecology and the Environment*, 1(3) :130–137, doi :10.1890/1540-9295(2003)001[0130 :ATIOGW]2.0.CO ;2.

Macias Fauria, M. and Johnson, E. A. (2008). Climate and wildfires in the North American boreal forest. *Philosophical Transactions of the Royal Society B : Biological Sciences*, 363(1501) :2315–2327, doi :10.1098/rstb.2007.2202.

Mansuy, N., Gauthier, S., Robitaille, A., and Bergeron, Y. (2011). The effects of surficial deposit-drainage combinations on spatial variations of fire cycles in the boreal forest of eastern Canada. *International Journal of Wildland Fire*, 19(8) :1083–1098, doi :10.1071/WF09144.

Marchal, J., Cumming, S. G., and McIntire, E. J. (2017). Land cover, more than monthly fire weather, drives fire-size distribution in Southern Québec forests : Implications for fire risk management. *PloS one*, 12(6) :e0179294, doi :10.1371/journal.pone.0179294.

Martell, D. L. and Sun, H. (2008). The impact of fire suppression, vegetation, and weather on the area burned by lightning-caused forest fires in Ontario. *Canadian Journal of Forest Research*, 38(6) :1547–1563, doi :10.1139/X07-210.

McKenney, D. W., Pedlar, J. H., Lawrence, K., Papadopol, P., and Campbell, K. (2014). Hardiness Zones and Bioclimatic Modelling of Plant Species Distributions in North America.

In *Proceedings of the 2014 Annual Meeting of the International Plant Propagators Society 1085*, pages 139–148, doi :10.17660/ActaHortic.2015.1085.24.

McKenney, D. W., Yemshanov, D., Pedlar, J. H., Allen, D. J., Lawrence, K. M., Hope, E., Lu, B., and Eddy, B. (2016). Canada's timber supply : current status and future prospects under a changing climate. Information Report GLC-X-15.

Mery, G., Katila, P., Galloway, G., Alfaro, R. I., Kanninen, M., Lobovikov, M., and Varjo, J. (2010). *Forests and society - responding to global drivers of change*. IUFRO, Vienna, Austria.

Michetti, M. and Zampieri, M. (2014). Climate-Human-Land Interactions : A Review of Major Modelling Approaches. *Land*, 3(3) :793–833, doi :10.3390/land3030793.

Miller, J. (2010). Species Distribution Modeling. *Geography Compass*, 4(6) :490–509, doi :10.1111/j.1749-8198.2010.00351.x.

Moritz, M. A., Krawchuk, M. A., and Parisien, M.-A. (2010). Pyrogeography : Understanding the ecological niche of fire. *PAGES News*, 18 :83–85, doi :10.22498/pages.18.2.83.

Natural Resources Canada (2017). The State of Canada's Forests. Annual Report 2017, available from http ://cfs.nrcan.gc.ca/pubwarehouse/pdfs/38871.pdf.

Nock, C. A., Vogt, R. J., and Beisner, B. E. (2016). Functional Traits. In *eLS*, Major Reference Works, pages 1–8. John Wiley & Sons, Ltd, Chichester edition.

Norby, R. J., Warren, J. M., Iversen, C. M., Medlyn, B. E., and McMurtrie, R. E. (2010). CO_2 enhancement of forest productivity constrained by limited nitrogen availability. *Proceedings of the National Academy of Sciences*, 107(45) :19368–19373, doi :10.1073/pnas.1006463107.

Oreskes, N. (2018). The Scientific Consensus on Climate Change : How Do We Know We're Not Wrong ? In *Climate Modelling*, pages 31–64. Springer, doi :10.1007/978-3-319-65058-62.

Pacé, M., Fenton, N. J., Paré, D., and Bergeron, Y. (2016). Ground-layer composition affects tree fine root biomass and soil nutrient availability in jack pine and black spruce forests under extreme drainage conditions. *Canadian Journal of Forest Research*, 47(4) :433–444, doi :10.1139/cjfr-2016-0352.

Pacé, M., Fenton, N. J., Paré, D., and Bergeron, Y. (2018). Differential effects of feather and sphagnum spp. mosses on black spruce germination and growth. *Forest Ecology and Management*, 415 :10–18, doi :10.1016/j.foreco.2018.02.020.

Pan, Y., Birdsey, R. A., Fang, J., Houghton, R., Kauppi, P. E., Kurz, W. A., Phillips, O. L., Shvidenko, A., Lewis, S. L., Canadell, J. G., Ciais, P., Jackson, R. B., Pacala, S. W., McGuire, A. D., Piao, S., Rautiainen, A., Sitch, S., and Hayes, D. (2011). A large and persistent carbon sink in the world's forests. *Science*, 333(6045) :988–993, doi :10.1126/science.1201609.

Parisien, M.-A., Miller, C., Parks, S. A., DeLancey, E. R., Robinne, F.-N., and Flannigan, M. D. (2016). The spatially varying influence of humans on fire probability in North America. *Environmental Research Letters*, 11(7) :075005, doi :10.1088/1748-9326/11/7/075005.

Parisien, M.-A., Parks, S. A., Krawchuk, M. A., Flannigan, M. D., Bowman, L. M., and Moritz, M. A. (2011). Scale-dependent controls on the area burned in the boreal forest of Canada, 1980-2005. *Ecological Applications*, 21(3) :789–805, doi :10.1890/10-0326.1.

Payette, S., Filion, L., and Delwaide, A. (2008). Spatially explicit fire-climate history of the boreal forest-tundra (Eastern Canada) over the last 2000 years. *Philosophical Transactions of the Royal Society of London B : Biological Sciences*, 363(1501) :2299–2314, doi :10.1098/rstb.2007.2201.

Peaucelle, M., Bellassen, V., Ciais, P., Peñuelas, J., and Viovy, N. (2017). A new approach to optimal discretization of plant functional types in a process-based ecosystem model with forest management : a case study for temperate conifers. *Global ecology and biogeography*, 26(4) :486–499, doi :10.1111/geb.12557.

Peh, K. S.-H., Corlett, R. T., and Bergeron, Y. (2015). *Routledge Handbook of Forest Ecology*. Routledge.

Périé, C., de Blois, S., Lambert, M.-C., and Casajus, N. (2014). *Effets anticipés des changements climatiques sur l'habitat des espèces arborescentes au Québec*. Ministère des Ressources naturelles du Québec, available from : https ://www.mffp.gouv.qc.ca/publications/forets/connaissances/recherche/Perie-Catherine/Memoire173.pdf.

Peterson, D., Wang, J., Ichoku, C., and Remer, L. A. (2010). Effects of lightning and other meteorological factors on fire activity in the North American boreal forest : implications for fire weather forecasting. *Atmospheric Chemistry and Physics*, 10(14) :6873–6888, doi :10.5194/acp-10-6873-2010.

Pfeiffer, M., Spessa, A., and Kaplan, J. O. (2013). A model for global biomass burning in preindustrial time : LPJ-LMfire (v1. 0). *Geoscientific Model Development*, 6(3) :643–685, doi :10.5194/gmd-6-643-2013.

Portier, J., Gauthier, S., Leduc, A., Arseneault, D., and Bergeron, Y. (2016). Fire regime along latitudinal gradients of continuous to discontinuous coniferous boreal forests in eastern Canada. *Forests*, 7(10) :211, doi :10.3390/f7100211.

Prentice, I. C., Kelley, D. I., Foster, P. N., Friedlingstein, P., Harrison, S. P., and Bartlein, P. J. (2011). Modeling fire and the terrestrial carbon balance. *Global Biogeochemical Cycles*, 25(3) :GB3005, doi :10.1029/2010GB003906.

Prévost, M. and Pothier, D. (2003). Partial cuts in a trembling aspen conifer stand : effects on microenvironmental conditions and regeneration dynamics. *Canadian Journal of Forest Research*, 33(1) :1–15, doi :10.1139/x02-147.

Prévost, M., Raymond, P., and Lussier, J.-M. (2010). Regeneration dynamics after patch cutting and scarification in yellow birch-conifer stands. *Canadian journal of forest research*, 40(2) :357–369, doi :10.1139/X09-192.

Price, D. T., Alfaro, R. I., Brown, K. J., Flannigan, M. D., Fleming, R. A., Hogg, E. H., Girardin, M. P., Lakusta, T., Johnston, M., McKenney, D. W., Pedlar, J. H., Stratton, T., Sturrock, R. N., Thompson, I. D., Trofymow, J. A., and Venier, L. A. (2013). Anticipating the consequences of climate change for Canada's boreal forest ecosystems. *Environmental Reviews*, 21(4) :322–365, doi :10.1139/er-2013-0042.

Pureswaran, D. S., De Grandpré, L., Paré, D., Taylor, A., Barrette, M., Morin, H., Régnière, J., and Kneeshaw, D. D. (2015). Climate-induced changes in host tree-insect phenology may drive ecological state-shift in boreal forests. *Ecology*, 96(6) :1480–1491, doi :10.1890/13-2366.1.

Quillet, A., Peng, C., and Garneau, M. (2010). Toward dynamic global vegetation models for simulating vegetation-climate interactions and feedbacks : recent developments, limitations, and future challenges. *Environmental Reviews*, 18(NA) :333–353, doi :10.1139/A10-016.

Rabin, S. S., Melton, J. R., Lasslop, G., Bachelet, D., Forrest, M., Hantson, S., Kaplan, J. O., Li, F., Mangeon, S., Ward, D. S., Yue, C., Arora, V. K., Hickler, T., Kloster, S., Knorr, W., Nieradzik, L., Spessa, A., Folberth, G. A., Sheehan, T., Voulgarakis, A., Kelley, D. I., Prentice, I. C., Sitch, S., Harrison, S., and Arneth, A. (2017). The Fire Modeling Intercomparison Project (FireMIP), phase 1 : experimental and analytical protocols with detailed model descriptions. *Geosci. Model Dev.*, 10(3) :1175–1197, doi :10.5194/gmd-10-1175-2017.

Régnière, J., Lysyk, T. J., and Auger, M. (1989). Population density estimation of spruce budworm, *Choristoneura fumiferana* (Clem.)(Lepidoptera : Tortricidae) on balsam fir and white spruce from 45-cm mid-crown branch tips. *The Canadian Entomologist*, 121(03) :267–281, doi :10.4039/Ent12127-1.

Régnière, J., Powell, J., Bentz, B., and Nealis, V. (2012). Effects of temperature on development, survival and reproduction of insects : experimental design, data analysis and modeling. *Journal of Insect Physiology*, 58(5) :634–647, doi :10.1016/j.jinsphys.2012.01.010.

Régnière, J., Saint-Amant, R., and Béchard, A. (2014). *BioSIM 10 - Guide de l'utilisateur.* Number LAU-X-137. Ressour. Nat. Can., Serv. can. for., Cent. for. Laurentides, Québec (Québec), available from : http ://www.cfs.nrcan.gc.ca/publications/ ?id=34817.

Rollinson, C. R., Liu, Y., Raiho, A., Moore, D. J. P., McLachlan, J., Bishop, D. A., Dye, A., Matthes, J. H., Hessl, A., Hickler, T., Pederson, N., Poulter, B., Quaife, T., Schaefer, K., Steinkamp, J., and Dietze, M. C. (2017). Emergent climate and CO_2 sensitivities of net primary productivity in ecosystem models do not agree with empirical data in temperate forests of eastern North America. *Global Change Biology*, 23(7) :2755–2767, doi :10.1111/gcb.13626.

Romps, D. M., Seeley, J. T., Vollaro, D., and Molinari, J. (2014). Projected increase in lightning strikes in the United States due to global warming. *Science*, 346(6211) :851–854, doi :10.1126/science.1259100.

Ruosch, M., Spahni, R., Joos, F., Henne, P. D., Knaap, W. O., and Tinner, W. (2016). Past and future evolution of *Abies alba* forests in Europe-comparison of a dynamic vegetation model with palaeo data and observations. *Global change biology*, 22(2) :727–740, doi :10.1111/gcb.13075.

Schibalski, A., Lehtonen, A., Hickler, T., and Schröder, B. (2017). Identifying important topics for model refinement in a widely used process-based model informed by correlative model analyses in a boreal forest. *SILVA FENNICA*, 51(4).

Sedano, F. and Randerson, J. T. (2014). Multi-scale influence of vapor pressure deficit on fire ignition and spread in boreal forest ecosystems. *Biogeosciences*, 11(14) :3739–3755, doi :10.5194/bg-11-3739-2014.

Shafer, S. L., Bartlein, P. J., Gray, E. M., and Pelltier, R. T. (2015). Projected Future Vegetation Changes for the Northwest United States and Southwest Canada at a Fine Spatial Resolution Using a Dynamic Global Vegetation Model. *PLOS ONE*, 10(10) :e0138759, doi :10.1371/journal.pone.0138759.

Sirois, L. (2000). Spatiotemporal variation in black spruce cone and seed crops along a boreal forest-tree line transect. *Canadian Journal of Forest Research*, 30(6) :900–909, doi :10.1139/x00-015.

Sitch, S., Smith, B., Prentice, I. C., Arneth, A., Bondeau, A., Cramer, W., Kaplan, J. O., Levis, S., Lucht, W., Sykes, M. T., Thonicke, K., and Venevsky, S. (2003). Evaluation of ecosystem dynamics, plant geography and terrestrial carbon cycling in the LPJ dynamic global vegetation model. *Global Change Biology*, 9(2) :161–185, doi :10.1046/j.1365-2486.2003.00569.x.

Smith, B., Prentice, I. C., and Sykes, M. T. (2001). Representation of vegetation dynamics in the modelling of terrestrial ecosystems : comparing two contrasting approaches within European climate space. *Global Ecology and Biogeography*, 10(6) :621–637, doi :10.1046/j.1466-822X.2001.t01-1-00256.x.

Solow, A. R. (2015). Extreme weather, made by us ? *Science*, 349(6255) :1444–1445, doi :10.1126/science.aad2132.

Splawinski, T., Gauthi, S., Fenton, N., Houle, D., and Bergeron, Y. (In press). The colonization of young fire initiated stands by the crustose lichen Trapeliopsis granulosa and its potential effect on conifer establishment and stand succession.

Stocks, B. J., Mason, J. A., Todd, J. B., Bosch, E. M., Wotton, B. M., Amiro, B. D., Flannigan, M. D., Hirsch, K. G., Logan, K. A., Martell, D. L., and Skinner, W. R. (2003). Large forest fires in Canada, 1959-1997. *Journal of Geophysical Research : Atmospheres*, 107(D1) :8149, doi :10.1029/2001JD000484.

Tang, G., Beckage, B., Smith, B., and Miller, P. A. (2010). Estimating potential forest NPP, biomass and their climatic sensitivity in New England using a dynamic ecosystem model. *Ecosphere*, 1(6) :1–20, doi :10.1890/ES10-00087.1.

Taylor, A. R., Boulanger, Y., Price, D. T., Cyr, D., McGarrigle, E., Rammer, W., and Kershaw, J. A. (2017). Rapid 21st century climate change projected to shift composition and growth of Canada's Acadian Forest Region. *Forest Ecology and Management*, 405(Supplement C) :284–294, doi :10.1016/j.foreco.2017.07.033.

Terrier, A., Girardin, M. P., Cantin, A., Groot, W. J., Anyomi, K. A., Gauthier, S., and Bergeron, Y. (2014). Disturbance legacies and paludification mediate the ecological impact of an intensifying wildfire regime in the Clay Belt boreal forest of eastern North America. *Journal of Vegetation Science*, 26(3) :588–602, doi :10.1111/jvs.12250/full.

Terrier, A., Girardin, M. P., Périé, C., Legendre, P., and Bergeron, Y. (2013). Potential changes in forest composition could reduce impacts of climate change on boreal wildfires. *Ecological Applications*, 23(1) :21–35, doi :10.1890/12-0425.1.

Thonicke, K., Spessa, A., Prentice, I. C., Harrison, S. P., Dong, L., and Carmona-Moreno, C. (2010). The influence of vegetation, fire spread and fire behaviour on biomass burning and trace gas emissions : results from a process-based model. *Biogeosciences*, 7(6) :1991–2011, doi :10.5194/bg-7-1991-2010.

Trenberth, K. E., Fasullo, J. T., and Shepherd, T. G. (2015). Attribution of climate extreme events. *Nature Climate Change*, 5(8) :725–730, doi :10.1038/nclimate2657.

Valdes, P. J., Armstrong, E., Badger, M. P., Bradshaw, C. D., Bragg, F., Crucifix, M., Davies-Barnard, T., Day, J. J., Farnsworth, A., Gordon, C., et al. (2017). The bridge hadcm3 family of climate models : Hadcm3@ bristol v1. 0. *Geoscientific Model Development*, 10(10) :3715, doi :10.5194/gmd-10-3715-2017.

Van Wagner, C. E. (1987). *Development and structure of the Canadian Forest Fire Weather Index System*. available from : https ://cfs.nrcan.gc.ca/publications ?id=19927.

Venevsky, S., Thonicke, K., Sitch, S., and Cramer, W. (2002). Simulating fire regimes in human-dominated ecosystems : Iberian Peninsula case study. *Global Change Biology*, 8(10) :984–998, doi :10.1046/j.1365-2486.2002.00528.x.

Verta, J.-P., Landry, C. R., and MacKay, J. J. (2013). Are long-lived trees poised for evolutionary change ? Single locus effects in the evolution of gene expression networks in spruce. *Molecular Ecology*, 22(9) :2369–2379, doi :10.1111/mec.12189.

Wotton, B., Martell, D., and Logan, K. (2003). Climate change and people-caused forest fire occurrence in Ontario. *Climatic Change*, 60(3) :275–295, doi :10.1023/A :1026075919710.

Wotton, B. M., Flannigan, M. D., and Marshall, G. A. (2017). Potential climate change impacts on fire intensity and key wildfire suppression thresholds in Canada. *Environmental Research Letters*, 12(9) :095003, doi :10.1088/1748-9326/aa7e6e.

Xia, J., McGuire, A. D., Lawrence, D., Burke, E., Chen, G., Chen, X., Delire, C., Koven, C., MacDougall, A., Peng, S., Rinke, A., Saito, K., Zhang, W., Alkama, R., Bohn, T. J., Ciais, P., Decharme, B., Gouttevin, I., Hajima, T., Hayes, D. J., Huang, K., Ji, D., Krinner, G., Lettenmaier, D. P., Miller, P. A., Moore, J. C., Smith, B., Sueyoshi, T., Shi, Z., Yan, L., Liang, J., Jiang, L., Zhang, Q., and Luo, Y. (2017). Terrestrial ecosystem model performance in simulating productivity and its vulnerability to climate change in the northern permafrost region. *Journal of Geophysical Research : Biogeosciences*, 122(2) :2016JG003384, doi :10.1002/2016JG003384.

Résumé

L'objectif principal est d'évaluer les effets potentiels du changement climatique (CC) sur la dynamique de végétation et des incendies, et de caractériser leurs effets conjoints sur la résilience de la forêt boréale de l'Est canadien. Des simulations ont été réalisées avec le modèle LPJ-LMfire à 100 km^2 de résolution et s'intéressent à : (1) la reconstruction de l'activité de feux entre 1901-2012 et relations avec la végétation et le climat, (2) projections de l'impact du CC sur la forêt boréale de l'Est canadien, (3) simulation des trajectoires des feux et de la végétation au cours de l'Holocène. LPJ-LMfire reproduit correctement les tendances spatio-temporelles de la fréquence des feux observée au cours du 20ème S.. Les trajectoires des feux et de la végétation simulées sur l'Holocène sont décalées spatialement par rapport aux reconstructions paléoécologiques et serait dû aux données climatiques fournies en entrée du modèle. La variabilité climatique et les impacts de foudre sont les facteurs déterminants de la répartition des feux au cours du 20ème S. alors que les rétroactions de la végétation sur les feux contrôlent la distribution de leur fréquence sur de longues échelles de temps. Nos résultats contredisent l'augmentation prévue du risque de feu futur, suggérant plutôt une diminution d'ici 2100, associée à une augmentation de la proportion des taxons feuillus et à une ouverture des paysages. Des pertes de biomasse causées par les feux et les chaleurs sont projetées; l'effet fertilisant du CO_2 atmosphériques sur la productivité forestière ne compensera pas ces pertes. En 2100, la baisse des stocks de biomasse pourraient menacer l'économie du secteur forestier.

Abstract

The objective is to assess the potential effects of climate change on vegetation dynamics and fires, and to characterize their joint effects on the resilience of eastern Canada's boreal forest. Simulations were carried out with the LPJ-LMfire model at 100 km^2 resolution from Manitoba to Newfoundland and focused on (1) fire activity reconstruction from 1901 to 2012 and relation to vegetation and climate, (2) projections of climate change impacts on the eastern Canada's boreal forest, (3) simulation of past fires and vegetation trajectories during the last 6000 years. LPJ-LMfire correctly reproduces the spatio-temporal trends in fire frequency observed in the 20th century. The Holocene trajectories of simulated fires and vegetation were spatially shifted compared to paleoecological reconstructions. The observed difference would be due to the Holocene climate data provided as input of LPJ-LMfire. Climate variability and lightning impacts are the determining factors in the distribution of fire frequency during the 20th century, while vegetation feedbacks on fires control the distribution of their frequency over long time scales. Our results contradict the predicted increase in future fire risk, suggesting a decrease in fire frequency by 2100, associated with an increase in the proportion of deciduous taxa and an opening of landscapes. Reductions of biomass incurred by fire and heat-induced tree mortality events are projected; the fertilizing effect of increasing atmospheric CO_2 on forest productivity is unlikely to compensate for these losses. By 2100, declining biomass stocks and increasing broadleaf proportion in the south could threaten the economy of the forest sector.

Mots Clés

Modélisation, LPJ-LMfire, Changements climatiques, Aménagement forestier, Forêt boréale, Feux, Dynamique de végétation

Keywords

Modelling, LPJ-LMfire, Climate change, Forest management, Boreal forest, Wildfires, Vegetation dynamic